UNIVERSIDADE FEDERAL FLUMINENSE

INSTITUTO DE BIOLOGIA

PROGRAMA DE PÓS-GRADUAÇÃO EM CIÊNCIAS E BIOTECNOLOGIA

RENATA DE LIMA BARBOSA

Investigação *in vitro* da associação de carbonatoapatita a membranas de concentrados plaquetários autólogos para a bioengenharia óssea.

Tese de Doutorado submetida a
Universidade Federal Fluminense visando à obtenção do grau de
Doutora em Ciências e Biotecnologia

Orientador: Dr. Gutemberg Gomes Alves

Coorientador: Dr. Carlos Fernando de Almeida Barros Mourão

Niterói
2023

RENATA DE LIMA BARBOSA

INVESTIGAÇÃO *IN VITRO* DA ASSOCIAÇÃO DE CARBONATOAPATITA A MEMBRANAS DE CONCENTRADOS PLAQUETÁRIOS AUTÓLOGOS PARA A BIOENGENHARIA ÓSSEA.

Trabalho desenvolvido no Laboratório de Unidade de pesquisa clínica, no Hospital Universitário Antônio Pedro HUAP – UFF do Departamento de Biologia Celular e Molecular (GCM) do Instituto de Biologia, Programa de Pós-Graduação em Ciências e Biotecnologia, Universidade Federal Fluminense. Apoio Financeiro: CAPES, CNPq, FAPERJ, UFF-FOPESQ

Tese de Doutorado submetida a Universidade Federal Fluminense como requisito parcial visando à obtenção do grau de Doutora em Ciências e Biotecnologia

Orientador(es): Dr. Gutemberg Gomes Alves

Dr. Carlos Fernando de Almeida Barros Mourão

RENATA DE LIMA BARBOSA

Ficha catalográfica automática - SDC/BCV
Gerada com informações fornecidas pelo autor

B238i Barbosa, Renata de Lima
Investigação in vitro da associação de carbonatoapatita a membranas de concentrados plaquetários autólogos para a bioengenharia óssea. / Renata de Lima Barbosa. - 2023.
184 f.: il.

Orientador: Gutemberg Gomes Alves.
Coorientador: Carlos Fernando Almeida Barros Mourão.
Tese (doutorado)-Universidade Federal Fluminense, Instituto de Biologia, Niterói, 2023.

1. Agregados plaquetários. 2. Bioengenharia óssea. 3. Células ósseas. 4. Biologia celular. 5. Produção intelectual. I. Alves, Gutemberg Gomes, orientador. II. Mourão, Carlos Fernando Almeida Barros, coorientador. III. Universidade Federal Fluminense. Instituto de Biologia. IV. Título.

CDD - XXX

Bibliotecário responsável: Debora do Nascimento - CRB7/6368

INVESTIGAÇÃO *IN VITRO* DA ASSOCIAÇÃO DE CARBONATOAPATITA A MEMBRANAS DE CONCENTRADOS PLAQUETÁRIOS AUTÓLOGOS PARA A BIOENGENHARIA ÓSSEA

Tese de Doutorado submetida à Universidade Federal Fluminense como requisito parcial visando à obtenção do grau de Doutora em Ciências e Biotecnologia

Banca Examinadora:

Dr. Gutemberg Gomes Alves – Departamento de Biologia Celular e Molecular UFF. (Orientador/Presidente)

Dra. Elena Mavropoulos – Centro Brasileiro de Pesquisas físicas (CBPF). (Membro externo)

Dra. Mônica Diuana Calasans Maia - Departamento de Odontologia – UFF. (Membro interno)

Dra. Mariana Rodrigues Pereira - Departamento de Neurobiologia (GNE) da UFF. (Membro interno)

Dra. Jéssica Dornelas da Silva - empresa NanoOnco3D (Membro externo)

Dr. Rafael Coutinho de Mello Machado - Inside Odontologia. (Membro externo)

Dr. Paulo Emílio Corrêa Leite - Departamento de Biologia Celular e Molecular– Universidade Federal Fluminense (UFF) (Revisor)

Dr. João Ricardo Almeida Soares - Laboratório de Desenvolvimento Tecnológico e Inovação do Instituto Vital Brazil (Suplente externo)

DEDICATÓRIA

A todos nós, que possamos nos beneficiar com avanços da ciência ao longo do tempo.

AGRADECIMENTOS

Agradeço ao Guto, meu orientador pelo aceite ao grupo, pelo trabalho e toda orientação e caminhada ao longo dos anos, muito obrigada!

Agradeço ao meu Coorientador pelo trabalho e toda orientação e caminhada ao longo dos anos, muito obrigada!

Agradeço aos órgãos de fomento CAPES, CNPq, FAPERJ, UFF-FOPESQ todo apoio financeiro e bolsa de pesquisa.

Agradeço aos doadores de sangue pela doação para o desenvolvimento desse trabalho.

Agradeço aos colegas de laboratório por colaborar para o desenvolvimento desse trabalho. Em especial Neilane, Manu e Victor, muito obrigada.

Agradeço ao Max e a Jéssica por sempre podermos jogar conversa fora, e falar sobre pesquisa.

Agradeço a minha família que sempre torceu muito, contribuiu e incentivou muito pela realização desse sonho.

Agradeço a minha irmã Aline pelos papos, incentivos e memes ao longo do tempo.

Agradeço ao João Ricardo, meu irmão de coração pelas conversas, por me ajudar a organizar minha cabeça, nos momentos mais angustiantes.

Agradeço ao Anderson, meu noivo pelo amor, carinho, paciência e compreensão nos períodos tensos.

Sumário

1. Lista de Abreviaturas **9**

2. Lista de Ilustrações **12**

RESUMO **15**

Abstract **16**

1 Introdução **17**

Protocol and Registry 29

Study selection 30

Critical Appraisal 31

Data extraction 31

RESULTS 32

Discussion **5**

Protocols for PRF production and preservation 5

Association of PRF and other materials/compounds 7

Cell-type related effects of PRF 9

Molecular effects of PRF on differentiation and mineralization 13

Final considerations **21**

Preparation of Alb-PRF and Alb-ncHA-PRF membranes 27

Production of the membrane eluates 28

Scanning electron microscopy 28

Observation of viable cells in the membranes 29

Quantification of cytokines and growth factor release 29

Statistical analysis 31

ConSIDERAÇÕES FINAIS **49**

2 Referências Biliográficas **51**

1 Anexo I **72**

2 Anexo II **77**

3 Anexo III **83**

4 Anexo IV **92**

5 ANEXO V 112

Lista de Abreviaturas

BMP2 - Proteína morfogenética óssea 2

CBPF Centro Brasileiro de Pesquisas Físicas

CCL11 – Quimiocina 11

CCL2 - Quimiocina 2

CCL3 - Quimiocina 3

CCL4 - Quimiocina 4

CCL5 - Quimiocina 5

cHA - Carbonatoapatita

CO_2 - Dióxido de carbono

CO_3 - Carbonato

CSF2 - Fator estimulador de colônias 2

CSF3 - Fator estimulador de colônias 3

CVDE - Cristal violeta

CXCL10 - Quimiocina 10

DAPI - (4',6-diamidino-2-fenilindol)

DMEM - Dulbecco's Modified Eagle's Medium – Meio de cultura de células

FGF – Fator de crescimento de fibroblastos

HA – Hidroxiapatita

HMDS - Hexametildisilazina

HUAP - Hospital Universitário Antônio Pedro

IFN-γ - Interferon-gamma

IL-10 - Interleucina - 10

IL-12 - Interleucina - 12

IL-13 - Interleucina - 13

IL-15 - Interleucina - 15

IL-17 - Interleucina – 17

IL-1RA - Antagonista do receptor de interleucina - 1 beta

IL-1β - Interleucina- 1 beta

IL-2 - Interleucina - 2

IL-4 - Interleucina - 4

IL-5 - Interleucina - 5

IL-6 - Interleucina - 6

IL-7 - Interleucina - 7

IL-8 - Interleucina - 8

IL-9 - Interleucina - 9

L-PRF - Fibrina Rica em Leucócitos e Plaquetas

MSCs - Células-tronco mesenquimais

NR - Vermelho neutro

OPG - Osteoprotegerina

PBS - Salina tamponada com fosfato

PDGF - Fator de crescimento derivado de plaquetas

PRF - Plasma rico em fibrinas

PRP - Plasma rico em plaquetas

RANKL - Receptor ativador do fator nuclear kappa B-ligante

RT-PCR - Reação da transcriptase reversa

Runx2 - Fator de Transcrição Relacionado ao Runt 2

SFB - Soro fetal bovino

TGF - Fator de transformação do crescimento

TNFα - Fator de necrose tumoral alfa

UPC - Unidade de Pesquisa Clínica

VEGF - Fator de Crescimento do Endotelial Vascular

XTT – (2,3-Bis-(2-Methoxy-4-Nitro-5-Sulfophenyl)-2H-Tetrazolium-5-Carboxanilide)

Lista de Ilustrações

Figura 1. Mercado europeu de biomateriais para regeneração óssea (iData research 2023).

Figura 2. Estrutura do osso. Adaptada e traduzida de Wang et al 2017.

Figura 3. Preparo da PRF, plasma acelular no início do tubo, coágulo de PRF no meio e células vermelhas (Lima, et al 2023).

Figure 4. The screening process, selection, and systematic steps according to the PRISMA Statement

Figure 5. Main biological events involved in the response of mineralizing cells to PRF, according to the literature evidence. Several growth factors and important mediators are released in the medium by PRF (1), many of which are able to activate mitogen-induced signaling pathways (2), known to modulate the expression of transcription factors, such as RunX2 and Osterix, directly involved on bone cell differentiation (3). These transcription factors are responsible for the altered expression and secretion of different proteins responsible for the formation of the mineralized matrix and the control of osteoclastogenesis (4). Furthermore, the exposure to PRF may induce increased secretion of growth factors, such as BMP-2, VEGF or IGF (5), indicating that exposed cells may also be activated by paracrine regulation in response to PRF. All of these processes result in increased nodule formation and, therefore, biological mineralization (6).

Figura 6 - Scanning electron microscopy (SEM) micrographs of nanostructured carbonated hydroxyapatite microspheres. Observe the morphology starting from 1 mm to 20 μm from the surface of the spheres, they are irregular and full of indentations.

Figura 7 - Scanning electron microscopy (SEM) micrographs of 24-hour PRF albumin membranes. Observe the morphology starting from 1 mm to 10 μm from the membrane indicates a very robust membrane.

Figura 8 - Scanning electron microscopy (SEM) micrographs of PRF albumin membranes associated with 24-hour nanostructured carbonated hydroxyapatite

microspheres. Observe the morphology starting from 1 mm to 20 μm from the membrane with cells wrapped in the fibrin network. It is possible to observe a different appearance, with cells trapped in the membrane and a sandy appearance. It is possible to observe two phases, one full of plots and the other very robust and dense.

Figura 9 - Scanning electron microscopy (SEM) micrographs of PRF albumin membranes associated with 21-day nanostructured carbonated hydroxyapatite microspheres. Note the morphology starting from 1 mm to 100 μm and the robust structure still present, associated with cells and carbonated hydroxyapatite microspheres.

Figura 10 - Scanning electron microscopy (SEM) micrographs of 21-day PRF albumin membranes. Observe the morphology starting from 1 mm to 100 μm of the membrane, indicating a membrane that remains structured at 21 days after polymerization.

Figura 11 – Histological sections of the Alb-PRF membranes. Note that he concentration of cells on the fibrin portion, in comparison with a dense denatured albumin portion.

Figura 12 – Histological sections of an Alb-PRF membrane associated with nanostructured carbonated hydroxyapatite microspheres.

Figura 13 – Microscope image of the Live/Dead assay of cells present in the membranes. Green (calcein) staining for live cells, red (EthD) for dead cells.

Figura 14 - Heatmap of the release of cytokines and growth factors from Alb-ncHA-PRF and Alb-PRF membranes after 24 hours of elution in culture medium. An asterisk indicates significant difference between groups ($p<0.05$).

Figura 15 - Cytocompatibility assessment of ALB-PRF and ALB-PRF + nCHA membrane extracts, in different dilutions in culture medium (DMEM), measured in MG63 cells, after 24 hours of exposure, using the XTT test. The bars show the mean and standard deviation of 3 independent experiments, in quintuplicates, represented as a percentage of the control group (cells exposed to culture medium). The line indicates a significant difference between groups ($p<0.05$). A positive cytotoxicity control was produced with latex extracts, showing 20.7% average survival.

Figura 16 - Proliferation of MG63 cells for up to 7 days after exposure to Alb-PRF,

Alb-nCHA-PRF extracts, or culture medium (control). Cell density was assessed thoruth the crystal violet dye exclusion test, with results expressed by the optical density at 540 nm. The letter (a) indicates a significant difference in relation to the control ($p<0.05$). The bars indicate mean ± standard deviation (n=5). Asterisks indicate a significant difference ($p<0.05$) in relation to all other experimental groups.

Figura 17 - In vitro calcification by MG63 cells exposed for up to 3 weeks to ALB-PRF or ALB-PRF + nCHA eluates. Bars indicate mean ± standard deviation (n=3) of alizarin-S labeling, expressed by optical density at 450nm. An asterisk indicates a significant difference ($p<0.05$) from the control group, exposed to culture medium.

Figura 18 - Assessment of alkaline phosphatase ezyme activity in the culture medium over 3 weeks, by MG63 osteoblasts exposed to extracts (25%) of ALB-PRF and ALB-PRF + nCHA membranes, or DMEM culture medium (control). The bars show the mean and standard deviation of 3 independent experiments, in quintuplicate, represented as the optical density of the medium, relative to the breakdown of the PNPP substrate. Asterisks indicate significant differences compared to all other groups at the same experimental time ($p<0.05$).

RESUMO

A fibrina rica em plaquetas (do inglês, Platelet Rich Fibrin, - PRF) é um concentrado sanguíneo de segunda geração utilizado na medicina regenerativa, que tem ganhado atenção como uma alternativa potencial para a terapia do tecido ósseo, com a capacidade de acelerar a regeneração óssea, embora os mecanismos subjacentes precisos ainda não sejam totalmente compreendidos. Além disso, o PRF pode ser integrado com outros biomateriais para estabelecer uma estrutura tridimensional versátil destinada a melhorar o recrutamento, proliferação e diferenciação celular na reparação óssea. Recentemente, nosso grupo propôs uma variante modificada do PRF enriquecida com albumina desnaturada (Alb-PRF,), além de uma preparação de "*sticky bone*", associando agregados plaquetários a microesferas nanoestruturadas de hidroxiapatita carbonatada (nCHA). Neste contexto, esta tese teve como objetivo (i) identificar, através de uma revisão sistemática de estudos *in vitro*, os principais eventos biológicos envolvidos nos efeitos do PRF sobre células ósseas e de tecidos mineralizados, e (ii) avaliar os efeitos da associação de Alb-PRF com esferas de nCHA (Alb-ncHA-PRF) sobre a capacidade de liberação de fatores de crescimento e moléculas imunomoduladoras e seu impacto no comportamento de osteoblastos humanos. A revisão sistemática de escopo, conduzida de acordo com a declaração PRISMA, identificou 76 estudos que demonstram que as membranas PRF influenciam a proliferação, diferenciação e mineralização de células ósseas, devido a mudanças notáveis em marcadores cruciais do metabolismo e comportamento das células ósseas. Por outro lado, os resultados experimentais demonstraram que a Alb-ncHA-PRF, quando comparado a Alb-PRF, exibiu uma liberação reduzida de fatores de crescimento e citocinas, o que posteriormente levou a menor proliferação de osteoblastos MG63, redução de sua atividade fosfatase alcalina e capacidade de mineralização in vitro. Estes achados apontam que a incorporação de esferas ncHA pode atenuar os efeitos biológicos pretendidos do Alb-PRF no comportamento dos osteoblastos. Estas descobertas sublinham o potencial de evolução do PRF na medicina regenerativa e a relevância de considerar a interação dinâmica com outros materiais para a eficácia terapêutica.

Palavras chave: Fibrina rica em plaquetas; gel de albumina; osteoblastos; compósitos; biomateriais.

ABSTRACT

Platelet-rich fibrin (PRF) is a second-generation blood concentrate used in regenerative medicine, that has gained attention as a potential alternative for bone tissue therapy, with the capacity to expedite wound healing and bone regeneration, although the precise underlying mechanisms remain incompletely understood. Additionally, PRF may be integrated with other biomaterials to establish a versatile three-dimensional framework aimed at enhancing cell recruitment, proliferation, and differentiation in bone repair. Recently, our group proposed Alb-PRF, a modified PRF variant enriched with denatured albumin, and a “sticky bone” preparation, associating platelet aggregates with nanostructured carbonated hydroxyapatite microspheres (nCHA). In this context, this thesis aimed to (i) identify, through a systematic review of in vitro studies, the main biological events involved in the effects of PRF on bone and mineralized tissue cells, and (ii) evaluate the effects of associating Alb-PRF with nCHA (Alb-ncHA-PRF) on the release capacity of growth factors and immunomodulatory molecules and their impact on the behavior of human osteoblasts. The comprehensive review, conducted according to the PRISMA Statement identified 76 studies that collectively demonstrate that PRF membranes influence the proliferation, differentiation, and mineralization of bone cells, due to notable changes in crucial markers of bone cell metabolism and behavior. On the other hand, the experimental results demonstrated that Alb-ncHA-PRF, when compared to Alb-PRF, exhibited a reduced release of growth factors and cytokines, which subsequently led to lower MG63 osteoblasts proliferation, alkaline phosphatase activity, and in vitro mineralization. These findings underscore that the incorporation of ncHA spheres may attenuate the intended biological effects of Alb-PRF on osteoblast behavior. Collectively, these findings underscore the evolving potential of PRF in regenerative medicine and the relevance of considering the dynamic interplay with other materials for therapeutic efficacy.

Keywords: Platelet-rich Fibrin; albumin gel; osteoblasts; sticky-bone; biomaterials.

1. INTRODUÇÃO

A bioengenharia de tecidos ósseos tem sido usada, nas últimas décadas, como uma ferramenta para a regeneração de defeitos críticos no sistema esquelético, os quais dificilmente sofrem reparo sem uma intervenção médica.

O mercado de enxertos e substitutos ósseos é categorizado com base nos produtos disponíveis, tais como aloenxertos, substitutos de enxertos ósseos e outros produtos. Além disso, as aplicações desses produtos incluem regiões craniomaxilofacial, odontológica, reconstrução articular, fusão espinhal e outras aplicações. O mercado de enxertos ósseos e substitutos está em constante crescimento. Há uma projeção de crescimento anual de 4% em termos de valor (em milhões de dólares) durante o período de e 2022 a 2027 (Figura 1). Notavelmente, prevê-se que a região da Ásia-Pacífico exiba a taxa de crescimento anual composta mais elevada durante o período de 2023 a 2027 (iData research 2023).

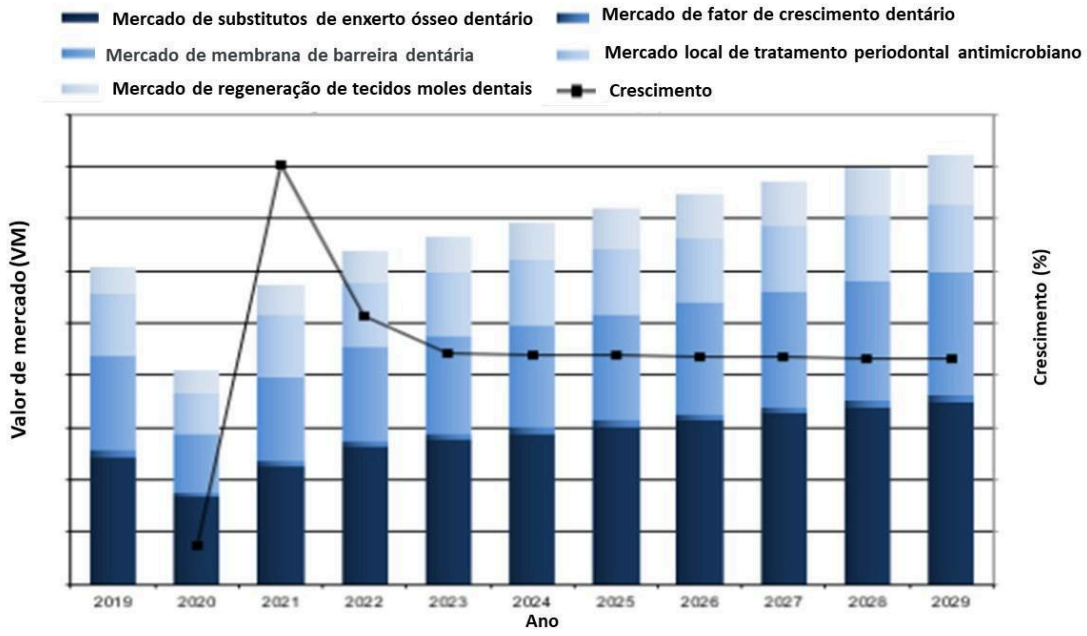

Figura 1. Mercado europeu de biomateriais para regeneração óssea (iData research 2023).

Um biomaterial ideal para a utilização em enxertos ósseos deve ser biocompatível, bioativo, osteocondutor e, preferencialmente, osteoindutor, além de ter composição química semelhante à parte mineral do osso natural a fim de evitar resposta inflamatória exacerbada (BERNARDS *et al.,* 2008). Existe a necessidade em desenvolver biomateriais adequados, que devem degradar e serem substituídos

por tecidos funcionalmente integrados ou devem ter a capacidade de crescer. Assim, é fundamental entender a natureza química e a resposta biológica para recuperação óssea (Hook *et al.* 2009). As pesquisas sobre formação óssea são direcionadas a processos importantes como a composição química, topografia, porosidade além de dureza, densidade e cristalinidade, estão associadas com a degradação dos biomateriais. Um desafio para regeneração óssea é a constituição de um arcabouço que possibilite uma dissolução controlada e cinética de liberação, garantindo que as concentrações necessárias de certos íons sejam liberadas no ambiente fisiológico de forma predeterminada (Hoppe et al 2011).

A busca crescente por substitutos ósseos com características importantes para integração óssea visa evitar problemas de morbidade ou rejeição do sítio doador e risco de transmissão de doenças, que são limitantes para o transplante de osso. O osso autólogo é o padrão ouro atualmente, mas sua disponibilidade é limitada, além da necessidade de uma segunda cirurgia necessária para sua colheita que está associada à morbidade do local doador e risco de infecção aumentado (Raina et al. 2016, Gupta et al. 2015). Dada a importância da composição inorgânica do osso, a HA (hidroxiapatita) sintética vem sendo estudada a bastante tempo devido às possíveis aplicações clínicas na construção de implantes e enxertos ósseos para o tratamento de danos e injúrias no tecido ósseo (Raina et al. 2016).

Em termos de composição, o tecido ósseo é um tecido conjuntivo especializado, formado por células e a matriz óssea. Os materiais orgânicos são principalmente fibras de colágeno. Os materiais inorgânicos são principalmente Cálcio (Ca) e Fósforo (P) na forma de cristais de hidroxiapatita (HA) (Figura 2) (Junqueira e Carneiro 2013, Gao et al 2017).

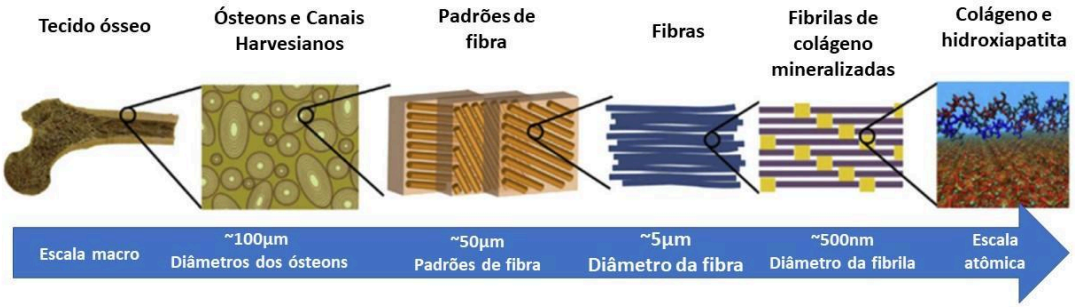

Figura 2. Estrutura do osso. Traduzida de Wang et al 2017.

A hidroxiapatita [Ca10 (PO4) 6 (OH) 2] (HA) é um dos principais componentes da fase mineral de ossos e dentes, e tem atraído a atenção como material de

substituição óssea devido à sua biocompatibilidade e osteointegração que estimulam o crescimento ósseo através de uma ação direta nos osteoblastos (Zambuzzi et al. 2011, Pepla et al. 2014). Biomateriais associados a HA são os mais utilizados em implantes para reparação óssea e reconstrução, devido a sua intensa combinação com os componentes minerais do osso. Sua composição química fornece propriedades diferenciais para um biomaterial, sendo biocompatível, bioativo e biofuncional, garantindo boa aplicabilidade em implantes (COSTA *et al.,* 2009). Além disso, a HA tem um arranjo sistemático de poros uniformes com interconexões, e tem sido usada com sucesso como material de enxerto ósseo para engenharia de tecidos, apresentando osteocondução, facilitando a migração das células osteogênicas e a vascularização do osso circundante (Doi et al. 2017).

Nesse sentido, diversas pesquisas têm desenvolvido e pesquisado materiais como as microesferas de carbonatoapatita (cHA), as quais possuem substituição de grupamentos hidroxila por carbonato, em uma alteração que contribui para conseguir uma estrutura altamente bioabsorvível para a bioengenharia de tecidos ósseos, permitindo substituição por osso novo regenerado (Mavropoulos et al. 2012, Calasans-Maia et al. 2015, Valiense et al. 2016, Carmo et al. 2018). A geometria e a ultraestrutura do material são de extrema importância para a adequação, absorção e integração, de maneira que haja infiltração por células, matriz orgânica e vasos sanguíneos (Habibovic et al. 2010). Diversos estudos comprovam que a hidroxiapatita carbonatada nanoestruturada é um material reabsorvível e que desaparece algumas semanas após o implante em defeitos críticos (Valiense et al. 2012; M. D. Calasans-Maia et al. 2015).Essa importante característica é conferida pela topografia de superfície do biomaterial para a adesão e proliferação de osteoblastos (Burg, Porter, and Kellam 2000).

O osso natural é um tipo especializado de tecido que produz matriz óssea formado por hidroxiapatita carbonatada (cHA), parte constituinte da matriz mineralizada, sendo formada principalmente muitos íons inorgânicos associados e outros traços de elementos, compondo assim a microestrutura óssea, dessa forma os favorece que osteoblastos reconheçam o implante desse material (Adams et al. 2014, Yao et al 2009).

Diversos estudos investigam a similaridade do osso, o tecido natural e a biocompatibilidade já bem estabelecida, e a liberação cálcio e fosfato no meio, os

íons necessários para a formação óssea quais são associados com a formação de novos tecidos ósseos (Enkel et al 2008). A topografia é um fator muito importante para a adesão e proliferação de osteoblastos. Uma vez nanoestruturado como o osso natural, durante o processo de degradação, ele não deve sofrer mudanças que comprometam a resposta celular de maneira a reconhecer como corpo estranho (Burg et al 2000). As células ósseas interagem facilmente com nanomateriais e esta interação pode ser crucial para o sucesso do implante, ou seja, um material nanoestruturado pode promover a adesão, proliferação e diferenciação celular (Li et al. 2009). Aperfeiçoar a geometria e a ultraestrutura do implante é, portanto, uma forma de fazer com que o material implantado se ajuste perfeitamente ao defeito ósseo e possa ser infiltrado por células, matriz orgânica e vasos sanguíneos (Habibovic et al. 2010).

Nesse sentido, as microesferas de carbonatoapatita nanoestruturada (cHA),que possuem substituição de grupamentos hidroxila por carbonato, apresentam uma alteração que contribui para conseguir uma estrutura altamente bioabsorvível para a bioengenharia de tecidos ósseos, permitindo substituição por osso novo regenerado (Mavropoulos et al. 2012, Calasans-Maia et al. 2015, Valiense et al. 2016, Carmo et al. 2018).

O desenvolvimento de biomateriais ósseos para imitar as propriedades estruturais e uma condição porosa do osso natural vem sendo amplamente investigado. As abordagens para a regeneração óssea estão mudando lentamente à medida que novos biomateriais e novas estratégias estão sendo desenvolvidas e a construção de um microambiente celular tornou-se um foco comum de várias disciplinas. Esse campo pode dar passos gigantescos devido ao entendimento da importância da convergência com nanotecnologia, ciência de células-tronco e biologia do desenvolvimento, e talvez outros campos (Gao *et al*. 2017, Yu *et al*. 2015). Estudos combinados procuram integrar propriedades biológicas e mecânicas adequadas para a concepção de biomateriais otimizados, que oferecem um microambiente propício para promover a diferenciação direcionada de células-tronco e, em sequência transformação artificial de biomateriais em formas biológicas (Gao *et al*. 2017).

A bioengenharia se baseia na tríade célula, arcabouço (biomaterial), e fatores de crescimento. Esses materiais ainda demandam o acréscimo de moléculas

osteoindutoras, tais como a proteína morfogenética óssea (BMP 2), para uma efetiva aplicação clínica. Isso representa um significativo aumento no custo do tratamento, uma vez que necessita de grandes doses para serem efetivas, ainda com o decréscimo na resposta com o aumento da idade do paciente (Carreira et al. 2014).

Nesse sentido, a regeneração tecidual tem avançado muito nos últimos anos com o desenvolvimento de agregados autólogos obtidos a partir do sangue, como a Fibrina Rica em Plaquetas (do inglês, Platelet Rich Fibrin, - PRF) e a Fibrina Rica em Leucócitos e Plaquetas (L-PRF), provocando considerável interesse nas áreas médicas e odontológicas. A PRF destaca-se como um biomaterial natural, autólogo, com alto potencial de compatibilidade e funcionalidade com o corpo humano. Como concentrado de plaquetário de segunda geração, a PRF passou por avanços significativos desde o seu início (Choukroun, et al 2006; Miron, et al 2017). A PRF demonstrou ser potencialmente benéfico em muitas aplicações já antes realizadas com PRP (do inglês, Platelet Rich Plasma, Plasma rico em plaquetas - PRP), como tratamentos dermatológicos, implantes ósseos, reconstrução de articulações, cirurgias plásticas e oftalmológicas (Pietrzak et al 2005, Dohan et al 2006a, Conde Montero et al 2013).

A PRF descrita por Choukroun e colaboradores, é uma técnica que não utiliza coagulantes e parte da imediata centrifugação de 10 ml de sangue a 3000 rpm (aproximadamente 400 g) por 10 min. A ausência de anticoagulante implica a ativação, em poucos minutos, da maioria das plaquetas da amostra de sangue em contato com as paredes do tubo, ativa a liberação das cascatas de coagulação da maioria das plaquetas, formando um coágulo de fibrina no meio do tubo, contendo plasma acelular no topo e glóbulos vermelhos no fundo (Figura 3) (Dohan et al 2006a).

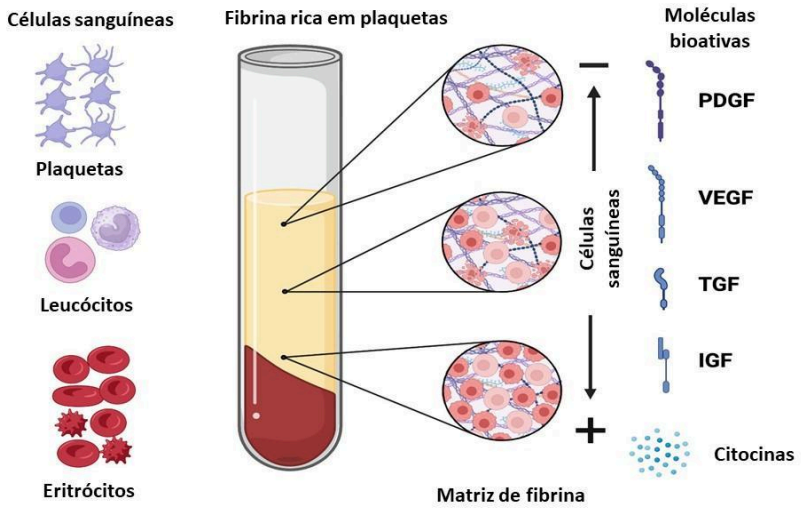

Figura 3. Preparo da PRF, plasma acelular no início do tubo, coágulo de PRF no meio e células vermelhas (Lima, et al 2023).

A PRF tem sido investigada há décadas, assim como o uso de fatores de crescimento autólogo do sangue do próprio paciente (Marx et al. 1998). Ela pertence a uma nova geração de concentrados de plaquetas (Dohan et al 2006a), com alta capacidade cicatricial. A polimerização da membrana cria uma estrutura física ideal para facilitar a cicatrização, promovendo a adesão de células osteoprogenitoras. E a presença de plaquetas e leucócitos garante a produção e liberação contínua de diferentes fatores de crescimento (FGF, VEGF, TGF, PDGF), sendo sua utilização caracterizada como uma técnica com custo benefício vantajoso, pois é obtida de única centrifugação de sangue humano sem adição de anticoagulantes (Choukroun et al.2006a, 2006b, Dohan et al. 2006a, 2006b, 2006c). Estas membranas permanecem significativas após três semanas, com um balanço de citocinas anti-inflamatórias, pró-inflamatórias e quimiocinas, apresentando equilíbrio necessário para a estabilidade em sua conformação (Lourenço et al 2018).

As inúmeras possibilidades terapêuticas do PRF podem ser obtidas pelas modificações em seu protocolo de produção, incluindo a associação com outros biomateriais. Um exemplo é o PRF enriquecido com albumina desnaturada (Alb-PRF) um biomaterial derivado do plasma sanguíneo desenvolvido e patenteado por nosso grupo de pesquisa (ANEXO I), que demonstrou ter interessantes propriedades biológicas para terapia tecidual. O Alb-PRF é obtido pelo aquecimento da fase líquida do PRF (fibrina rica em plaquetas) a 95°C por 5 minutos, o que provoca a desnaturação da albumina e de outras proteínas. A matriz semelhante a

gel resultante contém uma alta concentração de fatores de crescimento, citocinas e componentes da matriz extracelular que podem estimular a cicatrização e regeneração tecidual. Alb-PRF pode ser aplicado como membrana, preenchimento ou suporte para diversas aplicações clínicas, como cicatrização de feridas, regeneração óssea, aumento de tecidos moles e terapia periodontal. Alb-PRF tem diversas vantagens sobre o PRF convencional, como maior estabilidade, biocompatibilidade e bioatividade.

Nesse contexto, surge a hipótese de que a associação de microesferas de cHA nanoestruturada aos fatores de crescimento presentes no Alb-PRF podem oferecer uma alternativa de baixo custo para a obtenção dos elementos da tríade da bioengenharia para tratamentos ósseos. De fato, de acordo com um estudo clínico prévio (Mourão et al 2018b) com pacientes submetidos a procedimento para aumento do assoalho do seio maxilar, utilizando microesferas de hidroxiapatita carbonatada nanoestruturada associadas a um agregado plaquetário (concentrado de fatores de crescimento, ou CGF), foi possível observar que o procedimento cirúrgico quando associado ao biomaterial foi otimizado e apresentou rápida recuperação dos tecidos ósseos.

No entanto, diversas questões relevantes permanecem em aberto, tais como:

(i) quais os efeitos esperados de agregados plaquetários como o PRF sobre células ósseas e de tecidos mineralizados?

(i) a adição do cHA a membrana de Alb-PRF afetaria suas propriedades estruturais, bem como a liberação de fatores de crescimento?

(ii) Quais efeitos que esses componentes, em conjunto, terão sobre a viabilidade, proliferação e capacidade de mineralização de osteoblastos humanos?

A presente tese propôs um estudo *in vitro* capaz de acessar por meio de cultivo celular algumas dessas questões, a partir de uma revisão sistemática de escopo, seguida de uma investigação in vitro, que serão apresentadas em dois manuscritos independentes.

OBJETIVO GERAL:

Investigar as propriedades e aplicações do Plasma Rico em Fibrina (PRF) na regeneração óssea e avaliar seu impacto nas respostas celulares, bem como explorar os efeitos da associação de Alb-PRF com microesferas nanoestruturadas de hidroxiapatita carbonatada (Alb-ncHA-PRF) na liberação de mediadores biológicos e no comportamento de osteoblastos humanos.

OBJETIVOS ESPECÍFICOS:

1. Identificar as bases biológicas da aplicabilidade do PRF a partir de seus efeitos em eventos como proliferação, diferenciação e capacidade de mineralização de células ósseas a partir de evidências fornecidas por estudos controlados in vitro (**Manuscrito 1** - Effects of platelet-rich fibrin in the behavior of mineralizing cells related to bone tissue regeneration. A scoping review of in vitro evidence).

2. Avaliar a associação de Alb-PRF com microesferas nanoestruturadas de hidroxiapatita carbonatada (Alb-ncHA-PRF) com relação a capacidade de liberação de mediadores biológicos (citocinas, fatores de crescimento) e seu impacto no comportamento de osteoblastos humanos (**Manuscrito 2 - T**he association of nanostructured carbonated hydroxyapatite with denatured albumin and platetet-rich fibrin: impacts on growth factor release and osteoblast behavior).

MANUSCRITO I

Effects of platelet-rich fibrin in the behavior of mineralizing cells related to bone tissue regeneration. A scoping review of *in vitro* evidence

1. INTRODUCTION

In recent years, there has been significant advancement in bone tissue engineering, where damaged or diseased bones are repaired using materials that closely replicate the properties of natural bone while being safe for the body. A wide range of both synthetic and natural biomaterials have been extensively studied, each with its unique strengths and limitations. Being aware of the differences between these materials is vital for harnessing their respective benefits and pushing the boundaries of this field (DIMITRIOU *et al,* 2011; Miron *et al,* 2017 and Choukroun *et al,*2006).

Various artificially crafted (alloplastic) materials can be customized to meet spe-cific medical requirements nowadays. These synthetic biomaterials made from metals, ceramics, and polymers can be manufactured reproducibly on a large scale, with tuna-ble physical and chemical properties. Nevertheless, these materials usually lack the in-tricate structure and biological components found in natural materials of biological origin, such as xenografts, allografts, and autografts (DIMITRIOU *et al,* 2011; MIRON *et al,* 2017 and CHOUKROUN *et al,* 2006).

As a result, these materials of natural origin often have some advantages over synthetic biomaterials, such as in-creased biocompatibility, biodegradability, and biological activity.

In this context, the development of autologous blood-derived aggregates, such as Platelet-Rich Fibrin (PRF) or leukocyte- and platelet-rich fibrin (L-PRF), has garnered significant interest in the medical and dental fields for its importance in tissue regeneration (MIRON *et al,* 2017). PRF stands out as a promising choice for natural biomaterial due to its re-markable compatibility with the human body. As a second-generation blood concentrate, PRF has undergone significant advancements since its inception. It has built up-on the foundations of platelet-rich plasma (PRP) from the late 1990s and boasts enhanced attributes that make it valuable in numerous surgical procedures (CHOUKROUN *et al,* 2006; DOHAN, *et al,* 2006c; DOHAN, *et al,* 2006a; WONG, *et al, 2021*). Its concentration of essential cytokines and growth factors facilitates cell growth, migration, proliferation, and differentiation, allowing for smooth integration with native tissues (DIMITRIOU *et al,* 2011; MIRON *et al,* 2017 and CHOUKROUN *et al,* 2006).

Produced through the straightforward centrifugation of a patient's blood without the need for anticoagulants or activating agents, PRF manifests as a dense fibrin ma-trix rich in leukocytes, platelets, and a myriad of proteins pivotal for wound healing. This autologous biomaterial has been hailed for fostering angiogenesis, promoting cell specialization and differentiation, and serving as a supportive scaffold for bone cells, thereby expediting the bone healing and formation process (CHOUKROUN *et al,* 2006). Furthermore, the polymerization of PRF results in a membrane with a favorable physiological structure, offering a robust framework for osteoprogenitor cells to adhere to and facilitating the continuous release of vital growth factors such as Fibroblast Growth Factor (FGF) Vascular Endothelial Growth Factor (VEGF), Transforming Growth Factor (TGF), and Platelet-Derived Growth Factor (PDGF) (BORIE *et al,* 2015; PATEL *et al,* 2017; SHIVASHANKAR *et al,* 2013) (Figure 1). These are important cytokines that regulate various aspects of bone regeneration. While VEGF stimulates angiogenesis and osteogenesis, PDGF promotes chemotaxis and proliferation of mesenchymal stem cells and osteoblasts, FGF enhances osteoblast differentiation and bone matrix formation, and TGF modulates inflammation and immune response. These cytokines act synergistically to enhance bone healing and repair, and their delivery to bone defects can improve the outcome of bone regeneration therapies (CHEN *et al,* 2016; HAN *et al,* 2018; LOURENÇO *et al,* 2018; ZOU *et al,* 2021).

Despite the promising attributes of PRF, the scientific community continues to explore and debate its clinical efficacy compared to other biomaterials or conventional techniques. Particularly, inquiries concerning its direct positive influence on mineralizing cells such as osteoblasts have spurred numerous in vitro studies aimed at unraveling the biological mechanisms and impacts of PRF on mineralized tissues (BORIE *et al,* 2015; PATEL *et al,* 2017; SHIVASHANKAR *et al,* 2013). This scoping review aimed to elucidate the understanding of the biological basis of the applicability of different PRF derivations with potential use in bone therapy, compiling and comparing their effects on events such as proliferation, differentiation, and mineralization capacity of bone cells from evidence provided by controlled in vitro studies.

MATERIALS AND METHODS

Protocol and Registry

This scoping review was conducted based on the Preferred Reporting Items for Systematic Reviews and Meta-Analysis (PRISMA) Statement and its extension for Scoping Reviews (PRISMA-ScR) (MCGOWAN *et al,* 2020). The present research protocol is registered in the Open Science Framework database (https://doi.org/10.17605/OSF.IO/M6PE2).

Information sources and search strategy

The search strategy was developed based on a PICOS framework, where the following aspects were considered: Population: cell lines involved in bone regeneration; Intervention: exposure to second-generation autologous platelet aggregates (PRF); Comparison: cells not exposed to PRF; Outcome: positive effect on parameters related to regeneration (proliferation, differentiation, mineralization); Setting: in vitro assessments.

The search was conducted up to August 2023 in three different electronic databases: PubMed, Web of Science, and Scopus. The search key employed on each database is described in Figure 1. Adaptations were performed to fit the same terms into the different search engines and in combination with specific database filters when available. The entries were sent to Mendeley Desktop (Elsevier) software to eliminate replicas and thus consolidate the list of references for subsequent analysis.

Chart 1. The search key employed in the three consulted Databases.

DATABASE	Search Key
PubMed (https://pubmed.ncbi.nlm.nih.gov/)	(PRF OR “platelet rich fibrin” OR L-PRF OR i-PRF OR “Sticky bone” OR “concentrated growth factors” OR CGF) AND (Bone OR osteoblast* OR MSC OR “mesenchymal stem cell” OR “bone marrow” OR “Bone and bones” [mh] OR “bone cell” OR preosteoblast* OR Skeleton) AND (“in vitro” OR In Vitro Techniques” [mh] OR “Cell Lineage” [mh] OR “Cells, Cultured” [mh).
Web of Science (https://www.webofscience.com/)	((PRF OR “platelet rich fibrin” OR L-PRF OR i-PRF OR “Sticky bone” OR “concentrated growth factors” OR CGF) AND (Bone OR osteoblast OR MSC OR “mesenchymal stem cell” OR “bone marrow” OR “Bone and bones” OR “bone cell” OR preosteoblast OR PDL OR “periodontal ligament OR mineralization) AND (“in vitro” OR “In Vitro Techniques” OR “Cell Lineage” OR “Cells, Cultured”)) Refined by DOCTYPE: (ARTICLE)
Scopus	TITLE-ABS-KEY (prf OR “platelet rich fibrin” OR l-prf OR i-prf OR “Sticky bone” OR “concentrated growth factors” OR cgf) AND TITLE-ABS-KEY (bone

(https://www.scopus.com/search/form.uri?display=basic)	OR osteoblast OR MSC OR “mesenchymal stem cell” OR “bone marrow” OR “Bone and bones” OR “bone cell” OR preosteoblast OR pdl OR “periodontal ligament OR mineralization) AND TITLE-ABS-KEY ((“in vitro” OR “In Vitro Techniques” OR “Cell Lineage” OR “Cell Culture”) AND (LIMIT TO (DOCTYPE, “ar”))

Study selection

The eligibility criteria for the studies included the use of cell lines for bone regeneration, second-generation autologous platelet aggregate (PRF) exposure to cells, and a positive effect on parameters related to regeneration in vitro. Exclusion criteria comprised study designs and publication types that used other autologous materials that did not involve cell exposure or were case reports, exposure limited to non-mineralizing cells, such as fibroblasts and osteoclasts, articles that did not represented complete primary sources of evidence (abstracts, reviews, editorial letters, opinion letters, commentary articles), and in vivo or clinical studies. Subjects related to other research topics, such as meniscus, cartilage, cancer treatments, drug studies, and in vitro delivery, were considered "off-topic." There was no restriction on the publication date or language of publication.

Two reviewers (R.L.B. and E.S.L.) read all the titles and abstracts of the articles retrieved from the search, after performing a piloting and calibrating on data collection with a Cohen Kappa of 0,97 concordance. They analyzed and selected articles according to the eligibility criteria described above, eliminating duplicates. Any disagreement on study eligibility was resolved through discussion and consensus, or a third reviewer (G.G.A) made the final decision.

Critical Appraisal

The selected studies were evaluated by 3 reviewers (R.L.B., N.R.S.R, and G.G.A.), using the ToxRTool (Toxicological Data Reliability Assessment Tool) to assess the quality and reliability of in vitro data at the methodological level (SCHNEIDER *et al,* 2009). This tool includes 18 criteria that describe important aspects for developing reliable articles regarding the methodology applied and how the study was conducted. The checklist includes a description of the methodological aspects of each study, such as substance identification, test system, study design, and documentation of results. Each criterion corresponds to one point, where the article receives one point if it meets the criterion and zero points if it does not. Finally,

the scores are summed, generating a final score. Articles with scores less than 11 are considered unreliable, studies with scores between 11 and 14 are considered reliable with possible restrictions, and studies with scores between 15 and 18 are considered reliable without restrictions.

Data extraction

For data extraction, scientific and technical information were tabulated and analyzed using Microsoft Office Excel 2013. The data extracted included the authors and year of publication, cell type, growth factors detected, the presence of association/modification/addition with the PRF membranes, conditions of exposure of cells to PRF (time, volume), biological parameters evaluated, and main findings for the outcomes. These data were used for a qualitative evaluation and synthesis of evidence.

RESULTS

From the search key developed according to each database, 1157 articles were retrieved, and 429 duplicate records were excluded. Thus, 728 articles were evaluated for eligibility, applying the inclusion and exclusion criteria. Of these, 652 articles were excluded from the review because they did not meet the eligibility criteria (Figure 1). Therefore, 76 articles were evaluated in detail and used in the qualitative analysis of this review.

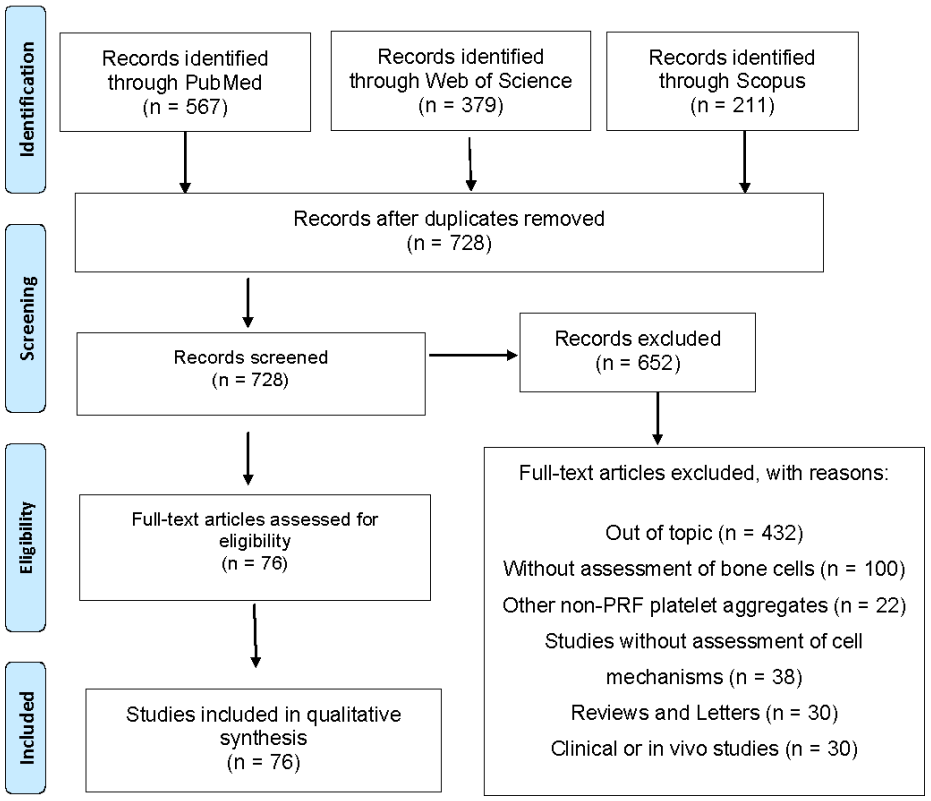

Figure 4. The screening process, selection, and systematic steps according to the PRISMA Statement

The ToxRTool was employed to assess the inherent quality of the selected studies of toxicological data as reported in a publication or a test report, with a reliability categorization performed as shown in Table 1. Among the 76 selected articles, around half (52%) achieved the maximum score (18 points), while further 48% (36 studies) presented only a few reporting limitations, with scores ranging from 15 to 17, rending a total of 100% of studies classified as reliable without restrictions (Table 1).

Table 1 - Critical appraisal of the selected studies, performed according to the ToxRTool (SCHNEIDER *et al,* 2009).

Publication	Group I: test substance identification (4)	Group II: test system characterization (3)	Group III: study design description (6)	Group IV: study Results documentation (3)	Group V: plausibility of study design and data (2)	Total (18)
AL-MAAWI *et al,* 2021	4	3	6	3	2	18
AL-MAAWI *et al,* 2022	4	3	6	3	2	18
BAGIO *et al,* 2021	3	3	6	3	2	17
BANYATWORAKUL *et al,* 2021	4	3	6	3	2	18
BI *et al,* 2020	4	3	6	3	2	18
BLATT *et al,* 2021	4	3	5	3	2	17
CHANG, TSAI & CHANG, 2010	4	2	5	3	2	16
CHEN *et al,* 2015	4	3	6	3	2	18
CHENG *et al,* 2022	4	3	5	3	2	17
CHI *et al,* 2019	4	3	5	3	2	17
CLIPET *et al,* 2012	4	3	6	3	2	18
DOHAN EHRENFEST *et al,* 2010	4	1	5	3	2	15
DOHLE *et al,* 2018	4	3	6	3	2	18
DOUGLAS *et al,* 2012	4	1	5	3	2	15
DUAN *et al,* 2018	4	1	5	3	2	15
EHRENFEST *et al,* 2009	4	1	5	3	2	15
ESMAEILNEJAD *et al,* 2022	4	3	6	3	2	18
FERNANDEZ-MEDINA *et al,* 2019	4	3	6	3	2	18
GASSLING *et al,* 2009	4	1	5	3	2	15
GASSLING *et al,* 2010	4	3	5	3	2	17
GASSLING *et al,* 2013a	4	3	6	3	2	18
GASSLING *et al,* 2013b	4	3	5	3	2	17
GIRIJA & KAVITHA, 2020	2	3	5	2	1	13
HE *et al,* 2009	4	3	5	3	2	17

HONG, CHEN & JIANG, 2018	4	3	6	3	2	18
HUANG *et al,* 2010	4	3	6	3	2	18
IRASTORZA *et al,* 2019	4	3	6	3	2	18
ISOBE *et al,* 2017	4	1	6	3	2	16
JI *et al,* 2015	4	3	6	3	2	18
KANG *et al,* 2011	4	3	6	3	2	18
KARDOS *et al,* 2018	4	2	5	3	2	16
KIM *et al,* 2017a	4	2	5	3	2	16
KIM *et al,* 2017b	4	3	5	3	2	17
KOSMIDIS *et al,* 2023	4	3	6	3	2	18
KOYANAGI *et al,* 2022	4	3	5	3	2	17
KYYAK *et al,* 2020	4	3	6	3	2	18
KYYAK *et al,* 2021	4	3	6	3	2	18
LI *et al,* 2013	4	2	6	3	2	17
LI *et al,* 2014	4	3	6	3	2	18
LI *et al,* 2018a	4	3	6	3	2	18
LI *et al,* 2018b	4	3	6	3	2	18
LIANG *et al,* 2021	3	3	6	3	2	17
LIU *et al,* 2019	4	3	6	3	2	18
LIU *et al,* 2022	4	3	6	3	2	18
LO MONACO *et al,* 2020	4	3	6	3	2	18
MARCHETTI *et al,* 2020	4	3	6	3	2	18
MORADIAN *et al,* 2017	4	2	5	3	2	16
NGUYEN *et al,* 2022	4	3	6	3	2	18
NIE *et al,* 2020	4	3	6	3	2	18
NUGRAHA *et al,* 2018a	4	2	5	3	2	16
NUGRAHA *et al,* 2018b	4	2	5	3	2	16
NUGRAHA *et al,* 2018c	4	2	5	3	2	16
NUGRAHA *et al,* 2019	4	2	5	3	2	16
RASTEGAR *et al,* 2021	4	3	6	3	2	18
SHAH *et al,* 2021	4	2	4	3	2	15
SONG *et al,*2018	4	3	6	3	2	18
STELLER *et al,* 2019a	4	3	6	3	2	18
STELLER *et al,* 2019b	4	3	6	3	2	18
SUI *et al,* 2023	4	3	6	3	2	18
THANASRISUEBWONG *et al,* 2020	4	2	6	3	2	16
VERBOKET et al., 2019	4	2	6	3	2	17
WANG *et al,*2015	4	3	6	3	2	18
WANG *et al,* 2018	4	3	6	3	2	18
WANG *et al,* 2022	4	3	5	3	2	17

WANG *et al,* 2023	4	3	5	3	2	17
WONG *et al,* 2021a	4	3	6	3	2	18
WONG *et al,* 2021b	4	3	6	3	2	18
WOO *et al,* 2016	4	1	5	3	2	15
WU *et al,* 2012	4	3	5	3	2	16
YU *et al,* 2016	4	3	6	3	2	18
YU *et al,* 2023	4	3	6	3	2	18
ZHANG *et al,* 2019	4	3	6	3	2	18
ZHANG *et al,* 2023	4	3	6	3	2	18
ZHAO *et al,* 2013	4	2	5	3	2	16
ZHENG *et al,* 2015	4	1	5	3	2	15
ZHENG *et al,* 2020	4	3	6	3	2	18

Of those, many articles did not specify the amount of medium used for membrane cultivation/extraction of PRF membranes, the number of replicates, or the passage of cells used in the experiments. These factors can influence the interpretation of the biological response, as the time of cultivation and sequential passages can affect the behavior of cells, changing their morphological, functional, and molecular characteristics, which may compromise the quality and reliability of the results obtained with in vitro cultured cells.

Table 2 shows the main data extracted from the selected studies regarding the effects of different protocols of PRF production on bone-related cells. Various studies propose ways to obtain and use PRF to optimize its handling characteristics storage and develop new application possibilities. These include the tube type, time and speed of centrifugation, mode of application, and even association with other materials.

More than half (56%) of the studies investigated the classical L-PRF protocol proposed by Choukrun, which forms a thick clotted yellow, jello-like moldable scaffold. Advanced PRF (A-PRF) is another type of platelet concentrate produced by centrifuging blood at a low speed and for a longer time, which results in a fibrin clot with a rich content of platelets, growth factors, and other bioactive molecules, which was studied in 9 (12%) of the selected studies. Further 9 studies investigated the effects of exposure to Injectable PRF (i-PRF), which is usually prepared by centrifuging blood samples at 1060 rpm for 14 minutes, forming a thinner unclotted liquid that can be injected into various sites where bone grafts have been placed or where infections have occurred. Two other studies assessed the biological properties

of H-PRF, which is produced by horizontal centrifugation. Finally, nine studies (12%) investigated the impact of freezing or lyophilizing L-PRF membranes on the effects of these materials over mineralizing cells. A few of the selected studies (six) compared the biological properties of two or more of these protocols, as will be discussed in the next section of this review.

One of the challenges in studying the effects of PRF on cell behavior is to choose the appropriate method of exposure. About half (51%) of the selected studies employed indirect exposure of cells to eluates, while other 42% (32 studies) cultivated cells in co-culture or directly seeded into the PRF matrices. The difference of direct or indirect in vitro exposure of cells to PRF eluates or co-culture is that the former simulates the initial contact of cells with PRF, while the latter mimics the long-term interaction of cells with PRF. Direct exposure of cells to PRF eluates can assess the cytotoxicity, inflammation, and differentiation potential of PRF, while co-culture of cells with PRF can evaluate the proliferation, migration, and mineralization ability of cells in the presence of PRF.

Table 2. The main biological information of the selected studies

Publication	PRF protocol	Mineralizing Cell type	Exposure time	Exposure method	Biological Parameters	Results
AL-MAAWI *et al,* 2021	A-PRF	Primary Human Osteoblasts	After 3 and 7 days	Eluate	VEGF; TGF-β1; PDGF, OPG, IL-8; OPN; ALP activity.	PRF produced according to the Low-Speed Centrifugation Concept, associated to a polymeric scaffold, had a significant effect on osteogenic markers of osteoblasts.
AL-MAAWI *et al,* 2022	L-PRF and H-PRF	Primary human osteoblasts (pOBs)	24h	Eluate	Cell adhesion.	Osteoblasts exposed to PRF produced with fixed-angle rotors presented higher adhesion than those exposed to PRF produced with variable angle.
BAGIO *et al,* 2021	A-PRF	Human dental pulp stem cells	5, 12, and 24 hours	Eluate	VEGF-A	5% A-PRF extracts increased VEGF-A expression by hDPSCs.
BANYATWORAKUL *et al,* 2021	L-PRF	Canine periodontal ligament cells	1,3 and 7 days	Eluate	Proliferation; migration; in vitro mineralization.	PRF derived from Thai buffalo blood promoted the proliferation, migration and increased mineral deposition in vitro. of canine periodontal ligament cells.
BI *et al,* 2020	L-PRF	Stem cells from the apical papilla (SCAP)	1,3 and 5 days	Eluate	Proliferation; migration; in vitro mineralization; ERK; pERK; ALP; DMP-1	PRF improved the proliferation, migration, and the osteo-/odontogenic differentiation of SCAPs by activating the ERK pathway.
BLATT *et al,* 2021	A-PRF and iPRF	Human Osteoblasts (HOB)	24hs	Co-culture	Cell viability; proliferation; migration; ALP; Col-I; BMP2; Runx-2.	The combination of PRF with bone substitute materials increased the viability, early proliferation and migration potential of human osteoblasts via RUNX2, alkaline phosphatase, collagen, and BMP2.

CHANG, TSAI & CHANG, 2010	L-PRF	Human Osteosarcoma osteoblast-like cells (U2OS)	1, 3, and 5 days	Co-culture	Proliferation; p-ERK, RANKL; OPG	PRF stimulated osteoblast proliferation with positive regulation of the expression of p-ERK, and increased the secretion of OPG.
CHEN *et al,* 2015	L-PRF	Canine dental pulp stem cells (DPSCs)	7, 14 and 21 days	Co-culture	Proliferation; ALP activity; ALP; DSPP; DMP 1; BSP	PRF not only provides a well-organized scaffold for cell adhesion and migration but also induces DPSC proliferation and differentiation markers.
CHENG *et al,* 2022	L-PRF	Rabbit bone marrow mesenchymal stem cells (BMSCs)	Up to 28 days	Co-culture	Mineralization; adipogenic differentiation; aggrecan, Col-II; Sox9; b-catenin; P-GSK3b; CaMKII; PKC.	Co-culture with PRF reversed the activation of Wnt/Ca2+ signaling in BMSCs under hydrostatic pressure, with increased expression of chondrogenic differentiation markers.
CHI *et al,* 2019	Decellularized PRF	Bone marrow stem cells	every 24 h for 9 days	Cultured on PRF	Adhesion; proliferation; Col I; ALP; OPN; OCN; Runx-2.	Decellularized PRF combined with chitosan/gelatin scaffolds accelerate attachment, proliferation, and osteogenesis-related marker expression of bone marrow stem cells.
CLIPET *et al,* 2012	L-PRF	Human Osteosarcoma osteoblast-like cells (Saos-2)	1 and 2 days	Eluate	Cytotoxicity; proliferation; Cell Cycle; cbfa1, Col1, OCN; OPN	Exposure to PRF conditioned medium increased cell viability, proliferation, and expression of the late and early markers of osteogenesis.
DOHAN EHRENFEST *et al,* 2010	L-PRF	Human bone mesenchymal stem cells (BMSC)	7,14, 21 and 28 days	Co-culture	Cytotoxicity; proliferation; ALP activity; mineralization; morphology (SEM)	increased proliferation and differentiation of BMSC when exposed to Choukroun's PRF.

DOHLE *et al,* 2018	iPRF	primary osteoblasts (pOB)	1 and 7 days	Cultured on PRF	VEGF; ICAM-1; ALP	The expression of E-selectin, ICAM-1, VEGF and ALP was significantly higher in co-culture of primary osteoblasts and outgrowth endothelial cells cultured in PRF *in vitro*, in addition to improving the angiogenesis process.
DOUGLAS *et al,* 2012	L-PRF	Human Osteosarcoma osteoblast-like cells (Saos-2)	3, 5 and 7 days	Co-culture	Cytocompatibility; migration.	PRF functionalized with ALP and induced to mineralization was not cytotoxic and promoted colonization by human osteoblasts.
DUAN *et al,* 2018	L-PRF	Rat periodontal ligament stem cells (PDLSCs)	1, 2, 3, 4, 7 and 14 days	Cultured on PRF	Proliferation; BSP; OCN; Runx-2; ALP activity	PRF enhanced cell proliferation and the expression of osteogenic markers in rat PDLSCs.
EHRENFEST *et al,* 2009	L-PRF	Human Maxillofacial osteoblasts	7,14, 21 and 28 days	Co-culture	Proliferation; mineralization; ALP activity	PRF stimulates the proliferation of several very different cell types, and the effects on osteoblastic differentiation are highly significant.
ESMAEILNEJAD *et al,* 2023	A-PRF and L-PRF	Human Osteosarcoma osteoblast-like cells (MG-63)	24 and 72h	Eluate	Proliferation; mineralization.	L-PRF increased proliferation, while A-PRF increased in vitro mineralization of MG-63 cells.
FERNANDEZ-MEDINA *et al,* 2019	A-PRF and I-PRF	Primary Human Osteoblasts	at 24 and 72 h	Eluate	Proliferation; migration; mineralization; cytokine release.	Cell viability and migration assay have demonstrated a detrimental effect when the concentration was ≥60. i-PRF demonstrated superior induction of mineralization. A negative impact of A-PRF was demonstrated at high concentrations.

GASSLING *et al,* 2009	L-PRF	human osteoblasts (HOB) and osteosarcoma (Saos-2)	10 days	Co-culture	PDGF; IGF; TGF-Beta	PRF exposure led to increased secretion of growth factors by osteoblasts.
GASSLING *et al,* 2010	L-PRF	Human periosteal cells	10 min, 1h. 1 day.	Eluate	Cell viability; proliferation.	PRF appears to be superior to collagen (Bio-Gide) as a scaffold for human periosteal cell proliferation.
GASSLING *et al,* 2013a	Mg-enhanced, enzymatically mineralized PRF	Human Osteosarcoma osteoblast-like cells (Saos-2)	1, 3 and 7 days	Co-culture	Cell viability; proliferation; morphology	The enzymatic mineralization of PRF did not affect osteoblast viability and proliferation on the membrane.
GASSLING *et al,* 2013b	L-PRF	Human osteoblasts	1, 5, 7 and 36 days	Eluate	Cell viability; proliferation, ALP activity.	The PRF membrane supports the proliferation of human osteoblast cells, in addition to being an adequate support for the cultivation of human osteoblasts *in vitro*.
GIRIJA & KAVITHA, 2020	PRF (undefined protocol)	Dental pulp cells	2h, overnight	Eluate	IL-6; IL-8; DMP-1, DSPP, STRO-1; mineralization.	The addition of bioactive radiopacifiers into PRF has a synergistic effect on the stimulation of odontoblastic differentiation of HDPCs, hence inducing mineralization.
HE *et al,* 2009	L-PRF	Rat calvaria osteoblasts	1, 7, 14, 21 and 28 days	Exudates	Proliferation; mineralization; ALP activity; cytokine release.	PRF released autologous growth factors gradually, and expressed stronger and more durable effects on proliferation and differentiation of rat osteoblasts than PRP *in vitro*.
HONG, CHEN & JIANG, 2018	freeze-dried L-PRF	Apical papilla (SCAPs)	7 and 14 days	Membrane dissolved in	Proliferation; migration; morphology; differentiation (CD45,	Freeze-dried PRF promotes the proliferation, migration, and differentiation of SCAPs

				10 mL DMEM	CD90, and CD146), mineralization; ALP; BSP; DMP-1; DSPP	
HUANG *et al,* 2010	L-PRF	Dental pulp cells (DPCs)	0, 1, 3, 5 days	Co-culture	Viability; Proliferation; OPG; ALP Activity	PRF stimulates cell proliferation and differentiation of DPCs by up-regulating OPG and ALP expression.
IRASTORZA *et al,* 2019	L-PRF	Pulp stem cells	4 days	Co-culture	Mineralization; ALP activity; ALP; Col-I; Osteonectin; Runx-2, OSX.	Osteoblastic differentiation from human pulp stem cells was achieved with a combination of biomimetic rough titanium surfaces (BASTM) with autologous plasma-derived fibrin-clot membranes.
ISOBE *et al,* 2017	L-PRF from stored (frozen) blood	Human periosteal cells	3 days	Eluate	Proliferation.	The quality of PRF clots prepared from stored whole blood samples is not significantly reduced and induced similar proliferation of periosteal cells as fresh PRF.
JI *et al,* 2015	L-PRF	Periodontal ligament stem cells, bone marrow mesenchymal stem cells	1, 2, 3, 4, 5, 6 and 7 days	Transwell insert	Migration; proliferation; BSP; OCN; OPN; Col-III.	The association of PRF and TDM (treated dentin matrix) induced cell differentiation according to different markers.
KANG *et al,* 2011	L-PRF	Human alveolar bone marrow stem cells (hABMSCs)	0, 0,5, 3, 6, 12hs. 1, 7, 14, 21, 28, and 35 days	Eluate	Proliferation; mineralization; migration; MMP9 activity	PRF increased proliferation, aggregation, activation of MMP9 and mineralization by decreasing migration of the hABMSCs.
KARDOS *et al,* 2018	Fresh, frozen, and	Mesenchymal Stem Cells	1, 7, and 14 days	Co-culture	Viability; proliferation; adhesion.	Preserved PRF membranes presented the same biological properties as fresh samples.

	freeze-dried L-PRF					
KIM *et al,* 2017a	L-PRF	Human Primary Osteoblasts	1, 2, 3, 7 days	co-culture	Proliferation; ALP activity.	PRF presented significantly higher data on DNA quantification, synthesis and proliferation, differentiation, and bone generation of osteoblasts, PDGFs and TGF-b.
KIM *et al,* 2017b	L-PRF	Human dental pulp cells (HDPCs)	1, 2, 3 days	Eluate	Viability; IL-1b; IL-6, and IL-8; VCAM-1, DSP; DMP-1; ALP Activity; Mineralization.	PRF presents odontogenic capacity in inflamed HDPCs.
KOYANAGI *et al,* 2022	Arterial blood-derived PRF (Ar-PRF), venous blood-derived PRF (Ve-PRF).	primary rabbit osteoblasts	At 1, 3, and 5 days	Eluate	Viability; Col-1; OCN; mineralization.	Exposed osteoblasts presented greater differentiation potential, including higher osteocalcin expression and mineralization with no difference between Ar and Ve-PRF.
KOSMIDIS *et al,* 2023	A-PRF, i-PRF, L-PRF	Human Osteosarcoma osteoblast-like cells (U2OS)	Up to 28 days	Eluate	Mineralization; ALP activity; ALP; OCN; ON; ICAM-1; Runx2; Col 1a	The three PRF preparations increased the osteogenic potential of U2OS cells. A-PRF presented the highest effect on mineralization, and i-PRF the highest potential for early cell differentiation.
KYYAK *et al,* 2020	i-PRF	Human Osteoblasts (HOB)	3, 7 and 10 days	Eluate	Viability; migration; proliferation; ALP; BMP-2; OCN.	i-PRF in combination with allogenic biomaterials enhances human osteoblasts activity when compared to xenogenic bone substitute material + i-PRF.

KYYAK *et al,* 2021	i-PRF	Human Osteoblasts (HOB)	3, 7, and 10 day	Eluate	Viability; migration; proliferation; ALP; BMP-2; OCN	The combination of four bovine bone substitute materials with i-PRF improved all cellular parameters, ALP and BMP-2 expression at earlier stages as well as osteonectin expression at later stages.
LI *et al,* 2013	L-PRF	Dental follicle (DF), alveolar bone (AB), periodontal ligament (PDL)	7, 14 and 21 days	Co-culture	Proliferation; migration; mineralization; ALP; MGP; Runx-2.	PRF induced an increase in the early osteoblast transcription factor RUNX2 and a reduction of the mineralization inhibitor MGP.
LI *et al,* 2014	lyophilized PRF	Rat alveolar bone cells	7, 14, and 21 days	Co-culture	Mineralization; proliferation; ALP; Runx-2.	Lyophilized PRF caused greater proliferation and elevation in the Runx2 expression in alveolar bone cells, compared to fresh PRF, and a more than 10-fold rise of ALP and in vitro mineralization.
LI *et al,* 2018a	L-PRF	Human periodontal ligament stem cells (hPDLCs)	21 days	Exudates	Adhesion; Proliferation; mineralization; ALP activity; ALP; OCN; OSX; Runx2.	PRF exudate enhances hPDLC adhesion, proliferation and induces the differentiation of hPDLC into mineralized tissue formation cells.
LI *et al,* 2018b	L-PRF	Human periodontal ligament cells (PDLSCs)	1, 2, 3, 7 and 14 days	Co-culture	Proliferation; Runx-2; MAPK; ERK1/2; pERK1/2; JNK1/2/3; pJNK1/2/3; P38; OSX; OCN; ALP activity.	PRF and IGF-1 can promote the osteogenic differentiation of PDLSCs and enhance their osteogenic mineralization through the regulation of the MAPK pathway.
LIU *et al,* 2022	Lyophilized L-PRF, crosslinked with genipin	Pulp stem cells from human exfoliated deciduous teeth (SHEDs)	Up to 14 days	Eluate	Proliferation; mineralization; Runx2; Col 1; OCN.	Genipin crosslinked L-PRF induced cell proliferation and enhanced the expression of key genes in osteogenesis.

LIANG *et al,* 2021	A-PRFe	Adipose-derived stem cells (ASCs)	7 days	Eluate	Proliferation; mineralization; adipogenesis; ALP, OPN; OCN; Runx-2.	A-PRF stimulated ASC proliferation, adipogenic and osteogenic differentiation on a dose-dependent manner.
LIU *et al,* 2019	Fresh/lyophilized PRF	Bone mesenchymal stem cells (BMSCs)	1-7 days	Eluate	Proliferation; mineralization.	fresh/lyophilized PRF (1:1) increased BMSC proliferation and in vitro mineralization.
LO MONACO *et al,* 2020	L-PRF	Dental pulp stem cells (DPSCs)	24, 48 e 72hs	Eluate	Chondrogenic differentiation; TIMP-1; proliferation.	L-PRF induced differential chondrogenesis on.DPSCs.
MARCHETTI *et al,* 2020	L-PRF	Periodontal ligament fibroblasts	24 h, 72 h and 7 days,	Eluate	Proliferation; viability; morphology.	L-PRF stimulated the onset of the growth of the periodontal ligament fibroblasts.
MORADIAN *et al,* 2017	L-PRF	Bone marrow mesenchymal stem cells (BMMSCs)	1, 5, 7, 9, and 12 days	Cultured on PRF	Proliferation; adhesion.	PRF significantly induced BMMSCs proliferation. Scanning electron microscopy showed that BMMSCs tightly adhered to thefibrin scaffold after seeding.
NGUYEN *et al,* 2022	A-PRF	Human Periodontal ligament stem cells (hPDLSCs)	at 1 h, 6 h, 24 h, 3 days, 5 days, and 7 days	Exudates	Proliferation; migration.	A-PRF in combination with xenogenic bone induced hPDLSC migration or proliferation, depending on the exudate concentration.
NIE *et al,* 2020	lyophilized L-PRF	MC3T3-E1 murine preosteoblasts	1, 3, and 5 days	Eluate	Proliferation; mineralization; OCN; OPN.	Eluates from lyophilized PRF added as a component for electrospinning preparation enhanced the proliferation, mineralization and expression of OCN and OPN of MEC3T3-E1 cells.
NUGRAHA *et al,* 2018a	L-PRF	Rat Gingival Mesenchymal	7, 14, and 21 days	Cultured on PRF	ALP; OC.	PRF induced increased ALP and OCN expression on GMSCs.

		Stem Cells (GMSCs)				
NUGRAHA *et al,* 2018b	L-PRF	Rat Gingival somatic cells (GSCs)	7, 14 and 21 days	Cultured on PRF	BSP-1.	PRF increases and stimulates GSCs BSP-1 expression.
NUGRAHA *et al,* 2018c	L-PRF	Rat Gingival stromal progenitor cells (GSPCs)	7, 14 and 21 days	Cultured on PRF	Cbfa-1; sox9.	GSPCs cultured in PRF possessed potential osteogenic differentiation ability as predicted by the cbfa-1/sox9 expression ratio.
NUGRAHA *et al,* 2019	L-PRF	Rat Gingival Mesenchymal Stem Cells (GMSCs)	7, 14 and 21 days	Cultured on PRF	Aggrecan.	Platelets Rich Fibrin increases aggrecan expression of GMSCs during osteogenic differentiation.
RASTEGAR *et al,* 2021	L-PRF	Human Osteosarcoma osteoblast-like cells (MG-63)	3 days	Co-culture	ALP activity; mineralization.	PRF loaded into PCL/chitosan core-shell fibers promoted in vitro mineralization and increased ALP activity.
SHAH *et al,* 2021	i-PRF	Human Osteosarcoma osteoblast-like cells (MG-63)	1, 7, 14, and 21 days	Co-culture	Proliferation; ALP activity; mineralization.	Coating of titanium discs with i-PRF causes increased proliferation, alkaline phosphatase production, and mineralization at day 1, 7, 14, and 21.
SONG *et al,* 2018	L-PRF	Rabbit Bone marrow-derived mesenchymal stem cells (BMSCs)	7 days	Eluate	Adhesion; proliferation; ALP; Col-1; OPN; Runx-2	Printed scaffolds of BCP/PVA associated to PRF promoted the adhesion, proliferation, and differentiation of BMSCs.

STELLER *et al,* 2019a	L-PRF	Human osteoblasts (HOB)	72h	Eluate	Proliferation; migration; viability.	The use of PRF improves the behavior of osteoblasts treated with zoledronic acid.
STELLER *et al,* 2019b	PRF	Human Primary Osteoblasts	24s	Eluate	Adhesion; viability; morphology.	Zoledronic acid decreased osteoblast adhesion on implant surfaces. PRF increased primary adhesion of zoledronic acid-treated osteoblasts on implant surfaces in vitro.
SUI *et al,* 2023	3D printed L-PRF composite scaffolds	MC3T3-E1 murine preosteoblasts	1 to 3 days	Cultured on PRF composite scaffold	Proliferation.	The proliferation of preosteoblasts into the scaffolds increased with the release of GFs, indicating that L-PRF remains bioactive after 3D printing.
THANASRISUE BWONG *et al,* 2020	Subfractioned (red and yellow) i-PRF	Periodontal ligament stem cells	0, 3, and 5 days	Eluate	Proliferation; Migration; Mineralization; ALP activity.	The factors released from the red i-PRF had a greater effect on cell proliferation and cell migration, while yellow i-PRF stimulated earlier osteogenic differentiation of periodontal ligament stem cells.
VERBOKET *et al,* 2019	High (208g) and Low (60g) RCF PRF	Bone marrow mononuclear cells (BMCs)	2, 7, 14 days	Eluate	Viability; Apoptosis; VEGFA; ICAM3; MMP2; MMP7; MMP9; TGF-β1; BCL2; BAX; ALP; COL-1; FGF2; SPP1.	PRF produced with low RCF significantly increased mediator contents and stimulatory effects on BMC with regard to gene expression of MMPs and metabolic activity/viability.
WANG *et al,* 2015	L-PRF	Rabbit Mesenchymal stem cells (MSCs)	1, 2, 3, 4, 5, 6, 7, 8, 14 days	Eluate	Proliferation; ALP; BMP2; OCN; OPN; Col-1.	PRF significantly stimulated MSC proliferation and osteogenesis in vitro.
WANG *et al,* 2018	i-PRF	Human Primary Osteoblasts	1, 3, 5, 7, 14 days	Co-culture	Proliferation; migration; adhesion; mineralization; ALP	i-PRF was able to influence osteoblast behavior, including migration, proliferation, and differentiation, at higher levels than PRP.

					activity; ALP; Col-1; OC.	
WANG *et al,* 2022	i-PRF	Human bone marrow stem cell (hBMSCs)	1 to 7 days	Eluate	Proliferation; survival; migration; mineralization; Col 1; OCN; OPN; Runx2; ERK 1/2; p-ERK.	i-PRF improved proliferation and migration of hBMSCs, with increased expression of osteogenic markers, mineralization, and activation of the ERK pathway.
WANG *et al,* 2022b	L-PRF	Rabbit mesenchymal stem cells from the Schneiderian membrane (SM-MSCs)	1 to 14 days	Eluate	Proliferation; migration; mineralization; ALP activity; ALP; Col 1; Runx2; ERK 1/2; p-ERK.	PRF stimulated proliferation, migration and osteogenic differentiation of SM-MSCs, with up-regulation of the ERK 1/2 signaling pathway.
WONG *et al,* 2021a	Large-pore PRF (LPPRF)	MC3T3-E1 preosteoblasts	6 days	Eluate	Proliferation; migration; mineralization.	large-pore LPPRF combined with a Mg ring increased preoteoblast proliferation, migration and in vitro calcium deposition.
WONG *et al,* 2021b	L-PRF	Rabbit primary osteoblasts	3 and 6 days	Eluate	Viability; ALP activity; Col-1; OPN; ALP.	L-PRF positively affected primary osteoblast behavior, and induced bone formation when associated to TCP.
WOO *et al,* 2016	L-PRF	Human dental pulp cells (HDPCs)	12hs. 1, 2 and 7 days	Eluate	Viability; ALP activity; DSP; DMP1; BMP 2/4; pSmad1/5/8	A combination of MTA and PRF synergistically stimulated odontoblastic differentiation of HDPCs by the modulation of the BMP/Smad pathway.
WU *et al,* 2012	L-PRF	Human Osteosarcoma osteoblast-like cells (U2OS)	2hs. 1, 3 and 5 days	Co-culture	Adhesion; proliferation p-Akt; HSP47; LOX.	PRF increased cell attachment and proliferation by the Akt pathway, and matrix synthesis via HSP47 and LOX accumulation.

YU *et al,* 2016	L-PRF	Canine deciduous and permanent dental pulp cells (DPCs)	1, 4, 7, and 11 days	Co-culture	Cytotoxicity; proliferation; ALP activity; mineralization; Col-1; OCN; OPN; Runx2, ALP	PRF stimulated the proliferation and differentiation of both deciduous and permanent DPCs, with deciduous pulp cells more responsive to the effects of PRF.
YU *et al,* 2023	H-PRF	Human osteoblasts (hFOBs)	3 days	Transwell insert	Migration	Culture medium from H-PRF bone blocks markedly promoted the migration of osteoblasts.
ZHANG *et al,* 2019	L-PRF	dental pulp stem cells (DPSCs)	1, 3, 5 and 7 days	Eluate	Migration; morphology; ALP activity; mineralization (SEM); OPN; Col-1; ALP.	Multifunctional triple-layered scaffolds combined with PRF significantly increased ALP activity and expression of differentiation markers on DPSCs.
ZHANG *et al,* 2023	i-PRF	Human dental pulp stem cells (hDPSCs)	Up to 21 days	Eluate	Proliferation; Mineralization; ALP activity; Runx2; DSPP; DMP1; BSP; Notch 1; Jagged 1; Hes 1.	I-PRF induce a dose dependent increase on proliferation of hDPSCs, and expression of osteo-/odontoblastic differentiation markers, as well as key proteins in the Notch signaling.
ZHAO *et al,* 2013	L-PRF	Periodontal ligament stem cells (PDLSCs)	7, 14, 21 days	Co-culture	Proliferation; mineralization (SEM); ALP activity; BSP; OCN; Col-I; and CP23	PRF induced proliferation in PDLSCs, while suppressing osteoblastic differentiation of PDLSCs by decreasing ALP activity and the gene expression of BSP and OCN while up-regulating the mRNA expression levels of Col-I and CP23 during the testing period. T.
ZHENG *et al,* 2015	Lyophilized PRF	Human Osteosarcoma osteoblast-like cells (MG63)	1, 3 and 5 days	Co-culture	Viability; adhesion; proliferation.	A combination of hydrogel and a nanostructured scaffold loaded with PRF improved the adhesion and proliferation of MG63 cells when compared to controls.

ZHENG *et al,* 2020	i-PRF	Human periodontal ligament cells (hPDLCs)	1, 3 and 5 days	Eluate	Migration; proliferation; ALP activity; mineralization; Runx2; Col-1; OCN; IL-1β, TNF-α and p65 (in the presence of LPS)	Liquid PRF promoted hPDLÇ proliferation and differentiation, and attenuated the inflammatory state induced by LPS.

The name of a protein indicates the assessment of its expression. L-PRF: Fibrin Rich in Platelets and Leukocytes produced by Choukrun´s protocol; i-PRF: liquid, injectable PRF; A-PRF: advanced PRF, produced with intermediary centrifugation forces; H-PRF: produced through horizontal centrifugation. RCF: Relative centrifugal force; ALP: Alkaline Phosphatase; OPN: Osteopontin; OPG: Osteoprotegerin; DMP-1: Dentin matrix protein 1; DSPP: Dentin Sialophosphoprotein; DSP: Dentin Sialoprotein; SPP: Sialophosphoprotein; BSP: Bone Sialoprotein; OCN: Osteocalcin; Col-1: Collagen type I; OSX: Osterix; MMP: Matrix Metalloproteinase; VCAM-1: Vascular cell adhesion molecule 1; BMP-2: Bone Morphogenetic Protein 2; MGP: Matrix Gla protein; LOX: Lysyl oxidase; LPS: Lipopolysaccharide; P-GSK3b: phosphorylated glycogen synthase kinase-3-beta.

Regarding the cell types employed in the studies, several different models were identified, from diverse mineralizing tissues of both human and animal origin. More than half of the studies (n=44, 58%) employed human cells, while the other half investigated cells from animal sources (42%), including cells from rabbits, canine and murine models. None of the selected studies performed a comparison between human or animal cells, in order to provide direct evidence of different responses to PRF between these origins. All studies that performed assessments of cell viability and proliferation after exposure of either human or animal cells to PRF presented similar descriptive results, even though with incomparable size effects, as the methodological settings were very heterogeneous (data not shown). Furthermore, very similar regulatory pathways are reported as activated by exposure to PRF, including the Cbfa-1/runx2, MAPK and Wnt signaling pathways, regardless of the human or animal origin of cells, as will be further described and discussed in the next section of this review. Nevertheless, it is important to notice that data resulting from human cells are usually considered more relevant and representative of human physiology and pathology than animal cells, which may have different molecular and cellular mechanisms, responses, and interactions. Furthermore, their obtention may reduce ethical and practical issues associated with the use of animals for research, such as animal welfare, availability, cost, and regulatory approval.

Several of the selected studies utilized primary cells, such as osteoblasts, dental pulp stem cells (hDPSCs), periodontal ligament cells (cPDLs), and bone marrow stem cells (BMSCs) (Table 2). Primary cells are isolated directly from living tissues or organs and offer several advantages over immortalized cell lines. They retain the physiological functions of their tissue of origin, such as gene expression, metabolism, and responsiveness to stimuli. They provide a more realistic model system, making them more suitable for studying complex biological processes. However, immortalized cell lines, which have been modified to proliferate indefinitely in culture, offer some benefits over primary cells. They are more homogeneous and consistent, easier to maintain and manipulate, and more readily available and cost-effective. Some of the selected studies utilized immortalized cell lines, including the well-established preosteoblasts from rat calvaria MC3T3-E1 and the human osteosarcoma cell lines SaOS2, MG-63, and U2OS (Table 2).

The majority of the selected articles investigated cells in monoculture. A single exception is the study by DOHLE *et al,* 2018, which employed a co-culture of outgrowth endothelial cells (OECs) and primary osteoblasts (pOBs), exposed together to injectable PRF. The authors presented evidence that i-PRF may have a positive effect on wound healing processes and angiogenic activation of endothelial cells, as the expression of E-selectin, ICAM-1, VEGF, and ALP were significantly higher in the exposed cells. OECs are a subpopulation of endothelial progenitor cells (EPCs) that have high proliferative and angiogenic potential, which have been already shown to interact with osteoblasts in a positive manner, enhancing osteogenic differentiation and increased mineralization. Additionally, osteoblasts secrete IL-8 which enhances their migration, survival, and expression of angiogenic factors and matrix metalloproteinases (FUCHS *et al,* 2010)**.** In this context, identifying that PRF may enhance these interactions may provide an interesting tool for bone tissue engineering.

Five studies investigated more than one cell type with the same methodology, even though not in co-culture, providing data that allow to identify some cell type-specific differences on the response to PRF preparations. The study by DOHAN EHRENFEST *et al,* 2010 was one of the first identified assessing different responses to L-PRF, by exposing gingival fibroblasts, dermal prekeratinocytes, preadipocytes, and maxillofacial osteoblasts. The results showed that PRF continually stimulates proliferation in all studied cell types, but this stimulation was stronger and dose-dependent in osteoblasts, while it was observed only at day 14 with fibroblasts. Adipocytes and prekeratinocytes also differed by presenting increased metabolic activity (as detected by mitochondrial activity), probably related to different regulations of metabolism in these cells. CLIPET *et al,* 2012 also compared human osteoblasts (SaOS2), fibroblasts (MRC5), and epithelial (KB) cell lines. Similar to the findings of Dohan et al., while PRF increased the proliferation of all cell types, the effects were more evident in osteoblasts at shorter experimental times. GASSLING *et al,* 2009, also compared the exposure of human osteoblasts, human fibroblasts, as well as human osteoblast-derived osteosarcoma cells (Saos-2) to PRF, assessing its effects not on proliferation but on the induction of the release of growth factors by these cells. While growth factors could be detected in all of the samples, fibroblasts secreted lower levels of PDGF-AB, PDGF-BB, IGF-I, and TGF-ß1 than osteoblasts,

especially those derived from osteossarcoma, suggesting increased paracrine activation by PRF in transformed cells. A similar pattern was also observed in the study by KARDOS *et al,* 2018, where mesenchymal stem cells presented higher rates of proliferation when exposed to fresh or lyophilized PRF samples, as compared to gingival fibroblasts. However, a recent study by AL-MAAWI *et al,* 2022, comparing different centrifugation protocols for PRF production, including L-PRF and H-PRF, reported relatively higher effects on the viability, proliferation, and adhesion of primary human dermal fibroblasts, when compared to osteoblasts. The very different methodologies employed impair the comparisons of these studies, but it is possible that the size of the effects of PRF on fibroblasts may be rather influenced by their tissue of origin, as fibroblasts from different anatomical sites may have distinct phenotypic and functional characteristics.

In the selected studies, different biological markers were observed that point to the molecular effects of PRF in cell differentiation and mineralization events (Table 1), depending on the cell type, including expression and secretion of alkaline phosphatase, sialoproteins and sialophosphoproteins, type 1 collagen, osteocalcin, ostepontin, bone morphogenetic protein-2 (BMP-2), and the regulation of the transcription factors Osterix and Runx2, that will be further discussed below.

Table 3 shows that a considerable proportion of the selected studies (n=19, 25%) investigated the association of PRF with other compounds or materials, in order to produce bioactive composites for different applications, which is a trend in the development of advanced, smart materials. These associations, which will be further discussed, include polymers (polycaprolactone meshes, chitosan/gelatin, polyvinyl alcohol/sodium alginate composites, PEG/PLGA copolymers), cements (MTA), calcium phosphates (nHA radiopacifiers, BCP, TCP) and allogenic or xenogeneic materials, including dentin chips and bovine bone substitutes. The myriad of methodologies and proposals impair the comparison of the relative performance of these materials between studies, and only a few of them included intra-study comparisons. Most of the studies indicated that the associations contribute to achieve the specific expected outcome, with increased cell response to the PRF-containing composites, either by increased attachment, proliferation, or differentiation. As an exception, the study by KYYAK *et al,* 2020, presented comparative evidence that the association of i-PRF with a xenogenic bone

substitute material (XBSM) is less bioactive, promoting lower osteoblastic activity than Allogenic bone substitute material (ABSM) associated to i-PRF. Nevertheless, further studies by KYYAK *et al,* 2021 indicated that sintering XBSM samples under high temperature could increase osteoblast viability and metabolic activity. Furthermore, NGUYEN *et al,* 2022 described that XBSM associated to other PRF type (A-PRF) enhanced human ligament stem cells proliferation and migration, even without sintering.

Table 3. The main data extracted from the studies with PRF associated to other materials and/or compounds.

References	Associated Material	Relevance	Results
AL-MAAWI *et al,* 2021	OsteoporeTM (OP), a commercially available PCL mesh	Combination of differently centrifuged PRF matrices with a polymeric resorbable scaffold to influence its biological properties on bone regeneration.	The presented results suggest that PRF produced according to the Low-speed centrifugation concept exhibits autologous blood cells and growth factors and seems to have a significant effect on osteogenesis, showing promising results to support bone regeneration.
CHI *et al,* 2019	Chitosan/gelatin (C/G)	Test whether decellularized PRF (DPRF) maintains its bioactive effects to improve chitosan/gelatin(C/G) base scaffolds, which display appropriate biocompatibility and mechanical properties, but lack biological activity to promote soft and hard tissue repair.	C/G/DPRF scaffolds accelerated attachment, proliferation, and osteogenesis-related marker expression of bone marrow stem cells. *In vivo*, C/G/DPRF scaffolds led to enhanced bone healing and defect closure in a rat calvarial defect model. Thus, it was concluded that DPRF remains bioactive and the prepared C/G/DPRF scaffold is a promising material for bone regeneration.
DOUGLAS *et al,* 2012; GASSLING *et al,* 2013	Calcium glycerophosphate (CaGP), ALP	Induce mineralization of PRF membranes, to achieve mechanical reinforcement of the gel and stability as a barrier membrane in guided bone regeneration.	The mineralization was confirmed, and WST test results showed that cell proliferation was inferior on PRF after addition of ALP, confirming its properties as a barrier.
GIRIJA AND KAVITHA, 2020	Bioactive radiopacifiers – nanohydroxyapatite (nHA) and dentin chips (DC)	Combine bioactive radiopacifiers – nanohydroxyapatite (nHA) and dentin chips (DC) to PRF, aiming to produce a traceable material for endodontic procedures, while still inducing adequate biological responses.	The results suggest that the addition of bioactive radiopacifiers into PRF has a synergistic effect on the stimulation of odontoblastic differentiation of HDPCs, hence inducing mineralization.
JI B *et al,* 2015	Treated dentin matrix (TDM)	Associate endogenous stem cells, PRF and TDM in the local microenvironment to contribute with the regeneration of periodontal tissues around the tooth root.	The study confirmed the roles of PRF as a bioactive agent with TDM as inductive scaffold for cells of the tooth socket microenvironment, involved in endogenous tooth root regeneration.

KYYAK *et al,* 2020	Allogenic (ABSM) and xenogenic bone substitute material (XBSM)	The comparison of an allogenic and xenogenic bone substitutes with i-PRF for the production of the more bioactive composite material for bone treatment.	i-PRF in combination with ABSM enhances HOB activity when compared to XBSM-i-PRF or untreated BSM in vitro. Therefore, addition of i-PRF to ABSM and – to a lower extent – to XBSM may influence osteoblast activity in vivo in an interesting way for bone therapy.
KYYAK *et al,* 2021	Cerabone R (CB), Bio-Oss R (BO), Creos Xenogain R (CX) and MinerOSS R X (MO)	Four bovine bone substitute materials (XBSM) were associated to i-PRF aiming to increase their osteoinductive properties.	XBSM sintered under high temperature showed increased HOB viability and metabolic activity through the whole period when compared to XBSM manufactured at lower temperatures. Overall, the combination of XBSM with i-PRF improved all cellular parameters, related to osteogenesis.
NGUYEN *et al,* 2022	Xenogenic bone substitute material (XBSM)	Advanced platelet-rich fibrin (A-PRF) and xenogenic bone substitute material (XBSM) were associated aiming to increase periodontal tissue regeneration.	The-PRF-XBSM mixture continuously released growth factors over 7 days and enhanced human ligament stem cells proliferation and migration.
NIE *et al,* 2020	Polyvinyl alcohol/sodium alginate	Addition of lyophilized PRF as a component for electrospinning preparations to increase the proliferation and osteogenesis of osteogenic precursor cells for bioengineering purposes.	The resulting material presented adequate physicochemical properties, and was able to increase osteogenic markers on bone cells.
RASTEGAR *et al,* 2021	PCL/chitosan	Platelet-rich fibrin (PRF)-loaded PCL/chitosan (PCL/CS-PRF) core-shell nanofibrous scaffold was made through a coaxial electrospinning method. The goal was to evaluate the effect of CS-RPF in the core layer of the nanofibrous on the osteogenic differentiation of human mesenchymal stem cells (HMSCs).	The formation of Ca-P on the surface of scaffold immersed in simulated body fluid solution indicated the suitable osteoconductivity of PCL/CS-PRF core-shell nanofibrous scaffold. Due to higher hydrophilicity and porosity of PCL/CS-PRF core-shell nanofibrous scaffold compared to PCL/CS scaffold, a better bone cell growth on the surface of PCL/CS-PRF scaffold was observed.
SONG *et al,* 2018	Nano - biphasic calcium phosphate (BCP), polyvinyl alcohol (PVA)	The low-temperature 3D printing of BCP/ PVA/PRF scaffolds would preserve the biological activity of	The biological activity of PRF was retained during the 3D printing process, and the presence of PRF in the biocompatible microenvironment of the scaffold provided cell binding sites and

		PRF and provide an innovative biomaterial for restoring segmental bone defects.	promoted the adhesion, proliferation, and differentiation of BMSCs.
STELLER *et al,* 2019a; 2019b	Zoledronic acid	Investigation of the effects or bone cells treated with bisphosphonates, as a potential mitigator of osteonecrosis associated with treatments with these drugs.	The negative effects of ZA on osteoblast survival and behavior (proliferation, morphology, adhesion to implant surface) was especially reduced when using PRF, indicating that the autologous material may have positive effects in the therapy of Bisphosphonate-Related Osteonecrosis of the Jaw.
SUI *et al,* 2023	Chitosan (CS)–hydroxyapatite (HAP) scaffolds	Study aiming to identify if 3D printing of a CS-HAP-PRF would compromise the biological properties of the platelet aggregate.	Based on the presented experimental results, it is possible to infer that the 2.5% P-C-H scaffold exhibits a remarkable biological activity. and, therefore, it is not negatively affected by 3D printing.
WOO *et al,* 2016	Mineral trioxide aggregate (MTA)	Combined PRF as a bioactive matrix and MTA as a root filling material beneficial for the endodontic management of an open apex.	The combination of MTA and PRF was proven as an odontogenic inducer in human dental pulp cells (HDPCs) in vitro.
WONG *et al,* 2021b	Magnesium Rings	The freeze drying enlarges the pores of PRF to engineer large-pore PRF (LPPRF), a type of PRF that has expanded pores for cell migration. Biodegradable Mg rings were used to provide stability to these pores, and release Mg ions during degradation, with potential to enhance osteoconduction and osteoinduction.	The results revealed that cell migration was more extensive when LPPRF was used rather than PRF. Moreover, the Mg ions released from the Mg rings significantly enhanced the calcium deposition by preosteoblasts, evidencing in vitro osteoinduction.
WONG *et al,* 2021	Tricalcium phosphate (TCP)	The development of a composite biomaterial combining the osteoconductive TCP incorporated with bioactive PRF for bio-synergistic bone regeneration.	The *in vitro* results showed that PRF plus TCP had excellent biosafety and was favorable for increasing osteoblast activity related to bone repair.

ZHANG *et al,* 2019	Polycaprolactone, chitosan and hydroxyapatite	Polycaprolactone/gelatin (PG) nanofiber films by electrospinning chitosan / poly (γ-glutamic acid) / hydroxyapatite (CPH) hydrogels were formed by electrostatic interaction and lyophilization, to exert osteoconduction; and platelet-rich fibrin (PRF) was added to promote bone induction through the release of growth factors.	This study provided evidence that the composite biomaterial positively affects dental pulp stem cells, with great potential for endodontics, but also in wider applications such as calvarial repair and oral alveolar bone regeneration.
ZHENG *et al,* 2015	Copolymer poly-polyethylene glycol (PEG)-PLGA (PLGA-PEG-PLGA)	A combination PRF with PLGA and nano-hydroxyapatite (nHA/PLGA) might produce a scaffold with high porosity, controlled pore size to better mimic natural bone; and improved osteogenic ability.	The resulting scaffold provided a good substrate for osteoblast proliferation, with sustained-release growth factors, producing a promising therapeutic agent for local applications in bone tissue engineering.

2. Discussion

Protocols for PRF production and preservation

As indicated in Table 2, apart from the classical Choukrun´s L-PRF, other production protocols were also identified in the selected studies. These platelet concentrates differ not only in their preparation methods, but also mechanical properties, degradation rates and growth factor release profiles, resulting in possible differences in the response of mineralizing cells after exposure. In this regard, a few studies compared such differences, with interesting findings that will be discussed below.

The study by MARCHETTI *et al,* 2020 compared L-PRF with two other autologous biomaterials: concentrated Growth Factors (CGF) and autologous platelet gel (APG). The authors reported stronger stimulation of the proliferation of human periodontal ligament fibroblasts (HPLF) by CGF, compared to L-PRF, and correlated these effects with the different secretion profiles of growth factors by these materials.

VERBOKET *et al,* 2019 used the Low-Speed Centrifugation Concept, reducing the centrifugal force in the production of L-PRF to produce a membrane with a higher concentration of cells and growth factors. The study compared the protocols of PRF medium-RCF (1300 RPM for 8 minutes) and PRF low-RCF (700 RPM for 3 minutes). Although there was significant heterogeneity between the protocols to produce platelet aggregates and experimental design, the positive effects observed on proliferation, differentiation, and mineralization were rather similar between the protocols.

FERNANDEZ-MEDINA *et al,* 2019 compared the biological activity of A-PRF and i-PRF, along with two PRP protocols. After 21 days, i-PRF induced superior mineralization by human primary osteoblasts, as compared to the other materials, while A-PRF presented a negative impact at high concentrations, related to increased cytotoxicity. Despite its low content in growth factors, the author concluded that i-PRF was the best candidate for bone tissue engineering applications, probably related to the prolonged release of BMP-2 by this material. ESMAEILNEJAD *et al,* 2023 also investigated the effects of A-PRF, this time compared to classic L-PRF, on the cellular activity of MG-63 osteosarcoma-derived osteoblasts. Their findings indicate that L-PRF induced

higher proliferation than A-PRF, while the latter was only capable of inducing *in vitro* mineralization at the employed experimental conditions, suggesting positive but very different effects of these materials. The study by KOSMIDIS *et al,* 2023, on the other hand, investigated the effects of A-PRF, L-PRF, and i-PRF on the osteogenesis of the human osteoblast-like U2OS cell line. Similar to the findings by ESMAEILNEJAD *et al,* 2023, A-PRF induced more mineralization and calcium production. The i-PRF induced more ALP activity, suggesting it has the potential to enhance early cell differentiation.

LOURENÇO *et al,* 2018 suggested using swing-out rotors instead of fixed-angle centrifugation to produce a product similar to L-PRF. According to some authors, the process known as H-PRF (platelet-rich fibrin produced through horizontal centrifugation), allows for a greater number of live cells and growth factors to be distributed more evenly in the final product. AL-MAAWI *et al,* 2022 compared the effects of PRF products produced by fixed-angle and horizontal centrifugation over osteoblast behavior, identifying very similar effects on proliferation and viability, with increased cell adhesion in the fixed-angle group. These results indicate that very similar materials may be produced with different centrifuge types, as long as the g-force is standardized.

The study by LI Q *et al,* 2014 included physical modifications in the PRF protocol to increase shelf-life, such as freeze-drying membranes. Their results indicated that proliferation and migration of periodontal progenitors were increased with exposure to lyophilized PRF, compared to fresh PRF, probably due to increased porosity and release of growth factors from the processed membranes. KARDOS *et al,* 2018 also analyzed PRF membranes in different presentations (fresh, frozen, and freeze-dried), compared different centrifugation protocols (1700 RCF in 5 min and 8 min) and the use of modified tubes (single-syringe closed system - hypACT Inject Auto). Living cells were observed only in fresh PRF membranes, while freezing induced, as expected, the disruption of leukocytes embedded in the PRF membrane. However, MSCs were reported as proliferating even faster over freeze-thawed PRF than over fresh samples, suggesting the adequacy of such procedure.

LIU *et al,* 2019 proposed the combination of fresh and lyophilized PRF at different ratios, tailored for different delivery rates of GFs in tissue healing. Their findings indicate a significant increase in proliferation and differentiation of BMSCs

exposed to eluates of different combinations, with the best results achieved with the fresh/lyophilized PRF ratio of 1:1. A subsequent study by the same group (LIU, X *et al,* 2022*)* proposed the use of a natural crosslinker agent, genipin, derived from gardenia flowers, to increase the stability and controlled release of growth factors by lyophilized PRF. Genipin-modified lyophilized PRF presented better biomechanical properties, slower biodegradation, and sustained release of growth factors, promoting the proliferation of pulp stem cells from human exfoliated deciduous teeth (SHEDs).

ISOBE *et al,* 2017 added the anticoagulant formulation acid citrate dextrose solution-A (ACD-A) in blood samples, with the objective of enabling its storage for later production of PRF, with its coagulation obtained by the addition of $CaCl_2$ (showing similarities with the protocol of PRP production), without significant reduction of its bioactivity. This method tends to improve the flexibility of successful PRF preparations and the quality of membranes prepared from whole blood samples stored until 2 days.

Association of PRF and other materials/compounds

Several of the selected studies investigated the association of PRF with other agents, including biomaterials, scaffolds, bioactive compounds, and ions, as described in Table 3. IRASTORZA *et al,* 2019 investigated the use of L-PRF as a biomimetic coat of titanium implant surfaces, aiming for improved osteointegration. When combined with hDPSCs (human dental pulp stem cells), the material induced both proliferation and osteogenic differentiation of stem cells. The study by STELLER *et al,* 2019 also assessed the use of PRF coating over titanium implants, this time to reverse the negative effects of a bisphosphonate (zoledronic acid) over osteoblast attachment to the implant surfaces. Indeed, zoledronic acid led to a decrease of osteoblast adherence onto the implant surface, but it was reversed by previous coating with L-PRF, suggesting that PRF may contribute to bone apposition in dental patients undergoing bisphosphonate treatment. Furthermore, L-PRF acted directly on the viability, migration, and proliferation of osteoblasts and fibroblasts treated with zoledronic acid (STELLER *et al,* 2019).

SONG *et al,* 2018 explored the effectiveness of 3D-printed Biphasic Calcium Phosphate/PVA scaffolds combined with PRF using a straightforward low-temperature method. These scaffolds demonstrated impressive biological

activity and biocompatibility in vitro. When implanted into critical bone defects in a rabbit's radius, the inclusion of PRF encouraged proper bone regeneration and repair by providing osteoconductive and osteoinductive stimuli (SONG *et al,* 2018). Similarly, SUI *et al,* 2023 proposed the production of 3D-printed L-PRF scaffolds composed by chitosan (CS)–hydroxyapatite (HAP) associated to lyophilized PRF. MC3T3-E1 murine preosteoblasts presented increased proliferation over the composite scaffold after association with PRF. The proliferation of preosteoblasts into the scaffolds increased with the release of GFs, indicating that L-PRF remains bioactive even after 3D printing. ZHANG *et al,* 2019 fabricated a complex, multifunctional triple-layered composite scaffolds including polycaprolactone/gelatin (PG) nanofiber films made by electrospinning, chitosan/poly (γ-glutamic acid)/hydroxyapatite (CPH) hydrogels, and platelet-rich fibrin (PRF). The resulting scaffold presented induced the proliferation of both fibroblasts and bone mesenchymal stem cells (BMSCs), also inducing osteogenic differentiation of the latter. Other calcium phosphates, such as tricalcium phosphate (TCP) also presented interesting outcomes after association with PRF, as reported by WONG *et al,* 2023, where the composite presented a controlled release of bioactive factors, with the increase in osteoblast attachment, cell proliferation, migration, and ECM formation.

Dentin, known for its bone-inducing properties, fuses and is gradually replaced by bone when grafted into it. This is likely due to its osteoinductive properties, biocompatibility, and BMP content (NIU *et al,* 2017). In a study by JI *et al,* 2015, after seven days of coculture with PRF and treated dentin matrix, BMSCs exhibited increased expression of BSP and OPN mRNA, while PDLSCs showed higher expression of BSP, OPN, and OCN. MAHENDRAN *et al,* 2019 combined PRF with dentin chips and nanohydroxyapatite to enhance radiopacity, creating a biocompatible structure that promoted cell proliferation as a mitogen. GIRIJA & KAVITHA 2020 compared the combination of PRF with 50 wt% of radiopacifier nanohydroxyapatite (nHA), or with 50 wt% dentin chips and their effects on odontoblastic differentiation. While both materials increased the expression of dentin sialophosphoprotein (DSP) and dentin matrix protein-1 (DMP-1), two important extracellular matrix proteins involved in the differentiation and mineralization of human dental pulp cells (HDPCs), exposure to PRF + 50 wt% nHA induced more mineralization nodules in these cells.

ZHENG et al. 2013 found that when developing a combination of PRF with a poly-polyethylene glycol (PEG)-PLGA copolymer, the hydrogel was evenly distributed on the inner surface of the PRF scaffolds. The hydrogel did not impact the inherently high porosity of the PRF scaffolds. A system containing nHA/PLGA/Gel/PRF allowed for slow and sustained release of PRF-derived growth factors, leading to increased adhesion and proliferation of MG63 human osteoblasts.

HDPCs treated with mineral trioxide aggregate (MTA) and PRF extracts exhibited significantly increased expression of dentin sialoprotein and dentin matrix protein-1, along with enhanced ALP activity and mineralization compared to MTA or PRF treatment alone. The MTA and PRF extracts together activated bone morphogenic proteins (BMP), while the BMP inhibitor LDN193189 diminished dentin sialophosphoprotein and dentin matrix protein-1 expression, ALP activity, and mineralization enhanced by MTA and PRF treatment (WOO *et al,* 2016).

In the study by BLATT *et al,* 2021, four different bone substitute materials (allogeneic, alloplastic, and two of xenogeneic origin) were associated with a combination of A-PRF and i-PRF. The addition of PRF increased cell proliferation and migration for all bone substitutes, but only the allogeneic and alloplastic materials significantly increased RUNX2 expression in human osteoblasts. On the other hand, bone morphogenic protein was expressed significantly higher when xenogeneic material was combined with PRF, suggesting that the biofunctionalization of bone substitutes with PRF might improve their performance, even for materials of different origins.

Cell-type related effects of PRF

PRF possesses significant proliferative potential due to its fibrin structure, which contains live leukocytes and activated platelets. This promotes the continuous release of growth factors such as FGF, PDGF, TGF-beta1, and VEGF. These factors act through specific signaling pathways, including MAPK and PI3K/Akt, which modulate gene expression and osteoblast proliferation and survival (CHEN *et al,* 2012).

Gingival stromal progenitor cells (GSPCs) are a population of mesenchymal stem cells derived from the gingival connective tissue that have been shown to possess multipotent differentiation capacity, including osteogenic, adipogenic, and

chondrogenic lineages. The study by NUGRAHA *et al,* 2018 investigated the effects of PRF on the osteogenic differentiation of GSPCs, identifying a role of Cbfa1/Sox9 expression ratio in this process, as it positively correlated with the osteogenic markers and mineralization of GSPCs. Later, another study by this group (NUGRAHA *et al,* 2019) showed that PRF also increased the expression of aggrecan, a chondrogenic differentiation marker that has a significant role in the early stage of osteogenic differentiation of gingival stem cells, which may contribute to accelerating the bone remodeling, with increased expression of alkaline phosphatase and osteocalcin (NUGRAHA *et al,* 2018; NUGRAHA *et al,* 2018).

Bone marrow stem cells (BMSCs) are multipotent progenitor cells with regenerative potential for various tissues, including bone (POLYMERI *et al,* 2016. In the selected studies, these cells exhibited increased proliferation when combined with PRF, irrespective of direct or indirect exposure (HAN *et al,* 2018; EHRENFEST *et al,* 2010; DOUGLAS *et al,* 2012; GASSLING *et al,* 2013; KARDOS *et al,* 2018; LIU *et al,* 2022). These results not only provide evidence for the potential clinical success of PRF but also lay the foundation for its further use in bone tissue engineering. Although BMSCs are widely used in cell therapy, one of the main challenges is ensuring their efficient migration and homing to target tissues following systemic or local administration. The proliferative effects of PRF on BMSCs, combined with its other properties such as biocompatibility, biodegradability, mechanical strength, porosity, and potential for vascularization (CANCEILL *et al,* 2023), could help overcome the limitations of conventional injection-based delivery of BMSC single-cell suspensions and enhance their retention and engraftment in injured tissues. The results by CHENG *et al,* 2022 with the exposure of BMSCs to L-PRF also provided some insights on its effects when combined to environmental factors, such as exposure to hydrostatic pressure, a mechanical stimulus that plays an important role in bone formation. In this sense, the co-culture of BMSCs with L-PRF reversed the activation of Wnt/Ca2+ signaling in BMSCs under hydrostatic pressure, with increased expression of chondrogenic differentiation markers, suggesting a modulation of the differentiation pathways by the released growth factors from PRF.

Human adipose stem cells (hASCs) are a type of mesenchymal stem cells (MSCs) that can be isolated from adipose tissue and have the potential to

differentiate into various cell types, including osteoblasts. This complex process involves multiple factors such as growth factors, signaling pathways, transcription factors, and epigenetic modifications (ZANETTI *et al,* 2013). hASCs are attractive for regenerative medicine applications because they are autologous, abundant, and easily accessible. However, various factors like age, disease, and culture conditions can influence the proliferation and differentiation capacities of hASCs. Consequently, enhancing hASC proliferation is crucial for their clinical use. Human ASCs exhibited increased proliferation when exposed to different concentrations of PRF eluates (LI *et al,* 2013). Platelet-derived growth factor (PDGF-BB), one of the main growth factors secreted by PRF, has been shown to be a potent mitogen for hASCs (LAI *et al,* 2018). It induces multiple signaling pathways such as ERK1/2, PI3K/Akt, and JNK, which regulate various cellular processes, including cell cycle progression through the expression of cyclins D1 and E. Previous studies have demonstrated that hASC proliferation may be blocked by inhibitors of PDGF receptor tyrosine kinase, ERK1/2, Akt, but not by a p38 inhibitor. These results suggest that the proliferation of hASCs through platelet concentrates like PRF may be mediated by PDGF-BB-induced activation of ERK1/2, PI3K/Akt, and JNK signaling pathways.

Apical papilla stem cells (SCAPs) are mesenchymal stem cells found at the root tip of developing teeth. They play a crucial role in root formation and dentin-pulp complex regeneration. SCAPs secrete various bioactive factors that can modulate their microenvironment and influence tissue repair and regeneration (ZHANG *et al,* 2019), including some involved in forming bone-like tissue. The present search revealed that SCAPs exhibited increased proliferation when exposed to PRF eluates (CHANG *et al,* 2010; GASSLING *et al,* 2013). These findings are promising for developing stem cell-based bone therapies combining PRF and SCAPs, with the feasibility of transplantation in treating bone defects already demonstrated in animal models.

Another type of mesenchymal stem cells investigated in association with PRF are those residing in the periodontal ligament, a connective tissue that anchors the tooth to the alveolar bone. Periodontal ligament stem cells (PDLSCs) have demonstrated osteogenic potential, meaning they can differentiate into osteoblasts and produce bone matrix, playing a vital role in periodontal tissue regeneration and bone repair (LEI *et al,* 2022). These cells exhibited proliferation

when co-cultured with PRF (NUGRAHA *et al,* 2018; WANG *et al,* 2022) or after exposure to eluates (RASTEGAR *et al,* 2021; WANG *et al,* 2022). These effects may contribute to the reported success in improving the regenerative potential and healing of PDL tissues presented by PRF in cases of late dental replantation or intraosseous defects.

Dental pulp stem cells (DPSCs) are also mesenchymal stem cells present in the dental pulp tissue of human teeth, which have the potential to differentiate into osteoblasts, odontoblasts, adipocytes, and neural cells. DPSCs have been shown to promote wound healing, bone regeneration, nerve regeneration, and pulp regeneration in animal models and clinical trials. DPSCs offer a promising source of autologous stem cells that can be used for tissue engineering and cell therapy of dental and oral diseases. In this sense, several selected studies assessed the exposure or association of DPSCs with PRF. HUANG *et al,* 2010 showed that L-PRF increases the proliferation and differentiation of human DPSCs (GASSLING *et al,* 2013). The study by BAGIO *et al,* 2021 evidenced that A-PRF induces an increase in the expression of VEGF-A by these cells, an important factor in the angiogenesis process in dental pulp regeneration. More recently, ZHANG *et al,* 2023 have shown that i-PRF eluates induce a dose-dependent increase in the proliferation of hDPSCs, and expression of osteo-/odontoblastic differentiation markers, as well as key proteins in the Notch signaling. This is a key pathway that regulates the fate and function of DPSCs, modulating the balance between self-renewal and differentiation, along with their angiogenic properties for tissue regeneration and repair. LO MONACO *et al,* 2020 exploited these effects by proposing the association of DPSCs with L-PRF for the treatment of osteoarthritis, as these cells can undergo chondrogenic differentiation and secrete growth factors associated with tissue repair. Indeed, the association with PRF promoted in vitro chondrogenesis and stimulated the survival of articular chondrocytes.

Osteoblasts are bone-forming cells that secrete extracellular matrix proteins supporting bone tissue formation and mineralization. These cells are derived from various progenitor populations, such as mesenchymal stromal/stem cells (MSCs), with their differentiation influenced by molecular mechanisms including signaling pathways, transcription factors, and epigenetic events[11]. Osteoblasts produce and respond to the main growth factors stimulating bone formation, typically released by PRF and its derivatives. The present search found evidence that

primary human osteoblasts and murine MC3T3-E1 preosteoblasts exhibit strong proliferative responses to PRF (HAN, *et al,* 2018; BLATT *et al,* 2021; ESMAEILNEJAD *et al,* 2023; GASSLING *et al,* 2009; IRASTORZA *et al,* 2019; JI *et al,* 2015; KIM *et al,* 2017; KIM *et al,* 2017; THANASRISUEBWONG *et al,* 2020; WANG *et al,* 2022). However, it is important to note that human osteosarcoma cell lines SaOS, MG63, and U2OS also showed consistent proliferative behavior after exposure to PRF (AL-MAAWI *et al,* 2021; CHANG *et al,* 2010; CLIPET *et al,* 2012; DOHLE *et al,* 2018; LI *et al, 2014;* LIU *et al,* 2022; LO MONACO *et al, 2020;* SONG *et al,* 2018; VERBOKET *et al, 2019;* WOO *et al,* 2016). This finding warrants further assessment and should be considered by clinicians for its potential risk of stimulating cancer cell growth and dissemination by creating a favorable niche for tumor development.

Due to the good cell response to PRF, some authors proposed the use of this material as a scaffold for bone cell therapy. It includes the proposal by GASSLING *et al,* 2009 and GASSLING *et al,* 2013 the use of PRF for periosteal tissue engineering, reporting an increased proliferation of periosteal cells (GASSLING *et al,* 2009) and human osteoblasts (GASSLING *et al,* 2013) over PRF, as compared to collagen scaffolds (Bio-Gides). As expected, PRF also promoted increased expression of osteogenic markers in osteoblasts, as compared to commercial collagen scaffolds.

In summary, the in vitro evidence from the selected studies highlights a robust effect on the proliferation of different cell types as an essential aspect of the clinical potential of PRF in treating bone and other mineralized tissues.

Molecular effects of PRF on differentiation and mineralization

Bone regeneration is a complex process involving the interaction of cells, growth factors, and extracellular matrix. Clinical studies have described PRF as effective in oral and maxillofacial bone regeneration, increasing the amount of bone formation following procedures such as sinus floor elevation (CHO *et al,* 2020). The molecular effects of PRF on the differentiation and mineralization of bone cells may involve various intracellular signaling pathways, as evidenced by the selected studies in this review and summarized in Figure 3.

Figure 5. Main biological events involved in the response of mineralizing cells to PRF, according to the literature evidence. Several growth factors and important mediators are released in the medium by PRF (1), many of which are able to activate mitogen-induced signaling pathways (2), known to modulate the expression of transcription factors, such as RunX2 and Osterix, directly involved on bone cell differentiation (3). These transcription factors are responsible for the altered expression and secretion of different proteins responsible for the formation of the mineralized matrix and the control of osteoclastogenesis (4). Furthermore, the exposure to PRF may induce increased secretion of growth factors, such as BMP-2, VEGF or IGF (5), indicating that exposed cells may also be activated by paracrine regulation in response to PRF. All of these processes result in increased nodule formation and, therefore, biological mineralization (6).

The mitogen-activated protein kinase (MAPK) pathway is a cell signaling route that regulates numerous biological processes, including cell differentiation. Among the MAPKs, ERK1/2 plays a crucial role in osteoblast differentiation by regulating the expression of osteogenesis-related genes (ZHENG *et al,* 2020). The phosphorylation of ERK was increased by exposure to PRF in the osteosarcoma-derived osteoblast cell line U2OS (CHANG *et al,* 2010; CHANG *et al,* 2011). Consequently, the expression of osteoprotegerin (OPG) was upregulated by PRF, while the expression of the receptor activator of NFkB ligand (RANKL) was not significantly altered. These results suggest that PRF could inhibit osteolytic activity by modulating osteoclastogenesis through the control of the OPG/RANKL ratio in osteoblasts (CHANG *et al,* 2010; CHANG *et al,* 2011).

The Runt-related transcription factor 2 (Runx2) is a key transcription factor that regulates the expression of genes involved in osteoblast differentiation and function. Research has demonstrated that various members of the MAPK family, including ERK1/2 and p38, can phosphorylate Runx2 at specific serine residues, enhancing its transcriptional activity and promoting osteogenic gene expression (JO *et al,* 2018). As a result, ERK1/2 and Runx2 are connected by a positive feedback loop that stimulates osteoblast differentiation and bone formation. In selected studies, a significant increase in the expression and/or phosphorylation of Runx2 was detected after exposure to platelet-rich fibrin (PRF) in different cell types (DOUGLAS *et al,* 2012; KOYANAGI *et al,* 2022; KYYAK *et al,* 2020; KYYAK *et al,* 2021; NUGRAHA *et al,* 2018; STELLER *et al,* 2019; ZHANG *et al,* 2019). The studies by WANG *et al,* 2022 and WANG *et al,* 2023) confirmed, with both human bone marrow and rabbit mesenchymal stem cells, that exposure to PRF preparations increases proliferation, expression of osteogenic markers, and in vitro mineralization concomitant to the up-regulation of the ERK 1/2 signaling pathway.

Additional evidence of these regulatory pathways comes from investigations of Osterix (Osx), a zinc-finger transcription factor essential for osteoblast differentiation and bone formation in bone homeostasis (LIU *et al,* 2020). Osx is a downstream target of Runx2 and regulates several target genes involved in osteoblast differentiation, such as Col5a1, Col5a3, and connexin43 (Cx43). Osx is controlled by multiple signaling pathways, including BMP, Wnt, FGF, and ERK1/2, which modulate its transcriptional activity and stability (NIU *et al,* 2017). Data from a study by LI *et al,* 2018 suggest that osterix levels significantly increase in periodontal ligament stem cells treated with PRF and IGF-1 at 14 days compared to the control group ($P < 0.01$). Furthermore, by the third day of exposure, the expression of genes controlled by Osx was upregulated in the PRF-exposed group. These findings imply that these transcription factors contribute to the stimulation of osteoblast differentiation by PRF, potentially through the activation of MAPKs in response to growth factors released by this autologous biomaterial.

The overexpression of Osx and Runx2 after exposure to PRF could potentially impact several essential proteins for osteoblast maturation and mineralization, whose expression is regulated by these factors, including collagen type-I a1 (Col1a1), osteonectin, osteopontin, bone sialoprotein, and osteocalcin. Osteocalcin is responsible for fixing calcium and hydroxyapatite in the extracellular matrix, contributing to the effective mineralization that occurs in bone tissue (CHEN *et al,* 2012). Molecular analyses through real-time PCR have shown a significant increase in RNA expression for osteocalcin in various mineralizing cells exposed to PRF (CHI *et al,* 2019; IRASTORZA *et al,* 2019; MORADIAN *et al,* 2017; NUGRAHA *et al,* 2018; STELLER *et al,* 2019; WANG *et al,* 2018). These findings were reinforced by a functional assessment through western blot, indicating increased levels of this protein in periodontal ligament stem cells, associated with increased bone formation in a rat in vivo model (DOUGLAS *et al,* 2012).

Different studies have reported that PRF also induces increased expression of dentin sialoprotein (DSP) and dentin sialophosphoprotein (DSPP) (CHEN *et al,* 2015; VERBOKET *et al,* 2019), which is enhanced in the presence of lipopolysaccharide (KARDOS *et al,* 2018). The results by HONG *et al,* 2018 suggest that this effect is dependent on the duration of exposure, as the expression level of DSPP was downregulated after incubation in PRF for seven

days and then significantly increased after 14 days of incubation. Bone sialoprotein (BSP) is also reported to increase when cells are exposed to PRF, primarily around 14 to 21 days (CHEN *et al,* 2015; DOUGLAS *et al,* 2012; GIRIJA, K. and KAVITHA, 2020; IRASTORZA *et al,* 2019; MORADIAN *et al,* 2017). Only human periodontal ligament stem cells had DSPP downregulated when co-cultured with PRF over extended experimental periods (WANG *et al,* 2023). These results are important since this non-collagenous protein plays a crucial role in the biomineralization of hard tissues such as bone and teeth, inducing the formation and growth of hydroxyapatite crystals in the extracellular matrix (LIU *et al,* 2021).

Osteopontin is another phosphorylated glycoprotein secreted into the mineralizing extracellular matrix by osteoblasts during bone development. Although osteopontin is an osteogenic marker that does not affect the cellular development of osteoblasts in vitro, it impacts the mineralization of bone tissue (WANG *et al,* 2019)**.** Various studies have shown that this osteogenic marker is present and highly expressed after exposure to PRF in osteoblasts (BANYATWORAKUL *et al,* 2021), dental pulp cells (WANG *et al,* 2018), and mesenchymal stem cells (MSCs) (STELLER *et al,* 2019). Real-time PCR revealed that bone marrow-derived mesenchymal stem cells (BMSCs) cultured on printed BCP/PVA/PRF scaffolds expressed significantly higher levels of osteopontin on days 7 and 14 compared to those cultured on other scaffolds ($P < 0.05$) (NUGRAHA *et al,* 2018). VERBOKET *et al,* 2019 observed higher expression in bone marrow cells exposed to medium and low RCF PRF, indicating that these protocols did not affect the expected effects of the material on the expression of matrix proteins.

The increase in collagen gene expression induced by PRF was reported in several studies (CLIPET *et al,* 2012; NUGRAHA *et al,* 2019; SUI *et al,* 2023; WANG *et al,* 2015; WANG *et al,* 2018), typically around the 14th to the 21st day of exposure. ZHAO *et al,* 2013 still observed slight upregulation by PRF in a dose-dependent manner after 14 or 21 days of culture ($P < 0.01$). In contrast, JI B *et al,* 2015 and VERBOKET *et al,* 2019 did not observe a significant difference in the expression of Col-III, the primary type of collagen in bone, between the control group and the test group.

ICAM-1 (intercellular adhesion molecule 1) is a protein that mediates cell-cell interactions and plays a role in inflammation and immune responses. ICAM-1 is expressed by various cell types, including osteoblasts, in which it may have different effects depending on the context (ZANETTI *et al,* 2013). In healthy individuals, ICAM-1 may facilitate osteoblast contact with lymphocytes, enhancing mineralization and bone formation through the downregulation of TGF-β1 (transforming growth factor beta 1), a negative regulator of osteogenesis. In pathological conditions such as osteoarthritis and osteoporosis, ICAM-1 expression by osteoblasts may be increased by proinflammatory cytokines and contribute to bone resorption and loss of bone mass. ICAM-1-positive osteoblasts can adhere to osteoclast precursors and stimulate their differentiation and activation through the osteoclastogenic factor RANKL (TANAKA *et al,* 2005). Moreover, ICAM-1-positive osteoblasts may have impaired proliferation and differentiation potential due to cell cycle arrest (LEI *et al,* 2022). When exposed to both regular and low-speed PRF, KANG *et al,* 2011 and VERBOKET *et al,* 2019, respectively, observed high expression of ICAM-1 in mesenchymal stem cells, including in the presence of lipopolysaccharide to simulate inflammation. On the other hand, DOHLE *et al,* 2018 reported that PRF appears to have no effect on the expression of the ICAM-1 protein by exposed primary human osteoblasts. This is an important finding since PRF is described as releasing considerable amounts of proinflammatory cytokines (LOURENÇO *et al,* 2018; LOURENÇO *et al,* 2021).

Alkaline phosphatase (ALP) is located on the outer surface of the cell membrane of osteoblasts. ALP is an early marker of osteoblast differentiation that indicates the transition of osteoprogenitor stem cells to immature pre-osteoblasts (JO *et al,* 2018). It plays an essential role in osteoid formation and mineralization and is recognized as a nonspecific marker of bone formation and osteoblast activity. ALP also regulates RUNX2, a master transcription factor in osteoblasts, through a positive feedback loop that modulates osteoblast differentiation. The present review identified several different studies assessing the effects of exposure to PRF on the expression of ALP, with increased levels evidenced from 14 to 21 days of culture (CHENG *et al,* 2022; CHI *et al,* 2019; DOHLE *et al,* 2018; GIRIJA, K. AND KAVITHA, M. 2020; KYYAK *et al,* 2020; LI *et al,* 2018; NGUYEN *et al,* 2022; WOO *et al,* 2016; YU *et al,* 2016). The study by WOO *et al,* 2016 observed that the effects of PRF associated with MTA on ALP and in vitro

mineralization of human dental pulp cells were impaired by pretreatment with a BMP inhibitor (LDN193189), indicating the participation of specific growth factors in the effects of PRF on ALP.

Osteoblast and bone cell activity are regulated by various growth factors, many of which are released by platelet-rich fibrin (PRF) membranes. Examples of these growth factors include transforming growth factor-beta (TGF-beta) and fibroblast growth factors (FGF). Osteoblasts themselves can produce and release growth factors that regulate the differentiation and activity of other bone cells, such as osteoclasts and osteocytes. These factors include RANKL/OPG, M-CSF, VEGF, PDGF, and BMP (HAN *et al,* 2018). These growth factors can act in paracrine or endocrine manners, influencing bone and systemic metabolism by promoting or inhibiting the differentiation and function of various bone cells. When exposed to PRF, osteoblasts engage in a complex cellular communication system involving both the exposure and secretion of growth factors that impact bone tissue, as evidenced by selected studies.

TGF-beta, a member of the TGF-beta superfamily of cytokines, regulates numerous cellular processes such as proliferation, differentiation, migration, and apoptosis. TGF-beta plays a significant role in bone formation and remodeling by influencing the balance between bone-forming cells (osteoblasts) and bone-resorbing cells (osteoclasts) (JANN *et al,* 2020). TGF-beta stimulates osteoblastic differentiation and activity by activating canonical and non-canonical signaling pathways and increasing the expression of osteogenic genes like Runx2, Osterix, and Collagen I in osteoblasts. Conversely, TGF-beta inhibits osteoclastogenesis and osteoclastic activity by modulating the interaction between osteoblasts and osteoclasts through OPG/RANKL, BMPs, and Wnt proteins, thereby affecting both aspects of the bone remodeling cycle.

Studies have shown that osteoblasts exposed to PRF demonstrate increased production of TGF-beta1. For instance, Saos-2 osteosarcoma-derived osteoblasts exposed to PRF exhibited significantly higher TGF-beta1 production (WANG *et al,* 2019). Rat calvaria osteoblasts exposed to PRF showed a time-dependent increase in TGF-beta1 production [48]. Human alveolar bone marrow stem cells treated with PRF extracts exhibited increased TGF-beta1 levels at 24 hours (KANG *et al,* 2011). A study by KIM *et al,* 2017 compared the release of TGF-beta1 associated with PRF in osteoblast cultures exposed to PRF

membranes produced by different protocols. The results indicated that the secreted levels of the growth factor were significantly higher in low-RCF PRF than in medium-RCF PRF ($p < 0.05$) (THANASRISUEBWONG *et al,* 2020). However, lyophilized PRF samples only slightly increased the release rate of TGF-beta1 in another osteosarcoma cell line, MG63 (YU *et al,* 2016).

Bone morphogenetic protein 2 (BMP-2) is a multifunctional protein belonging to the TGF-beta superfamily. It plays a crucial role in bone formation by stimulating the differentiation of mesenchymal stem cells (MSCs) into osteoblasts. Osteoblasts and osteocytes constitutively secrete BMP-2, which has been used as a therapy for bone fractures and diseases such as osteoporosis due to its osteogenic potential (ZOU *et al,* 2021). Rabbit mesenchymal stem cells exposed to PRF demonstrated a significant upregulation of BMP-2 mRNA expression, reaching levels that stimulate in vitro osteogenic differentiation (CANCEILL *et al,* 2023). Combining 1 mg/mL MTA with 1.25% PRF extracts increased BMP-2 expression in human dental pulp cells compared to PRF extracts alone, while MTA treatment alone showed no release (WOO *et al,* 2016). BMP-2 expression was also higher in co-cultures of i-PRF and primary osteoblasts (DOHLE *et al,* 2018).

Saos-2 cells exposed to PRF exhibited noticeably higher peaks of insulin-like growth factor-1 (IGF-1), especially compared to fibroblast cultures (WANG *et al,* 2019). Human alveolar bone marrow stem cells exposed to PRF extracts showed high expression of IGF-1 (LOURENÇO *et al,* 2021), similar to MG63 osteosarcoma cells and primary osteoblasts (NUGRAHA *et al,* 2018; THANASRISUEBWONG *et al,* 2020). These findings are significant since IGF-1 plays a crucial role in regulating osteoblast function and development (JANN *et al,* 2020). IGF-1 initiates a complex signaling pathway involving the PI3-K/PDK-1/Akt and Ras/Raf/MAPK pathways, which stimulate cell function and/or survival. IGF-1 also influences osteoclastogenesis by regulating RANKL and RANK expression.

The available data suggest that most of PRF's effects on bone and mineralizing cells may be attributed to the release of specific biological mediators that activate signaling pathways related to cell proliferation, survival, and differentiation. Investigating the release of growth factors, cytokines, and chemokines by PRF membranes could help understand these effects. However, only a few selected studies have detected such release in their in vitro assessments. ZHAO Y-H *et al,* 2013 observed a time-dependent decrease in

VEGF, IGF-1, and EGF release from PRF membranes within five days. In contrast, DOHLE *et al,* 2018 found the highest concentration of VEGF in osteoblast supernatants mixed with PRF and cultured for seven days, confirmed by relative gene expression of VEGF after 24 hours of osteoblast monocultures. ISOBE *et al,* 2017 observed that PDGF-BB concentration was significantly reduced in extracts from PRF membranes made from stored blood compared to fresh samples, indicating a potential drawback of long storage. ZHENG *et al,* 2015 observed a sustained release of PDGF, IGF-I, and TGF-B1 for up to four weeks when combining nHA/PLGA/GeI with lyophilized PRF, which positively affected MG63 cell mineralization. Studies evaluating platelet-derived growth factor (PDGF AA, AB, or BB) reported variations in the day of the highest in vitro release (CLIPET *et al,* 2012; GASSLING *et al,* 2013; IRASTORZA *et al,* 2019), ranging from the 1st to the 14th days of exposure. This suggests that the choice of extraction time may impact the observed effects of PRF treatment.

3. FINAL CONSIDERATIONS

Due to the considerable relevance of the theme for regenerative medicine and dentistry, several narrative and systematic reviews have been published issuing the clinical and biological effects of PRF. Many of these reviews are focused on the level of evidence supporting the use of PRF in regenerative dentistry and oral and maxillofacial surgery by assessing Randomized Clinical Trials (MIRON *et al,* 2017), including data indicating that PRF significantly improves bone tissue regeneration (GHANAATI *et al,* 2018), regardless of recent reviews on preclinical studies that failed to identify such effects on animal models (REIS *et al,* 2022). Despite any clinical controversies, only a few literature reviews visited the molecular and cellular evidence of PRF effects and are usually restricted to smaller groups of in vitro studies focusing on specific protocols, such as i-PRF (FARSHIDFAR *et al,* 2022). An exception is the interesting review by STRAUSS *et al,* 2020 assessed *in vitro* evidence of the biological effects of PRF in cells from different tissues, published up to 2018. However, unlike the present review, that study was not focused on bone and mineralized tissues and had a limited reach, as it was based on data retrieved from a single database (Medline). Therefore, more than an update on the literature, the present scoping review represents the most comprehensive mapping of the available evidence supporting the molecular mechanisms that set the basis of the PRF effects in the behavior of cells of bone and mineralized tissue.

While this approach provided valuable insights, it also introduced some limitations. By focusing exclusively on PRF, we ensured the feasibility and comparability of the review but may have overlooked data on other similar platelet aggregates or protocols, such as Concentrate of Growth Factors (CGF). Additionally, the scope of this review may be limited by the interpretation or reporting of the data, as some studies may have omitted important information necessary for a comprehensive understanding of the results. Nevertheless, it is possible to state, through the raised data, that the literature consistently provides in vitro evidence that PRF, produced by different protocols or in combination with other biomaterials, influences the proliferation, differentiation, and mineralization of cells from bone and mineralized tissue. These effects involve well-known pathways of cell survival, the activation of transcription factors (Runx2, OSX), and

increased expression of various proteins, including osteopontin, osteocalcin, collagen, ALP, BSPs, RANKL/OPG, and growth factors like TGF-beta, PDGF, and BMP2. Different studies have associated these effects with specific growth factors released by PRF, suggesting that this is an important factor to consider in the development and improvement of these autologous biomaterials for the treatment of mineralized tissue such as bone.

PRF is widely used in regenerative medicine and dentistry, and in vitro models represent only a small aspect of wound healing and bone regeneration. As such, it is not possible to guarantee that the reported results can be directly extrapolated to clinical settings. On the other hand, improved in vitro proliferation, differentiation and mineralization of osteoblasts may represent interesting evidence in support of enhanced regenerative activity, osteoinductive properties or enhanced osseointegration. Therefore, by gathering and analyzing information related to PRF and mineralizing cells, we can gain a better understanding of the mechanisms behind PRF's impact on bone regeneration and optimize its properties and applications. This includes determining optimal concentrations, exploring associations with other bone graft materials or drugs, and developing new production protocols to improve clinical outcomes of this promising autologous material.

MANUSCRITO II

The association of nanostructured carbonated hydroxyapatite with denatured albumin and platetet-rich fibrin: impacts on growth factor release and osteoblast behavior

ABSTRACT

Platelet Rich Fibrin (PRF), a second-generation blood concentrate, offers a versatile structure for bone regeneration due to its composition of fibrin, growth factors, and cytokines, with adaptations like denatured albumin-enriched PRF (Alb-PRF), showing potential for enhanced stability and growth factor dynamics. Researchers have also explored the combination of PRF with other biomaterials aiming to create a three-dimensional framework for enhanced cell recruitment, proliferation, and differentiation in bone repair studies. This study aimed to evaluate a combination of Alb-PRF with nanostructured carbonated hydroxyapatite microspheres (Alb-ncHA-PRF), and how this association affects the release capacity of growth factors and immunomodulatory molecules, and its impact on the behavior of MG63 human osteoblast-like cells. Alb-PRF membranes were prepared and associated to nanocarboapatite (ncHA) microspheres during polymerization. MG63 cells were exposed to eluates of both membranes to assess cell viability, proliferation, mineralization, and alkaline phosphatase (ALP) activity. The ultrastructural analysis has shown that the spheres were shattered, and fragments were incorporated into both the fibrin mesh and the albumin gel of Alb-PRF. Alb-ncHA-PRF presented reduced release of growth factors and cytokines, when compared to Alb-PRF ($p<0.05$). Alb-ncHA-PRF was able to stimulate osteoblast proliferation and ALP activity at lower levels than those observed by Alb-PRF, and was unable to positively affect in vitro mineralization by MG63 cells. These findings indicate that the addition of ncHA spheres reduces the biological activity of Alb-PRF, impairing its expected effects on osteoblast behavior.

Keywords: Platelet-rich Fibrin; albumin gel; osteoblasts; sticky-bone; biomaterials.

INTRODUCTION

In recent decades, several materials and techniques have been developed with the aim of optimizing the bone regeneration process. Blood-based materials have become the target of studies and improvements, giving rise to a range of different blood concentrates, featuring a three-dimensional constitution based on fibrin and regenerative potential. The first blood concentrate to gain prominence in the literature was Platelet Rich Plasma (PRP) (Use of platelet-rich fibrin in regenerative dentistry: a systematic review), obtained from the sequence of centrifuges and addition of chemical substances, such as sodium citrate. It is presented as a concentrate of platelets and growth factors higher than normal levels, which trigger cascades with different functions in the tissue regeneration environment, such as proliferation, migration, cell differentiation and angiogenesis. essential in tissue regeneration (Pietrzak et al 2005, Dohan et al 2006a, Conde Montero et al 2013).

The second generation of blood concentrates is established by Platelet Rich Fibrin (PRF), obtained through a single centrifugation of a blood aliquot and free from the addition of any substance (Dohan et al 2006a). Its structure is made up of fibrin, large concentrations of growth factors and cytokines. The benefits of using PRF for bone regeneration include the formation of a very versatile structure that provides a framework for the population of cells recruited to the site of its implantation, in addition to being a continuous reservoir of growth factors, such as growth factor platelet derivative (PDGF) and vascular endothelial growth factor (VEGF); activated platelets and cytokines that favor the tissue regeneration process (Choukroun et al. 2006; Mourão et al 2018; Lourenço et al 2019; Thanasrisuebwong et al 2020). Miscellaneous adaptations to the protocol for obtaining the PRF were described at literature with the aim of optimizing the composition biochemistry and stability of the PRF membrane (Dohan et al, 2018; Lourenço et al 2020). Such changes were made in the parameters of speed, time, angulation of the centrifuge rotor and three-dimensional structure, as presented in the membrane enriched with denatured albumin (Alb -PRF). In relation to Alb -PRF, the processing by denaturation of a portion of the blood centrifuge and its subsequent inclusion in the fibrin mesh causes relevant three-dimensional

changes, increasing its degradation time *in vivo* (In vivo evaluation of the biocompatibility and biodegradation of a new denatured plasma membrane combined with liquid PRF (Alb -PRF) and modifying the cellular distribution and release dynamics of growth factors and cytokines (Barros Mourão et al 2018).

In addition to production protocol adaptations, combinations of other biomaterials, such as bone and calcium phosphate, to blood concentrates were proposed in several studies, including the concept of the Sticky bone (Mourão et al., 2015; Gheno et al 2022). Mourão and collaborators combined the properties of platelet concentrates with carbonatoapatite (cHA) microspheres in a randomized clinical study (Mourão et al, 2017). This is a biomaterial with suitable properties to be used as a scaffold for cell migration and colonization, and feature the replacement of hydroxyl groups by carbonate, which contributes to the establishment of a highly resorbable three-dimensional structure, allowing its replacement with new regenerated bone (Mavropoulos et al. 2012, Calasans-Maia et al. 2015, Valiense et al. 2016, Carmo et al. 2018). The reabsorption capacity of nanostructured carbonated hydroxyapatite after a few weeks of its implantation in critical defects has been proven by several studies (Valiense et al. 2012; MD Calasans-Maia et al. 2015), this important characteristic being conferred by the surface topography of the biomaterial for the adhesion and proliferation of osteoblasts (Burg, Porter, and Kellam 2000). Although the association of platelet concentrate with cHA allows better manipulation of the spheres, there was no indication of acceleration of bone repair (Mourão et al 2017). Considering that several pieces of evidence point to a potential effect of PRF on bone tissue, contributing to its regeneration, it is not clear how its association with a biomaterial could affect the performance of this autologous product and its effects on bone cells.

In this context, the objective of this study was to evaluate the association of the membrane enriched with denatured albumin (Alb-PRF) with nanostructured carbonated hydroxyapatite microspheres, and to establish a comparison with the albumin membrane without the spheres. The researchers raised the hypothesis that the association of the biomaterial with albumin concentrates would produce a good three-dimensional framework, promoting a better response through cell recruitment, proliferation and differentiation, due to the availability of a structure based on calcium phosphate and important growth factors for the bone repair.

The specific objectives of the study were (i) to evaluate the three-dimensional structure of albumin membranes with and without cHA microspheres, (ii) to evaluate the *in vitro* release capacity of growth factors and immunomodulatory molecules and (iii) to evaluate cell viability, proliferation and mineralization of MG63 cells after exposure to membrane eluates.

METHODS

Ethical aspects

This project was conducted following the guidelines established by the 1975 international Helsinki agreement, after evaluation and approval by the ethics committee of the Hospital Universitário Antônio Pedro, approval number 3.432.068.

Preparation of nanocarboapatite spheres

The nanocarboapatite (cHA) microspheres were synthesized and characterized in the Biomaterial's Laboratory of the Brazilian Center for Research in Physics (Labiomat, CBPF, Rio de Janeiro) by the wet precipitation method at 37°C, without sintering, thus maintaining the nano-microscopic characteristics. The 425-600 µm spheres contained 6% CO_2 by weight, with a stoichiometry of 1.6 Ca/p <2.0. The biomaterial was characterized by scanning electron microscopy (SEM: JEOL FEG 250, JEOL®, Tokyo, Japan) to examine the morphology and surface of the spheres. The biomaterial was weighed (0.5g/vial) on a precision scale (UniblocAUY220, Shimadzu®, Kyoto, Japan) and then packaged and sterilized by gamma radiation (Gammacell 220, Nordion®, Ottawa, Canada) at 15 kGy/sample - a cobalt-60 irradiator at a dose rate of 19.72 Gy/min for 760 min.

Preparation of Alb-PRF and Alb-ncHA-PRF membranes

Peripheral blood samples were collected from 10 participants, of both sexes, aged between 20 and 46 years. Donors were healthy, with no history of recent use of anticoagulant medications. For collection, additive-free 9 mL tubes (Vacutube Seco, Biocon®, Brazil), adapters and 21G scalps were used. The protocol for Alb-PRF obtention (Gheno et al., 2020) was applied, which briefly consists of a single centrifugation at 700 RCF-max lasting 8 minutes in a horizontal rotor centrifuge (Bio-PRF, Venice , Florida, USA).

After centrifugation, the blood components settled, forming distinct layers depending on their respective densities. Therefore, for the production of activated albumin gel, the first two milliliters of the portion of platelet-poor plasma (PPP), located at the upper end of the tube, were collected with a 1 ml syringe (Injex®, Brazil). The albumin-rich serum underwent an activation cycle at 75º C lasting 10 minutes in the APAG equipment (Silfradent, Italy). Soon after the end of the process, the syringes containing the gel were stored at room temperature, protected from light, until use.

After the time required for the albumin gel to reach a temperature of approximately 37ºC, it was added to 6-well polystyrene plates (brand, manufacturer). For the production of Alb-PRF membranes, the entire available fraction of the liquid phase of the growth factor concentrate and the buffy coat was collected, added to the wells containing the activated albumin gel and carefully homogenized.

When preparing the Alb-ncHA-PRF membranes, in addition to the liquid phase of growth factor concentrate and buffy coat, carbonatoapatite microspheres (0.5 g per vial) were also added. In both cases, polymerization time varied between 5 and 10 minutes. After that, 4 mL of DMEM culture medium with 1% antibiotic (Penicillin–Streptomycin) was added.

Production of the membrane eluates

After polymerization, the Alb-PRF and Alb-nCHA-PRF membranes (n=5 per experimental group) were incubated in DMEM culture medium with 1% antibiotic for 24h. At the end of the period, the conditioned media were collected and stored in a -80º C freezer.

Scanning electron microscopy

In order to evaluate the ultrastructural characteristics of the Alb-PRF and Alb-nCHA-PRF membranes, scanning electron microscopy (SEM) was performed on samples from both groups, at experimental times of 24h, to evaluate their initial conformation, and at the time of 21 days to ascertain its ultrastructural stability over time. Processing for SEM began by washing the membranes with phosphate-saline buffer (PBS) pH 7.4. Afterwards, the samples were fixed with Karnovsky's solution (2.5% glutaraldehyde and 4% paraformaldehyde) for 1 hour.

Sequentially, post-fixation was performed with 1% osmium tetroxide, in a 0.2 M sodium cacodylate buffer solution, pH 7.4 in a 1:1 ratio. Soon after, samples from both experimental groups were dehydrated in ethyl alcohol at increasing concentrations ranging from 50% to 100%, and hexamethyldisilazane (HMDS). The materials were metallized with gold and observed at 15 kV with a scanning electron microscope (JEOL JSM-6490 LV, JEOL, Japan).

Histological analysis

Histological slides were produced to evaluate the organization of the platelet aggregates, their interaction with the biomaterial, in addition to the distribution of cells in the membranes. Two samples from each experimental group were fixed with 4% paraformaldehyde 24 hours after the end of their polymerization. The samples were embedded in paraffin and cut to a thickness of 7 μm. Subsequently, the histological sections were stained with hematoxylin and eosin (HE) and observed at 20X and 40X magnifications with an optical microscope (Axio Observer.A1, Zeiss, Germany).

Observation of viable cells in the membranes

Aiming to evaluate the viability of mononucleated blood cells trapped inside the membranes, a Live/Dead assay was performed. The membranes were maintained in cultures 7 days in 6-well polystyrene plates, in 4 mL of DMEM culture medium, without FBS and 1% antibiotics (Penicillin + streptomycin), with regular changes every 7 days at 37°C and 5% CO_2. A commercial cell imaging kit LIVE/DEAD® (Invitrogen), according to manufacturer's directions was employed, whose staining is based on the permeability of cytoplasmic membranes. Viable cells are stained in green by Fluorescein isothiocyanate (FITC), and non-viable cells are stained in red (Texas Red), with fluorescence in the wavelength ranges of 488 nm/515 nm and 570 nm/602 nm, respectively. Images were collected in a fluorescence microscope (Axio Observer.A1, Zeiss, Germany).

Quantification of cytokines and growth factor release

The concentrations of cytokines and growth factors released by the membranes were measured through the analysis of conditioned media at a concentration of 100%. For the detection of biomolecules, a multiparametric immunoassay based on magnetic microbeads labeled with XMap technology

(LuminexCorp, USA) was used, using a commercial kit (27-plex panel, Biorad Inc., USA) capable of quantifying IL-1β, IL-1RA, IL-2, IL-4, IL-5, IL-6, IL-7, IL-8 IL-9, IL-10, IL-12 (p70), IL-13, IL-15, IL-17, CCL11, FGF-b, CSF3, CSF2, IFN-γ, CXCL10, CCL2, CCL3, CCL-4, PDGF, CCL5, TNFα and VEGF. Quantification of magnetic beads and dosages was performed with a Bio-Plex MAGPIX system (Biorad Inc., USA). Results were analyzed using Xponent v. 3.0 software (Luminexcorp, USA).

Culture of human osteoblasts

The human osteosarcoma-derived MG-63 cell line was chosen in this study, due to its similarity with normal osteoblasts. The cells were obtained from the Rio de Janeiro Cell Bank (BCRJ) at the #104 passage and cultivated in DMEM (Dulbecco's Modified Eagle's Medium), supplemented with 10% fetal bovine serum (FBS) and 1% antibiotic (streptomycin/penicillin). Cultures were maintained in an incubator at 37°C and an atmosphere with 5% CO_2. Total changes of the culture medium were carried out at regular intervals of 72 hours, and subcultures occurred in a 1:4 ratio.

Evaluation of cell viability and proliferation

MG63 cells were subcultured for 24 hours on 96-well plates at a density of 10.000 cells/well (n=5 per experimental group), and then exposed for 24h to five concentrations of the Alb-PRF and Alb-ncAH-PRF eluates, diluted at 100%, 75%, 50%, 25% or 12.5% in DMEM. After the exposure, the cell viability was determined through the XTT (2,3-bis-(2-methoxy-4-nitro-5-sulphenyl) - (2H) – (tetrazolium-5-carboxanilide) assay by using a commercial kit (In Cytotox, Xenometrics, Germany). A group of cells were exposed to unconditioned media (n=5), as the experimental control. The Optical Density (O.D.) at 480nm was measured with a Sinergy II microplate reader (Biotek Inst., USA).

In order to evaluate the effects of the eluate on the cell proliferation, MG-63 cells were seeded in 96-well plates at a density of 1,000 cells/well, and treated with 150μ of culture medium conditioned with either 25% or 50% of the eluate from the membranes of both experimental groups. The experiment was carried out in quintuplicates, with each replicate treated with membrane eluate from a different donor. The conditioned medium was renewed every 72 hours, maintaining the

original eluate concentrations. A Crystal Violet Dye Exclusion assay (In Cytotox, Xenometrix, Germany) was performed to estimate cell density relative to the control group (cells exposed to unconditioned media), at 24h, 3, 5, and 7 days of treatment, by the measurement of the Optical Density at 540nm with a Sinergy II microplate reader (Biotek Inst., USA).

Determination of *in vitro* mineralization

To compare the osteoinductive potential of the Alb-PRF and Alb-PRF+nCHA membranes, an in vitro biomineralization assay was performed. MG-63 cells at passage 119 were seeded at a density of 20,000 cells/well in 48-well plates and treated with DMEM conditioned with 25% of the membrane eluates, supplemented with 5% FBS and 1% antibiotic (penicillin+streptomycin). Independent experiments were carried out with five technical replicates and five pooled biological replicates, employing cells exposed to unconditioned media as a control group. After the initial treatment, partial changes of the culture medium were carried out every 72 hours, equivalent to 50% of the final volume, always keeping the concentrations of conditioned medium unchanged throughout the entire experimental time.

At 1, 7, 14 and 21 days, the cell supernatant was collected and stored in a -80°C freezer, and the samples from each group were fixed in 4% paraformaldehyde and subsequently stained with 40mM alizarin in aqueous solution, to stain the deposits of calcium. After extraction with xxxx, the O.D. at 405 nm was read using a Sinergy II microplate reader (Biotek Inst., USA).

The collected cell supernatants were used to determine the alkaline phosphatase activity, using a p-nitrofenilphosphate (PNPP) based commercial kit (Labtest, Brazil), following the manufacturer's guidelines. To determine the enzyme activity by the hydrolysis of PNPP as a function of time, the optical density at 405 nm was monitored for 2 hours in kinetic mode on a Sinergy II microplate reader (Biotek Inst. USA). Three independent experiments were performed in quintuplicates.

Statistical analysis

Comparisons were performed between groups at different eluate concentrations and experimental times. The normality was assessed through the

Shapiro-Wilk test, and non-parametric analysis of variance was carried out using Kruskal-Wallis with Dunn post-hoc test, considering an alpha error of 5%. The statistical analysis was performed using GraphPad Prism 8 software (Graphpad inc., USA).

RESULTS

Soon after the synthesis, the ultrastructure of the carbonated hydroxyapatite spheres was evaluated, as shown in Figure 1. At higher magnification, it was possible to observe the roughness of the surface of the spheres, increasing their contact area.

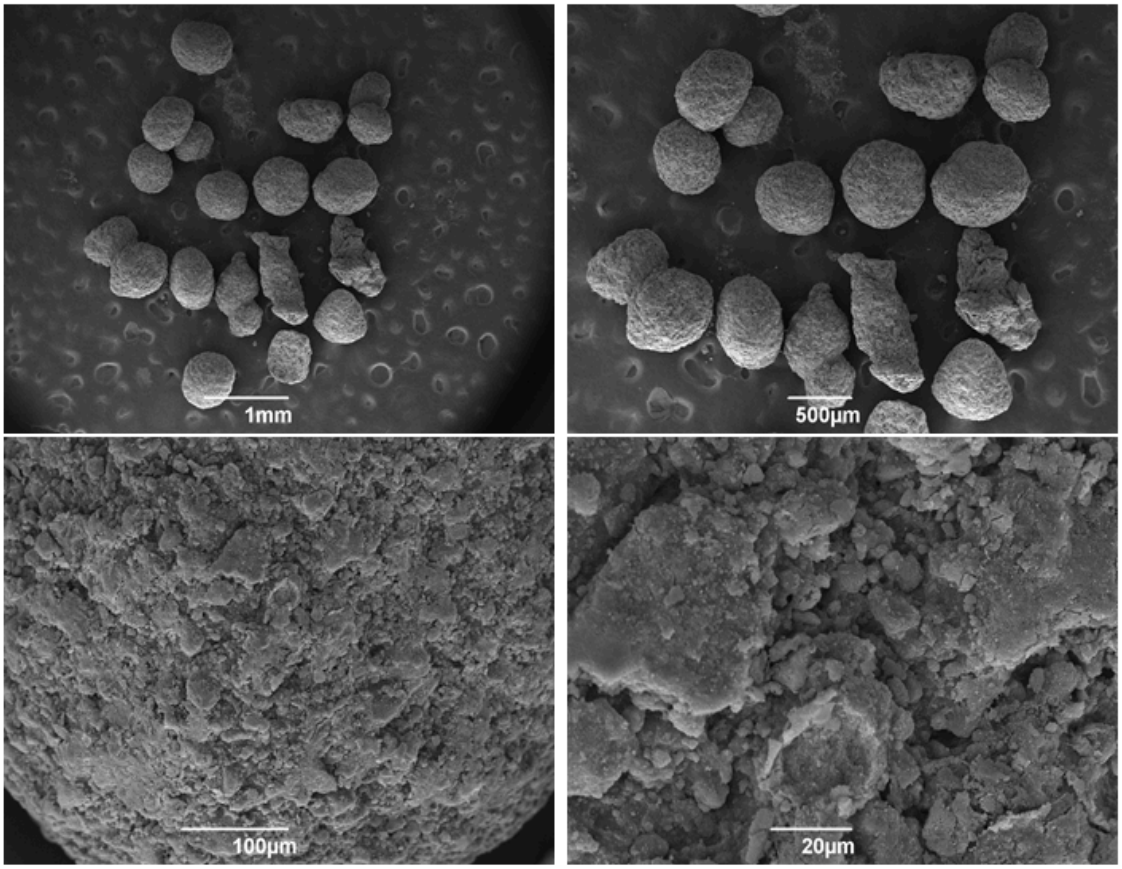

Figure 6 - Scanning electron microscopy (SEM) micrographs of nanostructured carbonated hydroxyapatite microspheres. Observe the morphology starting from 1 mm to 20 µm from the surface of the spheres, they are irregular and full of indentations.

The images obtained 24 hours after the synthesis of the Alb-PRF membranes demonstrate the structural robustness of the membrane, substantially different from other types of platelet aggregates (Figure 2).

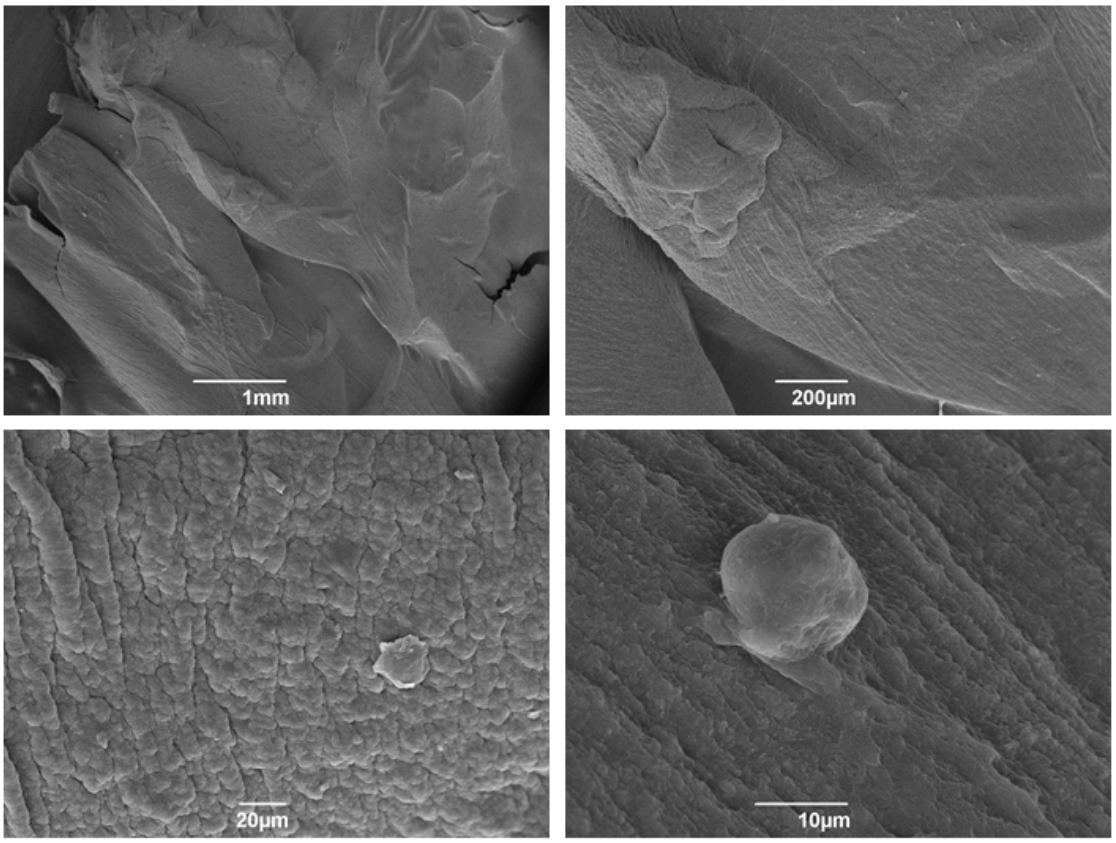

Figure 7 - Scanning electron microscopy (SEM) micrographs of 24-hour PRF albumin membranes. Observe the morphology starting from 1 mm to 10 µm from the membrane indicates a very robust membrane.

One day after integrating the spheres on the autologous material, producing the Alb-ncHA-PRF membranes, it is possible to observe the dense appearance resulting from the presence of denatured albumin (Figure 3), and a notable interaction between the fibrin network and the carbonated hydroxyapatite spheres.

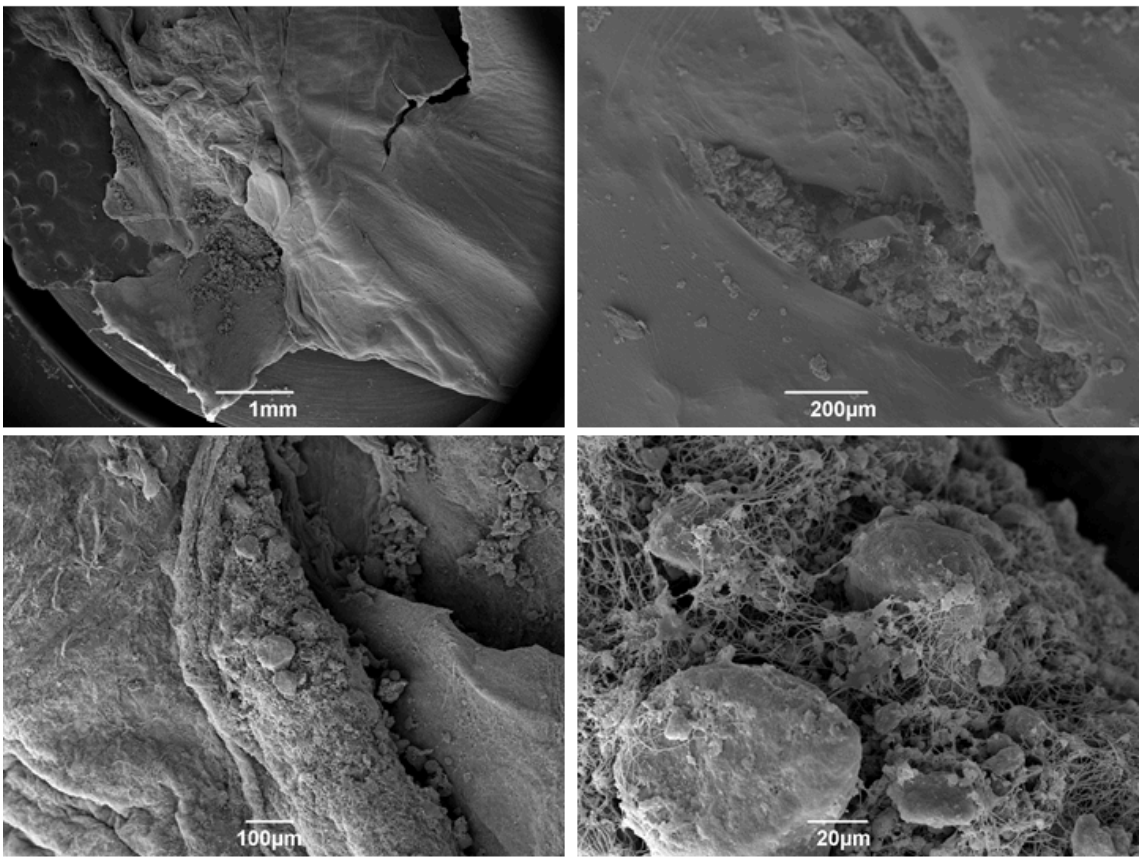

Figure 8 - Scanning electron microscopy (SEM) micrographs of PRF albumin membranes associated with 24-hour nanostructured carbonated hydroxyapatite microspheres. Observe the morphology starting from 1 mm to 20 µm from the membrane with cells wrapped in the fibrin network. It is possible to observe a different appearance, with cells trapped in the membrane and a sandy appearance. It is possible to observe two phases, one full of plots and the other very robust and dense.

After 21 days of the synthesis of the Alb-ncHA-PRF membranes, the micrographs show that the initial characteristics of the fibrin-albumin scaffold were maintained (Figure 4). Although slightly degraded, the carbonated hydroxyapatite spheres continue to adhere to the membrane, and a evident interaction with the fibrin network remains observable.

The micrographs of the Alb-PRF membranes at the experimental time of 21 days point to the integrity of the membrane over time (Figure 5).

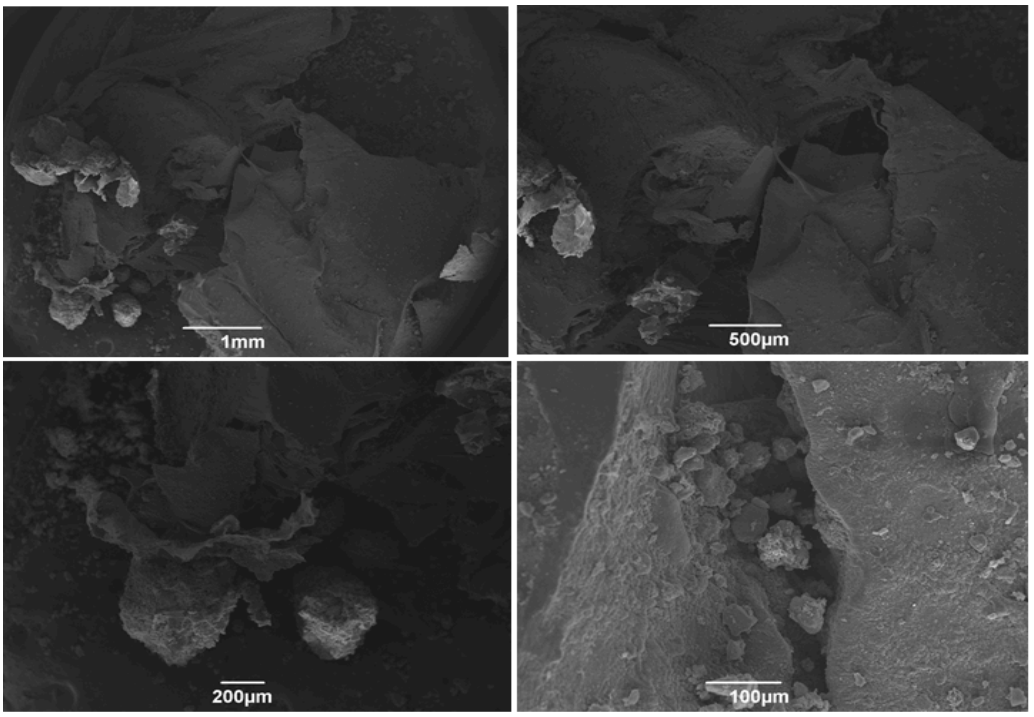

Figure 9 - Scanning electron microscopy (SEM) micrographs of PRF albumin membranes associated with 21-day nanostructured carbonated hydroxyapatite microspheres. Note the morphology starting from 1 mm to 100 µm and the robust structure still present, associated with cells and carbonated hydroxyapatite microspheres.

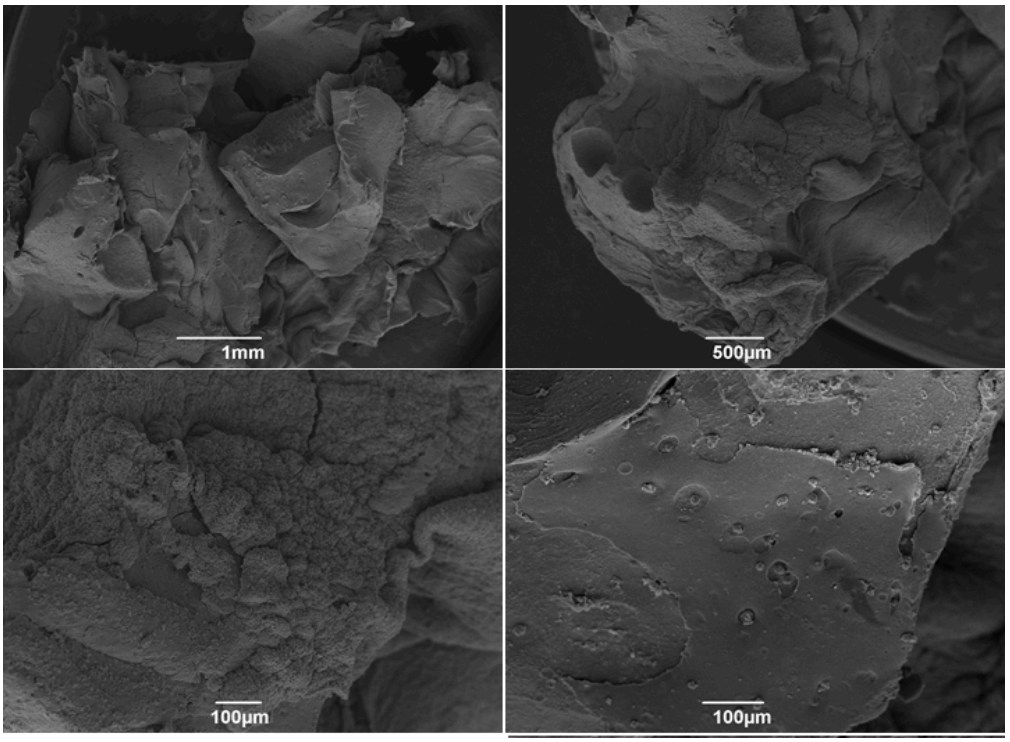

Figure 10 - Scanning electron microscopy (SEM) micrographs of 21-day PRF albumin membranes. Observe the morphology starting from 1 mm to 100 µm of the membrane, indicating a membrane that remains structured at 21 days after polymerization.

Figure 6 shows the ultrastructure of the Alb-PRF membranes, evidencing the characteristics of biphasic material, with a portion predominantly fibrous and rich in cells, and another dense phase composed by the denatured albumin. The addition of nanostructured cHA spheres did not seem to change this pattern, but the spheres were shattered in smaller pieces that often integrated in both albumin and fibrin phases (Figure 7).

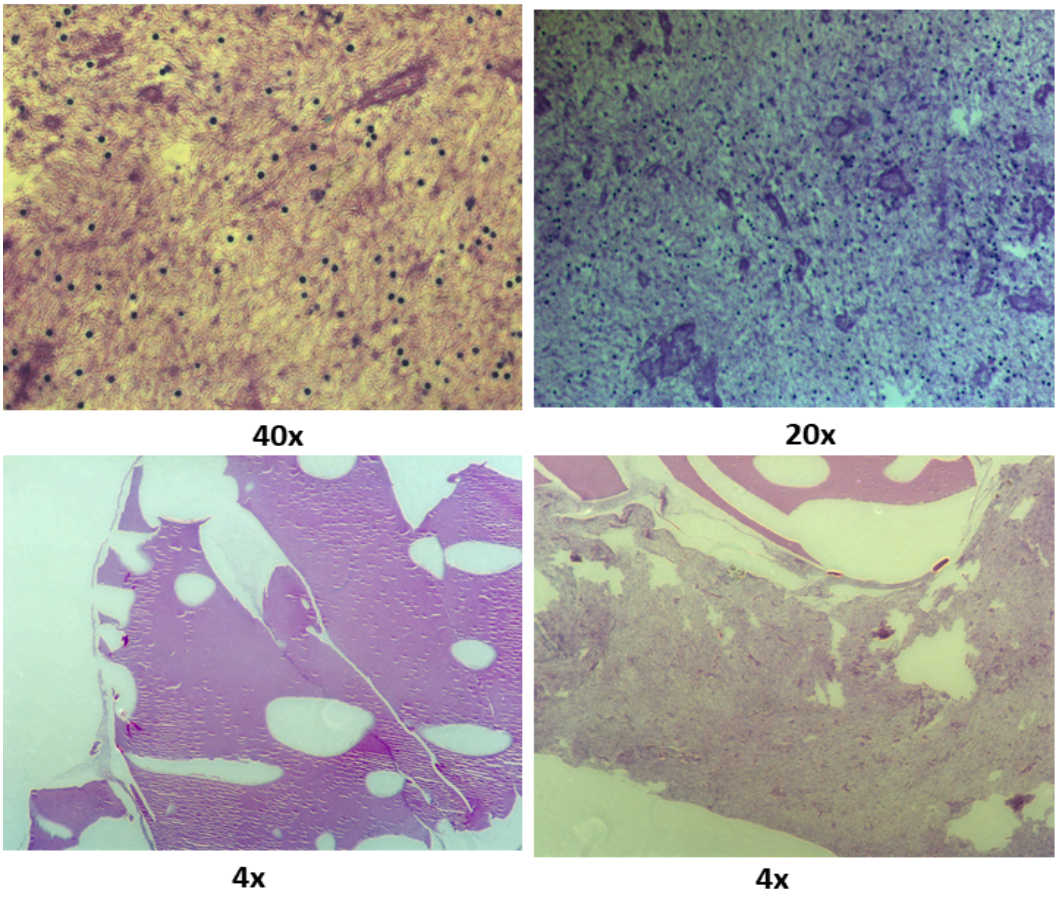

Figure 11 – Histological sections of the Alb-PRF membranes. Note that he concentration of cells on the fibrin portion, in comparison with a dense denatured albumin portion.

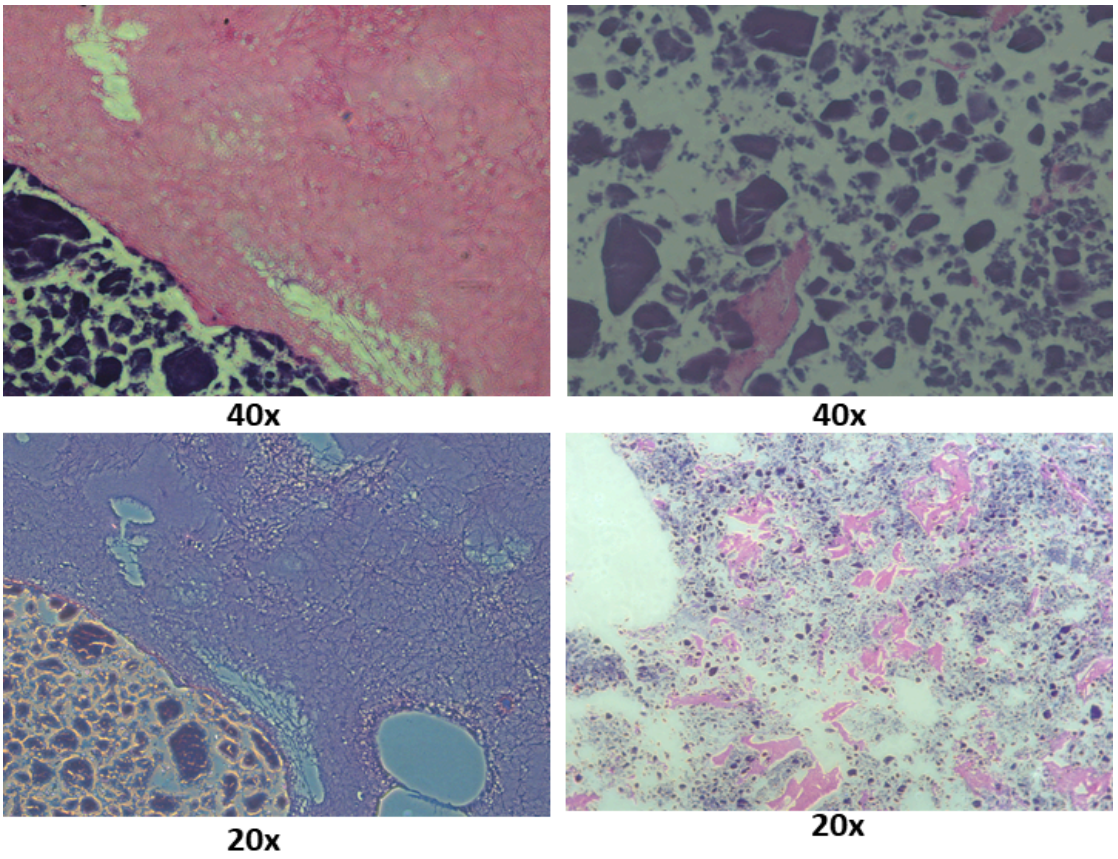

Figure 12 – Histological sections of an Alb-PRF membrane associated with nanostructured carbonated hydroxyapatite microspheres.

A live/dead assay was carried out either one seven days after the production of the membranes, to monitor the presence of living blood cells in the Alb-PRF and Alb-ncHA-PRF membranes over time (Figure 8). Both membranes were characterized by abundant calcein staining indicating the presence of viable cells. After seven days, cell density decreased as expected, but viable cells were still noticeable throughout the experimental period.

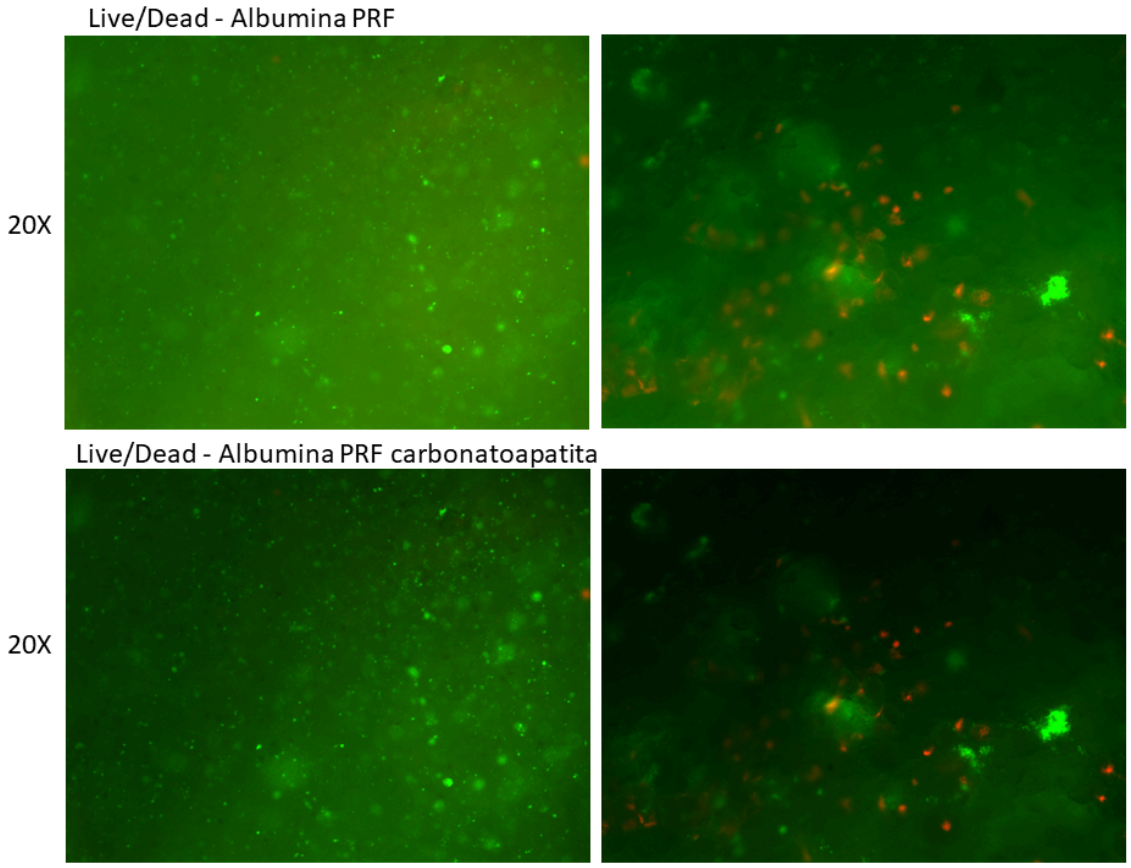

Figure 13 – Microscope image of the Live/Dead assay of cells present in the membranes. Green (calcein) staining for live cells, red (EthD) for dead cells.

The release of cytokines, chemokines and growth factors by the Alb-PRF and Alb-ncHA-PRF membranes was assessed in culture media within 24 hours. While both membranes were able to release biological mediators (Figure 9), 68% of the 25 assessed molecules were reduced in Alb-ncHA-PRF membranes when compared to Alb-PRF membranes ($p<0.05$), including all growth factors investigated (PDGF, VEGF, GM-CSF, G-CSF).

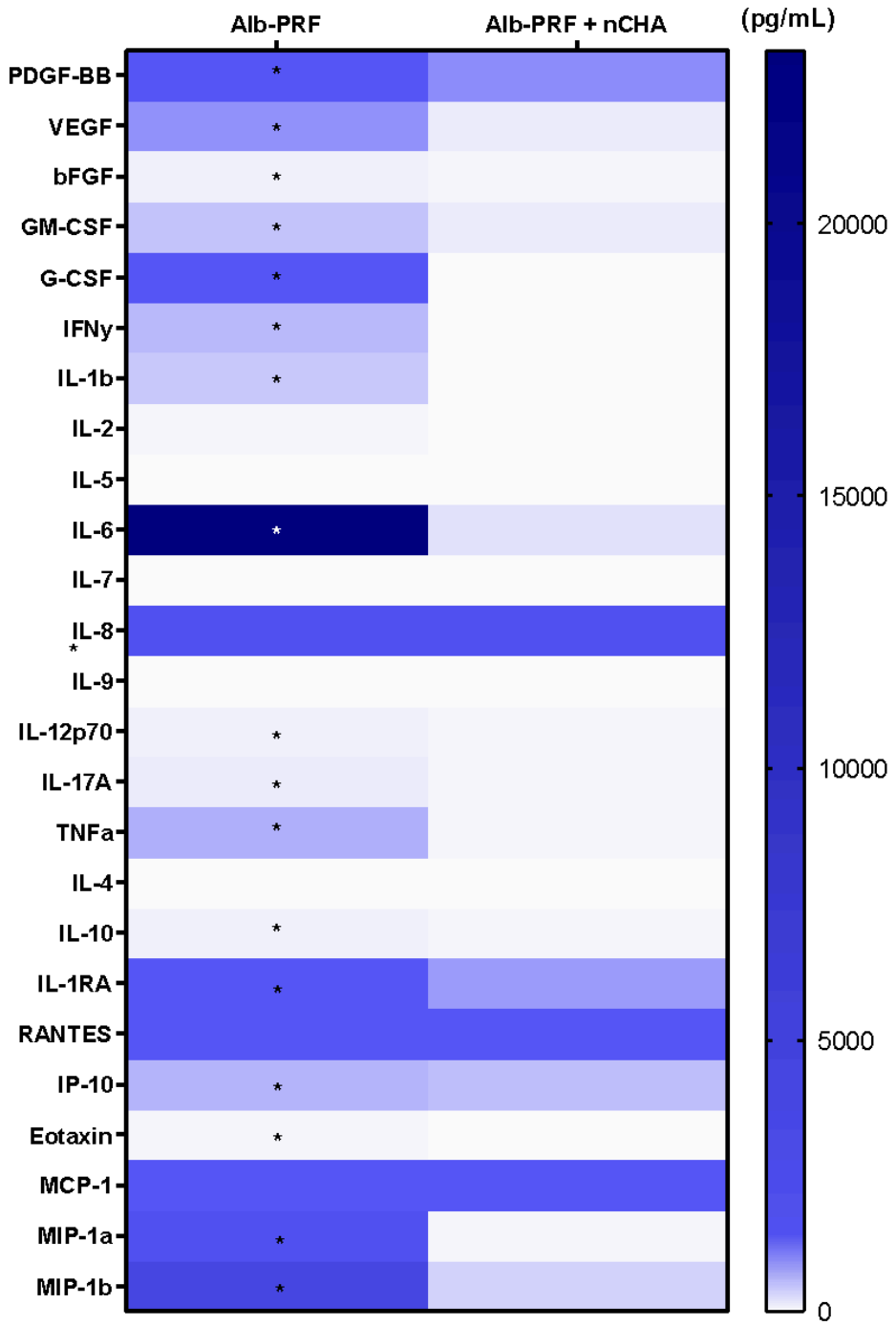

Figure 14 - Heatmap of the release of cytokines and growth factors from Alb-ncHA-PRF and Alb-PRF membranes after 24 hours of elution in culture medium. An asterisk indicates significant difference between groups ($p<0.05$).

The cytocompatibility of Alb-PRF and Alb-ncHA-PRF membranes with human bone cells was investigated through an XTT assay, carried out 24h after treatment of MG63 cells with different concentrations of membrane eluates. Both the Alb-PRF and Alb-ncHA-PRF membranes were biocompatible with cells at all

concentrations tested (Figure 10), as they induced similar viability to the unexposed control group ($p>0.05$). As an exception, when exposed to 100% eluates of Alb-PRF, cells showed significant higher levels of dehydrogenase/mitochondrial activity compared to Alb-ncHA-PRF and control ($p<0.05$).

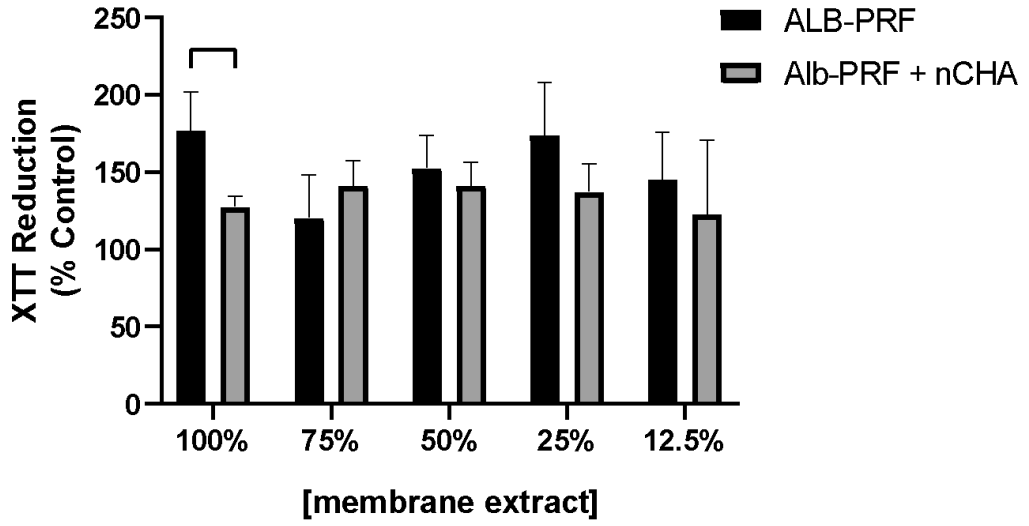

Figure 15. Cytocompatibility assessment of ALB-PRF and ALB-PRF + nCHA membrane extracts, in different dilutions in culture medium (DMEM), measured in MG63 cells, after 24 hours of exposure, using the XTT test. The bars show the mean and standard deviation of 3 independent experiments, in quintuplicates, represented as a percentage of the control group (cells exposed to culture medium). The line indicates a significant difference between groups ($p<0.05$). A positive cytotoxicity control was produced with latex extracts, showing 20.7% average survival.

The effects of Alb-PRF and Alb-ncHA-PRF membranes on bone cell proliferation was estimated in samples treated with conditioned media diluted at 25% or 50% (Figure 11). At day 1, only the Alb-PRF membranes significantly stimulated proliferation, without difference in performance between concentrations of 25% or 50%. On day 3, all experimental groups were effective in stimulating proliferation when compared to the control, but Alb-PRF membranes at a concentration of 50% were more effective than Alb-ncHA-PRF at the same concentration. On the remaining days, both membranes continued to perform better than the control, but without significant difference between them or between the different concentrations used.

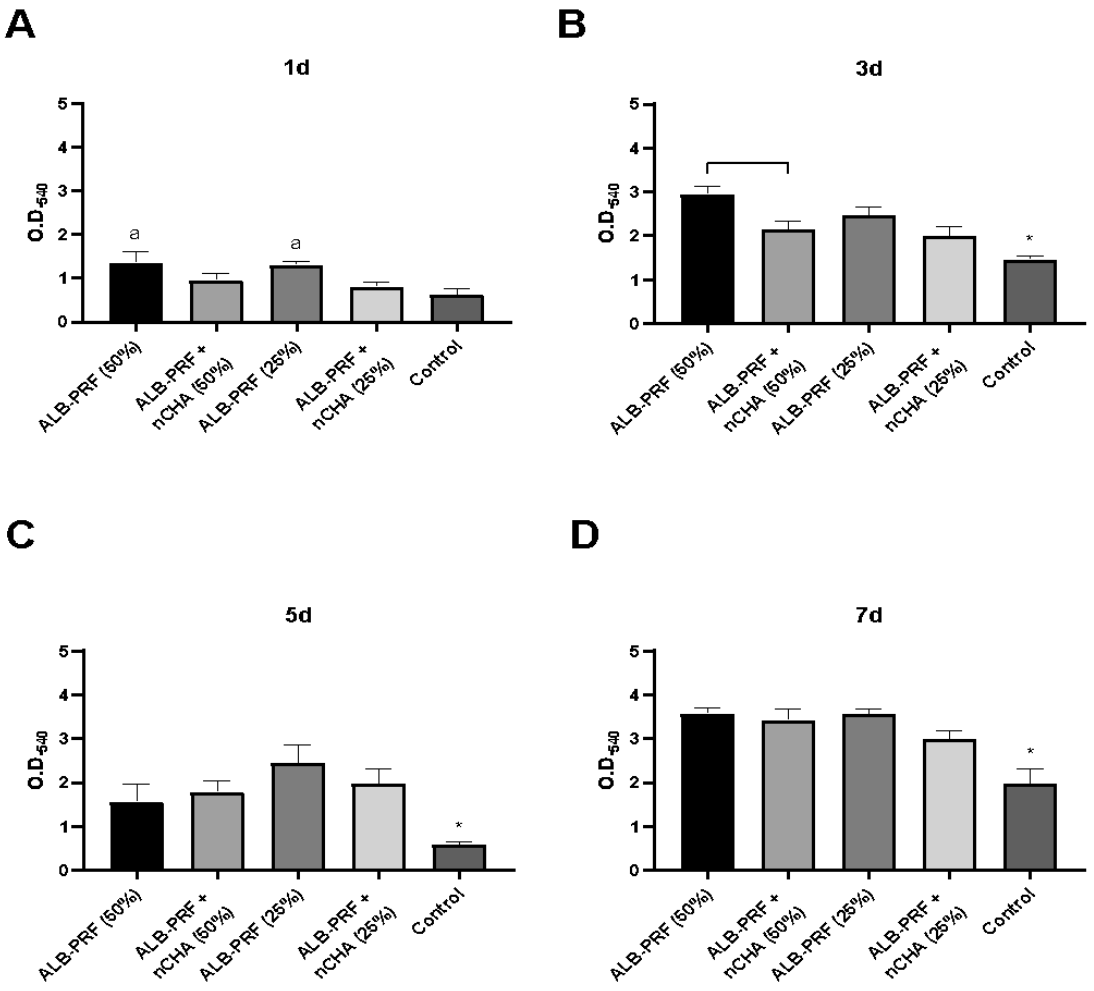

Figure 16. Proliferation of MG63 cells for up to 7 days after exposure to Alb-PRF, Alb-nCHA-PRF extracts, or culture medium (control). Cell density was assessed thoruth the crystal violet dye exclusion test, with results expressed by the optical density at 540 nm. The letter (a) indicates a significant difference in relation to the control ($p<0.05$). The bars indicate mean ± standard deviation (n=5). Asterisks indicate a significant difference ($p<0.05$) in relation to all other experimental groups.

The potential of the Alb-PRF and Alb-ncHA-PRF membranes to induce in vitro mineralization was evaluated by labeling extracellular calcium deposits with Alizarin Red (Figure 12). One day after exposure to 25% eluates, there was no variation between the experimental groups and the control. From day 7, and throughout days 14 and 21, it is possible to notice a consistent and progressive increase in mineralization induced by the Alb-PRF membrane ($p<0.05$). The Alb-ncHA-PRF membrane does not show signs of significantly favoring calcification (when compared to control) at any of the experimental times.

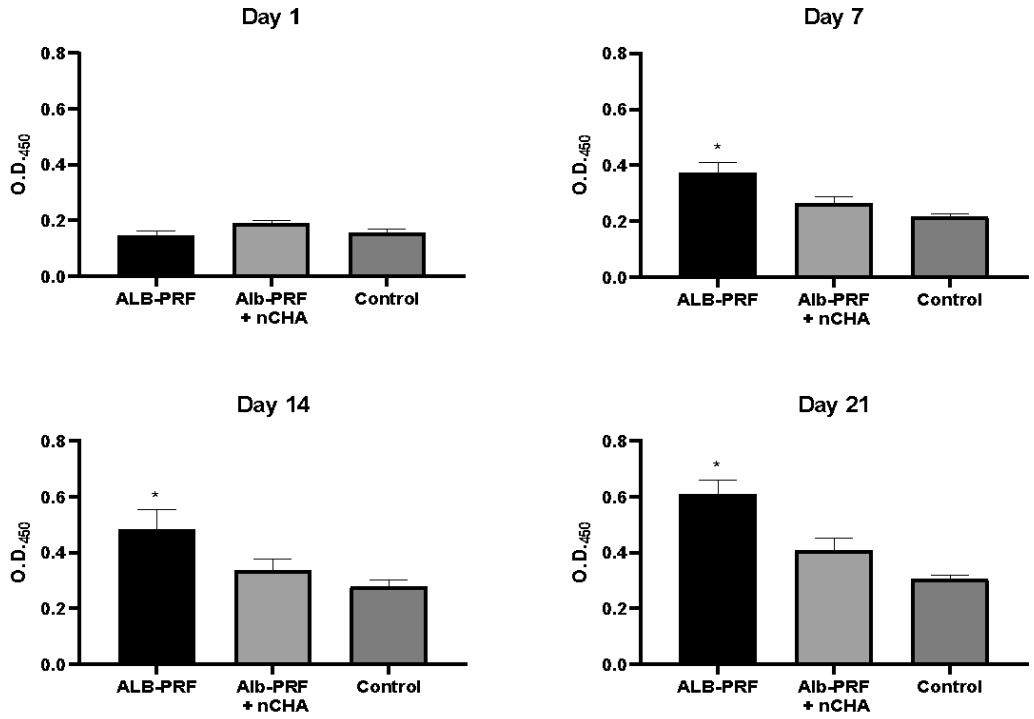

Figure 17. In vitro calcification by MG63 cells exposed for up to 3 weeks to ALB-PRF or ALB-PRF + nCHA eluates. Bars indicate mean ± standard deviation (n=3) of alizarin-S labeling, expressed by optical density at 450nm. An asterisk indicates a significant difference ($p<0.05$) from the control group, exposed to culture medium.

Alkaline phosphatase (ALP) enzyme activity was estimated in culture media over the three weeks of exposure to the eluates. At 24 hours, both the Alb-PRF and Alb-ncHA-PRF membranes showed the highest peaks of enzymatic activity, more than seventy times greater than the control group (Figure 13). From day 7 to day 21, cells stimulated with the Alb-PRF membrane showed increasing enzyme activity, although lower than the peak observed on day 1. The trend of progressive increase in enzyme activity was also seen on days 14 and 21 in cells treated with the Alb-ncHA-PRF membrane eluate, when compared to the control, but significantly lower than Alb-PRF ($p<0.05$).

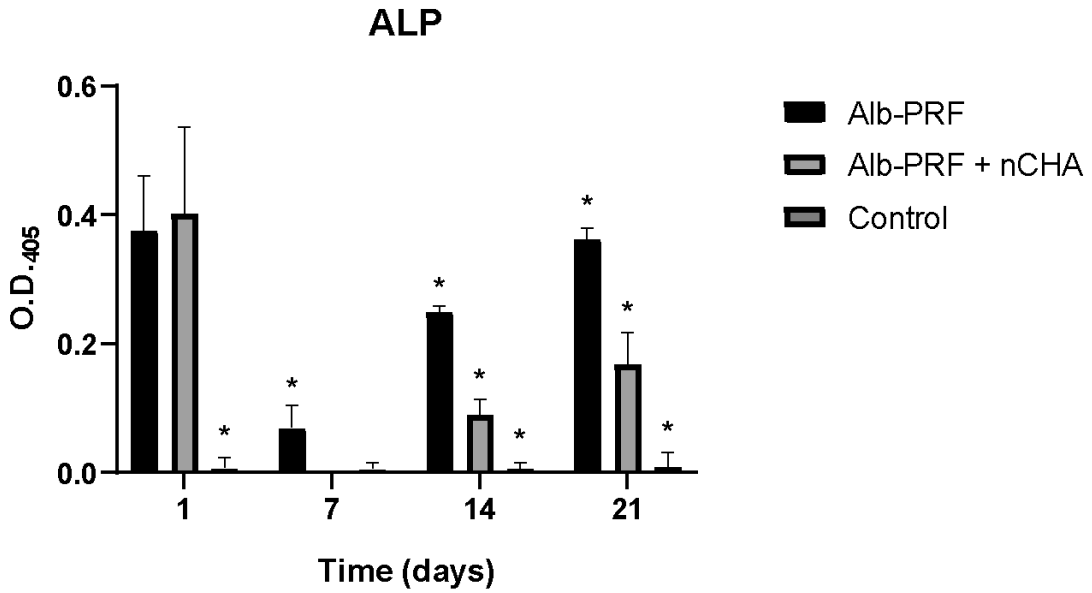

Figure 18. Assessment of alkaline phosphatase ezyme activity in the culture medium over 3 weeks, by MG63 osteoblasts exposed to extracts (25%) of ALB-PRF and ALB-PRF + nCHA membranes, or DMEM culture medium (control). The bars show the mean and standard deviation of 3 independent experiments, in quintuplicate, represented as the optical density of the medium, relative to the breakdown of the PNPP substrate. Asterisks indicate significant difference compared to all other groups at the same experimental time ($p<0.05$).

DISCUSSION

The present study aimed to contribute to the development of novel biomaterials by testing the hypothesis that the association of a nanostructured calcium phosphate allograft with Alb-PRF, in addition to representing a potential three-dimensional biodegradable barrier, would improve the behavior of bone cells, since the material provides both calcium phosphate and growth factors, all of which are important aspects for bone repair.

Due to its osteoconductive and biocompatible properties, hydroxyapatite (HA) is widely used as a bioceramic for bone replacement applications. The incorporation of carbonate into nanostructured HA causes significant changes in its physicochemical properties, resulting in increased *in vivo* dissolution rates, and enabling the production of bone substitutes with greater resorption (Anjos et al 2018). In this study, the ultrastructure of nCHA spheres was evaluated by scanning electron microscopy (SEM), enabling to observe a highly porous surface topography. The porosity of carbonated nanostructured hydroxyapatite spheres is

an important parameter that affects their performance as biomaterials for bone tissue engineering. It can be controlled by varying the synthesis parameters, such as temperature, time, pH, and concentration of the reactants, and usually range from 20% to 60% (Calasans-Maia et al 2015). The porosity of nanostructured cHA spheres affects their mechanical properties, biodegradability, bioactivity, and surface area, usually resulting in increased protein adsorption form biological media - a key factor that influences the cellular response and tissue integration of biomaterials (Mourão et al., 2018; Anjos et al 2019). According to the work of Anjos et al (2019), nutrients are consistently adsorbed from biological media by nanostructured nanohydroxyapatite, however without impact on cell growth or survival on the *in vitro* assessments performed by the authors.

The membranes produced by the Alb-PRF protocol were observed in detail by scanning electron microscopy and histology, identifying a very similar pattern form previous reports of the fibrin membrane enriched with denatured albumin (Gheno et al., 2020; Mourão et al., 2018), exhibiting a dense surface, in which the deposition of a layer of denatured protein was evident that entirely surrounded the fibrin fibers, as well as the retention of leucocytes and platelets. This structural configuration can be considered advantageous for guided-bone regeneration (GBR) purposes, where resorbable membranes facilitate the growth of new bone tissue, providing mechanical stability but preventing the invasion of soft tissue cells into the defect area, while allowing the passage of nutrients and oxygen.

The addition of nCHA spheres produced membranes with a similar pattern, however with the presence of smaller shards of biomaterial resulting from the disintegration of the spheres, which could be observed in both phases. It is important to notice, however, that some spheres that interacted with the fibrin portion (wrapped inside fibrils, as observed by SEM) remained relatively integrous along at least 21 days, suggesting that this combination might reduce the solubility of this material and may potentially modulate its solubility. It is an interesting factor to be considered and investigated in future studies, as controlling bioresorption may optimize the bioavailability of calcium and phosphate ions, which are essential for bone mineralization and osteogenesis. Conversely, by decreasing the solubility of CHS, it is possible to prolong their retention time in the bone defect site and provide a sustained release of therapeutic ions (S. Bose et al, 2017; A. Bigi et al, 2018).

The release of cytokines and growth factors by PRF membrane has been widely known since studies in the early 2000s (Choukroun et al. 2006; Dohan et al 2009; Mourão et al 2018; Lourenço et al 2019; Thanasrisuebwong et al 2020), resulting in effects on the promotion of angiogenesis, migration, proliferation and differentiation of mesenchymal cells, fibroblasts, and osteoblasts, among others (Barbosa et al, 2023). In this study, high levels of growth factors such as PDGF, VEGF and FGF2 were released by Alb-PRF within 24 hours. However, with the addition of the nanostructured cHA spheres, the release was significantly reduced for all these molecules, along with several cytokines and chemokines. This finding suggests that the spheres may be trapping different proteins contained within the fibrin scaffold, a feature with great potential of impact on the biological effects of PRF during tissue regeneration. Indeed, hydroxyapatite and other calcium phosphates are well known for their ability to adsorb proteins, including growth factors from biological media, such as blood plasma, serum, and cell culture media (Dorozhkin, 2013). While such interactions may be interesting for controlled delivery of biological mediators in some settings (Dorozhkin, 2013; Chen et al., 2015), the insufficient control over the release profile of GFs may be an issue in the applicability of composite materials such as alb-ncHA-PRF, as they could cause the loss of expected effects.

To identify the potential impact of these changes observed in the properties of Alb-PRF caused by the association with ncHA on the behavior of bone cells, we have performed an in vitro assessment employing human osteoblast-like cells derived from osteossarcoma, from the cell line MG63. This is a cell type commonly used as an experimental bone cell model due to their similarity to primary human osteoblasts: although there are variations in terms of morphology and shorter duplication time, these cells express the main biological markers of osteoblast behavior, are regulated by the same differentiation regulatory pathways, and can produce a mineralized matrix when adequately stimulated. In this way, they present important characteristics for testing biomaterials in medical applications (Czekanska et al 2013; Staehlke et al 2018; ATCC, 2023).

The cytotoxicity of platelet-rich fibrin (PRF) on osteoblasts is a topic of interest for tissue engineering and regenerative medicine since the optimal concentration of PRF and its cytokines for osteoblast viability and function is still under debate. Silva et al (2020) investigated the effects of different concentrations

of PRF and its cytokines on the cytotoxicity of osteoblasts, reporting that higher doses of PRF elutes induced significant cell death and reduced cell viability. These effects were mainly correlated with the concentration of cytokines such as IL-6 and TNF-α. In the present study, Alb-PRF membranes (added or not with cHA) presented a good cytocompatibility in all tested concentrations, and regardless of the high release of cytokines already identified after 24 hours elution. These results are in accordance with previous in vitro assessments of alb-PRF with other cell types, such as fibroblasts (Al- Maawi S et al 2021; Shirakata Y et al 2021). Nevertheless, since the cumulative production and release of cytokines by alb-PRF membranes has already been reported in the literature (Mourão et al., 2019), we decided to perform the subsequent biological assessments with diluted membrane eluates (50% or 25%), in order to avoid potential cytotoxicity in longer experimental times.

Cell proliferation is a very important phenomenon in tissue regeneration, and one of the most positively affected by the growth factors usually released by PRF (such as VEGF, PDGF and TGF-Beta). The present results confirm that alb-PRF is able to stimulate proliferation of human osteoblasts, and its effects at the first 1 to 3 days are significantly stronger than those of Alb-ncHA-PRF. This result provides a first glance at the potential impact of the lower release of biological mediators induced by the addition of ncHA to the platelet aggregate. PDGF, FGF2 and VEGF are important cytokines that contribute on the regulation of the proliferation of osteoblasts, as they bind to specific receptors and activate intracellular signaling pathways that regulate gene expression, cell cycle progression, and survival. PDGF and VEGF also modulate the expression of other factors that influence osteoblast function, such as osteoprotegerin, osteocalcin, and bone morphogenetic proteins (Wang et al., 2019). The balance between these growth factors, which was strongly affected on the eluates of determines the rate and extent of osteoblast proliferation and differentiation, as well as their interactions with other cells in the bone microenvironment (Chen et al., 2012).

In vitro mineralization is another of the main parameters investigated to predict the impacts of platelet aggregates and PRF derivatives, as it is a marker of the osteogenic potential of these materials, and fundamental for bone regeneration. This mineralization involves osteoblast differentiation pathways, such as the cbfa-1/runx2 pathway, activated, in the case of PRF, by growth factors

released by the autologous biomaterial (Lima et al 2023). The presence of calcium phosphate (hydroxyapatite) in osteoblastic cell cultures is commonly quantified by the alizarin red staining method, an established approach to characterize a mineralized matrix resulting from osteogenic cell differentiation (Palmieri et al., 2018; Bernar et al., 2022). Through these methods, a significant difference was observed in the calcification induced by alb-PRF and alb-ncHA-PRF: while the exposure to Alb-PRF eluates greatly induced in vitro mineralization, this effect was reversed by the presence of ncHA spheres, since the Alb-ncHA-PRF eluates were statistically equivalent to the control group ($p>0.05$). This is yet another indication that the presence of the spheres affected the biological properties of Alb -PRF, by impairing behaviors that are often modulated by growth factor stimulation.

Alkaline phosphatase (ALP) is widely expressed in mineralized tissue cells and plays a crucial role in the formation of hard tissue, being considered an early marker of osteogenic differentiation (Vimalraj et al, 2020). Alkaline phosphatase secretion by osteoblasts increases during early differentiation, as cells are preparing for bone matrix synthesis. In the extracellular matrix formation phase, ALP facilitates the mineralization of the newly formed bone matrix. The most significant peak in alkaline phosphatase activity occurs during mineralization and deposition of hydroxyapatite crystals onto the bone matrix, followed by a decrease in ALP levels, reflecting a reduction in active osteoblasts, with some transitioning into osteocytes embedded within the bone matrix, or undergoing apoptosis. In this study, ALP activity presented two peaks, at days #1 and #21 for both stimulated groups, without relevant ALP secretion by unstimulated cells (control). As recently reviewed by Lima et al. (2023), this is one of the most common responses of bone/mineralized tissue cells to stimulation by L-PRF (and its derivative protocols), that was once again, in our study, strongly reduced by the addition of nanostructured cHA spheres into the platelet aggregate scaffold.

Altogether, these findings suggest that the association of denatured albumin-enriched platelet-rich fibrin with nano-carbo hydroxyapatite spheres decrease the expected stimulation of bone cells by the PRF component, most probably through a lower release of cytokines and growth factors. This hypothesis may both explain and be reinforced by the clinical study by Mourão et al. (2017), which reported a lack of stimulation of novel bone formation by a “sticky bone” preparation composed by concentrated growth factors (CGF) associated to nCHA

spheres very similar to those of the present work. It is possible that the difference between this and other studies, reporting a clinical success obtained with associations of PRF and calcium phosphates, lies in a lower protein absorption of proteins due to different physicochemical properties – another hypothesis that still demands confirmation by further studies.

CONCLUSION

The results indicate that the addition of carbonatoapatite spheres reduces the biological activity of Alb-PRF, associated to a lower release of proteins such as growth factors, which impairs its expected effects on proliferation, *in vitro* mineralization, and alkaline phosphatase activity of osteoblasts.

4. CONSIDERAÇÕES FINAIS

É possível afirmar, através dos dados levantados nesta tese, que a literatura fornece consistentemente evidências *in vitro* de que o PRF, produzido por diferentes protocolos ou em combinação com outros biomateriais, influencia a proliferação, diferenciação e mineralização de células de ossos e tecidos mineralizados. Esses efeitos envolvem vias bem conhecidas de sobrevivência celular, a ativação de fatores de transcrição (Runx2, OSX) e aumento da expressão de várias proteínas, incluindo osteopontina, osteocalcina, colágeno, ALP, BSPs, RANKL/OPG e fatores de crescimento como TGF- beta, PDGF e BMP2. Diferentes estudos associaram esses efeitos a fatores de crescimento específicos liberados pelo PRF, sugerindo que este é um fator importante a ser considerado no desenvolvimento e aprimoramento desses biomateriais autólogos para o tratamento de tecidos mineralizados como o osso.

O PRF é amplamente utilizado na medicina regenerativa e na odontologia, e os modelos *in vitro* representam apenas um pequeno aspecto da cicatrização de feridas e da regeneração óssea. Como tal, não é possível garantir que os resultados *in vitro* identificados possam ser diretamente extrapolados para ambientes clínicos. Por outro lado, a melhoria da proliferação, diferenciação e mineralização in vitro dos osteoblastos pode representar uma evidência interessante em apoio à atividade regenerativa aumentada, às propriedades osteoindutoras ou à osseointegração melhorada. Portanto, ao reunir e analisar informações relacionadas ao PRF e às células mineralizantes, podemos compreender melhor os mecanismos por trás do impacto do PRF na regeneração óssea e otimizar suas propriedades e aplicações. Isto inclui a determinação de concentrações ideais, a exploração de associações com outros materiais de enxerto ósseo ou medicamentos e o desenvolvimento de novos protocolos de produção para melhorar os resultados clínicos deste promissor material autólogo.

A associação do PRF com a albumina desnaturada, como no caso do Alb-PRF, tem um potencial significativo nas áreas da medicina regenerativa e odontologia. A albumina desnaturada possui propriedades bioativas que podem aprimorar a eficácia do PRF em processos de regeneração tecidual, como na reparação óssea, e um papel de barreira na regeneração óssea guiada. No entanto, os resultados apresentados na seção experimental desta Tese apontam

que a associação de fibrina rica em plaquetas enriquecida com albumina desnaturada com esferas de nano-carbohidroxiapatita diminui a estimulação esperada das células ósseas pelo componente PRF, muito provavelmente através de uma menor libertação de citocinas e fatores de crescimento. Esta hipótese pode tanto explicar como ser reforçada pelo estudo clínico de Mourão et al. (2017), que relatara uma baixa estimulação da formação de novos ossos por uma preparação de "*sticky bone*" composta por fatores de crescimento concentrados (CGF) associados a esferas nCHA muito semelhantes às do presente trabalho. É possível que a diferença entre este e outros estudos, que relatam um sucesso clínico obtido com associações de PRF e fosfatos de cálcio, esteja na menor absorção proteica de proteínas devido às diferentes propriedades físico-químicas – outra hipótese que ainda necessita de confirmação por novos estudos.

CONCLUSÃO

Os resultados demonstram que a inclusão de esferas de carbonatoapatita diminui a atividade biológica do Alb-PRF, resultando em uma redução na liberação de proteínas, como os fatores de crescimento. Essa diminuição compromete os efeitos esperados dos derivados do PRF na proliferação, mineralização in vitro e atividade da fosfatase alcalina dos osteoblastos.

5. Referências Biliográficas

ADAMS, Brandy R., *et al,* 2014. Osteoblast Response to Nanocrystalline Calcium Hydroxyapatite Depends on Carbonate Content. *Journal of Biomedical Materials Research Part A* 102(9): 3237–42. doi:10.1002/jbm.a.34994.

AL-MAAWI, S.; *et al,* 2021. Biologization of Pcl-mesh using platelet rich fibrin (Prf) enhances its regenerative potential in vitro. *International journal of molecular sciences* 2021, *22*, 2159.

AL-MAAWI, S.; *et al,* 2022. A standardized g-force allows the preparation of similar platelet-rich fibrin qualities regardless of rotor angle. *Tissue Engineering Part A* 2022, *28*, 353-365.https://pubmed.ncbi.nlm.nih.gov/34555949/

ANJOS, S *et al,* 2019 Impact of crystallinity and crystal size of nanostructured carbonated hydroxyapatite on pre-osteoblast in vitro biocompatibility J Biomed Mater Res. DOI: 10.1002/jbm.a.36709

ATTIA MS, *et al,* 2019. Histological and histomorphometric evaluation of hydroxyapatite-based biomaterials in surgically created defects around implants in dogs. J Periodontol. 2019; 90 (3): 281-7)

A. BIGI et al,2018. Nanosized hydroxyapatite as a drug delivery system for bone regeneration. Nanomedicine: Nanotechnology, Biology and Medicine, vol. 14, no. 2, pp. 441-449, 2018.

BAGIO, D.A. *et al,* 2021 Increased VEGF-A Expression of Human Dental Pulp Stem Cells (hDPSCs) Cultured with Advanced Platelet Rich Fibrin (A-PRF). *The Open Dentistry Journal* 2021, *15*.

BANYATWORAKUL, P. *et al,* 2021. Responses of canine periodontal ligament cells to bubaline blood derived platelet rich fibrin in vitro. *Scientific reports* 2021, *11*, 11409.

BARROS MOURÃO *et al,* 2018. Characterization of a new membrane from concentrated growth factors associated with denaturized Albumin (Alb-CGF) for clinical applications: A preliminary study. Int J Growth Factors Stem Cells Dent [serial online] 2018; 1:64-9. Available from: https://www.cellsindentistry.org / text.asp?2018 / 1 / 2 /64/235911

BI, J. *et al,* 2020 X. Platelet-rich Fibrin Improves the Osteo-/Odontogenic Differentiation of Stem Cells from Apical Papilla via the Extracellular Signal–regulated Protein Kinase Signaling Pathway. *Journal of Endodontics* 2020, *46*, 648-654.

BLATT, S. *et al,* 2021. Possible implications for improved osteogenesis? The combination of platelet-rich fibrin with different bone substitute materials. *Frontiers in Bioengineering and Biotechnology* 2021, *9*, 640053.

BHULLAR, SK, *et al,* 2015. “SMART BIOMATERIALS – A REVIEW.” Rev. Adv. Mater. Sci 40:303–14. http://www.ipme.nw.ru/e-journals / RAMS / no_34015 / 10_34015 _ bhullar.pdf.

BORIE, E. *et al,*2015. Platelet-rich fibrin application in dentistry: a literature review. *International journal of clinical and experimental medicine* 2015, *8*, 7922.

BOTTINO, Marco C. et al. 2012 “Recent advances in the development of GTR/GBR membranes for periodontal regeneration—A materials perspective.” Dent Mater 28:703–721.

BURG, KJ, *et al,* 2000. Biomaterial Developments for Bone Tissue Engineering. *Biomaterials* 21 (23): 2347–59. http:// www.ncbi.nlm.nih.gov / pubmed / 11055282.

CALASANS-MAIA, Mônica Diuana et al. 2015 “Cytocompatibility and biocompatibility of nanostructured carbonated hydroxyapatite spheres for bone repair.” J. Appl. Oral Sci., Bauru, v. 23, no. 6, p. 599-608

CANCEILL, T. *et al,* 2023. Characterization and Safety Profile of a New Combined Advanced Therapeutic Medical Product Platelet Lysate-Based Fibrin Hydrogel for Mesenchymal Stromal Cell Local Delivery in Regenerative Medicine. *International journal of molecular sciences* 2023, *24*, doi:10.3390/ijms24032206.

CARREIRA, AC, *et al,* 2014. “Bone morphogenetic proteins: Structure, biological function and therapeutic applications” 0003-9861/2014 Published by Elsevier Inc.

CARMO, André Boziki Xavier do *et al,* 2018. Alveolar bone repair with strontium-containing nanostructured carbonated hydroxyapatite. J. Appl. Oral Sci., Bauru, v. 26, e20170084, 2018.

CHANG, I.C. *et al,* 2010. Platelet-rich fibrin modulates the expression of extracellular signal-regulated protein kinase and osteoprotegerin in human osteoblasts. *Journal of biomedical materials research Part A* 2010, *95*, 327-332.

CHANG, Y.C. *et al,* 2011. Effects of platelet-rich fibrin on human periodontal ligament fibroblasts and application for periodontal infrabony defects. *Australian dental journal* 2011, *56*, 365-371.

CHAPIN, J. *et al,* 2014. Fibrinolysis and the control of blood coagulation, Blood Rev (2014), Volume 29, Issue 1, January 2015, Pages 17-24 http://dx.doi.org/10.1016/j.blre.2014.09.003

CHENG, B. *et al,* 2022. Distinctive roles of Wnt signaling in chondrogenic differentiation of BMSCs under coupling of pressure and platelet-rich fibrin. *Tissue Engineering and Regenerative Medicine* 2022, *19*, 823-837.

CHEN, G. *et al,* 2012. TGF-β and BMP signaling in osteoblast differentiation and bone formation. International journal of biological sciences, 8(2), 272–288. https://doi.org/10.7150/ijbs.2929

CHEN, Q. *et al,* 2016. Fate decision of mesenchymal stem cells: adipocytes or osteoblasts? *Cell Death & Differentiation* 2016, *23*, 1128-1139.

CHEN, Y.-J. *et al,* 2015. Potential dental pulp revascularization and odonto-/osteogenic capacity of a novel transplant combined with dental pulp stem cells and platelet-rich fibrin. *Cell and tissue research* 2015, *361*, 439-455.

CHEN X, *et al,* 2015. Growth factor delivery systems for tissue engineering and regenerative medicine. J Control Release. 2015;219:169-80

CHI, H.; *et al*, 2019. Chitosan-gelatin scaffolds incorporating decellularized platelet-rich fibrin promote bone regeneration. *ACS Biomaterials Science & Engineering* 2019, *5*, 5305-5315.

CHO, Y.S. *et al,* 2020. Radiologic comparative analysis between saline and platelet-rich fibrin filling after hydraulic transcrestal sinus lifting without adjunctive bone graft: a randomized controlled trial. *Clinical oral implants research* 2020, *31*, 1087-1093.

CHOUKROUN, J, *et al,* 2006a. Platelet-Rich Fibrin (PRF): A Second-Generation Platelet Concentrate. Part IV: Clinical Effects on Tissue Healing. Oral surgery, oral medicine, oral pathology, oral radiology, and endodontics 101(3): e56-60.

CHOUKROUN, J, *et al,* 2006b. “Platelet-Rich Fibrin (PRF): A Second-Generation Platelet Concentrate. Part V: Histologic Evaluations of PRF Effects on Bone Allograft Maturation in Sinus Lift.” Oral surgery, oral medicine, oral pathology, oral radiology, and endodontics 101(3): 299–303.

CLIPET, F. *et al,* 2012. In vitro effects of Choukroun's platelet-rich fibrin conditioned medium on 3 different cell lines implicated in dental implantology. *Implant dentistry* 2012, *21*, 51-56.

COSTA ACF M. *et al,* 2009. Hydroxyapatite: Obtaining, characterization and applications. Magazine Electronics of Materials and Processes. 2009; 4(3):29-38.

CZEKANSKA, E M. *et al,* 2013. A phenotypic comparison of osteoblast cell lines versus human primary osteoblasts for biomaterials testing Journal of Biomedical Materials Research: Part A

DAVIS, J., Caldwell, S., E Intagliata, N. 2018. *Coagulation Pathways, Hemostasis, and Thrombosis in Liver Failure. Seminars in Respiratory and Critical Care Medicine, 39(05), 598–608.* (2018), doi:10.1055/s-0038-1673658

DE VAL J, *et al,* 2016. Influence of hydroxyapatite granule size, porosity, and crystallinity on tissue reaction in vivo. Part A: synthesis, characterization of the materials, and SEM analysis. Clin Oral Implants Res. 2016; 27 (11): 1331-8.

DE VAL J, *et al,* 2018. Influence of hydroxyapatite granule size, porosity, and crystallinity on tissue reaction in vivo. Part B: a comparative study with biphasic synthetic biomaterials. Clin Oral Implants Res. 2018 Nov; 29 (11): 1077-1084.

DIEZ-ESCUDERO, A., *et al,* 2017. *In vitro degradation of calcium phosphates: Effect of multiscale porosity, textural properties and composition. Acta Biomaterialia, 60, 81–92.* doi:10.1016/j.actbio .2017.07.033

DIMITRIOU, Rozalia *et al,* 2011 Bone regeneration: current concepts and future directions. BMC Medicine 2011, 9:66

DOHAN DM, *et al,* 2006. Platelet-rich fibrin (PRF): a second-generation platelet concentrate. Part I: technological concepts and evolution. Oral Surg Oral Med Oral Pathol Oral Radiol Endod. 2006 Mar;101(3): e37-44. doi: 10.1016/j.tripleo.2005.07.008. Epub 2006 Jan 19. PMID: 16504849.

DOHAN, DM, *et al,* 2006 c. “Platelet-Rich Fibrin (PRF): A Second-Generation Platelet Concentrate. Part III: Leucocyte Activation: A New Feature for Platelet Concentrates?” Oral surgery, oral medicine, oral pathology, oral radiology, and endodontics 101(3): e51-5.

DOHAN Ehrenfest DM, *et al,* 2018. The impact of the centrifuge characteristics and centrifugation protocols on the cells, growth factors, and fibrin architecture of a leukocyte- and platelet-rich fibrin (L-PRF) clot and membrane. Platelets. 2018 Mar;29(2):171-184. doi: 10.1080/09537104.2017.1293812. Epub 2017 Apr 24. PMID: 28437133.

DOHLE, E.; *et al,* 2018. Platelet-rich fibrin-based matrices to improve angiogenesis in an in vitro co-culture model for bone tissue engineering. *Journal of tissue engineering and regenerative medicine* 2018, *12*, 598-610.

DOUGLAS, T.E. *et al,* 2012. Enzymatically induced mineralization of platelet-rich fibrin. *Journal of Biomedical Materials Research Part A* 2012, *100*, 1335-1346.

DOROZHKIN SV. 2013. Protein interactions with calcium phosphates: mechanisms and applications. Prog Biomater. 2013;2(1):1-23.

DUAN, X. *et al,* 2018. Study of platelet-rich fibrin combined with rat periodontal ligament stem cells in periodontal tissue regeneration. *Journal of cellular and molecular medicine* 2018, *22*, 1047-1055.

E. MAVROPOULOS *et al,* 2012 "Biocompatibility of Carbonated Hydroxyapatite Nanoparticles with Different Crystallinities", Key Engineering Materials, Vols. 493-494, pp. 331-336

EHRENFEST, D.M.D. *et al,* 2009. In vitro effects of Choukroun's PRF (platelet-rich fibrin) on human gingival fibroblasts, dermal prekeratinocytes, preadipocytes, and maxillofacial osteoblasts in primary cultures. *Oral Surgery, Oral Medicine, Oral Pathology, Oral Radiology, and Endodontology* 2009, *108*, 341-352.

EHRENFEST, D.M.D. *et al,* 2010. Choukroun's platelet-rich fibrin (PRF) stimulates in vitro proliferation and differentiation of human oral bone mesenchymal stem cell in a dose-dependent way. *Archives of oral biology* 2010, *55*, 185-194.

ENKEL B. *et al,* 2008. Bioactive materials in endodontics. Expert Rev. Med. Devices. 2008; 5(4):475-494.

ESMAEILNEJAD, A. *et al,* 2023. Comparative evaluation of the effect of two platelet concentrates (a-PRF and L-PRF) on the cellular activity of pre-osteoblastic MG-63 cell line: An in vitro study. *Journal of dentistry* 2023, *24*, 235.

FARSHIDFAR, N. *et al,* 2022. The application of injectable platelet-rich fibrin in regenerative dentistry: A systematic scoping review of In vitro and In vivo studies. *Japanese Dental Science Review* 2022, *58*, 89-123.

FERNÁNDEZ-MEDINA, T. *et al,* 2019. Systematic comparison of the effect of four clinical-grade platelet rich hemoderivatives on osteoblast behaviour. *International journal of molecular sciences* 2019, *20*, 6243.

FUCHS, S. *et al,* 2010. Outgrowth endothelial cells: sources, characteristics and potential applications in tissue engineering and regenerative medicine. *Bioreactor Systems for Tissue Engineering II: Strategies for the Expansion and Directed Differentiation of Stem Cells* 2010, 201-217.

GHANAATI, S. *et al,* 2018. Fifteen years of platelet rich fibrin in dentistry and oromaxillofacial surgery: how high is the level of scientific evidence? *Journal of Oral Implantology* 2018, *44*, 471-492.

GAO C. *et al,* 2017. Bone biomaterials and interactions with stem cells. Bone Research (2017) 5, 17059-17059

GASSLING, V.L. *et al,* 2009. Platelet-rich plasma and platelet-rich fibrin in human cell culture. *Oral surgery, oral medicine, oral pathology, oral radiology, and endodontics* 2009, *108*, 48-55, doi:10.1016/j.tripleo.2009.02.007.

GASSLING, V. *et al,* 2010. Platelet-rich fibrin membranes as scaffolds for periosteal tissue engineering. *Clinical oral implants research* 2010, *21*, 543-549.

GASSLING, V. *et al,* 2013. Magnesium-enhanced enzymatically mineralized platelet-rich fibrin for bone regeneration applications. *Biomedical Materials* 2013, *8*, 055001.

GASSLING, V. *et al,* 2013. Comparison of platelet rich fibrin and collagen as osteoblast-seeded scaffolds for bone tissue engineering applications. *Clinical oral implants research* 2013, *24*, 320-328.

GIRIJA, K. E Kavitha, M. 2020. Comparative evaluation of platelet-rich fibrin, platelet-rich fibrin+ 50 wt% nanohydroxyapatite, platelet-rich fibrin+ 50 wt% dentin chips on odontoblastic differentiation-An in vitro study-part 2. *Journal of Conservative Dentistry: JCD* 2020, *23*, 354.

GLOBAL INDUSTRY ANALYSTS, Inc. 2016. “Bone Grafts (MCP-1637) - Global Industry Analysts, Inc.” http://www.strategyr.com/MCP1637.asp#sthash. JXus3mzP.dpbs.

GONDA Y, *et al,* 2009. Stimulatory effect of hydrothermally synthesized biodegradable hydroxyapatite granules on osteogenesis and direct association with osteoclasts. Biomaterials. 2009; 30 (26): 4390-400.

GUPTA, Anil Kumar, *et al,* 2015. Hydroxyapatite Crystals as a Bone Graft Substitute in Benign Lytic Lesions of Bone. *Indian Journal of Orthopedics* 49 (6). Wolters Kluwer -- Medknow Publications: 649–55. doi:10.4103/0019-5413.168767.

GREEN, D. 2006. *Coagulation cascade. Hemodialysis International, 10(S2), S2–S4.* (2006). doi:10.1111/j.1542-4758. 2006.00119.x

HABIBOVIC, Pamela, *et al,* 2010. Comparison of Two Carbonated Apatite Ceramics in Vivo.” *Acta Biomaterialia* 6(6):2219–26. doi:10.1016/j.actbio.2009.11.028.

HAN, Y. *et al,* 2018. Paracrine and endocrine actions of bone—the functions of secretory proteins from osteoblasts, osteocytes, and osteoclasts. *Bone research* 2018, *6*, 16.

HE, L. *et al,* 2009. A comparative study of platelet-rich fibrin (PRF) and platelet-rich plasma (PRP) on the effect of proliferation and differentiation of rat osteoblasts in vitro. *Oral Surgery, Oral Medicine, Oral Pathology, Oral Radiology, and Endodontology* 2009, *108*, 707-713.

HONG, S. *et al,* 2018. A Comparative Evaluation of Concentrated Growth Factor and Platelet-rich Fibrin on the Proliferation, Migration, and Differentiation of Human Stem Cells of the Apical Papilla. *J Endod* 2018, *44*, 977-983, doi:10.1016/j.joen.2018.03.006.

HOLZAPFEL BM; *et al,* 2012. DW How smart do biomaterials need to be? A translational science and clinical point of view.Advanced Drug Delivery Reviews. 2012; 65(4):1-23.

HOOK AL; *et al,* 2010. MR High throughput methods applied in biomaterial development and discovery. Biomaterials 2010; 31:187–198.

HUANG, F.M. *et al,* 2010. Platelet-rich fibrin increases proliferation and differentiation of human dental pulp cells. *J Endod* 2010, *36*, 1628-1632, doi:10.1016/j.joen.2010.07.004.

iData research 2023 - Taxa de crescimento anual composta mais elevada durante o período de 2023 a 2027

IRASTORZA, I. *et al,* 2019. Adhesion, integration and osteogenesis of human dental pulp stem cells on biomimetic implant surfaces combined with plasma derived products. *European cells & materials* 2019, *38*, 201-214, doi:10.22203/eCM.v038a14.

ISOBE, K. *et al,* 2017. Platelet-rich fibrin prepared from stored whole-blood samples. *Int J Implant Dent* 2017, *3*, 6, doi:10.1186/s40729-017-0068-4.

JANN, J. *et al,* 2020. Influence of the TGF-β Superfamily on Osteoclasts/Osteoblasts Balance in Physiological and Pathological Bone Conditions. *International journal of molecular sciences* 2020, *21*, doi:10.3390/ijms21207597.

JANIS, J. E., E Harrison, B. 2016. *Wound Healing. Plastic and Reconstructive Surgery, 138, 9S–17S.* doi:10.1097/prs.0000000000002773

JI, B. *et al,* 2015. The combination use of platelet-rich fibrin and treated dentin matrix for tooth root regeneration by cell homing. *Tissue engineering. Part A* 2015, *21*, 26-34, doi:10.1089/ten.tea.2014.0043.

JO, S. *et al,* 2018. Identification and characterization of human bone-derived cells. *Biochemical and biophysical research communications* 2018, *495*, 1257-1263, doi:10.1016/j.bbrc.2017.11.155.

Junqueira e Carneiro. Histologia Básica. 11°edição, editora Guanabara, 2008 p. (6) 136-142. 2013

KANG, Y.H. *et al,* 2011. Platelet-rich fibrin is a Bioscaffold and reservoir of growth factors for tissue regeneration. *Tissue engineering. Part A* 2011, *17*, 349-359, doi:10.1089/ten.TEA.2010.0327.

KARDOS, D. *et al,* 2018. Biological and Mechanical Properties of Platelet-Rich Fibrin Membranes after Thermal Manipulation and Preparation in a Single-Syringe Closed System. *International journal of molecular sciences* 2018, *19*, doi:10.3390/ijms19113433.

KIM, J.; *et al,* 2017. Effects of Growth Factors From Platelet-Rich Fibrin on the Bone Regeneration. *The Journal of craniofacial surgery* 2017, *28*, 860-865, doi:10.1097/scs.0000000000003396.

KIM, J.H. *et al,* 2017. Effect of Platelet-rich Fibrin on Odontoblastic Differentiation in Human Dental Pulp Cells Exposed to Lipopolysaccharide. *J Endod* 2017, *43*, 433-438, doi:10.1016/j.joen.2016.11.002.

KOLMAS, J. *et al,* 2017. *Effect of carbonate substitution on physicochemical and biological properties of silver containing hydroxyapatites. Materials Science and Engineering: C, 74, 124–130.* doi:10.1016/j.msec .2017.01.003

KOSMIDIS, K. *et al,* 2023. An in vitro study into three different PRF preparations for osteogenesis potential. *Journal of periodontal research* 2023, *58*, 483-492.

KOYANAGI, M. *et al,* 2021. Regenerative Potential of Solid Bone Marrow Aspirate Concentrate Compared with Platelet-Rich Fibrin. *Tissue engineering. Part A* 2022, *28*, 749-759, doi:10.1089/ten.TEA.2021.0225.

KYYAK, S. *et al,* 2020. Combination of an allogenic and a xenogenic bone substitute material with injectable platelet-rich fibrin - A comparative in vitro study. *Journal of biomaterials applications* 2020, *35*, 83-96, doi:10.1177/0885328220914407.

KYYAK, S. *et al,* 2021. Activation of Human Osteoblasts via Different Bovine Bone Substitute Materials With and Without Injectable Platelet Rich Fibrin in vitro. *Front Bioeng Biotechnol* 2021, *9*, 599224, doi:10.3389/fbioe.2021.599224.

LAI, F. *et al,* 2018. Platelet-rich plasma enhances the proliferation of human adipose stem cells through multiple signaling pathways. *Stem cell research & therapy* 2018, *9*, 107, doi:10.1186/s13287-018-0851-z.

LEI, F. *et al,* 2022. Treatment of inflammatory bone loss in periodontitis by stem cell-derived exosomes. *Acta Biomater* 2022, *141*, 333-343, doi:10.1016/j.actbio.2021.12.035.

LEE, Esther J. *et al,* 2014. Biomaterials for Tissue Engineering Ann Biomed Eng. 2014 February; 42(2): 323–337. doi:10.1007/s10439-013-0859-6.

LI, Q. *et al,* 2013. Platelet-rich fibrin promotes periodontal regeneration and enhances alveolar bone augmentation. *BioMed research international* 2013, *2013*, 638043, doi:10.1155/2013/638043.
LI, Q. *et al,* 2014. Lyophilized platelet-rich fibrin (PRF) promotes craniofacial bone regeneration through Runx2. *International journal of molecular sciences* 2014, *15*, 8509-8525, doi:10.3390/ijms15058509.

LI, X. *et al,* 2018. Platelet-rich fibrin exudate promotes the proliferation and osteogenic differentiation of human periodontal ligament cells in vitro. *Molecular medicine reports* 2018, *18*, 4477-4485, doi:10.3892/mmr.2018.9472.

LI, X. *et al,* 2018. Roles of PRF and IGF-1 in promoting alveolar osteoblast growth and proliferation and molecular mechanism. *Int J Clin Exp Pathol* 2018, *11*, 3294-3301.

LIANG, Z. *et al,* 2021. Advanced-platelet-rich fibrin extract promotes adipogenic and osteogenic differentiation of human adipose-derived stem cells in a dose-dependent manner in vitro. *Tissue & cell* 2021, *71*, 101506, doi:10.1016/j.tice.2021.101506.

LI, B, *et al,* 2009. Fabrication and Cellular Biocompatibility of Porous Carbonated Biphasic Calcium Phosphate Ceramics with a Nanostructure. *Acta Biomaterialia* 5 (1): 134–43. doi:10.1016/j.actbio.2008.07.035.

LIMA BARBOSA, R. de *et al,* 2023. The Effects of Platelet-Rich Fibrin in the Behavior of Mineralizing Cells Related to Bone Tissue Regeneration—A Scoping Review of In Vitro Evidence. J. Funct. Biomater. 2023, 14, 503. https://doi.org/10.3390/jfb14100503

LIU, Z. *et al,* 2019. Controlled Release Strategies for the Combination of Fresh and Lyophilized Platelet-Rich Fibrin on Bone Tissue Regeneration. *BioMed research international* 2019, *2019*, 4923767, doi:10.1155/2019/4923767.

LIU, X. *et al,* 2022. Genipin modified lyophilized platelet-rich fibrin scaffold for sustained release of growth factors to promote bone regeneration. *Frontiers in Physiology* 2022, *13*, 1007692.

LIU, Q. *et al,* 2020. Recent Advances of Osterix Transcription Factor in Osteoblast Differentiation and Bone Formation. *Front Cell Dev Biol* 2020, *8*, 601224, doi:10.3389/fcell.2020.601224.

LIU, M.M. *et al,* 2021. Dentine sialophosphoprotein signal in dentineogenesis and dentine regeneration. *European cells & materials* 2021, *42*, 43-62, doi:10.22203/eCM.v042a04.

LO MONACO, M. *et al,* 2020. Therapeutic Potential of Dental Pulp Stem Cells and Leukocyte- and Platelet-Rich Fibrin for Osteoarthritis. *Cells* 2020, *9*, doi:10.3390/cells9040980.

LOURENÇO ES, *et al,* 2018. The *in vitro* release of cytokines and growth factors from fibrin membranes produced through horizontal centrifugation. J Biomed Mater Res Part A 2018:106A:1373–1380.

LOURENÇO, E.S. *et al,* 2021. Effects of rotor angle and time after centrifugation on the biological in vitro properties of platelet rich fibrin membranes. *Journal of biomedical materials research. Part B, Applied biomaterials* 2021, *109*, 60-68, doi:10.1002/jbm.b.34680.

MAHENDRAN, K. *et al,* 2019. Comparative evaluation of radiopacity and cytotoxicity of platelet-rich fibrin, platelet-rich fibrin + 50wt% nano-hydroxyapatite, platelet-rich fibrin + 50wt% dentin chips: An in vitro study. *Journal of conservative dentistry : JCD* 2019, *22*, 28-33, doi:10.4103/jcd.Jcd_281_18.

MARCHETTI, E. *et al,* 2020. Evaluation of Different Autologous Platelet Concentrate Biomaterials: Morphological and Biological Comparisons and Considerations. *Materials (Basel, Switzerland)* 2020, *13*, doi:10.3390/ma13102282.

MARX RE, *et al,* 1998. Platelet-rich plasma: growth factor enhancement for bone grafts. OralSurg, OralMed, OralPathol, OralRadiol, Endod 85(6):638–646

MCGOWAN, J. *et al,* 2020. Reporting scoping reviews-PRISMA ScR extension. *J Clin Epidemiol* 2020, *123*, 177-179, doi:10.1016/j.jclinepi.2020.03.016.

MAVROPOULOS E, *et al,* 2010. Adsorption and bioactivity studies of albumin onto hydroxyapatite surface Colloids and Surfaces B: Biointerfaces 83 (2011) 1–9

MIRON, R.J. *et al,* 2017. Use of platelet-rich fibrin in regenerative dentistry: a systematic review. *Clinical oral investigations* 2017, *21*, 1913-1927, doi:10.1007/s00784-017-2133-z.

MORADIAN, H. *et al,* 2017. Design and Fabrication of a Novel Transplant Combined with Human Bone Marrow Mesenchymal Stem Cells and Platelet-rich Fibrin: New Horizons for Periodontal Tissue Regeneration after Dental Trauma. *Iran J Pharm Res* 2017, *16*, 1370-1378.

MOURÃO CF, *et al,* 2018. Characterization of a new membrane from concentrated growth factors associated with denaturized albumin (Alb -Cgf) for clinical applications: A preliminary study. Int J Growth Factors Stem Cells Dent 0;0:0 .

MOURÃO, CF, *et al,* 2018. Does the association of blood-derived growth factors to nanostructured carbonated hydroxyapatite contribute to the maxillary sinus floor elevation? A randomized clinical trial. Clinical Oral Investigations

MOURÃO, CF, *et al,* 2018. The use of platelet – rich fibrin as a hemostatic material in oral soft tissues. Oral and Maxillofacial Surgery https://doi.org/10.1007/s10006-018-0708-8

MURPHY, Ciara M. et al. 2013 Cell-scaffold interactions in the bone tissue engineering triad. European Cells and Materials Vol. 26 2013 (pages 120-132)

NGUYEN, M. *et al,* 2022. Effects of advanced platelet-rich fibrin combined with xenogenic bone on human periodontal ligament stem cells. *Clin Exp Dent Res* 2022, *8*, 875-882, doi:10.1002/cre2.563.

NIU, B. *et al,* 2017. In vitro evaluation of electrospun silk fibroin/nano-hydroxyapatite/BMP-2 scaffolds for bone regeneration. *Journal of biomaterials science. Polymer edition* 2017, *28*, 257-270, doi:10.1080/09205063.2016.1262163.

NIE, J. *et al,* 2020. Electrospinning With Lyophilized Platelet-Rich Fibrin Has the Potential to Enhance the Proliferation and Osteogenesis of MC3T3-E1 Cells. *Front Bioeng Biotechnol* 2020, *8*, 595579, doi:10.3389/fbioe.2020.595579.

NUGRAHA, A. *et al,* 2018. Osteogenic potential of gingival stromal progenitor cells cultured in platelet rich fibrin is predicted by core-binding factor subunit-α1/Sox9 expression ratio (in vitro). *F1000Research* 2018, *7*, 1134, doi:10.12688/f1000research.15423.1.

NUGRAHA, A. *et al,* 2018. In vitro bone sialoprotein-I expression in combined gingival stromal progenitor cells and platelet rich fibrin during osteogenic differentiation. *Tropical Journal of Pharmaceutical Research* 2018, *17*, 2341-2345, doi:10.4314/tjpr.v17i12.4.

NUGRAHA, A.P. *et al,* 2018. Bone alkaline phosphatase and osteocalcin expression of rat's Gingival mesenchymal stem cells cultured in platelet-rich fibrin for bone remodeling (in vitro study). *European journal of dentistry* 2018, *12*, 566-573, doi:10.4103/ejd.ejd_261_18.

NUGRAHA, A. *et al,* 2019. The Aggrecan Expression Post Platelet Rich Fibrin Administration in Gingival Medicinal Signaling Cells in Wistar Rats (Rattus

novergicus) During the Early Osteogenic Differentiation (In Vitro). *Kafkas Universitesi Veteriner Fakultesi Dergisi* 2019.

PEPLA, Erlind, *et al,* 2014. Nano-Hydroxyapatite and Its Applications in Preventive, Restorative and Regenerative Dentistry: A Review of Literature. Annali Di Stomatologia 5 (3). CIC Editori Internazionali: 108–14.

PATEL, G.K. *et al,*2017. Platelet-Rich Fibrin in Regeneration of Intrabony Defects: A Randomized Controlled Trial. *Journal of periodontology* 2017, *88*, 1192-1199, doi:10.1902/jop.2017.130710.

POLYMERI, A. *et al,* 2016. Bone Marrow Stromal Stem Cells in Tissue Engineering and Regenerative Medicine. *Horm Metab Res* 2016, *48*, 700-713, doi:10.1055/s-0042-118458.

RAINA, DB, *et al,* 2016. Muscle as an Osteoinductive Niche for Local Bone Formation with the Use of a Biphasic Calcium Sulphate / hydroxyapatite Biomaterial. *Bone & Joint Research* 5 (10). British Editorial Society of Bone and Joint Surgery: 500–511. doi:10.1302/2046-3758.510.BJR -2016-0133.R1.

RAHAVI SS, *et al, 2017*. A comparative study on physicochemical properties of hydroxyapatite powders derived from natural and synthetic sources. Russ Non-Fer Met. 2017; 58 (3): 276-86.

RASTEGAR, A. *et al,* 2021. Platelet-rich fibrin-loaded PCL/chitosan core-shell fibers scaffold for enhanced osteogenic differentiation of mesenchymal stem cells. *Carbohydrate polymers* 2021, *269*, 118351, doi:10.1016/j.carbpol.2021.118351.

REIS, N.T.d.A. *et al,* 2022. Use of platelet-rich fibrin for bone repair: a systematic review and meta-analysis of preclinical studies. *Brazilian Oral Research* 2022, *36*.

SADAT-SHOJAI M, *et al,* 2013. Synthesis methods for nanosized hydroxyapatite with diverse structures. Acta Biomater. 2013; 9 (8): 7591-621.)

S. BOSE *et al,* 2017. Carbonated hydroxyapatite spheres: A novel injectable scaffold for bone tissue engineering. Journal of Biomedical Materials Research Part A, vol. 105, no. 4, pp. 1110-1120, 2017.

SCHNEIDER, K. *et al,* 2009. "ToxRTool", a new tool to assess the reliability of toxicological data. *Toxicol Lett* 2009, *189*, 138-144, doi:10.1016/j.toxlet.2009.05.013.

SHIRAKATA Y, *et al,* 2021. Histological Evaluation of Gingival and Intrabony Periodontal Defects Treated with Platelet-rich Fibrin Using Different Protocols: A Canine Study. Oral Health 88 Prev Dent [Internet]. 2021 https://pubmed.ncbi.nlm.nih.gov/34673845/

SHIVASHANKAR, V.Y. *et al,* 2013. Combination of platelet rich fibrin, hydroxyapatite and PRF membrane in the management of large inflammatory periapical lesion. *Journal of conservative dentistry : JCD* 2013, *16*, 261-264, doi:10.4103/0972-0707.111329.

SHAH, R. *et al,* 2021. In Vitro Evaluation of Osteoblast Response to the Effect of Injectable Platelet-rich Fibrin Coating on Titanium Disks. *The journal of contemporary dental practice* 2021, *22*, 107-110.

SILVA, JM, *et al,* 2020. Cytotoxicity of platelet-rich fibrin on human osteoblasts is associated with increased production of inflammatory mediators. Journal of Biomedical Materials Research Part A, 108(2), 406-415.

SONG, Y. *et al,* 2018. Nano-biphasic calcium phosphate/polyvinyl alcohol composites with enhanced bioactivity for bone repair via low-temperature three-dimensional printing and loading with platelet-rich fibrin. *Int J Nanomedicine* 2018, *13*, 505-523, doi:10.2147/ijn.S152105.

STAEHLKEA, S, *et al,* 2018. Phenotypic stability of the human MG-63 osteoblastic cell line at different passages Cell Biology International doi: 10.1002/cbin.11072

STELLER, D. *et al,* 2019. Positive impact of Platelet-rich plasma and Platelet-rich fibrin on viability, migration and proliferation of osteoblasts and fibroblasts treated with zoledronic acid. *Scientific reports* 2019, *9*, 8310, doi:10.1038/s41598-019-43798-z.

STELLER, D. *et al,* 2019. Impacts of platelet-rich fibrin and platelet-rich plasma on primary osteoblast adhesion onto titanium implants in a bisphosphonate in vitro model. *J Oral Pathol Med* 2019, *48*, 943-950, doi:10.1111/jop.12944.

STRAUSS, F.-J. *et al,* 2020. Effect of platelet-rich fibrin on cell proliferation, migration, differentiation, inflammation, and osteoclastogenesis: a systematic review of in vitro studies. *Clinical oral investigations* 2020, *24*, 569-584.

SUI, X. *et al,* 2023. 3D printing of ‘green’thermo-sensitive chitosan-hydroxyapatite bone scaffold based on lyophilized platelet-rich fibrin. *Biomedical Materials* 2023, *18*, 025022.

TANAKA, Y. *et al,* 2005. Osteoblasts and osteoclasts in bone remodeling and inflammation. *Curr Drug Targets Inflamm Allergy* 2005, *4*, 325-328, doi:10.2174/1568010054022015.

TATTERSALL, L, *et al,* 2019. Encyclopedia of Bone Biology https://doi.org/10.1016/B978-0-12-801238-3.62259-6 1

THANASRISUEBWONG, P. *et al,* 2020. Red and Yellow Injectable Platelet-Rich Fibrin Demonstrated Differential Effects on Periodontal Ligament Stem Cell Proliferation, Migration, and Osteogenic Differentiation. *International journal of molecular sciences* 2020, *21*, doi:10.3390/ijms21145153.

VALIENSE H, *et al,* 2016. *In vitro* and *in vivo* evaluation of strontium - containing nanostructured carbonated hydroxyapatite/sodium alginate for sinus lift in rabbits. *J Biomed Mater Res Part B* 2016:103B:274–282.

VERBOKET, R. *et al,* 2019. Influence of concentration and preparation of platelet rich fibrin on human bone marrow mononuclear cells (in vitro). *Platelets* 2019, *30*, 861-870, doi:10.1080/09537104.2018.1530346.

WANG, P.-H. *et al,* 2018. Wound healing. Journal of the Chinese Medical Association, 81(2), 94–101. doi: 10.1016/j.jcma .2017.11.002

WANG, Y. *et al,* 2019. The hypoxia-inducible factor α pathway couples' angiogenesis to osteogenesis during skeletal development. Journal of Clinical Investigation, 117(6), 1616-1626.

WANG, Z. *et al,* 2015. Osteoblastic mesenchymal stem cell sheet combined with Choukroun platelet-rich fibrin induces bone formation at an ectopic site. *Journal of biomedical materials research. Part B, Applied biomaterials* 2015, *103*, 1204-1216, doi:10.1002/jbm.b.33288.

WANG, Z. *et al,* 2019. Preparation and effect of lyophilized platelet-rich fibrin on the osteogenic potential of bone marrow mesenchymal stem cells in vitro and in vivo. *Heliyon* 2019, *5*, e02739, doi:10.1016/j.heliyon.2019.e02739.

WANG, X. *et al,* 2018. Effects of an injectable platelet-rich fibrin on osteoblast behavior and bone tissue formation in comparison to platelet-rich plasma. *Platelets* 2018, *29*, 48-55, doi:10.1080/09537104.2017.1293807.

WANG, J. *et al,* 2022. Effects of platelet-rich fibrin on osteogenic differentiation of Schneiderian membrane derived mesenchymal stem cells and bone formation in maxillary sinus. *Cell Communication and Signaling* 2022, *20*, 88.

WANG, J. *et al,* 2023. Injectable platelet-rich fibrin positively regulates osteogenic differentiation of stem cells from implant hole via the ERK1/2 pathway. *Platelets* 2023, *34*, 2159020.

WONG, P.C. *et al,* 2021. Large-Pore Platelet-Rich Fibrin with a Mg Ring to Allow MC3T3-E1 Preosteoblast Migration and to Improve Osteogenic Ability for Bone

Defect Repair. *International journal of molecular sciences* 2021, *22*, doi:10.3390/ijms22084022.

WONG, C.C. *et al,* 2021. Effectiveness of treating segmental bone defects with a synergistic co-delivery approach with platelet-rich fibrin and tricalcium phosphate. *Materials science & engineering. C, Materials for biological applications* 2021, *129*, 112364, doi:10.1016/j.msec.2021.112364.

WOO, S.M. *et al,* 2016. Combination of Mineral Trioxide Aggregate and Platelet-rich Fibrin Promotes the Odontoblastic Differentiation and Mineralization of Human Dental Pulp Cells via BMP/Smad Signaling Pathway. *J Endod* 2016, *42*, 82-88, doi:10.1016/j.joen.2015.06.019.

WU, C.L. *et al,*2012. Platelet-rich fibrin increases cell attachment, proliferation and collagen-related protein expression of human osteoblasts. *Aust Dent J* 2012, *57*, 207-212, doi:10.1111/j.1834-7819.2012.01686.x.

YAO, Fang, *et al,* 2009. Simultaneous Incorporation of Carbonate and Fluoride in Synthetic Apatites: Effect on Crystallographic and Physico -Chemical Properties. *Acta Biomaterialia* 5 (6). Elsevier: 2169–77. doi:10.1016/J.ACTBIO.2009.02.007.

YU, J. *et al,* 2016. Platelet-rich fibrin as a scaffold in combination with either deciduous or permanent dental pulp cells for bone tissue engineering. 2016, *9*, 15177-15184.

ZAMBUZZI, Willian F. *et al,* 2011. Biological Behavior of Pre-Osteoblasts on Natural Hydroxyapatite: A Study of Signaling Molecules from Attachment to Differentiation. Journal of Biomedical Materials Research Part A 97A (2): 193–200. doi:10.1002/jbm.a.32933.

ZANETTI, A.S. *et al,* 2013. Human adipose-derived stem cells and three-dimensional scaffold constructs: a review of the biomaterials and models currently used for bone regeneration. *Journal of biomedical materials research. Part B, Applied biomaterials* 2013, *101*, 187-199, doi:10.1002/jbm.b.32817

ZHANG, L. *et al,* 2019. Multifunctional Triple-Layered Composite Scaffolds Combining Platelet-Rich Fibrin Promote Bone Regeneration. *ACS Biomater Sci Eng* 2019, *5*, 6691-6702, doi:10.1021/acsbiomaterials.9b01022.

ZHANG, J. *et al,* 2023. Platelet-rich Fibrin Promotes the Proliferation and Osteo-/odontoblastic Differentiation of Human Dental Pulp Stem Cells. *Curr Stem Cell Res Ther* 2023, *18*, 560-567, doi:10.2174/1574888x17666220704092411.

ZHAO, Y.H. *et al,* 2013. The combined use of cell sheet fragments of periodontal ligament stem cells and platelet-rich fibrin granules for avulsed tooth reimplantation. *Biomaterials* 2013, *34*, 5506-5520, doi:10.1016/j.biomaterials.2013.03.079.

ZHENG, L. *et al,* 2015. New Biodegradable Implant Material Containing Hydrogel with Growth Factors of Lyophilized PRF in Combination with an nHA/PLGA Scaffold. *Journal of Hard Tissue Biology* 2015, *24*, 54-60, doi:10.2485/jhtb.24.54.

ZHENG, S. *et al,* 2020. Liquid platelet-rich fibrin promotes the regenerative potential of human periodontal ligament cells. *Oral diseases* 2020, *26*, 1755-1763, doi:10.1111/odi.13501.

ZOU, M.L. *et al,* 2021. The Smad Dependent TGF-β and BMP Signaling Pathway in Bone Remodeling and Therapies. *Front Mol Biosci* 2021, *8*, 593310, doi:10.3389/fmolb.2021.593310.

1 ANEXO I

UFF - HOSPITAL UNIIVERSITÁRIO ANTÔNIO PEDRO / FACULDADE DE

PARECER CONSUBSTANCIADO DO CEP

DADOS DO PROJETO DE PESQUISA

Título da Pesquisa: Desenvolvimento de novos materiais para tratamento ósseo a partir de derivados de sangue humano

Pesquisador: Gutemberg Gomes Alves

Área Temática:

Versão: 3

CAAE: 12126919.7.0000.5243

Instituição Proponente: Instituto de Biologia-UFF

Patrocinador Principal: Financiamento Próprio

DADOS DO PARECER

Número do Parecer: 3.432.068

Apresentação do Projeto:

A bioengenharia tem sido amplamente utilizada como ferramenta para estratégias terapêuticas envolvendo tecidos ósseos. Neste intuito, células humanas são associadas a fatores de crescimento e a arcabouços compostos por biomateriais compatíveis para promover a regeneração tecidual. O pesquisador tem desenvolvido com seu grupo de pesquisa microesferas de carbonatoapatita nanoestruturada (nCHA) como meio para obter uma estrutura altamente bioabsorvível, permitindo substituição por osso novo regenerado. A associação à moléculas capazes de induzir a diferenciação óssea, representadas por fatores de crescimento representa custo elevado. Por outro lado, a Fibrina Rica em Plaquetas (PRF) é um biomaterial autólogo produzido a partir de sangue total humano, com comprovada capacidade de produzir/liberar fatores ativadores do reparo tecidual. O presente projeto propõe o estudo da associação de esferas de carbonatoapatita a membranas de PRF. Será coletado o sangue venoso de 20 voluntários saudáveis. Essas amostras passarão por um processamento para produção de derivados plaquetários autólogos, os quais serão submetidos a uma série de testes estruturais, de estabilidade e de biocompatibilidade in vitro, gerando dados preditivos de sua eficácia em futuros estudos clínicos. Para isso, investigarão: (i) se a associação de cHA e PRF afeta as caraterísticas estruturais de ambos os materiais, através de estudos de microscopia eletrônica e de fluorescência; (ii) se o biomaterial resultante é capaz de produzir/liberar fatores de crescimento e citocinas relevantes para o reparo ósseo, quando imerso em meio de cultura; e (iii) se osteoblastos

Endereço: Rua Marquês de Paraná, 303 - 4º Andar (Prédio Anexo)
Bairro: Centro **CEP:** 24.033-900
UF: RJ **Município:** NITEROI
Telefone: (21)2629-9189 **Fax:** (21)2629-9189 **E-mail:** etica@vm.uff.br

humanos são afetados positivamente por estes fatores, através de ensaios de proliferação e diferenciação. Ainda, o presente projeto propõe também investigar tais efeitos biológicos em membranas de PRF produzidas por meio de um protocolo modificado que inclui a associação a um gel de albumina de plasma ativado (APAG), capaz de estabilizar o arcabouço de fibrina para aplicações que requerem maior estabilidade da matriz. Esperamos que esta pesquisa de forte viés translacional e interdisciplinar permita o desenvolvimento de biomateriais autólogos de baixo custo para aplicações clínicas que demandem a regeneração de tecido ósseo, com alto impacto científico-tecnológico e social, contribuindo para a melhora na qualidade de vida da população.

Critério de Inclusão:
Indivíduos maiores de idade, entre 18 e 69 anos, saudáveis de acordo com os critérios de doação de sangue do Ministério da Saúde (pesando mais de 50 kg, e declarando com sensação de bem-estar) e fora de condição de risco social.
Critério de Exclusão:
Serão excluídos indivíduos: que tenham doado sangue recentemente (60 dias para homens, 90 dias para mulheres); com histórico de diabetes; que estejam sob tratamentos anticoagulantes; que tenham diagnóstico de hepatite após os 11 anos de idade; mulheres grávidas ou que estejam amamentando; pessoas que estejam expostas a doenças transmissíveis pelo sangue, como aids, hepatite, sífilis e doença de Chagas.

Objetivo da Pesquisa:
Os objetivos declarados da pesquisa são:
"Objetivo Primário:
Avaliar in vitro as propriedades biológicas de novos arcabouços autólogos de fibrina para aplicações em terapia óssea, associados a biomateriais tais como esferas de nano carbonatoapatita (CHA) e Gel de Albumina Plasmática Termicamente Ativada.

Objetivo Secundário:
1. Padronizar um protocolo de produção de membranas de PRF/albumina/CHA."

Avaliação dos Riscos e Benefícios:
O pesquisador apresenta como riscos e benefícios:
*RISCOS: "Os riscos aos participantes são os mesmos vinculados à doação voluntária de sangue, e

não serão aumentados pela participação na presente pesquisa. A quebra de sigilo das informações colhidas no questionário pode se configurar como um risco para os participantes. As cautelas e providências que serão adotadas para evitar a identificação dos participantes da pesquisa, garantindo seu anonimato, incluem: a) codificação imediata das amostras no ato da coleta; antes do envio ao laboratório; b) arquivamento do TCLE e dados secundários que venham a ser coletados será realizado em uma sala de arquivos apropriada, com controle de acesso e vigiada por câmera, presente no local da Pesquisa (Unidade de Pesquisa Clínica)."

*BENEFÍCIOS: "A pesquisa não trará benefícios diretos aos participantes. Os benefícios à sociedade, por outro lado, se caracterizam pela possibilidade de desenvolver novos biomateriais autólogos para tratamento de defeitos ósseos,de baixíssimo custo e fácil produção, com potencial impacto na qualidade de vida de indivíduos com problemas ósseos."

Riscos e benefícios da pesquisa bem descritos.

Comentários e Considerações sobre a Pesquisa:

A proposta de pesquisa apresentada tem grande relevância acadêmica uma vez que pretende desenvolver novos biomateriais, associando malha densa de fibrina autóloga a albumina sérica desnaturada e/ou a esferas de carbonatoapatita, que apresentem maior extensão e alta estabilidade, capazes de atuar postivamente sobre células ósseas.

Após cumprimento de todas as pendências, este colegiado entende que a proposta do projeto apresenta-se adequada em todos os aspectos considerados e sobre os quais foram solicitados esclarecimentos.

A equipe de pesquisa inserida nas informações básicas do projeto na Plataforma Brasil corresponde exatamente àquela apresentada no projeto.

Desenho de estudo corretamente definido.

Riscos e benefícios muito bem reelaborados.

A hipótese bem elaborada.

Tamanho amostral adequado à proposta.

Os critérios de inclusão e exclusão bem definidos.

A metodologia proposta adequada.

Metodologia de Análise de Dados bem descrita e adequada.

O TCLE foi ajustado e está bem estruturado.

O cronograma adequado à proposta.

O pesquisador apresentou orçamento financeiro coerente com as análises a serem realizadas.

Considerações sobre os Termos de apresentação obrigatória:

Sobre os termos de apresentação obrigatória, foram apresentados os documentos:

- Carta de anuência assinada pelo diretor Acadêmico HUAP/EBSERH
- Folha de rosto: devidamente assinada;
- termo de Biorrepositório: devidamente apresentado;
- TCLE: adequado.

Conclusões ou Pendências e Lista de Inadequações:

O projeto foi considerado aprovado por este Colegiado.

Considerações Finais a critério do CEP:

Este parecer foi elaborado baseado nos documentos abaixo relacionados:

Tipo Documento	Arquivo	Postagem	Autor	Situação
Informações Básicas do Projeto	PB_INFORMAÇÕES_BÁSICAS_DO_PROJETO_1117184.pdf	01/07/2019 15:00:06		Aceito
Outros	Carta_ao_CEP.pdf	29/05/2019	Gutemberg Gomes	Aceito

Endereço: Rua Marquês de Paraná, 303 - 4º Andar (Prédio Anexo)
Bairro: Centro **CEP:** 24.033-900
UF: RJ **Município:** NITEROI
Telefone: (21)2629-9189 **Fax:** (21)2629-9189 **E-mail:** etica@vm.uff.br

Outros	Carta_ao_CEP.pdf	21:15:20	Alves	Aceito
Projeto Detalhado / Brochura Investigador	Projeto_Plataforma_Brasil.docx	29/05/2019 21:11:59	Gutemberg Gomes Alves	Aceito
TCLE / Termos de Assentimento / Justificativa de Ausência	TCLE.pdf	29/05/2019 21:09:04	Gutemberg Gomes Alves	Aceito
Folha de Rosto	Folha_de_rosto.pdf	25/03/2019 20:14:48	Gutemberg Gomes Alves	Aceito
Declaração de Instituição e Infraestrutura	declaracao.pdf	14/03/2019 15:30:48	Gutemberg Gomes Alves	Aceito
Declaração de Manuseio Material Biológico / Biorepositório / Biobanco	estabelecimentodebiorrepositorio.pdf	14/03/2019 15:21:13	Gutemberg Gomes Alves	Aceito
Cronograma	Cronograma.docx	12/03/2019 14:28:01	Gutemberg Gomes Alves	Aceito

Situação do Parecer:
Aprovado

Necessita Apreciação da CONEP:
Não

NITEROI, 02 de Julho de 2019

Assinado por:
José Carlos Carraro Eduardo
(Coordenador(a))

2 Anexo II

Original Article

Characterization of a New Membrane from Concentrated Growth Factors Associated with Denaturized Albumin (Alb-CGF) for Clinical Applications: A Preliminary Study

Carlos Fernando de Almeida Barros Mourão[1,2,3], Ezio Gheno[2], Emanuelle Stellet Lourenço[1], Renata de Lima Barbosa[1], Gregori M. Kurtzman[4], Kayvon Javid[4], Elena Mavropoulos[5], Stefano Benedicenti[2], Mônica Diuana Calasans-Maia[3], Rafael Coutinho de Mello Machado[3], Gutemberg Gomes Alves[1]

[1]Department of Molecular and Cell Biology, Institute of Biology, Fluminense Federal University, Brazil, [2]Department of Surgical Sciences and Integrated Diagnostics, University of Genova, Genova, Italy, [3]Department of Oral Surgery, Dentistry School, Federal Fluminense University, Niterói, Brazil, [4]Private Clinical Practice, United States, [5]Brazilian Center for Physics Research, Rio De Janeiro, Brazil

Abstract

Background: One of the main issues pertaining to the use of fibrin membranes today, is their clinical efficacy for guided bone regeneration. This requires the need for membrane stability and a controlled resorption that enables the barrier to remain functionally during a relevant clinical time span. Human serum albumin is known to have an impact in the formation and stability of the fibrin networks density and permeability. Therefore, its interaction with fibrin aggregates may provide interesting features to autologous blood-derived biomaterials. **Aim:** In this context, the present study sought to characterize membranes produced through a modified protocol for concentrated growth factors (CGF) associated with activated plasma albumin gel (APAG). **Method:** Mixing denaturized albumin with CGF from the same blood samples into glass containers resulted in solid malleable membranes, with a modified denser ultrastructure as revealed by scanning electron microscopy (SEM). **Results:** The membranes presented a high density of nucleated cells, uniformly distributed along its length, and were able to release growth factors such as PDGF, VEGF, and FGF2 for 7 days. **Conclusion:** This preliminary study indicates that the protocol may provide autologous moldable and stable biomaterials for use as a soft tissue barrier, offering the basis for further research on its effectiveness for guided tissue regeneration.

Keywords: Activated plasma albumin gel, albumin, biological membrane, concentrated growth factors, *in vitro*

Introduction

Over the last several decades, different methods have been developed with the purpose of promoting the regeneration of soft and hard tissue in the dental clinic, including the use of biomaterials.[1] In this context, blood concentrates are promising clinically relevant products by offering an alternative source of minimally invasive autologous regeneration. Platelet aggregates can be generated from the patients' own peripheral blood and concentrated by centrifugation, thus being able to release different growth factors (GFs)[2] with well-documented desirable effects in tissue regeneration.

Platelet-rich fibrin (PRF) is considered the second generation of platelet concentrates,[3] being characterized as a simple and low-cost protocol obtained from single centrifugation without the addition of anticoagulants.[4,5] During centrifugation, a solid-fibrin matrix is generated by the activation of platelets through the interaction with the blood tube's surface. The resulting PRF matrix consists of a fibrin framework that includes platelets, leukocytes, and plasma proteins and may be used as a membrane for protection of soft tissues and in guided bone regeneration.[6-9]

In almost 20 years since its proposal, different protocols to produce PRF have been presented in the scientific literature aiming to improve the biological properties of these autologous biomaterials.[10] Most protocols seek to increase cellularity within the fibrin mesh, trying to improve the distribution and

Access this article online

Quick Response Code:

Website: www.cellsindentistry.org

DOI: 10.4103/GFSC.GFSC_21_18

Address for correspondence: Prof. Carlos Fernando de Almeida Barros Mourão,
Rua Miguel de Fries 9, Icaraí, Niterói, Rio de Janeiro 24220-900, Brazil.
E-mail: mouraocf@gmail.com

How to cite this article: Barros Mourão CF, Gheno E, Lourenço ES, Barbosa Rd, Kurtzman GM, Javid K, *et al.* Characterization of a new membrane from concentrated growth factors associated with denaturized Albumin (Alb-CGF) for clinical applications: A preliminary study. Int J Growth Factors Stem Cells Dent 2018;1:64-9.

production of cytokines, mainly GFs, in the receptor site. However, while different protocols for autologous platelet concentrates are often suitable for specific clinical applications, limitations in the stability of the fibrin mesh may compromise their applicability to surgical procedures that demand improved stability.

In cases where there is an attempt to use the biologically derived membrane as a protective barrier to prevent the advancement of soft tissue in the bone graft, the efficiency of the fibrin mesh for guided bone regeneration procedures is not well defined.[9] A recent study demonstrated its stability and the ability to release cytokines for up to 28 days after production when in a biological environment.[9] However, there are precise estimates neither of the actual residence time of this membrane under the bone graft after the operative procedure nor of the effect of enzymes such as metalloproteinases in their degradation, which could impact its efficacy as an autologous barrier. This desired clinical application indicates the need for further development of protocols aiming to further modulate this stability without losing the controlled release of cytokines from the blood at the site of surgery.

The use of serum albumin in the field of tissue engineering is widely reported,[11] which is a protein abundant in the human body and easy to isolate, from blood plasma precipitation with high purity and homogeneity.[11] In addition to providing a compatible structure for cell proliferation, biomaterials enriched with albumin showed little reduction of their dimensions over time (dimensional stability) suggesting less degradation *in vitro*.[11] Furthermore, one study has demonstrated that the association with albumin can modulate the fibrin network ultrastructure and permeability, inducing fibers with increased thickness and a coarse nodular appearance.[12] In view of these data, the association with denatured serum albumin could represent a possible improvement in the PRF-based framework, which is a totally autologous, biocompatible and possibly more durable material with a longer duration of action.

In this context, the present work proposes a protocol for the production of an autologous biomaterial for the treatment of osseous defects, presenting extension and high stability related to association of a dense fibrin matrix of concentrated growth factors (CGFs) with denaturized serum albumin. This preliminary study additionally presents an assessment of the initial controlled release of GFs. The cellularity of such membranes offers the basis for further research on the effectiveness of said material for guided tissue regeneration.

Materials and Methods

The procedures were developed according to the principles recommended for experimentation with humans determined in the Declaration of Helsinki, revised in 2000. The procedures of this study are part of the project approved by the Research Ethics Committee HUAP-UFF (CAAE 57080116.0.0000.5243).

Production of the albumin-concentrated growth factors membranes

Peripheral blood was collected from four healthy donors, with no history of anticoagulant medication use, using 9 ml tubes, without adding any additives (Vacutube, Biocon®, Brazil). For the production of each membrane, two tubes were positioned in the vertical rotor and fixed angle centrifuge (Medifuge®, Silfradent, Italy), and the protocol was applied to obtain the CGF in the liquid phase (LPCGF), as described by the manufacturer. After processing, it was possible to observe plasma and the remaining decanted blood material containing red cells.

Two milliliters of the initial portion of plasma (platelet-poor plasma [PPP]) was collected with a syringe (Injex®, Brazil), while the other blood portions (buffy coat, LPCGF, and red blood cells) were reserved at room temperature (20°C). The syringes containing PPP were inserted into a device for human serum albumin denaturation activated plasma albumin gel (APAG®, Silfradent, Italy). After 10 min in an operating temperature of 75°C, the syringes were stored at room temperature for another 10 min and protected from ambient light (as recommended by the manufacturer). The denaturized albumin was deposited into a glass container, to obtain the desired shape.

Subsequently, using a 10 ml syringe (Injex®, Brazil) and an 18G hypodermic needle (Injex®, Brazil), the LPCGF and buffy coat portions were collected in an approximate volume of 4 ml, added to the denaturized albumin on the glass container, and then gently mixed with tweezers. After waiting for the fibrin polymerization process (approximately 5 min), the membrane was formed with the previously established format. Figure 1 demonstrates a scheme of the production of the Alb-CGF membranes.

Ultrastructural evaluation

Immediately after production, the membrane was fixed with Karnovsky's solution and postfixed with 0.2 M sodium cacodylate solution and 1% osmium tetroxide solution, finally being dehydrated in alcohol solutions (ranging from 15% to 100%) and hexamethyl disilazine. The Alb-CGF membrane had its structure analyzed through scanning electron microscopy (SEM). The material was metalized with gold and observed at 15 kV with a scanning electron microscope (JEOL JSM-6490 LV, JEOL, Japan).

Assessment of cellularity

Fluorescence microscopy was utilized as a tool to evaluate the presence of nucleated cells within the Alb-CGF membranes. Seven days after production, three membranes were fixed in 4% paraformaldehyde for 25 min and stained with 1:5000 4',6-diamidino-2-phenylindole and then diluted in saline. Samples were observed in an inverted fluorescence microscope (Axio A1, Zeiss®), and three adjacent and nonoverlapping fields were photographed for three different areas of the membrane: center, left, and right borders. The cell density in each field was calculated with the help of Image-Pro Plus 6 (Media Cybernetics, Maryland, USA) software.

Elution and quantification of growth factors

To analyze the dynamics of the release of GFs over time, PRF membranes were cultured for 7 days after their preparation. Membranes were incubated in triplicate in 6-well culture plates (TPP, USA) in the presence of 4 ml of Dulbecco's modified Eagle's medium (GIBCO, USA) without antibiotics, in a humidified atmosphere at 37°C/5% CO_2. Aliquots of the extracts were collected at 1 h and 7 days of culture and stored in an ultra-freezer at −80°C. The eluates were used for the determination of GFs. For the detection of biomolecules, conventional enzyme-linked immunosorbent assay (ELISA) assays were used. Aliquots of 1 h and 7 days were analyzed for the presence of fibroblast growth factor (FGF)-b, vascular endothelial growth factor (VEGF), and platelet-derived growth factor (PDGF)-bb by ELISA using commercial kits (PeproTech®, Rocky Hills, NJ, USA).

Statistical analysis

The comparison of the cellularity in the three portions of the membrane, as well as the GF release between the two different experimental times was performed by one-way ANOVA with posttest of Bonferroni, considering an alpha error of 5%. Statistical analysis was performed using GraphPad Prism 6 software (GraphPad Inc., California, USA).

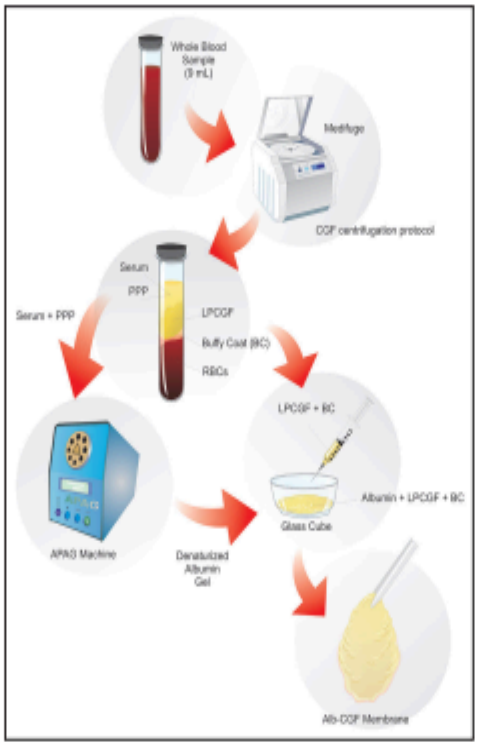

Figure 1: Scheme for the production of albumin-concentrated growth factor membranes. A whole blood sample is concentrated employing the concentrated growth factor protocol. The platelet-poor plasma portion is used in an activated plasma albumin gel machine to produce activated plasma albumin gel. This gel is mixed in a glass vessel with the liquid-phase concentrated growth factor and buffy coat (containing CD34+ cells). The contact with the glass contributes to produce a stable denser fibrin mesh in the form of a strong but malleable membrane (albumin-concentrated growth factor)

Results

The proposed association of LPCGF and denaturized albumin by mixing on a glass vessel [Figure 1] resulted in a solid, opaque moldable membrane [Figure 2]. Ultrastructural evaluation of the Alb-CGF membrane was performed through SEM as shown in Figure 3. It is possible to observe a very dense surface [Figure 3a and b], with very evident deposition of a layer of denaturized protein [Figure 3c and d], which is clearly coating the fibrin fibers [Figure 3c and e] and surrounding the trapped cells and platelets [Figure 3f].

Regarding the presence and distribution of cells within the membrane, Figure 4 demonstrates that nucleated cells are observable at similar densities both at the center of the membrane [Figure 4b] and in its left and right borders [Figure 4a and c, respectively]. The counting of nuclei in three independent fields for each membrane portion indicates no statistical difference on cellularity along the membrane [Figure 4d, $P < 0.05$].

Figure 5 shows that, during an elution assay, the membranes were able to release GFs such as PDGF, VEGF, and FGF2 in considerable concentrations within the 1st h. Curiously, similar levels of noncumulative release of VEGF and FGF2 were observed after 7 days of culture, without significant difference from 1 h ($P > 0.05$), indicating a continuous release with time for at least 1 week. PDGF presented a strong release at 1 h and a reduction on the mean GF concentration after 7 days of incubation, without statistical significance ($P > 0.05$).

Discussion

One of the main issues pertaining to the use of fibrin membranes today is their clinical efficacy for guided bone regeneration.[13] Nonetheless, until the present, there are no consistent studies that demonstrate the efficacy of membrane-derived blood-GFs as a barrier against the invasion of soft tissue in the bone repair process. One intended characteristic of the final membrane is controlled resorption, which is highly dependent on the fibrin mesh stability, enabling the barrier to continue during a relevant clinical timespan.

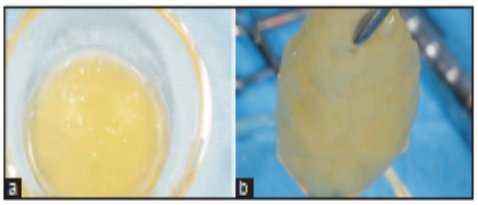

Figure 2: Images of the final step of production of the albumin-concentrated growth factor membrane, being mixed in a glass vessel (a), forming a solid but malleable membrane (b)

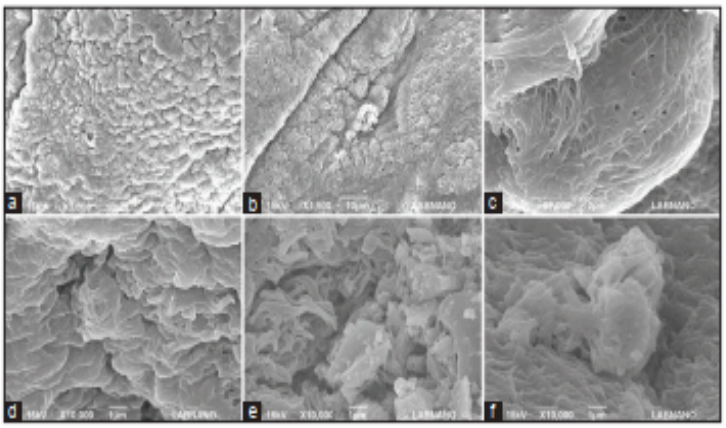

Figure 3: Scanning electron micrographs of the albumin concentrated growth factor membrane, obtained at 15 kV, at different magnifications (JEOL JSM 6490 LV, JEOL, Japan). (a and b) Very dense surface, with very evident deposition of a layer of the denaturized protein (c and d), which is clearly coating the fibrin fibers (c and e); (f) The fibers surrounding the trapped cells and platelets

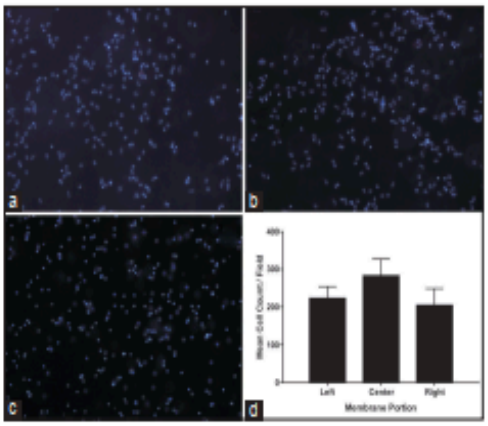

Figure 4: Estimation of cellularity within the albumin-concentrated growth factor membrane 7 days after production. Cell nuclei were evidenced by fluorescence microscopy after staining with 4',6-diamidino-2-phenylindole in the left border (a), center (b), or right border of the membrane (c) (images obtained with a ×20 objective). (d) The mean nucleated cell number ($n = 3$) for each membrane portion. No statistical difference was found ($P < 0.05$)

Modifications of the protocol for production of PRF,[9,14] as well as its associated other biomaterials,[15] may represent a source of novel strategies to improve its clinical efficacy. Such is the case of CGF,[16] an alternative protocol for the production of autologous fibrin derivatives, which modifies the original Choukroun's PRF centrifugation parameters through a patented concentration system (Medifuge®, Silfradent, Italy). This process results in a biomaterial that contains CD34+ cells, releases GFs, presents a fibrin matrix with potential use as a scaffold,[16] provided interesting results in diverse clinical settings,[17-19] mostly employed as the injectable LPCGF. The same company patented a commercial device to produce APAG (Silfradent, Italy), through the heat-induced aggregation of human serum albumin originated from PPP. According to the manufacturer, the denaturized proteins aggregate mostly through hydrophobic interactions and disulfide bonds, resulting in a biocompatible polymeric material that is proposed as an injectable filler material for esthetic interventions (https://www.silfradentasia.com/apag.html). While albumin is nonadhesive to leukocytes and platelets, since it lacks integrin-binding motif such as fibrin Arginyl-glycil-aspartic acid (RGD), studies suggest that platelets may adhere to unfolded albumin through receptor-mediated mechanisms.[20] Moreover, it is proposed that APAG may be mixed with LPCGF in a syringe, to produce an injectable esthetic filler containing CD34+ cells and GFs.[21] Nevertheless, the scientific literature still lacks on reports that describe the structural properties of this biomaterial, as well as its capability of releasing GFs and providing desired clinical outcomes.

In the present work, a protocol is proposed employing the production of a denaturized albumin gel with the use of the APAG system and its association to LPCGF, however, with an important modification in its final step, i.e., the mixing of CGF and albumin. Differing from the manufacturer's proposed protocol, the syringe was substituted by a glass vessel aiming to (i) ensure the integrity of viable cells from the buffy coat, which could possibly suffer from the pressure imposed by the syringe pumping, and (ii) induce fibrin polymerization through activation by contact with the glass surface, resulting in a denser fibrin network. The resulting biomaterial is a moldable and yet resistant membrane, therefore presenting potential characteristics for adequate use as a barrier on tissue regeneration.

Indeed, the dense appearance of the material, as revealed by SEM analysis, suggests that strong albumin-fibrin mesh interactions are occurring, modifying the usual fibrin scaffold appearance of CGF. Previous reports in the literature indicate that in the presence of albumin, there was an increased tendency for fibrin fibers to be aggregated into clumps during polymerization.[12] There is a possibility that this resulting

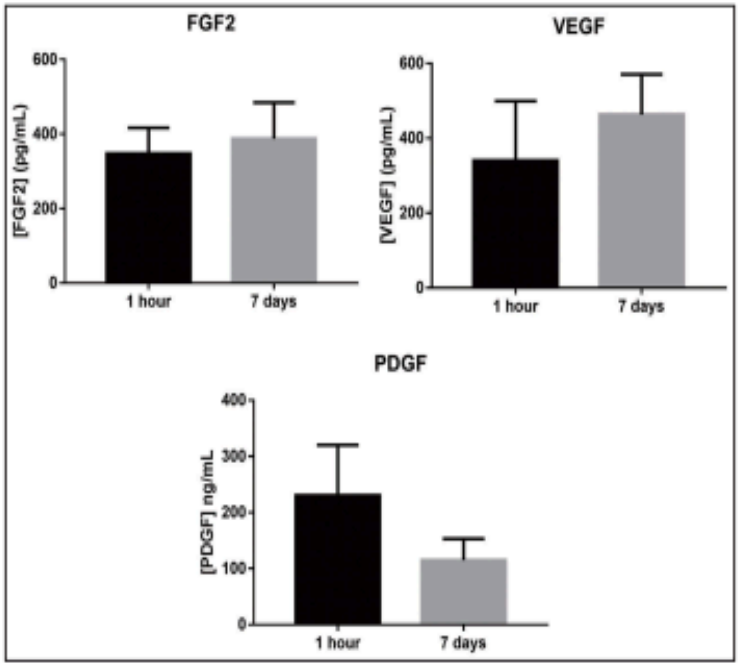

Figure 5: Assessment of the release of growth factors from the albumin-concentrated growth factor into cell culture media. Bars represent mean ± standard deviation of three biological and three technical replicates. There was no statistically significant difference between experimental times ($P > 0.05$)

denser product could be modulated to provide a less clumped network for use not as a barrier, but as a cell scaffold, by employing lower proportions of APAG related to CGF, as further studies should investigate. Nevertheless, while the micrographs of the proposed membrane did not evidence the presence of cells in the surface of the material, the fluorescence assay revealed that the mixing protocol resulted in a very uniform distribution of nucleated cells entrapped in the membrane. In the hypothesis that some of these cells are leukocytes able to produce GFs (as remains to be investigated with surface marker assays), this uniformity might become a very interesting benefit, since a moldable material grafted over a wider wound surface would be able to release similar levels of regenerative mediators along the entire repair area. This could possibly be an improvement over the rather polarized concentration of nucleated and CD34+ cells in the buffy coat distal region of PRF membranes.[9,22,23]

However, as stated earlier, there was no scientific evidence in the literature assessing the ability of APAG + CGF to still produce/release GFs. In this sense, the present report demonstrates that the Alb-CGF, produced as proposed, is capable of both immediate and prolonged release (after 1 week) of important GFs related to tissue regeneration such as PDGF, VEGF, and FGF2, all described among the main factors responsible for the desired clinical outcomes of PRF therapy.[5,9] Curiously, the levels of released cytokines are in the same order of magnitude as those found for PRF in previous reports employing equivalent and comparable elution methodologies.

Conclusion

While several questions remain to be answered by further studies, the present protocol proposed for the production of an Alb-CGF membrane may represent an important step toward the development of autologous moldable and stable biomaterials for use as soft tissue barriers and potential for different applications in the oral cavity, as in periodontal regenerations, for example. Consequently, this proposal opens the way for further scientific efforts for *in vitro*, *in vivo*, and clinical assessments that could confirm adequate desirable clinical outcomes for the association of denaturized albumin and autologous CGF.

Acknowledgment

We acknowledge the multiuser platform Labnano (CBPF, Brazil) for the use of the electron microscope.

Financial support and sponsorship

Nil.

Conflicts of interest

There are no conflicts of interest.

References

1. Bottino MC, Thomas V, Schmidt G, Vohra YK, Chu TM, Kowolik MJ, *et al.* Recent advances in the development of GTR/GBR membranes for periodontal regeneration – A materials perspective. Dent Mater 2012;28:703-21.
2. Dohan DM, Choukroun J, Diss A, Dohan SL, Dohan AJ, Mouhyi J, *et al.*

Platelet-rich fibrin (PRF): A second-generation platelet concentrate. Part II: Platelet-related biologic features. Oral Surg Oral Med Oral Pathol Oral Radiol Endod 2006;101:e45-50.
3. Dohan DM, Choukroun J, Diss A, Dohan SL, Dohan AJ, Mouhyi J, *et al.* Platelet-rich fibrin (PRF): A second-generation platelet concentrate. Part III: Leucocyte activation: A new feature for platelet concentrates? Oral Surg Oral Med Oral Pathol Oral Radiol Endod 2006;101:e51-5.
4. Choukroun J, Diss A, Simonpieri A, Girard MO, Schoeffler C, Dohan SL, *et al.* Platelet-rich fibrin (PRF): A second-generation platelet concentrate. Part V: Histologic evaluations of PRF effects on bone allograft maturation in sinus lift. Oral Surg Oral Med Oral Pathol Oral Radiol Endod 2006;101:299-303.
5. Dohan Ehrenfest DM, de Peppo GM, Doglioli P, Sammartino G. Slow release of growth factors and thrombospondin-1 in Choukroun's platelet-rich fibrin (PRF): A gold standard to achieve for all surgical platelet concentrates technologies. Growth Factors 2009;27:63-9.
6. Bolukbasi N, Ersanli S, Keklikoglu N, Basegmez C, Ozdemir T. Sinus augmentation with platelet-rich fibrin in combination with bovine bone graft versus bovine bone graft in combination with collagen membrane. J Oral Implantol 2015;41:586-95.
7. Soydan SS, Uckan S. Management of bisphosphonate-related osteonecrosis of the jaw with a platelet-rich fibrin membrane: Technical report. J Oral Maxillofac Surg 2014;72:322-6.
8. Tajima N, Ohba S, Sawase T, Asahina I. Evaluation of sinus floor augmentation with simultaneous implant placement using platelet-rich fibrin as sole grafting material. Int J Oral Maxillofac Implants 2013;28:77-83.
9. Lourenço ES, Mourão CFAB, Leite PEC, Granjeiro JM, Calasans-Maia MD, Alves GG, *et al.* The *in vitro* release of cytokines and growth factors from fibrin membranes produced through horizontal centrifugation. J Biomed Mater Res A 2018;106:1373-80.
10. Dohan Ehrenfest DM, Andia I, Zumstein MA, Zhang CQ, Pinto NR, Bielecki T, *et al.* Classification of platelet concentrates (Platelet-rich plasma-PRP, platelet-rich fibrin-PRF) for topical and infiltrative use in orthopedic and sports medicine: Current consensus, clinical implications and perspectives. Muscles Ligaments Tendons J 2014;4:3-9.
11. Horváthy DB, Simon M, Schwarz CM, Masteling M, Vácz G, Hornyák I, *et al.* Serum albumin as a local therapeutic agent in cell therapy and tissue engineering. Biofactors 2017;43:315-30.
12. van Gelder JM, Nair CH, Dhall DP. Colloid determination of fibrin network permeability. Blood Coagul Fibrinolysis 1996;7:747-60.
13. Miron RJ, Zucchelli G, Pikos MA, Salama M, Lee S, Guillemette V, *et al.* Use of platelet-rich fibrin in regenerative dentistry: A systematic review. Clin Oral Investig 2017;21:1913-27.
14. Mourão CF, Valiense H, Melo ER, Mourão NB, Maia MD. Obtention of injectable platelets rich-fibrin (i-PRF) and its polymerization with bone graft: Technical note. Rev Col Bras Cir 2015;42:421-3.
15. de Almeida Barros Mourão CF, Lourenço ES, Nascimento JR, Machado RC, Rossi AM, Leite PEC, *et al.* Does the association of blood-derived growth factors to nanostructured carbonated hydroxyapatite contributes to the maxillary sinus floor elevation? A randomized clinical trial. Clin Oral Investig 2018. https://doi.org/10.1007/s00784-018-2445-7.
16. Rodella LF, Favero G, Boninsegna R, Buffoli B, Labanca M, Scari G, *et al.* Growth factors, CD34 positive cells, and fibrin network analysis in concentrated growth factors fraction. Microsc Res Tech 2011;74:772-7.
17. Borsani E, Bonazza V, Buffoli B, Cocchi MA, Castrezzati S, Scari G, *et al.* Biological characterization and in vitro effects of human concentrated growth factor preparation: An innovative approach to tissue regeneration. Biol Med (Aligarh) 2015;7:5. Doi: 10.4172/0974-8369.1000256.
18. Kang JS, Zheng Z, Choi MJ, Lee SH, Kim DY, Cho SB, *et al.* The effect of CD34+ cell-containing autologous platelet-rich plasma injection on pattern hair loss: A preliminary study. J Eur Acad Dermatol Venereol 2014;28:72-9.
19. Mackie AR, Losordo DW. CD34-positive stem cells: In the treatment of heart and vascular disease in human beings. Tex Heart Inst J 2011;38:474-85.
20. Sivaraman B, Latour RA. Time-dependent conformational changes in adsorbed albumin and its effect on platelet adhesion. Langmuir 2012;28:2745-52.
21. Matthews-Brzozowska T, Krzyżanowska A, Lichaj M. Revitalization of facial skin based on preparations of patient own blood. J Med Sci 2016;86:173-6.
22. Nishimoto S, Fujita K, Sotsuka Y, Kinoshita M, Fujiwara T, Kawai K, *et al.* Growth factor measurement and histological analysis in platelet rich fibrin: A pilot study. J Maxillofac Oral Surg 2015;14:907-13.
23. Bansal M, Kumar A, Puri K, Khatri M, Gupta G, Vij H, *et al.* Clinical and histologic evaluation of platelet-rich fibrin accelerated epithelization of gingival wound. J Cutan Aesthet Surg 2016;9:196-200.

3 ANEXO III

Received: 15 November 2019 | Revised: 29 May 2020 | Accepted: 16 June 2020

DOI: 10.1002/jbm.b.34680

ORIGINAL RESEARCH REPORT

WILEY

Effects of rotor angle and time after centrifugation on the biological in vitro properties of platelet rich fibrin membranes

Emanuelle Stellet Lourenço[1] | Gutemberg Gomes Alves[2] | Renata de Lima Barbosa[4] | Carolina Nascimento Spiegel[2] | Rafael Coutinho de Mello-Machado[1] | Sarah Al-Maawi[3] | Shahram Ghanaati[3] | Carlos Fernando de Almeida Barros Mourão[1,4]

[1]Post-Graduation Program in Dentistry, Fluminense Federal University, Niterói, Rio de Janeiro, Brazil

[2]Department of Molecular and Cell Biology, Institute of Biology, Fluminense Federal University, Niterói, Rio de Janeiro, Brazil

[3]Department of Maxillofacial, Clinic for Maxillofacial and Plastic Surgery, Johann Wolfgang Goethe University, Frankfurt Am Main, Germany

[4]Post-Graduation Program in Science and Biotechnology, Fluminense Federal University, Niterói, Rio de Janeiro, Brazil

Correspondence
Gutemberg Gomes Alves, Hospital Universitário Antônio Pedro, Av. Marquês do Paraná, 303 - Centro, Niterói, Rio de Janeiro, Brazil.
Email: gutopepe@yahoo.com.br

Funding information
Coordenação de Aperfeiçoamento de Pessoal de Nível Superior; Fundação Carlos Chagas Filho de Amparo à Pesquisa do Estado do Rio de Janeiro

Abstract

This study evaluated the impact of rotor angle and time of storage after centrifugation on the in vitro biological properties of platelet-rich fibrin (PRF) membranes. Blood samples ($n = 9$) were processed with a vertical fixed-angle (V) or a swing-out horizontal (H) centrifuge, with 20–60 min of sample storage after centrifugation. Leukocytes, platelets, and red blood cells were counted, and fibrin architecture was observed by scanning electron microscopy (SEM). The release of FGF2, PDGFbb, VEGF, IL-6, and IL-1β was measured after incubation on culture media for 7–21 days. Cell content was equivalent in all experimental groups ($p > .05$). The fibrin matrix was similar for fixed-angle and horizontal centrifugation. Horizontal centrifugation induced a twofold increase in PDGF and 1.7x increase on FGF release as compared to V samples, while IL-1β was significantly reduced ($p < .05$). No significant difference was observed on the release of growth factors and cytokines at different times after centrifugation ($p < .05$). These data suggest that both angles of centrifugation produce PRF membranes with similar structure and cellularity, but horizontal centrifugation induces a higher release of growth factors. Higher times of storage after centrifugation did not impact on cell content and the release of growth factors.

KEYWORDS
blood platelets, centrifugation, fibrin, platelet-rich fibrin

1 | INTRODUCTION

The development and improvement of technologies applied to tissue regeneration have been challenging in recent decades, with the increasing use of hemo-components as autologous biomaterials. Given its characteristics, among which the potential for bioactivity (Ahmed, Dare, & Hincke, 2008; Anitua, Pino, & Orive, 2017; Borie et al., 2015), platelet concentrates have been widely applied in procedures such as the treatment of chronic wounds, osteonecrosis, infra-osseous defects, plastic, and orthopedic surgeries and as hemostatic agents (Dohan Ehrenfest et al., 2014; Jubert, Rodríguez, Reverté-Vinaixa, & Navarro, 2017; Mourão, Calasans-Maia, Mello-Machado, Resende, & Alves, 2018; Piccin et al., 2017).

The second generation of platelet aggregates is obtained from the processing of blood aliquots, usually by centrifugation. Initially described by Choukroun and colleagues (Dohan et al., 2006a), platelet-rich fibrin (PRF) presents a fully autologous protocol, consisting of centrifugation of the peripheral blood samples, collected in glass or silica-coated tubes without the addition of anticoagulants. The resulting material consists of a three-dimensional fibrin network allowing the entrapment of cells, such as platelets and leukocytes, as well as growth factors and cytokines, promoting their

continuous release over time (Dohan et al., 2006b; Dohan et al., 2006c).

While PRF is recognized for its simplified protocol, low cost, and extensive description in the scientific literature (Miron & Choukroun, 2017), some controversial points remain regarding the standardization of its production. Parameters of centrifugation such as time, g-force and angulation of the centrifuge rotor, represent another point of controversy and protocol bias, with several different PRF protocols proposed in the literature, which may produce materials with possible structural and functional differences (Dohan Ehrenfest et al., 2018). Recent studies (Lourenço et al., 2018; Miron et al., 2019) have reported the production of membranes from the adaptation of the PRF protocol through the use of variable angulation horizontal rotor centrifuges. The option to use this type of centrifuge is based on the usually easy access to this type of equipment, which is widely available in hospitals and clinics. With such protocol, it was possible to produce a fibrin structured material (Lourenço et al., 2018), presenting cellularity, fibrin organization, and in vitro stability similar to that described for regular PRF membranes, and able to a consistent time-dependent release of growth factors and cytokines. Furthermore, a recent study has suggested several advantages of the horizontal centrifugation when compared to the fixed-angle centrifugation (Miron, Chai, et al., 2019). However, there are only scarce data available on the differences on the final membrane produced with these different types of centrifugation, including the structure of the fibrin scaffold, the cellular composition, and the release of growth factors and cytokines.

Another technical aspect of PRF production is the lack of consensus regarding how much time a membrane may rest after centrifugation and before its clinical use without affecting its biological properties and usefulness. The initially proposed protocol for PRF production (Dohan et al., 2006a) offers an empirical recommendation of waiting ~10 min before its use, which should be sufficient for polymerization and serum release (Borie et al., 2015). However, the scientific literature lacks evidence of the effects of long waiting times after centrifugation on the biological properties of PRF membranes.

In order to contribute to the understanding of methodological issues in the production of platelet-rich fibrin membranes, this work aimed to assess two different hypotheses: (a) that the time after centrifugation impacts on the in vitro biological properties of PRF membranes and (b) that the use of horizontal and vertical centrifugation protocols produce PRF membranes with similar in vitro biological properties, such as cell content, fibrin scaffold structure and the retention/release of growth factors and pro-inflammatory cytokines.

2 | MATERIALS AND METHODS

2.1 | Participants and research ethics

Blood samples were collected with the informed consent of nine healthy volunteer donors, from both sexes, with ages between 30 and 45. The study was approved by the Federal Fluminense University Ethical Committee (CAAE number 12126919.7.0000.5243) and performed following the ethical standards of the institutional ethics research committee and with the 1964 Helsinki declaration, revised in 2000.

2.2 | Membrane preparation

A DUO machine (DUO®Process for PRF, Nice, France) was selected to represent the vertical, fixed angle (V) protocol for the PRF production, while a local clinical swing-out centrifuge (B-40, RDE®, Brazil) was chosen as the representative of a horizontal (H) rotor centrifuge. Two 9 ml aliquots of blood were collected from each donor with a 21G vein needle (BD, Brazil), from the antecubital fossa, using red cover glass collection tubes (Vacuette, Greiner Bio-One, Brazil), without the addition of any substance. One aliquot was immediately centrifuged in the fixed-angle centrifuge (DUO® Process for PRF, Nice, France), using the L-PRF process considering RCF-clot proposed previously (Fujioka-Kobayashi et al., 2017), with a 41.3° fixed angle rotor, ~708 g and 12 min duration. The second aliquot was immediately centrifuged in a swing-out horizontal rotor centrifuge (B-40, RDE®, Brazil) on the same conditions of time and relative centrifugal force (RCF) (12 min at ~708 g), with the RCF calculated for the maximum radius as described previously (Miron, Choukroun, & Ghanaati, 2018).

After centrifugation, the tubes were placed vertically on a shelf for 20, 40, or 60 min at room temperature. The material was collected from each centrifuge, and with the aid of a piece of sterile gauze, slight compression was applied, producing a gelatinous structure, identified as a fibrin membrane rich in platelets. These procedures were performed by the same researcher (CFM).

2.3 | Estimation of cellularity of PRF membranes

Blood Samples (n = 3) were processed as described above, with the two centrifugation methods. In the referred times after centrifugation, the formed membranes were removed from the tubes, and the areas of semi-coagulated thrombus were separated with the aid of surgical scissors, 1 cm below the area referring to the Buffy Coat. Subsequently, the membranes were taken to the PRF compressor (PRF Box, Biohorizons, Birmingham, AL), where fibrin clot exudates were collected and placed into purple cap glass tubes containing EDTA (Greiner Bio-One, Brazil). During processing, the supernatant serum fractions (PPP) and the bottom semi-coagulated thrombus with red blood cells (RBC) (1 cm below the area referring to the Buff Coat) were also collected and pooled with the exudate in the EDTA-containing tubes. The tubes were gently homogenized for the complete dissolution of clots. A further 9 ml sample was collected on the EDTA-containing tube, representing the Whole Blood sample. To quantify platelets, RBCs, and leukocytes, these samples evaluated with a Counter 19 CP Hematology Analyzer (Wiener Lab, Argentina). The cell content on the PRF membranes was estimated considering the subtraction method, in which:

PRF cell count = Whole blood − Postprocessing blood fractions (Exudate + PPP + RBC).

2.4 | Evaluation of the fibrin scaffold structure

The structure of the fibrin matrices of the PRF membranes was observed through scanning electron microscopy (SEM). The membranes produced during the cell estimation assay were used for this evaluation. After the resting times (20, 40, and 60 min), the membranes were fixed with a Karnovsky's solution and post-fixed with 0.2 M sodium cacodylate and 1% osmium tetroxide, and finally dehydrated in alcohol solutions (ranging from 15 to 100%) and hexamethyldisilazane (HMDS). The samples were mounted on metallic supports with adhesive tape, coated with a gold layer, and examined under a JEOL JSM 6390LV scanning electron microscope (Akishima, Tokyo, Japan) operated at 15 kV.

Micrographs collected at ×5000 magnification were used for a quantitative evaluation of the fibrin fiber diameter on a method adapted from a previous protocol (Pretorius, Steyn, Engelbrecht, Swanepoel, & Oberholzer, 2011). Two micrographs were taken from three samples of each material, always from the surface of their medial portion. A 10 × 10 grid was superimposed over each micrograph, and one individual primary or stem fiber (not originated from a distinct branch) was measured by a blinded observer (without knowledge of the experimental groups) using the Manual Measurements function of the Image Pro Plus 6.0 Software (Media Cybernetics Inc.). Since it was not possible to identify an unrepeated primary fiber in some squares, the evaluation generated a mean of 522 ± 49 measurements out of the theoretical 600 hundred for each material/experimental condition.

2.5 | Elution and quantification of growth factors and cytokines

For the elution of biological mediators from the membranes, 9 ml blood samples were produced as described above, and maintained in 4 ml of DMEM medium without antibiotics for the experimental times of 1, 7, and 21 days, in a humid atmosphere at 37°C and 5% of CO_2. After each incubation period, the conditioned medium was collected and stored in a freezer at −80°C (−112 °F) for further evaluation and replaced by an equal volume of fresh medium for the next experimental time point.

The conditioned media samples were used for the evaluation of the release of basic Fibroblastic Growth Factor (FGF2), Platelet-Derived Growth Factor (PDGFbb), and Vascular Endothelial Growth Factor (VEGF), as well as the pro-inflammatory cytokines IL1β and IL-6. This assay was performed through ELISA sandwich enzyme immunoassays using commercially available kits (Peprotech®), employing horseradish peroxidase and ABTS as the reporting system. The Optical Density (OD) at 405 nm was measured using a Synergy II Microplate Reader (Biotek®). The experiments were performed in biological quintuplicates and technical triplicates, that is, each of the five membranes was evaluated three times.

2.6 | Statistical analysis

Results were calculated as means and the standard error of the mean (SEM). The results from the cell counts, fiber diameter, and ELISA assays obtained for horizontal and angled rotor centrifuges were compared with nonparametric, two-tailed Mann–Whitney U tests, considering an alpha error of 5%, using the software GraphPad Prism 7.0 (GraphPad®).

3 | RESULTS

After the production of PRF membranes using two centrifuges with different angles of the rotor, and sample resting times ranging from 20 to 60 min, the cell content of the resulting biomaterials was determined by a subtraction method, as shown in Table 1. Platelet concentrations obtained from the analysis of all participants were within the normal laboratory reference range (170–400 × 10^3/μl). Platelets and leucocytes were preferentially concentrated on the polymerized

TABLE 1 Evaluation of the content of cells on PRF membranes produced with different centrifugation angles and times after centrifugation

	Red blood cells (RBC) (10^6/μl)	Platelets (PLT) (10^3/μl)	Leucocytes (LY) (10^3/μl)
Whole blood	4.81 ± 1.13	230.5 ± 19.09	1.7 ± 1.1
Vertical centrifugation			
20 min	0.46 ± 0.21	226.5 ± 18.5	1.5 ± 0.6
40 min	0.64 ± 0.12	225.5 ± 10.2	1.6 ± 0.3
60 min	0.66 ± 0.09	225.5 + 10.0	1.1 ± 0.4
Horizontal centrifugation			
20 min	0.48 ± 0.18	224.5 + 5.0	1.3 ± 0.3
40 min	0.59 ± 0.12	223.5 ± 0.0	1.4 ± 0.5
60 min	0.62 ± 0.1	226.5 ± 12.0	1.3 ± 0.3

Note: Results are expressed as mean ± *SD* of three biological replicates.

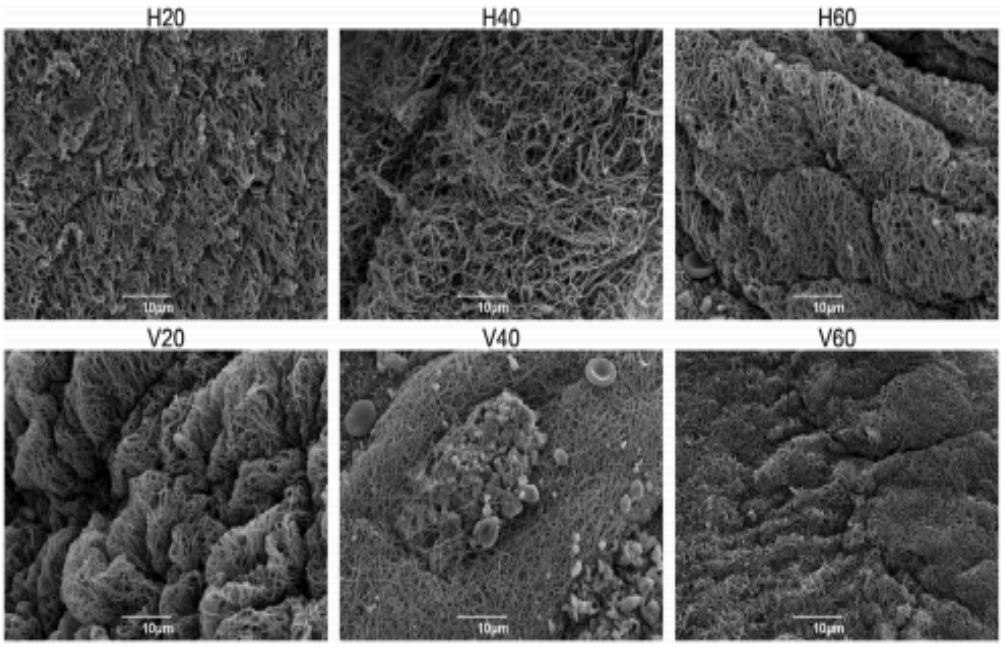

FIGURE 1 Electron micrographs, produced at x10.000 magnification, of the fibrin scaffolds produced with either vertical or horizontal rotor centrifugation, 20, 40, or 60 min after centrifugation

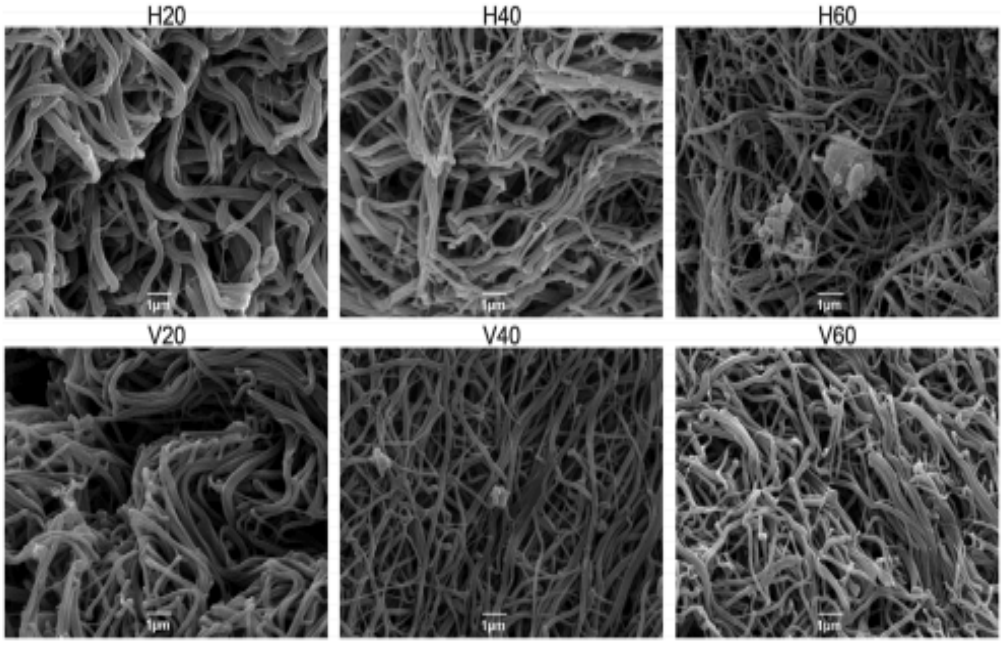

FIGURE 2 Electron micrographs, produced at x2000 magnification, of the fibrin scaffolds produced with either vertical or horizontal rotor centrifugation, 20, 40, or 60 min of after centrifugation

matrices, with more than 90% of the platelets retained in the biomaterial, while a much lower content of red blood cells was found on these membranes, as compared to the whole blood samples. No significant difference was found on leukocyte, RBS, and platelets between the two centrifugation protocols, or between samples that rested for different times after centrifugation ($p > .05$).

The morphological pattern of the PRF clots produced with the different protocols was observed through scanning electron microscopy (Figures 1 and 2). All membranes presented a dense fibrin matrix, with apparent network porosity (Figure 1). While these networks seem very similar comparing the centrifugation protocols (H and V), the fibrin network shows evidence of slight differences in the thickness and density considering the time (Figure 2), where thicker and less compacted filaments are apparent with 20 min after centrifugation. The image analysis for fibrin fiber thickness confirmed a significant reduction on mean diameter from 20 to 60 min after centrifugation in both horizontal (from 358 ± 79 to 205 ± 57 nm, $p = .04$) and fixed-angle centrifugation (from 311 ± 63 to 138 ± 35 nm, $p = .037$).

Figures 3 to 5 show the concentrations of the growth factors PDGFbb, FGF2, and VEGF, eluted from fixe-angle PRF, and horizontal

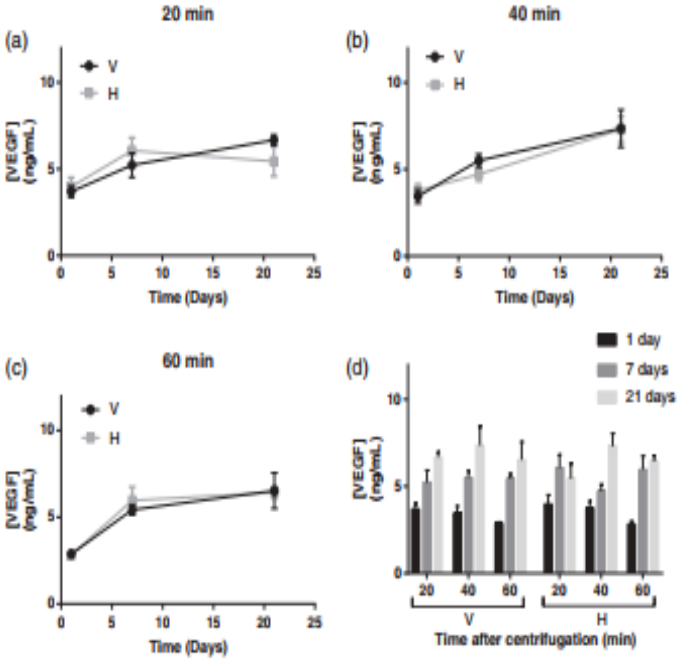

FIGURE 3 VEGF release from 7 to 21 days of elution in culture media by PRF membranes produced by fixed-angle (V, black circle) or horizontal (H, gray square) centrifugation and left to rest by 20 (a), 40 (b), or 60 min (c). Panel D shows the same results as a function of time after centrifugation. Bars and symbols indicate mean ± SEM

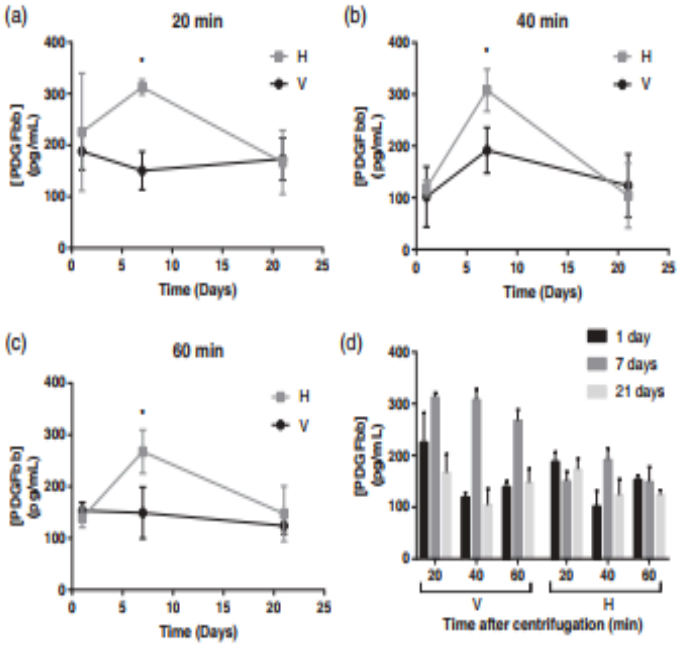

FIGURE 4 PDGFbb release from 7 to 21 days of elution in culture media by PRF membranes produced by fixed-angle (V, black circle) or horizontal (H, gray square) centrifugation and left to rest by 20 (a), 40 (b), or 60 min (c). Panel d shows the same results as a function of time after centrifugation. Bars and symbols indicate mean ± SEM. An asterisk indicates a significant difference among groups ($p < .05$)

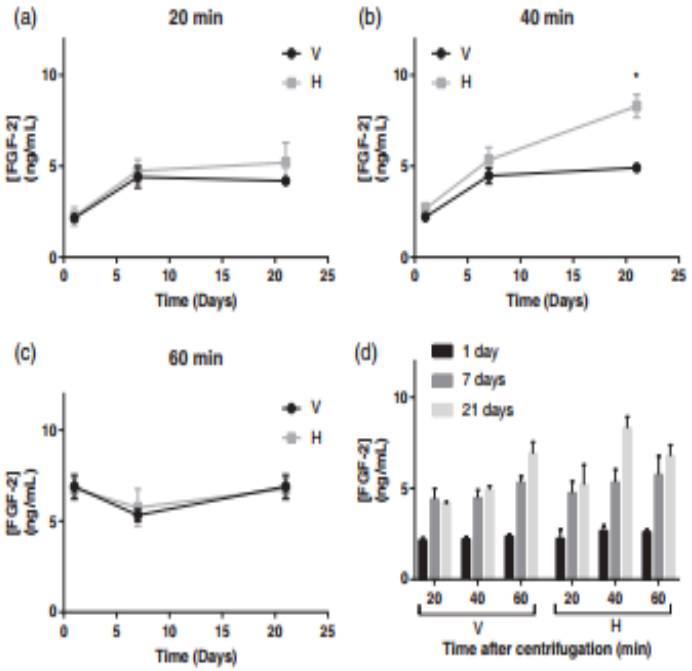

FIGURE 5 FGF2 release from 7 to 21 days of elution in culture media by PRF membranes produced by fixed-angle (V, black circle) or horizontal (H, gray square) centrifugation and left to rest by 20 (a), 40 (b), or 60 min (c). Panel d shows the same results as a function of time after centrifugation. Bars and symbols indicate mean ± *SEM*. An asterisk indicates a significant difference among groups ($p < .05$)

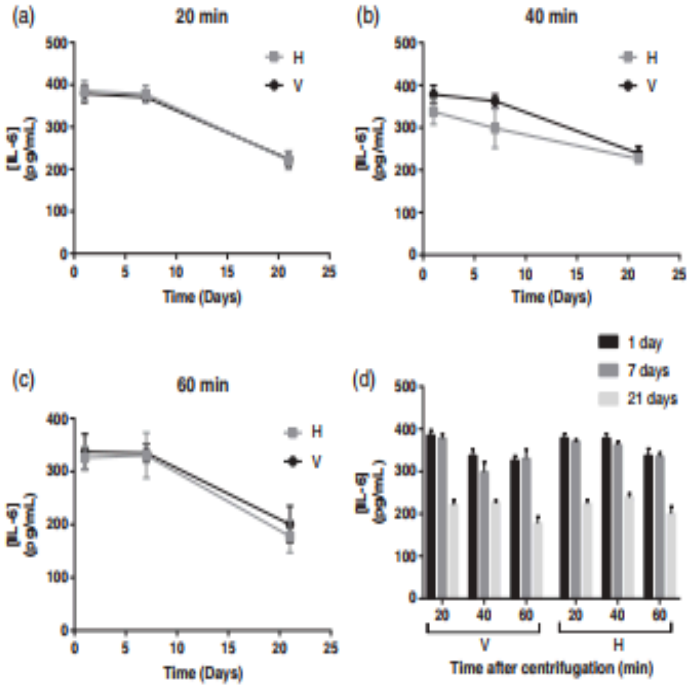

FIGURE 6 IL-6 release from 7 to 21 days of elution in culture media by PRF membranes produced by fixed-angle (V, black circle) or horizontal (H, gray square) centrifugation and left to rest by 20 (a), 40 (b), or 60 min (c). Panel d shows the same results as a function of time after centrifugation. Bars and symbols indicate mean ± *SEM*

centrifugation membranes, according to the time of incubation in culture media and time after centrifugation. All analytes presented a sustained release from 7 to 21 days. Figure 3 shows a similar pattern of VEGF release between centrifugation protocols ($p > .05$). Figure 4 shows a peak of PDGFbb release at day 7 in all storage times for the horizontal centrifugation, which attained a significant ($p < .05$) 1.5–2x increase as compared to vertical centrifugation. Figure 5 indicates a very similar pattern of FGF2 release by the two centrifugation protocols, except for a significantly higher release (1.7X, $p < .05$) from horizontal centrifugation at day 21 in the 40 min resting samples, as compared with the vertical centrifugation.

Regarding the release of inflammatory cytokines, Figure 6 shows a similar pattern of release for IL-6 for all centrifugation and sample resting protocols ($p > .05$), which seemed to decrease with time of

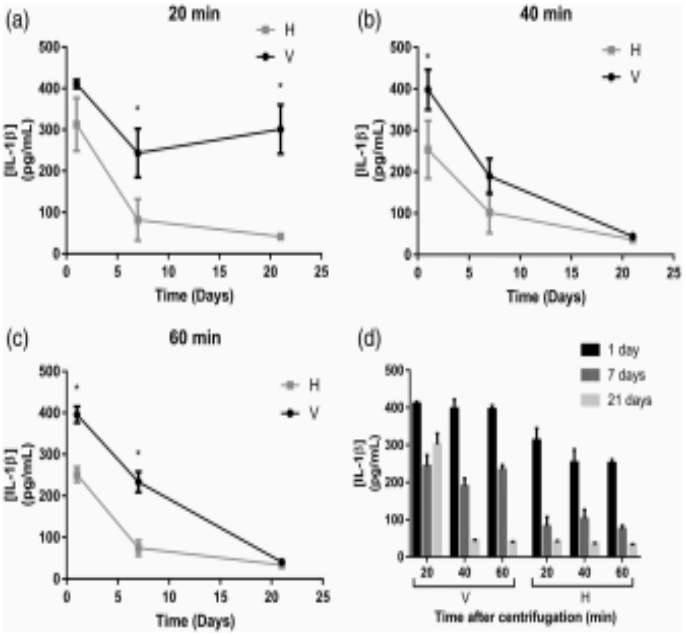

FIGURE 7 IL-1β release from 7 to 21 days of elution in culture media by PRF membranes produced by fixed-angle (V, black circle) or horizontal (H, gray square) centrifugation and left to rest by 20 (a), 40 (b), or 60 min (c). Panel d shows the same results as a function of time after centrifugation. Bars and symbols indicate mean ± SEM. An asterisk indicates a significant difference among groups ($p < .05$)

incubation. For IL-1β, however, different dynamics were observed, where the vertical centrifugation resulted in a higher release of the cytokine in different incubation times, depending on the post-centrifugation resting protocol (Figure 7). Regarding the time after centrifugation, the 20 min samples centrifuged by the fixed-angle vertical protocol presented a release of IL-1β around 7× higher ($p < .05$) than the other resting times.

4 | DISCUSSION

The profusion of PRF production protocols available in literature led to the formulation and test of two hypotheses regarding PRF biological properties that could be assessed in vitro. Our results suggest that, while the choice between horizontal and fixed-angle rotor centrifugation may produce membranes with similar properties, some interesting differences are also induced, that may be considered when applying/designing PRF production protocols.

Recently, our research group has demonstrated that blood-derived fibrin membranes with high structural stability and cell content can be generated by horizontal centrifugation, which are capable of sustained production/release of growth factors and anti-inflammatory cytokines (Lourenço et al., 2018). The present study compared this mode of centrifugation with a commercially available centrifuge designed to produce PRF using a fixed-angle rotor. The results show that these protocols produce similar membranes regarding the apparent fibrin network structure, as observed by SEM, and cell retention, as shown by the equivalent counts of leukocytes, platelets, and RBC. However, these results are in contrast with the observation of Miron et al. (Miron, Chai, et al., 2019), reporting increased leukocyte retention, and a more homogeneous cell distribution on PRF produced through horizontal centrifugation as compared to fixed-angle rotors. However, both studies differ in the tested centrifuge models, as well as the PRF production protocol and method for cellularity determination. In this regard, that previous study proposed the use of anticoagulants during centrifugation to simulate the PRF production, allowing the immediate cell counting in different collected sample fractions (Miron, Chai, et al., 2019). However, it might have limited the observation of the effects of fibrin polymerization on cell retention/distribution. On the other hand, the subtraction method employed in this study remains a currently accepted method for determination of cellularity on platelet aggregates, even though several limitations have been discussed in recent years (Kitamura et al., 2018), such as low accuracy, and the inability to account for aggregated platelets or cells lost during compression steps. Therefore, the present results may be affected by such limitations, which could be the source of the differences from the previous report. In this context, the work by Kitamura et al. (Watanabe et al., 2017) provides an interesting method for direct counting of polymerized membranes by digestion with tissue-plasminogen activator, which may solve such discrepancies in further studies.

The results from the elution assays show that the initial release of FGF, VEGF, and PDGF was sustained by both materials for weeks in the in vitro test system. This data suggests that more than just retaining soluble growth factors from blood or platelets, both membranes were able to produce these mediators through the presence of lymphocytes, as well-known and documented for PRF (Dohan Ehrenfest et al., 2018). It is interesting to note, however, that for PDGF and FGF2, significantly higher levels of release could be identified for the H-PRF membranes, as well as a lower release of IL-1beta ($p < .05$), indicating the existence of differences on the resulting biologically active membranes. Miron et al. (Miron, Chai, et al., 2019) theorized that the horizontal centrifugation provides a means to better

separate cells based on density, as swing-out rotors allow for an increased difference between RCF-min and RCF-max produced within a tube, facilitating the separation of cell layers. In addition, they hypothesized that horizontal centrifugation might cause less damage to cells, allowing direct flow with less friction against the tube walls. In the present work, the differences observed in the release of some growth factors and cytokines at longer elution times suggest that the phenomenon may be at least to some extent related to production by platelet/lymphocytes after centrifugation, which conflicts with the absence of differences observed in the cell content. Therefore, such differences suggest the possibility that the subtraction method has been unable to detect changes on platelet and/or lymphocyte related to the centrifugation protocol. This hypothesis reinforces the need for further assessments of the horizontal protocol through a direct cell counting approach.

A second hypothesis for the differences in cytokine and growth factor release between horizontal and fixed-angle centrifugation is related to the possibility of differential entrapment of growth factors/cytokines. While such a hypothesis is not tested on the present work, there is evidence on the literature that the centrifugation step affects the entrapment of growth factors on the fibrin lattice and its distribution along the PRF membrane (Bai, Wang, Wang, Lin, & Chan, 2017). Furthermore, studies have also shown that PDGF, VEGF, and FGF bind to specific sites of fibrin/fibrinogen, such as the heparin domain, with diverse affinities and, consequently, present differential cumulative releases from fibrin matrices at up to 7 days (Martino, Briquez, Ranga, Lutolf, & Hubbell, 2013). IL-1β was also demonstrated as presenting a binding site to fibrin (Sahni, Guo, Sahni, & Francis, 2004), influencing clot formation, and even competing/displacing growth factors such as FGF-2. Such complex interactions might help justify, if not explain, the singular changes observed for PDGF or IL-β, as compared to IL-6 and VEGF.

The present study also issued a question relevant to the clinical use of PRF membranes, related to changes in PRF biological properties after extended times of storage after centrifugation. Answers to these questions may be of paramount importance to understand the best moment of application of the PRF membrane. In cases involving more extensive surgeries, as blood may be collected and immediately processed, alterations on the material properties with time become a justifiable surgeon's concern. A recent study has already shown that the time between blood extraction and the start of centrifugation can impact the biological properties of PRF (Miron et al., 2019), causing interferences in the size of PRF membranes. Regarding storage after centrifugation, Peck, Hiss, Stephen, Satti, and Majeed (2015) reported a small (1.5%) increase in platelet count in PRF membranes 60 min after centrifugation. Dohan Ehrenfest (Ehrenfest, 2010) advised against the permanence in silica-coated plastic centrifugation tubes for more than 15 min, at risk of clot shrinkage, and merging with the red blood cell base, leading to an unusable material loaded with red blood cells.

While such shrinkage and merging were not observed in the present study employing glass tubes, our findings suggest that resting samples inside glass tubes for longer times after centrifugation (20 to 60 min) do not affect platelet or leukocyte retention, or the overall formation of a dense fibrin matrix. However, the data also suggest that increasing times of storage might result in changes in some properties of these fibers, with a significant reduction in the diameter of fibers ($p < .05$). It is important to notice that such observation came from SEM examination followed by a quantitative assessment through image analysis often used to estimate fibrin fiber thickness (Pretorius et al., 2011). However, while considered adequate for qualitative morphological assessments, the quantitative use of SEM is subject to several limitations which, in the case of fibrin matrices, may include artifacts from manipulation or fixing steps, and differences in fiber thickness depending on the evaluated region (core or surface), the origin of fiber (stem or branch), and the difficulty of calibration with an adequate resolution at the submicron scale. Therefore, despite methodological care on blinding and standardization of regions and fiber-type, this finding based only on a limited number of surface observations must be considered carefully. Nevertheless, the result gives preliminary evidence that some phenomena might occur with the PRF fibrin network at more extended times of storage. Previous reports indicate the presence of in vitro fibrinolysis on blood clots provided by limited activation of plasma proteins with time (Elnager et al., 2014), which may cause a reduction in mean fiber diameter (Hudson, 2017). Furthermore, there is evidence on the literature that posttranslational changes on fibrinogen (de Vries, Snoek, Rijken, & de Maat, 2020) caused by low levels of oxidation and photooxidation results in more dense fibrin clots with thinner fibers. Therefore, this is an intriguing finding which remains to be confirmed with other quantitative approaches in order to understand better the effects of storage of PRF membranes after centrifugation and its possible clinical implications.

5 | CONCLUSION

The use of horizontal centrifugation produces PRF membranes with equivalent cell content and similar fibrin scaffold morphology, but with significantly increased in vitro release of PDGF, FGF2, and decreased release of IL-1β, as compared to fixed-angle vertical centrifugation. Higher times of resting after centrifugation, regardless of the angle of rotor, did not impact on its cell content and in vitro release of growth factors, but evidence suggests minor changes on structural features of the fibrin matrix of PRF.

ACKNOWLEDGMENT

Authors acknowledge the financial support of the Brazilian government agencies CAPES and FAPERJ and thank the Electron Microscopy Platform of the Instituto Oswaldo Cruz, Fiocruz.

CONFLICT OF INTEREST

The authors declare no conflict of interest during the conduction of this study, and no benefit of any kind was received either directly or indirectly by the author(s).

ORCID

Gutemberg Gomes Alves https://orcid.org/0000-0003-0016-4809
Shahrom Ghanaati https://orcid.org/0000-0002-7897-0854

Carlos Fernando de Almeida Barros Mourão https://orcid.org/0000-0001-5775-0222

REFERENCES

Ahmed, T. A., Dare, E. V., & Hincke, M. (2008). Fibrin: A versatile scaffold for tissue engineering applications. *Tissue Engineering. Part B, Reviews*, *14*(2), 199–215.

Anitua, E., Pino, A., & Orive, G. (2017). Opening new horizons in regenerative dermatology using platelet-based autologous therapies. *International Journal of Dermatology*, *56*(3), 247–251.

Bai, M. Y., Wang, C. W., Wang, J. Y., Lin, M. F., & Chan, W. P. (2017). Three-dimensional structure and cytokine distribution of platelet-rich fibrin. *Clinics*, *72*(2), 116–124.

Borie, E., Olivi, D. G., Orsi, I. A., Garlet, K., Weber, B., Beltrán, V., & Fuentes, R. (2015). Platelet-rich fibrin application in dentistry: A literature review. *International Journal of Clinical and Experimental Medicine*, *8*(5), 7922–7929.

de Vries, J. J., Snoek, C. J., Rijken, D. C., & de Maat, M. P. (2020). Effects of post-translational modifications of fibrinogen on clot formation, clot structure, and fibrinolysis: A systematic review. *Arteriosclerosis, Thrombosis, and Vascular Biology*, *40*(3), 554–569.

Dohan, D. M., Choukroun, J., Diss, A., Dohan, S. L., Dohan, A. J., Mouhyi, J., & Gogly, B. (2006a). Platelet-rich fibrin (PRF): A second-generation platelet concentrate. Part I: Technological concepts and evolution. *Oral Surgery, Oral Medicine, Oral Pathology, Oral Radiology, and Endodontics*, *101*(3), e37–e44.

Dohan, D. M., Choukroun, J., Diss, A., Dohan, S. L., Dohan, A. J., Mouhyi, J., & Gogly, B. (2006b). Platelet-rich fibrin (PRF): A second-generation platelet concentrate. Part II: Platelet-related biologic features. *Oral Surgery, Oral Medicine, Oral Pathology, Oral Radiology, and Endodontics*, *101*(3), e45–e50.

Dohan, D. M., Choukroun, J., Diss, A., Dohan, S. L., Dohan, A. J., Mouhyi, J., & Gogly, B. (2006c). Platelet-rich fibrin (PRF): A second-generation platelet concentrate. Part III: Leucocyte activation: A new feature for platelet concentrates? *Oral Surgery, Oral Medicine, Oral Pathology, Oral Radiology, and Endodontics*, *101*(3), e51–e55.

Dohan Ehrenfest, D. M., Andia, I., Zumstein, M. A., Zhang, C. Q., Pinto, N. R., & Bielecki, T. (2014). Classification of platelet concentrates (platelet-rich plasma-PRP, platelet-rich fibrin-PRF) for topical and infiltrative use in orthopedic and sports medicine: Current consensus, clinical implications and perspectives. *Muscles Ligaments Tendons Journal*, *4*(1), 3–9.

Dohan Ehrenfest, D. M., Pinto, N. R., Pereda, A., Jiménez, P., Corso, M. D., Kang, B. S., … Quirynen, M. (2018). The impact of the centrifuge characteristics and centrifugation protocols on the cells, growth factors, and fibrin architecture of a leukocyte- and platelet-rich fibrin (L-PRF) clot and membrane. *Platelets*, *29*(2), 171–184.

Ehrenfest, D. M. D. (2010). How to optimize the preparation of leukocyte- and platelet-rich fibrin (L-PRF, Choukroun's technique) clots and membranes: Introducing the PRF box. *Oral Surgery, Oral Medicine, Oral Pathology, Oral Radiology, and Endodontics*, *110*(3), 275–278.

Elnager, A., Abdullah, W. Z., Hassan, R., Idris, Z., Wan Arfah, N., Sulaiman, S. A., & Mustafa, Z. (2014). In vitro whole blood clot lysis for fibrinolytic activity study using D-dimer and confocal microscopy. *Advances in Hematology*, *2014*, 814684.

Fujioka-Kobayashi, M., Miron, R. J., Hernandez, M., Kandalam, U., Zhang, Y., & Choukroun, J. (2017). Optimized platelet-rich fibrin with the low-speed concept: Growth factor release, biocompatibility, and cellular response. *Journal of Periodontology*, *88*(1), 112–121.

Hudson, N. E. (2017). Biophysical mechanisms mediating fibrin fiber lysis. *BioMed Research International*, *2017*, 2748340.

Jubert, N. J., Rodríguez, L., Reverté-Vinaixa, M. M., & Navarro, A. (2017). Platelet-rich plasma injections for advanced knee osteoarthritis: A prospective, randomized, double-blinded clinical trial. *Orthopaedic Journal of Sports Medicine*, *5*(2), 2325967116689386.

Kitamura, Y., Watanabe, T., Nakamura, M., Isobe, K., Kawabata, H., Uematsu, K., … Kawase, T. (2018). Platelet counts in insoluble platelet-rich fibrin clots: A direct method for accurate determination. *Frontiers in Bioengineering and Biotechnology*, *6*, 4.

Lourenço, E. S., Mourão, C. F. A. B., Leite, P. E. C., Granjeiro, J. M., Calasans-Maia, M. D., & Alves, G. G. (2018). The in vitro release of cytokines and growth factors from fibrin membranes produced through horizontal centrifugation. *Journal of Biomedical Materials Research. Part A*, *106*(5), 1373–1380.

Martino, M. M., Briquez, P. S., Ranga, A., Lutolf, M. P., & Hubbell, J. A. (2013). Heparin-binding domain of fibrin(ogen) binds growth factors and promotes tissue repair when incorporated within a synthetic matrix. *Proceedings of the National Academy of Sciences of the United States of America*, *110*(12), 4563–4568.

Miron, R., Choukroun, J., & Ghanaati, S. (2018). Controversies related to scientific report describing g-forces from studies on platelet-rich fibrin: Necessity for standardization of relative centrifugal force values. *International Journal of Growth Factors and Stem Cells in Dentistry*, *1*, 80–89.

Miron, R. J., Chai, J., Zheng, S., Feng, M., Sculean, A., & Zhang, Y. (2019). A novel method for evaluating and quantifying cell types in platelet rich fibrin and an introduction to horizontal centrifugation. *Journal of Biomedical Materials Research. Part A*, *107*(10), 2257–2271.

Miron, R. J., & Choukroun, J. (2017). *Platelet rich fibrin in regenerative dentistry: Biological background and clinical indications*, 1, Hoboken, New Jersey: Wiley.

Miron, R. J., Dham, A., Dham, U., Zhang, Y., Pikos, M. A., & Sculean, A. (2019). The effect of age, gender, and time between blood draw and start of centrifugation on the size outcomes of platelet-rich fibrin (PRF) membranes. *Clinical Oral Investigations*, *23*(5), 2179–2185.

Mourão, C. F. A. B., Calasans-Maia, M. D., Mello-Machado, R. C., Resende, R. F. B., & Alves, G. G. (2018). The use of platelet-rich fibrin as a hemostatic material in oral soft tissues. *Oral and Maxillofacial Surgery*, *22*(3), 329–333.

Peck, M. T., Hiss, D., Stephen, L., Satti, A., & Majeed, A. (2015). Platelet-rich fibrin (PRF)-the effect of storage time on platelet concentration. *South African Dental Journal*, *70*(10), 448–451.

Piccin, A., Di Pierro, A. M., Canzian, L., Primerano, M., Corvetta, D., Negri, G., … Fontanella, F. (2017). Platelet gel: A new therapeutic tool with great potential. *Blood Transfusion*, *15*(4), 333–340.

Pretorius, E., Steyn, H., Engelbrecht, M., Swanepoel, A. C., & Oberholzer, H. M. (2011). Differences in fibrin fiber diameters in healthy individuals and thromboembolic ischemic stroke patients. *Blood Coagulation & Fibrinolysis*, *22*(8), 696–700.

Sahni, A., Guo, M., Sahni, S. K., & Francis, C. W. (2004). Interleukin-1β but not IL-1α binds to fibrinogen and fibrin and has enhanced activity in the bound form. *Blood*, *104*(2), 409–414.

Watanabe, T., Isobe, K., Suzuki, T., Kawabata, H., Nakamura, M., Tsukioka, T., … Kawase, T. (2017). An evaluation of the accuracy of the subtraction method used for determining platelet counts in advanced platelet-rich fibrin and concentrated growth factor preparations. *Dentistry Journal (Basel)*, *5*(1), 7.

How to cite this article: ES Lourenço, GG Alves, R de Lima Barbosa, et al. Effects of rotor angle and time after centrifugation on the biological in vitro properties of platelet rich fibrin membranes. *J Biomed Mater Res*. 2020;1–9. https://doi.org/10.1002/jbm.b.34680

4 Anexo IV

applied sciences

MDPI

Article

Effects of Leukocyte-Platelet-Rich Fibrin (L–PRF) on Pain, Soft Tissue Healing, Growth Factors, and Cytokines after Third Molar Extraction: A Randomized, Split-Mouth, Double-Blinded Clinical Trial

Madelaine Torres da Silva [1], Carlos Fernando de Almeida Barros Mourão [2,3,*], Rafael Coutinho Mello-Machado [1], Pietro Montemezzi [4], Renata de Lima Barbosa [2], Suelen Cristina Sartoretto [3], Paulo Emílio Correa Leite [5], Kayvon Javid [1], Tomoyuki Kawase [6], Gutemberg Gomes Alves [2] and Mônica Diuana Calasans-Maia [3]

1 Graduate Program, Dentistry School, Universidade Federal Fluminense, Niteroi 24020-140, Brazil; madtorres.mt@gmail.com (M.T.d.S.); rafaelcoutinhodemello@yahoo.com.br (R.C.M.-M.); onecure@aol.com (K.J.)
2 Biotechnology Department, Universidade Federal Fluminense, Niteroi 24020-140, Brazil; renata_licaa@hotmail.com (R.d.L.B.); gutopepe@yahoo.com.br (G.G.A.)
3 Oral Surgery Department, Universidade Federal Fluminense, Niteroi 24020-140, Brazil; susartoretto@hotmail.com (S.C.S.); monicacalasansmaia@gmail.com (M.D.C.-M.)
4 Private Practice, 24128 Bergamo, Italy; m.montemezzi@libero.it
5 Bioengineering Program, Nacional Institute of Metrology, Quality and Technology, Duque de Caxias 25250-020, Brazil; leitepec@gmail.com
6 Division of Oral Bioengineering, Institute of Medicine and Dentistry, Niigata University, Niigata 951-8514, Japan; kawase@dent.niigata-u.ac.jp
* Correspondence: mouraocf@gmail.com; Tel.: +1-941-830-1302

check for updates

Citation: da Silva, M.T.; de Almeida Barros Mourão, C.F.; Mello-Machado, R.C.; Montemezzi, P.; de Lima Barbosa, R.; Sartoretto, S.C.; Leite, P.E.C.; Javid, K.; Kawase, T.; Alves, G.G.; et al. Effects of Leukocyte-Platelet-Rich Fibrin (L–PRF) on Pain, Soft Tissue Healing, Growth Factors, and Cytokines after Third Molar Extraction: A Randomized, Split-Mouth, Double-Blinded Clinical Trial. *Appl. Sci.* **2021**, *11*, 1666. https://doi.org/10.3390/app11041666

Academic Editors: Vanessa Nicolin and Claudio Stacchi
Received: 20 January 2021
Accepted: 3 February 2021
Published: 12 February 2021

Publisher's Note: MDPI stays neutral with regard to jurisdictional claims in published maps and institutional affiliations.

Abstract: This study assessed the effects of leukocyte-platelet-rich fibrin (L–PRF) on soft tissue healing and the correlation with the local concentration of growth factors (GF) and cytokines in the dental socket of lower third molars. Forty lower-third molars (20 participants) were included in this randomized, double-blinded, split-mouth study. After extractions, randomized sides received alveolar filling with L–PRF on one side and a natural blood clot on the other side. The pain was assessed for up to seven days and soft tissue healing (Landry index) for 14 days post-extraction. Swabs were collected from the surgical sites for GF and cytokine assessment by flow luminometry. Participants reported lower postoperative pain on the sides grafted with L–PRF, which also presented increased tissue healing scores ($p < 0.05$). There were increased levels of all GFs and several cytokines at the L–PRF site at day one, while vascular endothelial growth factor (VEGF), IL–10, and IL1–RA remained higher throughout for seven days ($p < 0.05$). VEGF concentration at L–PRF sites correlated positively with the participants' blood platelet content ($\rho = 0.769$). PDGF correlated negatively with pain experience on days 2 and 3, and positively with soft tissue healing scores, while FGFb presented a weak correlation with a reduction of pain on day 3. The use of L–PRF improves the soft tissue healing process and decreases postoperative pain after the third molar extractions, which correlates with an increase in the local concentration of growth factors such as PDGF and FGFb.

Keywords: platelet-rich fibrin; third molar; clinical trial; growth factors; cytokines

1. Introduction

Lower third molar tooth extraction is one of the most common surgeries performed by dental surgeons in the daily clinic. However, some postoperative complications, such as pain, trismus, swelling, and alveolitis, are possible after this procedure [1–3]. Therefore, different strategies have been developed to reduce the risk of these complications and improve tissue healing.

One of the current strategies is the implantation of the leukocyte-platelet-rich fibrin (L–PRF) immediately after tooth extraction. Prior studies have demonstrated the effectiveness of this autologous biomaterial in reducing postoperative complications in third molars [4,5]. This second-generation autologous blood-derived biomaterial contains a dense fibrin mesh with increased contents of platelets and leukocytes, as well as increased concentrations of essential growth factors and cytokines that will assist in tissue repair, especially concerning soft tissue healing [6,7]. Among those, the Transforming Growth Factor Beta (TGF–β), the Platelet-Derived Growth Factor (PDGF), the Vascular Endothelial Growth Factor (VEGF), and the basic Fibroblast Growth Factor (FGF–2) are considered some of the essential mediators produced by leukocytes and platelets in L–PRF membranes. There is strong in vitro evidence of continuous production and release of these mediators by the new autologous biomaterials [7–9].

Several studies on post-extraction sockets assessing the contribution of L–PRF have shown evaluations that indicated better postoperative and substantial improvements in soft tissue healing and pain reduction, employing tools such as the Landry index for soft tissue repair, and the Visual Analogue Scale (VAS) for pain [4,5,10,11]. These analyses contribute to a qualitative assessment related to the patient's recovery in the postoperative period. It may be supposed that these effects are mainly related to the continuous release of growth factors, previously described by different in vitro studies [9,12]. However, there is a lack of clinical evidence on the local release of growth factors and cytokines by grafted L–PRF membranes in this model and their correlation with the improvement in pain and tissue healing on the management of third molar extractions. Even though the local release assessment is challenging to transpose from in vitro to clinical settings, surface protein extraction methods using tapes and swabs have been successfully used in clinical studies [13,14]. In this context, the present study aimed to evaluate the tissue repair and postoperative pain in lower third molar extraction sockets treated with L–PRF, assessing the correlation between these outcomes and the presence of growth factors and cytokines quantified at the surface of the surgical site by using a swab extraction method.

2. Materials and Methods

2.1. Study Design and Outcomes

The present prospective study was conducted in a randomized, double-blind, and split-mouth design. The study was conducted at the Associate Laboratory of Clinical Research in Dentistry (LPCO) of the Dentistry School at Fluminense Federal University, Niterói, Rio de Janeiro, Brazil, between March and July 2019. The study adhered to the principles described in the Declaration of Helsinki and approved by the Ethical Committee of the Antonio Pedro University Hospital under the registration no. 2.721.351. All participants were informed of the study procedures/objectives and were included only after providing written informed consent. The Consolidated Standards of Reporting Trials (CONSORT) statement [15] guidelines were followed to ensure the quality and transparency of this trial.

The primary outcome was represented by postoperative pain and soft tissue healing. For the pain assessments, the primary outcome measures included the pain experienced until the 7th day after surgery according to VAS scores (days 1, 2, 3, and 7) and the Sum of Pain Intensity Differences (SPID) from 24 h to 48 h, 72 h, or 196 h after surgical procedures, while for soft tissue healing the measures were the Landry indexes at the 7th and 14th day after surgery. The secondary outcome was the content of tissue-healing and inflammatory mediators present in the mucosa at 24 h and seven days after surgery.

2.2. Sample Calculation and Randomization

This study's sample size calculation was performed using the software SPSS, version 22.0 (IBM Corporation, Armonk, NY, USA). The primary outcomes (pain and tissue healing) were chosen to calculate the sample size based on the availability of supporting data from the literature. The data from previous studies related to third molars extraction and L–PRF placement [5,10] and a pilot study with 5 patients (included in the present research) shows

that a sample size of at least 16 extractions in each group is required to achieve 80% power at a significance level of 5% ($\alpha = 0.05$) [16]. Therefore, a sample size of 20 extractions for each group was adopted (two extractions per patient, for a total of 20 participants). Randomization was performed through the flipping of a coin, where each side represented an experimental group. The sides—the right or left dental sockets—were distributed into two groups: L–PRF ($n = 20$) and Clot ($n = 20$). The allocation sequence was concealed until participants were enrolled and assigned to interventions.

2.3. Inclusion and Exclusion Criteria

The complete medical and dental history of each participant was obtained. Participants between 18 to 30 years old requiring lower third molar extractions with Level A and Class I, according to the Pell–Gregory classification [17], were included. Participants were excluded from the study if they were smokers, presented local infection (e.g., pericoronitis), had motor difficulties that impeded or hampered hygiene, had prior pain in the orofacial region (e.g., joints and/or masticatory muscles issues), were pregnant, had decompensated metabolic diseases or periodontal disease without previous treatment, or had a history of radiotherapy or use of bisphosphonates.

All research participants were previously informed of the physical and psychological criteria required to participate in this project. The psychological criteria for project participation included no history of anxiety, mood, eating, and/or psychotic disorders that could compromise participation and collaboration in the study.

2.4. Participant Selection

Recruitment of research participants was carried out by a trained investigator (R.C.M.-M.), who diagnosed the indication of the lower third molar extractions after the admission of the patients to the School of Dentistry. The initial evaluation and diagnosis of the teeth indicated for extraction was confirmed by two other trained professionals who were not a part of this research team. All the participants were masked to the studied groups.

2.5. Pre-Surgical Procedures

Venipuncture was performed prior to any treatment (median basilica vein, median cubital vein, median cephalic vein). Blood was drawn into two sterile red cover 10 mL tubes without anticoagulant (BD Vacutainer®, Becton Serum Blood Collection Tubes, Dickinson & Company, Franklin Lakes, NJ, USA). This process was performed at room temperature (20 °C).

L–PRF clots were produced using tubes according to the fabricant (IntraSpin™, Biohorizons®, Birmingham, AL, USA), and immediately centrifuged at 2700 rpm for 12 min (~708 g) using a vertical/fixed-angle centrifuge (IntraSpin™, Biohorizons®, Birmingham, Alabama, AL, USA). This centrifugation protocol considered the g-force value referenced at the bottom of the centrifugation tubes (RCF–max) [18]. After centrifugation, each L–PRF clot was removed from the tube and separated from the red element phase at the base using cotton pliers.

A further blood sample was collected in a 4 mL EDTA tube (BD Vacutainer Lavender K2–EDTA Blood Collection Tubes, Dickinson and Company, USA) for hematological analysis. The analysis was performed using the Wiener lab. Counter 19/19 CP (Labinbraz Comercial Ltd.a, Sao Paulo, Brazil), obtaining the platelet and white blood cells (WBC) counts of each participant.

2.6. Surgical Procedures

Panoramic radiographs were taken by the same professional operator and with the use of the same machine (i–CAT, Kavo, Brazil). The participants were informed to avoid the use of any anti-inflammatory drugs before the surgery, or any other medication to prevent the influence on the healing process. All surgeries were performed by the same operator (C.F.M.) with the same pre-, trans-, and postoperative protocol. The examiner

responsible for postoperative evaluations (M.T.S.) was not present in any surgery, blinding the study for the evaluation. The participants were also not informed about the location of the sockets that received the L–PRF or the sockets that were clot-filled.

Local asepsis was performed by rinsing with 0.12% chlorhexidine digluconate (Periogard® Colgate, São Paulo, Brazil) for one minute and with extraoral use of 4% chlorhexidine soap (Riohex Rioquímica®, Rio de Janeiro, Brazil). The local anesthesia was administered using a Carpule syringe (Quinelato®, Schobell Industrial Ltd.a., São Paulo, SP, Brazil) to block the inferior alveolar lingual and buccal nerves, using 2% alphacaine with 1:100,000 epinephrine (DFL Indústria e Comércio®, Rio de Janeiro, RJ, Brazil). Both sides were blocked before the third molar extractions. Soft tissue release around the tooth was performed using a no. 3 scalpel handle (Bard Park, Quinelato®, Sao Paulo, SP, Brazil) and a no. 15 blade (Solidor, Lamelid®, SãoPaulo, Brazil) to test the success of deep anesthesia and for better apical positioning of the elevators and forceps. Tissue detachment was performed using a Molt no. 9 detacher (Quinelato®, São Paulo, SP, Brazil) around the tooth, followed by elevator and forceps dislocation (Quinelato®, Sao Paulo, SP, Brazil) for later removal. After the extraction was completed, the dental socket was gently explored with a Lucas no. 4 Curette (Quinelato®, Sao Paulo, SP. Brazil) and irrigated with 0.9% physiological saline solution (~20 mL).

For each participant, one dental socket was left as is to be filled with blood as a physiological condition after tooth removal. A few minutes after extraction, the clot could be noticed at the level of the alveolar border. In the absence of a blood clot, a gentle curettage of the alveolar socket was performed to cause slight bleeding. For the sockets receiving the L–PRF, after removing the third molar, four L–PRF clots were placed directly in the dental socket with the aid of an alveolar curette. The tissue was sutured using the traditional single stitch suturing technique with a Johnson 4–0 silk thread (Johnson & Johnson, Ethicon®, São Paulo, Brazil). The number of stitches was determined by the surgeon's criteria, who performed a primary closure in all cases. It is essential to mention that after tooth extraction, there was a simulated manipulation of the tissue to hide to the research participant the side in which the L–PRF grafting occurred.

Paracetamol (500 mg, Tylenol, Johnson & Johnson, Brazil) was prescribed every six hours for pain. In the case of severe pain reported, a protocol was adopted, including an emergency medication (Ibuprofen 400 mg, Advil, Pfizer, USA) every eight hours for three days. Oral hygiene instructions were provided to avoid the accumulation of bacterial plaque above the suture. Participants were instructed to use 0.12% chlorhexidine digluconate rinse (Periogard®, Colgate, São Paulo, Brazil) twice daily for seven days. All sutures were removed after seventy days.

2.7. Clinical Measurements

The participants were scheduled for postoperative evaluation after 1, 2, 3, 7, and 14 days. During those appointments, the evaluation of clinical measurements was performed by the same examiner masked to the study, including parameters such as soft tissue healing, pain, and the number of analgesics consumed. Postoperative pain was measured in all participants on days 1, 2, 3, and 7, while the healing index was measured on days 7 and 14 (even though the routine clinical examination was performed on the first days).

The assessment of soft tissue healing around the sockets was performed using the healing index system described by Landry et al. [19]. The following parameters were used to assess the level of healing: the color of tissues, epithelialization of wound margins, the presence of bleeding on palpation, granulation, and suppuration. The level of healing was scored as 1–very poor, 2–poor, 3–good, 4–very good, or 5–excellent. As an example, very poor healing was attributed to sites with tissue color that was more than 50% red, and the presence of bleeding, tissue granulation, and suppuration. On the other hand, excellent healing was attributed to sites with a healthy pink color and without bleeding, tissue granulation, or exposed connective tissue.

Pain analysis was performed according to the VAS on a 0–10 scale, where 0 indicates the absence of pain and 10 was attributed to the most severe pain ever felt, along with the

graphic classification scale [20]. The participants were previously oriented regarding the pain assessment and asked to report any difficulty in distinguishing between sites. The number of painkillers consumed was also recorded. In this study, a score ≥ 5 was considered as an indicator of severe pain after the third molar extraction [21], resulting in the use of emergency medication for the patients. A derived time-weighted endpoint, the Sum of Pain Intensity Differences (SPID), was also calculated from the available times of data collection, considering the first measure (24 h) as a baseline, and its difference score calculated at each subsequent time point, in hours (SPID24–48, SPID24–72, and SPID24–196).

2.8. Quantification of Cytokines and Growth Factors

On the first and seventh postoperative days, the participants submitted to a swab collection in the surgical region on both sides in order to collect the surface cytokines and growth factors present in the site. The alveolar ridge was isolated with cotton rollers to avoid saliva collection, and after that it was dried with an air jet for 10 s. The samples were collected through friction in the central portion of the socket, in addition to the buccal, lingual, distal, and mesial portion of the gingival border of the operated region. Sterile swabs were used for this procedure (Plastic-Cotton Tipped Applicators, MedLine Industries, IL, USA). The swabs were then placed on 15 mL falcon tubes containing 1.5 mL phosphate-buffered saline solution (PBS) with 0.2% sodium dodecyl sulfate (SDS) and 0.5% propylene glycol and sonicated for 30 min on an ultrasonic bath maintained at 4 °C with ice, for the extraction of proteins. The liquid was collected and stored in different aliquots in cryovials and kept in an ultra-freezer at −80 °C until the quantification assays. The quantification was performed by a masked operator.

For the detection of the biomolecules, a multiparametric immunoassay based on XMap-labeled magnetic microbeads (LuminexCorp, Blvd Austin, TX, USA) was used, through a commercial kit (27–plex panel, Biorad Inc., USA) capable of quantifying IL–1β, IL1-RA, IL-4, IL-6, IL8, IL–10, IL–12 (p70), IL–13, IL–15, IL–17, CCL11, FGF–b, CSF3, CSF2, IFN–γ, CXCL10, CCL2, CCL3, CCL–4, PDGF, CCL5, TNFα and VEGF, and a 1–plex kit containing TGF–β1 beads. Quantification of the magnetic beads and dosages was performed with a BioPlex MAGPIX system (Biorad Inc., Hercules, CA, USA). Results were analyzed using the Xponent v. 3.0 software (Luminexcorp, USA).

2.9. Statistical Analysis

Wilcoxon nonparametric two-tailed tests were used for the comparison of the clinical data in the postoperative period. Data from the cytokine and growth factor assessment for the control and L–PRF sites were analyzed by nonparametric, paired Mann-Whitney U tests. The correlation between the molecule concentrations and the clinical parameters or the blood cell count (WBC and platelet) was investigated through a two-tailed Spearman's rank correlation matrix, where coefficients between 0.3–0.5 indicated weak correlations, 0.5–0.7 indicated moderate correlations, and coefficients above 0.7 indicated strong correlations, according to a rule of thumb proposed previously [22]. The data was also evaluated through multiple regression analyses using the least squares method, where each outcome measure (VAS, CI, SPID) was considered to be the independent variable on a test. The normality of residuals was assessed by the D'Agostino-Pearson omnibus and Kolmogorov–Smirnov tests. For all tests, an alpha error of 5% was considered. The tests were performed with the help of the GraphPad Prism 8.0 (GraphPad Software Inc., San Diego, CA, USA).

3. Results

3.1. Clinical Evaluation

The sample of recruited participants (March–July 2019) was composed of fourteen females and six males, with a mean age of ~23 years old (range 18–29) (Table 1). The follow-up during the postoperative period indicated a good recovery in all cases without serious complications, intolerance to the medication used, or side effects. There was no

alveolar osteitis, tissue necrosis, abscess, or delayed healing. The CONSORT chart of participant flow is shown in Figure 1.

Table 1. Socio-demographic data of the patients included in the study.

Gender	n = 20 (Participants)
Male	6
Female	14
Age (years), mean ± SD	23 ± 3.28
Education Level	
High school diploma	14 (9 female and 5 male)
Bachelor's degree	6 (5 female and 1 male)
Extraction indication	n = 40 (dental extractions)
Previous pericoronitis	17
Dental caries	9
Orthodontic treatment	14

SD = Standard deviation.

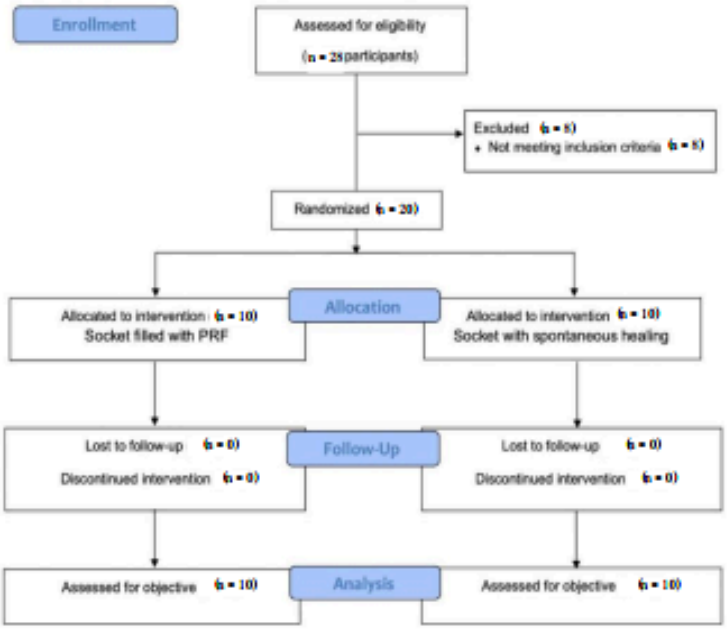

Figure 1. Flowchart illustrating the procedure of the clinical trial (CONSORT) [15].

No participant reported difficulties in differentiating the pain between both surgical sites. On the first postoperative day, a total of 70% of the participants reported severe pain on the site without the use of L–PRF, while 30% experienced severe pain in the L–PRF site. On the second day, the results were 30% and 10%, respectively. Only 10% of the patients reported severe pain in the clot site on the third day, while no severe pain was reported in both groups on the seventh day. Figure 2A shows that the mean score on VAS was significantly lower on the L–PRF sites in all the assessed days ($p < 0.05$). Overall, the average use of Paracetamol per participant was 1.4 tablets per day in the first three days. Of the 20 participants, six made use of emergency medication (Ibuprofen) for three days in the same period and the pain was controlled after that. When the pain was compared using the time-weighted endpoint SPID, there was no significant difference ($p < 0.05$) between control and L–PRF groups from 24 h after surgery to either 48 h (26 ± 26 for

L–PRF versus 39 ± 36 for Control), 72 h (84 ± 46 for L–PRF versus 90 ± 56 for Control), or 196 h (439 ± 150 for L–PRF versus 565 ± 160 for Control). Figure 2B shows the assessments for the cicatrization index.

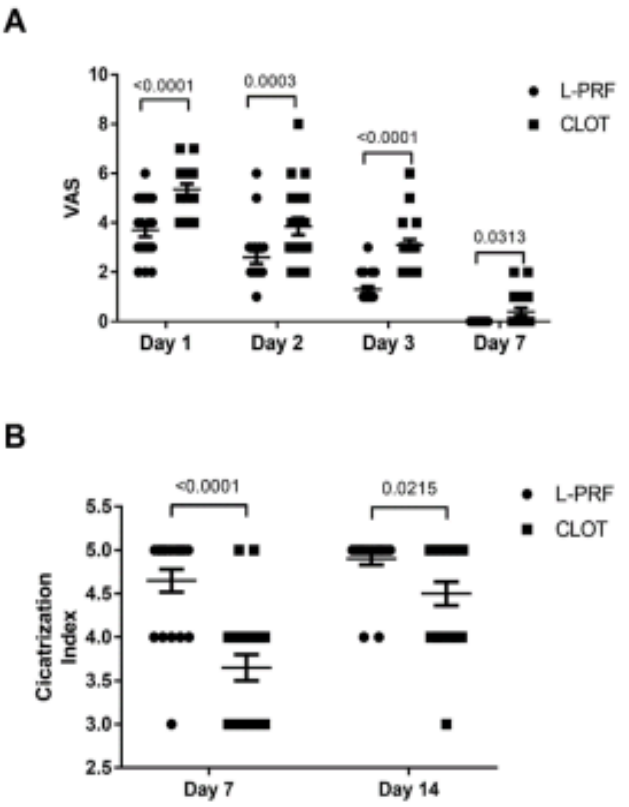

Figure 2. (A) Pain evaluation by Visual Analog Scale (VAS) for 1, 2, 3, and 7 days in the postoperative period. (B) Comparison of the soft tissue healing, as measured by the Landry´s index, at seven and 14 days of the postoperative period. Squares indicate the score for the clot site of each participant, while circles indicate the scores for the leukocyte-platelet-rich fibrin (L-PRF) sites. Lines indicate the mean ± SD. Connecting lines indicate statistical difference (p value indicated on the figure).

On the seventh day, it was possible to find a highly significant difference after the comparison to the Clot group ($p < 0.0001$). After 14 days, a significant difference was also observed, showing a better healing process to the L–PRF group ($p = 0.0215$). It is possible to observe the healing follow-up in Figure 3.

3.2. *Biochemical Analysis*

Figure 4 shows the mean content of growth factors and cytokines measured on the surface of the surgical sites (control and L–PRF), on the first and seventh days after the procedure. From the 28 analytes initially assessed, twelve had detectable levels after extraction from the swabs. From those, all growth factors (VEGF, FGF–2, PDGFbb, TGF–β1) and the majority of the inflammatory cytokines (IL–1β, IL–4, TNF–α, IL1–RA, IL–10, and IFN–gamma) were present at significantly higher levels in the L–PRF sites, as compared to Clot at day 1 ($p < 0.05$). However, by the end of one week most of the analytes were present at similar levels at the L–PRF and Clot sites, with the exceptions of VEGF, which attained a

two-fold increase as compared to control, and the anti-inflammatory cytokines IL–10 and IL–1RA, which were around 1.5 × increased at the L–PRF sites ($p < 0.05$).

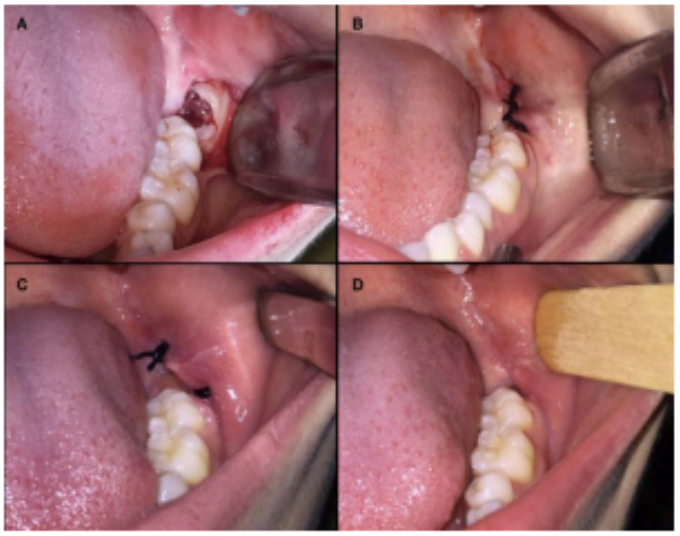

Figure 3. (A) L–PRF placed at the dental socket; (B) Immediate postoperative area, after suturing; (C) Evaluation of soft tissue healing after seven days, socket showing good healing (Landry's Index 3) (D) After 14th day with excellent healing (Landry's Index 5) of soft tissues.

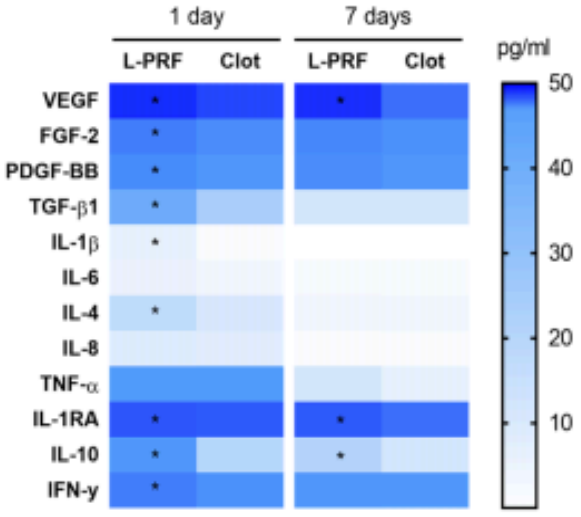

Figure 4. Heatmap of the cytokines extracted from swabs of the L–PRF and Clot sites at 1 and 7 days after surgery. The intensity of the blue color indicates the mean concentration (n = 20) of each analyte, as detected by flow luminometry. An asterisk indicates a significant difference between L–PRF and Clot at the same experimental time ($p < 0.05$).

In order to observe if the content of growth factors and cytokines could correlate with hematological parameters (WBC and platelets) of each participant, an analysis was

performed with blood samples collected before the production of L–PRF. The hematological analysis showed that the WBC (6.99 ± 1.30) and platelets (262.7 ± 14.90). The WBC count (×103/microL) were within normal ranges in all participants. A Spearman's rank correlation test was performed between the WBC and platelet contents, and the values of analytes detected for each participant (Table 2). From all interactions, a significant positive correlation was detected between the blood platelet count of the participants and the surface concentration of VEGF ($p = 0.04$, rho = 0.769). TGF–β1 presented a coefficient comparable to a moderate correlation with platelet content, even with a non-significant borderline p value ($p = 0.05$, rho = 0.634).

In order to identify relationships between the outcome measurements and the detected biological mediators, several multiple regression analyses were performed, as shown in Table 3 for the control group and Table 4 for the L–PRF sites. The multiple r^2 from the tests varied from 0.596 to 0.741, and the residuals passed normality in all tests ($p < 0.05$). However, no significant association was identified between any pain or cicatrization index and the concentrations of growth factors and cytokines in both surgical sites ($p > 0.05$). However, when a correlation matrix was produced between the local growth factor/cytokine concentrations and the clinical evaluation scores through a two-tailed analysis, significant correlations were observed between some endpoints and growth factors, as shown in Table 5. FGFb presented a weak negative correlation with the pain score on the third day (Rho = −0.479, $p = 0.033$), while PDGF negatively correlated with pain scores on both the second and third days (Rho = 0.524, $p = 0.018$ and Rho = −0.709, $p = 0.009$, respectively) and with the cicatrization indexes on the seventh (Rho = 0.516, $p = 0.020$) and 14th days (Rho = 0.522, $p = 0.018$).

Table 2. Analysis of correlation between cell counts and surface cytokine/growth factor concentration on each site of the participants (Clot and L–PRF), at day one after surgery.

		VEGF	TGF–β1	FGFb	PDGF–bb	TNF–α	IL–10	IL–6	IL–4	IL–1β	IL–8	IL–1RA	IFN–γ
Clot Leucocytes (WBC)	Spearman ρ	−0.432	0.0365	0.335	0.054	−0.032	−0.275	0.450	−0.481	0.098	−0.429	−0.372	−0.243
	p value	0.212	0.924	0.341	0.884	0.933	0.435	0.191	0.159	0.789	0.216	0.286	0.494
Platelets	Spearman ρ	0.079	0.382	−0.468	−0.395	0.110	0.176	0.123	0.175	0.132	0.129	0.1963	0.060
	p value	0.899	0.272	0.173	0.256	0.764	0.620	0.734	0.620	0.713	0.719	0.578	0.871
L–PRF Leucocytes (WBC)	Spearman ρ	−0.561	0.465	−0.226	−0.287	−0.440	−0.440	0.000	−0.142	−0.218	−0.258	0.017	0.278
	p value	0.096	0.177	0.529	0.420	0.202	0.203	1.009	0.694	0.553	0.467	1.000	0.431
Platelets	Spearman ρ	**0.769 ***	0.634	0.012	0.049	0.430	0.021	−0.389	−0.135	−0.359	0.051	−0.638	−0.490
	p value	**0.040**	0.050	0.980	0.899	0.212	0.957	0.264	0.708	0.308	0.889	0.067	0.154

Bold numbers with an asterisk indicate a significative correlation ($p < 0.05$, Rho > 0.3).

Table 3. Results for the multiple regression analysis between the different outcomes and the detected growth factors and cytokines on the Control site.

		VEGF	TGF-b1	FGFb	PDGF-bb	TNF-alfa	IL-10	IL-6	IL-4	IL-1b	IL-8	IL-1RA	IFN-Gamma
VAS (day one)	Coefficient	−0.002922	0.3448	−2.08	0.3448	0.3501	0.0003067	−2.669	0.9531	−5.03	2.771	0.02966	−0.1704
Multiple R2 = 0.6538	SE	1.74609×10^{11}	8.689×10^{14}	1.352×10^{14}	1.071×10^{15}	7.551×10^{14}	3.43×10^{10}	7.609×10^{15}	2.202×10^{14}	$2,514 \times 10^{15}$	$4,265 \times 10^{15}$	$7,81449 \times 10^{12}$	$1,59 \times 10^{14}$
	95% CI	-4.12×10^{11} to 4.12×10^{12}	-2.055×10^{15} to 2.055×10^{15}	-3.196×10^{14} to 3.196×10^{14}	-2.533×10^{15} to 2.533×10^{15}	-1.785×10^{15} to 1.785×10^{15}	-8.11×10^{10} to 8.11×10^{10}	-1.799×10^{16} to 1.799×10^{16}	-5.207×10^{14} to 5.207×10^{14}	-5.946×10^{15} to 5.946×10^{15}	-1.009×10^{16} to 1.009×10^{16}	-1.84×10^{12} to 1.84×10^{12}	-3.760×10^{14} to 3.760×10^{14}
	p value	>0.9999	>0.9999	>0.9999	>0.9999	>0.9999	>0.9999	>0.9999	>0.9999	>0.9999	>0.9999	>0.9999	>0.9999
VAS (day 2)	Coefficient	0.01323	−0.916	−1.279	−0.916	0.8711	0.0001924	−2.471	2.224	−10.74	4.307	0.006912	−0.2313
Multiple R2 = 0.5957	SE	2.98372×10^{11}	1.485×10^{15}	2.31×10^{14}	1.83×10^{15}	1.29×10^{15}	58,631,858,055	1.3×10^{16}	3.763×10^{14}	4.297×10^{15}	7.288×10^{15}	1.33534×10^{13}	2.717×10^{14}
	95% CI	−70,553,7947,738 to 705,537,947,738	-3.511×10^{15} to 3.511×10^{15}	-5.462×10^{14} to 5.462×10^{14}	-4.328×10^{15} to 4.328×10^{15}	-3.051×10^{15} to 3.051×10^{15}	−138,642,313,474 to 138642313474	-3.074×10^{16} to 3.074×10^{16}	-8.898×10^{14} to 8.898×10^{14}	-1.016×10^{16} to 1.016×10^{16}	-1.723×10^{16} to 1.723×10^{16}	−315,75,789,661,657 to 31,575,789,661,657	-6.424×10^{14} to 6.424×10^{14}
	p value	>0.9999	>0.9999	>0.9999	>0.9999	>0.9999	>0.9999	>0.9999	>0.9999	>0.9999	>0.9999	>0.9999	>0.9999
VAS (day 3)	Coefficient	−0.008301	−0.3741	−2.558	−0.3741	0.6477	−0.0000004932	−4.217	3.077	−9.134	2.942	0.02786	−0.2079
Multiple R2 = 0.5957	SE	1.78067×10^{11}	8.862×10^{14}	1.378×10^{14}	1.092×10^{15}	7.7×10^{14}	34,991,205,207	7.759×10^{15}	2.246×10^{14}	2.564×10^{15}	4.35×10^{15}	7.96925×10^{12}	1.621×10^{14}
	95% CI	-4.21×10^{11} to 4.21×10^{11}	-2.095×10^{15} to 2.095×10^{15}	-3.259×10^{14} to 3.259×10^{14}	-2.583×10^{15} to 2.583×10^{15}	-1.821×10^{15} to 1.821×10^{15}	-8.27×10^{10} to 8.27×10^{10}	-1.835×10^{16} to 1.835×10^{16}	-5.310×10^{14} to 5.310×10^{14}	-6.063×10^{15} to 6.063×10^{15}	-1.028×10^{16} to 1.028×10^{16}	-1.88×10^{13} to 1.88×10^{13}	-3.834×10^{14} to 3.834×10^{14}
	p value	>0.9999	>0.9999	>0.9999	>0.9999	>0.9999	>0.9999	>0.9999	>0.9999	>0.9999	>0.9999	>0.9999	>0.9999
CI (day 7)	Coefficient	−0.003013	0.02395	−0.06562	0.02394	0.2534	0.00002793	−1.158	2.91	−5.612	−0.6447	−0.006342	−0.0268
Multiple R2 = 0.6824	SE	1.25912×10^{11}	6.266×10^{14}	9.74692×10^{13}	7.724×10^{14}	5.445×10^{14}	24742518484	5.487×10^{15}	1.588×10^{14}	1.813×10^{15}	3.076×10^{15}	5.63511×10^{12}	1.147×10^{14}
	95% CI	-2.97×10^{11} to 2.97×10^{11}	-1.482×10^{15} to 1.482×10^{15}	-2.305×10^{14} to 2.305×10^{14}	-1.826×10^{15} to 1.826×10^{15}	-1.287×10^{15} to 1.287×10^{15}	-5.85×10^{10} to 5.85×10^{10}	-1.297×10^{16} to 1.297×10^{16}	-3.755×10^{14} to 3.755×10^{14}	-4.287×10^{15} to 4.287×10^{15}	-7.273×10^{15} to 7.273×10^{15}	-1.3×10^{13} to 1.3×10^{13}	-2.711×10^{14} to 2.711×10^{14}
	p value	>0.9999	>0.9999	>0.9999	>0.9999	>0.9999	>0.9999	>0.9999	>0.9999	>0.9999	>0.9999	>0.9999	>0.9999
CI (day 14)	Coefficient	0.002542	−0.1547	0.03387	−0.1547	−0.226	0.00008631	−0.1141	−2.935	6.486	−0.4847	0.009534	0.0623
Multiple R2 = 0.6667	SE	1.10432×10^{11}	5.496×10^{14}	8.54861×10^{13}	6.774×10^{14}	4.775×10^{14}	21,700,624,254	4.812×10^{15}	1.393×10^{14}	1.59×10^{15}	2.697×10^{15}	4.94232×10^{12}	1.006×10^{14}
	95% CI	-2.61×10^{11} to 2.61×10^{11}	-1.300×10^{15} to 1.300×10^{15}	-2.021×10^{14} to 2.021×10^{14}	-1.602×10^{15} to 1.602×10^{15}	-1.129×10^{15} to 1.129×10^{15}	-5.13×10^{10} to 5.13×10^{10}	-1.138×10^{16} to 1.138×10^{16}	-3.293×10^{14} to 3.293×10^{14}	-3.760×10^{15} to 3.760×10^{15}	-6.378×10^{15} to 6.378×10^{15}	-1.16×10^{13} to 1.16×10^{13}	-2.378×10^{14} to 2.378×10^{14}
	p-value	>0.9999	>0.9999	>0.9999	>0.9999	>0.9999	>0.9999	>0.9999	>0.9999	>0.9999	>0.9999	>0.9999	>0.9999
SPID 24–48	Coefficient	−0.3877	30.26	−19.21	30.26	−12.5	0.002744	−4.739	−30.49	137	−36.86	0.5459	1.462
Multiple R2 = 0.7039	SE	7.68153×10^{12}	3.823×10^{16}	5.946×10^{15}	4.712×10^{16}	3.322×10^{16}	1.50947×10^{12}	3.347×10^{17}	9.688×10^{15}	1.106×10^{17}	1.876×10^{17}	3.438×10^{14}	6.995×10^{15}
	95% CI	-1.82×10^{13} to 1.82×10^{13}	-9.039×10^{16} to 9.039×10^{16}	-1.406×10^{16} to 1.406×10^{16}	-1.114×10^{17} to 1.114×10^{17}	-7.855×10^{16} to 7.855×10^{16}	-3.56×10^{12} to 3.56×10^{12}	-7.915×10^{17} to 7.915×10^{17}	-2.291×10^{16} to 2.291×10^{16}	-2.616×10^{17} to 2.616×10^{17}	-4.437×10^{17} to 4.437×10^{17}	-8.129×10^{14} to 8.129×10^{14}	-1.654×10^{16} to 1.654×10^{16}
	p value	>0.9999	>0.9999	>0.9999	>0.9999	>0.9999	>0.9999	>0.9999	>0.9999	>0.9999	>0.9999	>0.9999	>0.9999
SPID 24–72	Coefficient	−0.2586	47.51	−7.727	47.51	−19.65	0.01022	32.42	−81.46	235.5	−40.96	0.5892	2.362
Multiple R2 = 0.7411	SE	1.26831×10^{13}	6.312×10^{16}	9.818×10^{15}	7.78×10^{16}	5.485×10^{16}	2.49231×10^{12}	5.527×10^{17}	1.6×10^{16}	1.826×10^{17}	3.098×10^{17}	5.676×10^{14}	1.155×10^{16}
	95% CI	-2.99×10^{13} to 2.99×10^{13}	-1.492×10^{17} to 1.492×10^{17}	-2.322×10^{16} to 2.322×10^{16}	-1.840×10^{17} to 1.840×10^{17}	-1.297×10^{17} to 1.297×10^{17}	-5.89×10^{12} to 5.89×10^{12}	-1.307×10^{18} to 1.307×10^{18}	-3.782×10^{16} to 3.782×10^{16}	-4.319×10^{17} to 4.319×10^{17}	-7.326×10^{17} to 7.326×10^{17}	-1.342×10^{15} to 1.342×10^{15}	-2.731×10^{16} to 2.731×10^{16}
	p value	>0.9999	>0.9999	>0.9999	>0.9999	>0.9999	>0.9999	>0.9999	>0.9999	>0.9999	>0.9999	>0.9999	>0.9999

Table 3. *Cont.*

		VEGF	TGF-b1	FGFb	PDGF-bb	TNF-alfa	IL-10	IL-6	IL-4	IL-1b	IL-8	IL-1RA	IFN-Gamma
SPID 24–168	Coefficient	−0.1601	69.64	−28.6	69.64	−15.58	0.0581	57.51	−133.7	136.4	116.9	1.578	−4.764
Multiple R2 = 0.6888	SE	2.91903×10^{13}	1.453×10^{17}	2.26×10^{16}	1.791×10^{17}	1.262×10^{17}	5.73606×10^{12}	1.272×10^{18}	3.681×10^{16}	4.203×10^{17}	7.13×10^{17}	1.306×10^{15}	2.658×10^{16}
	95% CI	-6.9×10^{13} to 6.9×10^{13}	-3.435×10^{17} to 3.435×10^{17}	-5.343×10^{16} to 5.343×10^{16}	-4.234×10^{17} to 4.234×10^{17}	-2.985×10^{17} to 2.985×10^{17}	-1.35×10^{12} to 1.35×10^{12}	-3.008×10^{18} to 3.008×10^{18}	-8.705×10^{16} to 8.705×10^{16}	-9.939×10^{17} to 9.939×10^{17}	-1.686×10^{18} to 1.686×10^{18}	-3.089×10^{15} to 3.089×10^{15}	-6.285×10^{16} to 6.285×10^{16}
	p value												

VAS—Visual analog scale of pain; CI—Cicatrization Index; SPID—Sum of Pain Intensity Difference for the determined interval, in hours; 95% CI—95% confidence interval; SE—standard error.

Table 4. Results for the multiple regression analysis between the different outcomes and the detected growth factors and cytokines on the L–PRF surgical site.

		VEGF	TGF–b1	FGFb	PDGF–bb	TNF–alfa	IL–10	IL–6	IL–4	IL–1b	IL–8	IL–1RA	IFN–Gamma
VAS (day one)	Coefficient	0.02764	−0.1627	0.1696	−2.716	−0.04526	0.04117	2.914	−0.4218	−3.725	0.8876	0.0283	−0.0944
Multiple R2 = 0.6538	SE	2.26727×10^{12}	6.864×10^{14}	1.84×10^{14}	4.094	6.66499×10^{13}	3.52915×10^{12}	6.25×10^{15}	2.292×10^{15}	3.893×10^{15}	2.153×10^{15}	5.89863×10^{12}	7.88918×10^{13}
	95% CI	-5.36×10^{12} to 5.36×10^{12}	-1.62×10^{15} to 1.623×10^{15}	-4.351×10^{14} to 4.351×10^{14}	−12.40 to 6.965	-1.576×10^{14} to 1.576×10^{14}	-8.34×10^{12} to 8.34×10^{12}	-1.478×10^{16} to 1.478×10^{16}	-5.421×10^{15} to 5.421×10^{15}	-9.205×10^{15} to 9.205×10^{15}	-5.091×10^{15} to 5.091×10^{15}	-1.39×10^{12} to 1.39×10^{12}	-1.865×10^{14} to 1.865×10^{14}
	p value	>0.9999	>0.9999	>0.9999	0.5283	>0.9999	>0.9999	>0.9999	>0.9999	>0.9999	>0.9999	>0.9999	>0.9999
VAS (day 2)	Coefficient	0.001511	0.03459	2.165	−2.875	0.2745	−0.01392	−0.4092	−0.05736	−0.1734	0.4868	0.00836	−0.03179
Multiple R2 = 0.5957	SE	2.34162×10^{12}	7.089×10^{14}	1.901×10^{14}	4.175	6.88358×10^{13}	3.64489×10^{12}	6.455×10^{15}	2.368×10^{15}	4.02×10^{15}	2.224×10^{15}	6.09207×10^{12}	8.14791×10^{13}
	95% CI	-5.54×10^{12} to 5.54×10^{12}	-1.676×10^{15} to 1.676×10^{15}	-4.494×10^{14} to 4.494×10^{14}	−12.75 to 6.998	-1.628×10^{14} to 1.628×10^{14}	-8.62×10^{12} to 8.62×10^{12}	-1.526×10^{16} to 1.526×10^{16}	-5.599×10^{15} to 5.599×10^{15}	-9.507×10^{15} to 9.507×10^{15}	-5.258×10^{15} to 5.258×10^{15}	-1.44×10^{12} to 1.44×10^{12}	-1.92×10^{14} to 1.92×10^{14}
	p value	>0.9999	>0.9999	>0.9999	0.5133	>0.9999	>0.9999	>0.9999	>0.9999	>0.9999	>0.9999	>0.9999	>0.9999
VAS (day 3)	Coefficient	0.0009442	0.04703	0.2057	−1.876	0.131	−0.01446	0.5434	−0.2135	−0.776	0.9408	0.002328	−0.03558
Multiple R2 = 0.5957	SE	1.17081×10^{12}	3.544×10^{14}	9.50296×10^{13}	1.64	3.44179×10^{13}	1.82244×10^{12}	3.228×10^{15}	1.184×10^{15}	2.01×10^{15}	1.112×10^{15}	3.04604×10^{12}	4.07395×10^{13}
	95% CI	-2.77×10^{12} to 2.77×10^{12}	-8.381×10^{14} to 8.381×10^{14}	-2.247×10^{14} to 2.247×10^{14}	−5.755 to 2.003	-8.13×10^{14} to 8.13×10^{14}	-4.30×10^{12} to 4.30×10^{12}	-7.632×10^{15} to 7.632×10^{15}	-2.799×10^{15} to 2.799×10^{15}	-4.753×10^{15} to 4.753×10^{15}	-2.629×10^{15} to 2.629×10^{15}	-7.20×10^{12} to 7.20×10^{12}	-9.63×10^{14} to 9.63×10^{14}
	p value	>0.9999	>0.9999	>0.9999	0.2903	>0.9999	>0.9999	>0.9999	>0.9999	>0.9999	>0.9999	>0.9999	>0.9999
CI (day 7)	Coefficient	−0.01202	−0.4186	−2.129	1.224	−0.1411	0.01456	4.754	0.4722	−2.011	0.8682	0.0071	−0.05192
Multiple R2 = 0.6824	SE	1.09519×10^{12}	3.315×10^{14}	8.8892×10^{13}	2.042	3.2195×10^{13}	1.70474×10^{12}	3.019×10^{15}	1.107×10^{15}	1.88×10^{15}	1.04×10^{15}	2.84931×10^{12}	3.81083×10^{13}
	95% CI	-2.59×10^{12} to 2.59×10^{12}	-7.840×10^{14} to 7.840×10^{14}	-2.102×10^{14} to 2.102×10^{14}	−3.604 to 6.052	-7.62×10^{13} to 7.62×10^{13}	-4.03×10^{12} to 4.03×10^{12}	-7.139×10^{15} to 7.139×10^{15}	-2.619×10^{15} to 2.619×10^{15}	-4.446×10^{15} to 4.446×10^{15}	-2.459×10^{15} to 2.459×10^{15}	-6.73×10^{12} to 6.730×10^{12}	-9.0×10^{13} to 9.0×10^{13}
	p value	>0.9999	>0.9999	>0.9999	0.567795	>0.9999	>0.9999	>0.9999	>0.9999	>0.9999	>0.9999	>0.9999	>0.9999
CI (day 14)	Coefficient	−0.009527	−0.2259	0.3207	0.7161	−0.04191	0.0129	2.573	0.5418	−0.2613	−0.1487	−0.006896	0.009277
Multiple R2 = 0.6667	SE	5.85406×10^{11}	1.772×10^{14}	4.75148×10^{13}	1.046	1.72089×10^{13}	9.11222×10^{11}	1.614×10^{15}	5.919×10^{14}	1.005×10^{15}	5.56 × 10^{14}	1.52302×10^{12}	2.03698×10^{13}
	95% CI	-1.38×10^{11} to 1.38×10^{11}	-4.190×10^{14} to 4.190×10^{14}	-1.124×10^{14} to 1.124×10^{14}	−1.757 to 3.189	-4.06×10^{13} to 4.06×10^{13}	-2.15×10^{12} to 2.15×10^{12}	-3.816×10^{15} to 3.816×10^{15}	-1.400×10^{15} to 1.400×10^{15}	-2.377×10^{15} to 2.377×10^{15}	-1.315×10^{15} to 1.315×10^{15}	-3.60×10^{12} to 3.60×10^{12}	-4.81×10^{13} to 4.81×10^{13}
	p value	>0.9999	>0.9999	>0.9999	0.5156	>0.9999	>0.9999	>0.9999	>0.9999	>0.9999	>0.9999	>0.9999	>0.9999
SPID 24–48	Coefficient	0.627	−4.734	−47.89	3.795	−7.674	1.322	79.75	−8.746	−85.24	9.621	0.4785	−1.502
Multiple R2 = 0.7039	SE	4.65977×10^{13}	1.411×10^{16}	3.782×10^{15}	103.1	1.37×10^{15}	7.25323×10^{13}	1.285×10^{17}	4.712×10^{16}	8.001×10^{16}	4.425×10^{16}	1.212×10^{14}	1.621×10^{15}
	95% CI	-1.102×10^{14} to 1.102×10^{14}	-3.336×10^{16} to 3.336×10^{16}	-8.943×10^{15} to 8.943×10^{15}	−240.1 to 247.7	-3.239×10^{15} to 3.239×10^{15}	-1.715×10^{14} to 1.715×10^{14}	-3.038×10^{17} to 3.038×10^{17}	-1.114×10^{17} to 1.114×10^{17}	-1.892×10^{17} to 1.892×10^{17}	-1.046×10^{17} to 1.046×10^{17}	-2.867×10^{14} to 2.867×10^{14}	-3.834×10^{15} to 3.834×10^{15}
	p value	>0.9999	>0.9999	>0.9999	0.9717	>0.9999	>0.9999	>0.9999	>0.9999	>0.9999	>0.9999	>0.9999	>0.9999
SPID 24–72	Coefficient	1.268	−9.767	−48.76	−16.37	−11.9	2.658	136.6	−13.74	−156	8.344	1.102	−2.914
Multiple R2 = 0.7411	SE	7.94774×10^{13}	2.406×10^{16}	6.451×10^{15}	175.2	2.336×10^{15}	1.237×10^{14}	2.191×10^{17}	8.036×10^{16}	1.365×10^{17}	7.548×10^{16}	2.068×10^{14}	2.765×10^{15}
	95% CI	-1.879×10^{14} to 1.879×10^{14}	-5.689×10^{16} to 5.689×10^{16}	-1.525×10^{16} to 1.525×10^{16}	−430.6 to 397.8	-5.525×10^{15} to 5.525×10^{15}	-2.925×10^{14} to 2.925×10^{14}	-5.181×10^{17} to 5.181×10^{17}	-1.900×10^{17} to 1.900×10^{17}	-3.227×10^{17} to 3.227×10^{17}	-1.785×10^{17} to 1.785×10^{17}	-4.889×10^{14} to 4.889×10^{14}	-6.539×10^{15} to 6.539×10^{15}
	p value	>0.9999	>0.9999	>0.9999	0.9282	>0.9999	>0.9999	>0.9999	>0.9999	>0.9999	>0.9999	>0.9999	>0.9999

Table 4. *Cont.*

		VEGF	TGF-b1	FGFb	PDGF-bb	TNF-alfa	IL-10	IL-6	IL-4	IL-1b	IL-8	IL-IRA	IFN-Gamma
SPID 24-168	Coefficient	3.921	−25.38	−32.48	−277.1	−16.25	6.61	416.4	−54.23	−513.6	93.56	3.819	−11.98
Multiple R2 = 0.6888	SE	2.767×10^{14}	8.378×10^{16}	2.246×10^{16}	536.4	8.135×10^{15}	4.308×10^{14}	7.629×10^{17}	2.798×10^{17}	4.752×10^{17}	2.628×10^{17}	7.2×10^{14}	9.63×10^{15}
	95% CI	-6.544×10^{14} to 6.544×10^{14}	-1.981×10^{17} to 1.981×10^{17}	-5.312×10^{16} to 5.312×10^{16}	−1546 to 991.3	-1.924×10^{16} to 1.924×10^{16}	-1.019×10^{15} to 1.019×10^{15}	-1.804×10^{18} to 1.804×10^{18}	-6.617×10^{17} to 6.617×10^{17}	-1.124×10^{18} to 1.124×10^{18}	-6.215×10^{17} to 6.215×10^{17}	-1.703×10^{15} to 1.703×10^{15}	-2.277×10^{16} to 2.277×10^{16}
	p value	>0.9999	>0.9999	>0.9999	0.6213	>0.9999	>0.9999	>0.9999	>0.9999	>0.9999	>0.9999	>0.9999	>0.9999

VAS - Visual analog scale of pain; CI—Cicatrization Index; SPID—Sum of Pain Intensity Difference for the determined interval, in hours; 95% CI—95% confidence interval; SE—standard error.

Table 5. Analysis of correlation between pain/tissue healing indicators and the surface concentration of cytokine and growth factors on each side of the participants (clot and L–PRF) at day one after surgery.

Outcome Measure		VEGF	TGF–β1	FGFb	PDGF–bb	TNF–α	IL–10	IL–6	IL–4	IL–1β	IL–8	IL–1RA	IFN–γ
Clot													
VAS (day 1)	Spearman ρ	−0.013	0.317	0.299	0.317	−0.316	0.068	−0.273	−0.209	−0.050	−0.387	0.046	−0.300
	p value	0.957	0.173	0.200	0.173	0.175	0.776	0.244	0.378	0.836	0.092	0.847	0.199
VAS (day 2)	Spearman ρ	0.074	0.042	0.107	0.042	−0.274	−0.107	−0.191	−0.152	−0.044	−0.055	−0.133	−0.299
	p value	0.758	0.859	0.655	0.859	0.243	0.653	0.421	0.521	0.853	0.819	0.576	0.200
VAS (day 3)	Spearman ρ	−0.020	−0.127	−0.077	−0.127	−0.268	−0.069	−0.037	−0.002	0.191	−0.008	0.008	−0.292
	p value	0.933	0.594	0.748	0.594	0.254	0.773	0.876	0.994	0.420	0.975	0.972	0.211
CI (day 7)	Spearman ρ	−0.182	−0.045	−0.010	−0.045	0.234	0.222	−0.036	−0.027	−0.197	−0.146	0.098	0.234
	p value	0.443	0.850	0.967	0.850	0.321	0.346	0.882	0.910	0.405	0.540	0.682	0.321
CI (day 14)	Spearman ρ	−0.349	0.091	0.172	0.091	0.404	0.326	0.163	0.057	0.089	−0.076	0.442	0.366
	p value	0.132	0.703	0.469	0.703	0.077	0.161	0.492	0.810	0.710	0.752	0.051	0.113
$SPID_{24-48}$	Spearman ρ	−0.136	0.116	0.105	0.116	−0.002	0.146	−0.031	−0.060	0.021	−0.194	0.090	−0.017
	p value	0.567	0.626	0.659	0.626	0.992	0.538	0.895	0.803	0.930	0.413	0.707	0.942
$SPID_{24-72}$	Spearman ρ	−0.096	0.214	0.212	0.214	−0.081	0.143	−0.129	−0.144	−0.055	−0.260	0.035	−0.095
	p value	0.686	0.365	0.368	0.365	0.734	0.547	0.588	0.545	0.819	0.268	0.884	0.691
$SPID_{24-196}$	Spearman ρ	−0.159	0.276	0.320	0.276	−0.062	0.197	−0.162	−0.191	−0.065	−0.299	0.120	−0.086
	p value	0.502	0.238	0.168	0.238	0.797	0.405	0.495	0.421	0.784	0.200	0.613	0.720
L-PRF													
VAS (day 1)	Spearman ρ	−0.228	−0.122	0.147	−0.403	−0.199	0.278	−0.300	−0.250	−0.138	−0.379	0.031	−0.240
	p value	0.333	0.609	0.536	0.078	0.400	0.235	0.198	0.288	0.560	0.100	0.896	0.309
VAS (day 2)	Spearman ρ	−0.050	−0.243	−0.302	**−0.524 ***	−0.154	0.207	−0.165	−0.138	0.093	−0.223	0.072	−0.301
	p value	0.833	0.301	0.195	**0.018**	0.516	0.381	0.488	0.563	0.697	0.344	0.763	0.198
VAS (day 3)	Spearman ρ	0.120	−0.208	**−0.479 ***	**−0.709 ***	−0.091	−0.003	−0.249	−0.216	−0.135	−0.215	0.013	−0.172
	p value	0.615	0.378	**0.033**	**0.009**	0.704	0.989	0.289	0.360	0.570	0.363	0.957	0.468
CI (day 7)	Spearman ρ	−0.171	0.202	−0.328	**0.516 ***	0.040	−0.105	0.106	0.042	−0.067	0.025	0.042	0.247
	p value	0.470	0.392	0.159	**0.020**	0.868	0.660	0.655	0.861	0.778	0.915	0.862	0.294
CI (day 14)	Spearman ρ	−0.348	0.362	−0.174	**0.522 ***	−0.150	−0.098	0.309	0.117	0.214	0.261	0.166	0.261
	p value	0.133	0.117	0.463	**0.018**	0.529	0.681	0.184	0.622	0.365	0.265	0.485	0.265
$SPID_{24-48}$	Spearman ρ	−0.229	0.134	−0.133	0.078	−0.185	0.073	−0.069	−0.086	−0.104	−0.153	0.076	0.068
	p-value	0.332	0.572	0.575	0.743	0.434	0.759	0.774	0.719	0.662	0.520	0.750	0.776
$SPID_{24-72}$	Spearman ρ	−0.261	0.043	−0.110	−0.003	−0.174	0.204	−0.133	−0.112	−0.080	−0.250	0.076	−0.053
	p value	0.267	0.856	0.646	0.990	0.464	0.388	0.575	0.637	0.738	0.287	0.750	0.824
$SPID_{24-196}$	Spearman ρ	−0.258	−0.083	0.073	−0.288	−0.179	0.277	−0.309	-0.256	−0.188	−0.382	−0.008	−0.215
	p value	0.273	0.727	0.759	0.218	0.451	0.238	0.185	0.275	0.428	0.096	0.975	0.363

VAS—Visual analog scale of pain; CI—Cicatrization Index. SPID—Sum of Pain Intensity Differences. Bold numbers with an asterisk indicate a significative relevant correlation ($p < 0.05$, Rho > 0.3). The Spearman´s correlation rank test could not be performed for VAS at day 7 since all results were null.

4. Discussion

The purpose of the present study was to assess the effects of L–PRF on the healing process of the lower third molars extraction socket and its relationship with the local concentration of growth factors and cytokines. For this, a randomization unit was employed consisting of the participant's extraction socket and not that of a different participant. Such a study design, besides reducing inter-individual and demographic variables such as age and gender, usually provides relevant data without the necessary use of larger samples [13,14]. Another important fact about the present study design was the double blinding at the levels of both participants and data evaluation (clinical and laboratory parameters). These are essential steps to reduce the risk of bias and improve the quality of data from clinical trials. Blinding was a topic of particular concern in the study design in order to ensure that both participants and researchers who assessed the outcomes remained unaware of the treatment on each surgical site. Special care was taken in the dental socket's primary closure, and the local anesthesia by regional block was performed so the participants would not feel the introduction of the L–PRF membranes. Furthermore, the membranes' compressing and natural shrinkage contributed to reducing differences between sites, as shown in Figure 4. With such a model, the present findings indicate that the use of L–PRF impacts the local surface concentration of growth factors, with repercussions on clinical parameters of recovery, such as the perception of pain and the quality of soft tissue repair.

Regarding the local concentration of cytokines and growth factors, the present study employed a method of extraction based on previous reports for epithelial surfaces [23,24]. The current findings show that the use of surface swabs may provide an alternative approach to compare the local release of growth factors by L–PRF. However, the data should also be considered with care, as the method may also be subjected to diverse sources of bias, since some methodological steps may interfere with the final amount of collected analytes, including the time of pressing, area of collection, and previous removal of saliva, which represents another well-known source of cytokines [25]. Besides, the examiner's experience was essential to avoid contamination, e.g., saliva and food debris in the suture region. Therefore, careful steps were taken in this study during sample collection, and the examiner guided the oral hygiene of all study participants to reduce the risk of bias during the evaluations performed. The description of this care may help to increase reproducibility and minimize the risk of bias on this kind of clinical/molecular assessment.

The results show that the method of collection was adequate to detect significant differences between grafted and control sites for at least nine molecules, including all four growth factors investigated. FGF–2 or basic FGF (FGFb) is a potent mitogen, promoting angiogenesis and inducing connective tissue remodeling by the production of the extracellular matrix (ECM) by fibroblasts [26]. VEGF, besides its well-known angiogenic properties, also induces collagen deposition and epithelization through mitogenic and chemotactic actions [27]. PDGF is another GF that promotes mitogenesis, angiogenesis, cellular differentiation, and even the upregulation of other growth factors that promote fibroblastic function [28]. TGF–β1 is a multifunctional mediator that acts mainly by chemotaxis and mitogenesis of fibroblasts and macrophages, as well as stimulation of collagen deposition for connective tissue wound healing [29]. Through these mechanisms, these growth factors are expected to be directly associated with the regenerative properties of L–PRF [12,30]. Remarkably, the data indicate that the presence of L–PRF may also be linked to increased local levels of some pro-inflammatory mediators such as IFN–gamma and IL–1beta, which have already been reported as produced and released by L–PRF preparations [9]. While these cytokines mediate inflammatory changes of the gingival tissues, including angiogenesis and edema [31] that could affect the soft tissue healing improvement, the present data suggest that the supraphysiological concentrations released by L–PRF on dental sockets of the third molars are not sufficient to increase postoperative discomfort. On the other hand, the concentrations of most cytokines decreased to levels similar to the control sides within seven days, with the persistent difference found only to VEGF and the anti-inflammatory

cytokines IL–10 and the antagonist of the receptor of IL–1 (IL–1RA), which might contribute to an immunomodulatory role for L–PRF, as previously proposed by Dohan et al. [8].

Another interesting finding was the identification of a strong positive correlation between the platelet count of the samples used to produce L–PRF and the local content of VEGF and, to a lower extent, TGF–β1. The relatively small sample from the present study may have impaired the identification of possible correlations for other analytes present at smaller concentrations. Still, this finding is in agreement with the idea that individual traits may impact biological factors related to the materials effectivity; in this case, the local release of growth factors, reinforcing the need for point-of-care quality assurance of individual L–PRF preparations, including platelet counts of whole blood and prepared membranes [32,33].

Concerning the analysis of pain and healing of soft tissue, the present findings are in agreement with previous reports on good outcomes related to the use of L–PRF on extracted dental sockets [5,10,34]. L–PRF implanted in the third molar socket improved postoperative discomfort ($p < 0.05$) and significantly enhanced soft tissue healing on the seventh and fourteenth day, a timeframe where several other studies also report good clinical results of L–PRF [5,10,34]. Furthermore, the present study provides direct evidence of the connection between released growth factors and clinical improvement by different outcome measures, represented mainly by the strong correlation of PDGF–bb concentration at the L–PRF site with the reduction of pain on the third day after surgery, and the moderate correlation with the cicatrization index at the 7th and the 14th days after surgery. It is essential to notice that PDGF is considered one of the essential mediators released by platelet aggregates. Its proven efficacy in the regeneration of both soft and hard tissue has even led to its approval by the FDA for clinical uses, such as periodontal therapy [31]. Together with the weak-to-moderate negative correlation of FGFb with pain scores on the third day, these findings should encourage further studies on the release of this growth factor by L–PRF, including larger samples and other biomolecular, histological, and histomorphometric analyses at different times of tissue repair.

One of the main limitations of the present study is related to the fact that the sample size was calculated based on the primary clinical outcomes. While the resulting small sample indeed has proven sufficient for the detection of differences between L–PRF and blood clot, as well as a correlation between PDGF and clinical improvement at the L–PRF site, it might have been insufficient for the identification of direct relationships between the clinical and biochemical outcomes through the multiple regression analysis. We were also unable to identify L–PRF treatment's effects through the time-weighted endpoint of pain assessment SPID, employed mainly in clinical trials of analgesics. In this case, rather than a small sample, the very nature of L–PRF mechanisms, which are possibly anti-inflammatory rather than analgesic, may explain the results. Therefore, the participants experienced lower pain from the baseline (24 h) to the last time of follow-up (7 days). On the other hand, they reported high levels of pain at the baseline, with a significant reduction until the 7th day after surgery, thus producing better time-weighted scores. Therefore, the comparison of the pain scores at each time of follow-up proved more sensitive to the effects of L–PRF treatment, as shown in the present results using VAS, a reliable, valid, sensitive, and appropriate scale commonly used in dental, oral, and maxillofacial surgery [35].

Finally, another important limitation of the study was the choice for a split-mouth design, which makes it difficult to compare some variables such as trismus and the number of painkillers consumed and increased the difficulty of achieving symmetrical patterns of dental position. Furthermore, there is always the risk of the patients experiencing difficulties distinguishing between the left and right sides when assessing pain. Nevertheless, we chose to employ this widely used methodology since it avoids other biases, such as in memory of pain, and avoids the need to submit the control group to a venipuncture (to simulate L–PRF production). In this research, the participants were previously oriented regarding the pain assessment, and none of them reported difficulties differentiating the source of pain. This occurred most likely because the pain after surgical removal of the mandibular

third molar could originate from the periodontal ligament or the adjacent tooth's bone and usually does not surpass the midsagittal plan [35]. Split-mouth designs also have been successfully employed on oral pain assessments with low risk of "carry-across" effects [36].

Regardless of these limitations, the present study adds to the body of evidence on the effectiveness of L–PRF in the recovery of third molar extractions by indicating that clinical parameters may improve after L–PRF implantations and provide firsthand clinical evidence that these effects are correlated with the local increase on growth factor concentration. These results suggest that the collection of local growth factors and mediators from the surface of surgical sites may be generalized for other clinical studies of platelet aggregates and may encourage further studies of the correlation between clinical and molecular parameters to enhance the understanding of the mechanisms of action of this autologous biomaterial on the recovery of soft tissues.

5. Conclusions

The use of L–PRF improves the soft tissue healing process and decreases postoperative pain after the third molar extractions, which correlates with an increase in the local concentration of growth factors such as PDGF and FGFb.

Author Contributions: M.T.d.S.: investigation, methodology, writing—original draft preparation; C.F.d.A.B.M.: conceptualization, investigation, methodology, validation, supervision, writing—review and editing; funding acquisition; R.C.M.-M.: investigation, methodology, writing—original draft preparation; P.M.: investigation, validation, funding acquisition; K.J.: investigation, validation, data curation; R.d.L.B.: investigation, software; S.C.S.: data curation, validation; P.E.C.L.: investigation, software, data curation, validation; T.K.: data curation, validation; G.G.A.: conceptualization, investigation, methodology, validation, writing—review and editing; M.D.C.-M.: conceptualization, investigation, methodology, supervision, writing—review and editing, funding acquisition. All authors have read and agreed to the published version of the manuscript.

Funding: This research was funded by Fundação Carlos Chagas Filho de Amparo à Pesquisa do Estado do Rio de Janeiro, FAPERJ, Rio de Janeiro, Brazil. Grant number: E-26/202.713/2019.

Institutional Review Board Statement: The study was conducted according to the guidelines of the Declaration of Helsinki and approved by the Institutional Ethics Committee of the Antonio Pedro University Hospital under the registration no. 2.721.351. Rio de Janeiro, Brazil (protocol code #874527185.0000.5243 and date of approval 02.06.2018).

Informed Consent Statement: Informed consent was obtained from all subjects involved in the study.

Data Availability Statement: Data is contained within the article.

Conflicts of Interest: The authors declare no conflict of interest.

References

1. Osunde, O.D.; Adebola, R.A.; Saheeb, B.D. A comparative study of the effect of suture-less and multiple suture techniques on inflammatory complications following third molar surgery. *Int. J. Oral Maxillofac. Surg.* **2012**, *41*, 1275–1279. [CrossRef]
2. Kaewkumnert, S.; Phithaksinsuk, K.; Changpoo, C.; Nochit, N.; Muensaiyat, Y.; Wilaipornsawai, S.; Piriyaphokai, U.; Powcharoen, W. Comparison of intraosseous and submucosal dexamethasone injection in mandibular third molar surgery: A split-mouth randomized clinical trial. *Int. J. Oral Maxillofac. Surg.* **2020**, *49*, 529–535. [CrossRef] [PubMed]
3. Zandi, M.; Amini, P.; Keshavarz, A. Effectiveness of cold therapy in reducing pain, trismus, and oedema after impacted mandibular third molar surgery: A randomized, self-controlled, observer-blind, split-mouth clinical trial. *Int. J. Oral Maxillofac. Surg.* **2016**, *45*, 118–123. [CrossRef] [PubMed]
4. Afat, I.M.; Akdoğan, E.T.; Gönül, O. Effects of Leukocyte-and Platelet-Rich Fibrin Alone and Combined With Hyaluronic Acid on Pain, Edema, and Trismus after Surgical Extraction of Impacted Mandibular Third Molars. *J. Oral Maxillofac. Surg.* **2018**, *76*, 926–932. [CrossRef] [PubMed]
5. Ritto, F.G.; Pimentel, T.; Canellas, J.V.S.; Junger, B.; Cruz, M.; Medeiros, P.J. Randomized double-blind clinical trial evaluation of bone healing after third molar surgery with the use of leukocyte- and platelet-rich fibrin. *Int. J. Oral Maxillofac. Surg.* **2019**, *48*, 1088–1093. [CrossRef]
6. Ghanaati, S.; Booms, P.; Orlowska, A.; Kubesch, A.; Lorenz, J.; Rutkowski, J.; Landes, C.; Sader, R.; Kirkpatrick, C.; Choukroun, J. Advanced platelet-rich fibrin: A new concept for cell-based tissue engineering by means of inflammatory cells. *J. Oral Implantol.* **2014**, *40*, 679–689. [CrossRef] [PubMed]

7. Kang, Y.H.; Jeon, S.H.; Park, J.Y.; Chung, J.H.; Choung, Y.H.; Choung, H.W.; Kim, E.S.; Choung, P.H. Platelet-rich fibrin is a Bioscaffold and reservoir of growth factors for tissue regeneration. *Tissue Eng. Part A* 2011, *17*, 349–359. [CrossRef]
8. Dohan, D.M.; Choukroun, J.; Diss, A.; Dohan, S.L.; Dohan, A.J.; Mouhyi, J.; Gogly, B. Platelet-rich fibrin (PRF): A second-generation platelet concentrate. Part III: Leucocyte activation: A new feature for platelet concentrates? *Oral Surg. Oral Med. Oral Pathol. Oral Radiol. Endod.* 2006, *101*, e51–e55. [CrossRef]
9. Lourenco, E.S.; Mourao, C.; Leite, P.E.C.; Granjeiro, J.M.; Calasans-Maia, M.D.; Alves, G.G. The in vitro release of cytokines and growth factors from fibrin membranes produced through horizontal centrifugation. *J. Biomat. Mater. Res. Part A* 2018, *106*, 1373–1380. [CrossRef]
10. de Almeida Barros Mourão, C.F.; de Mello-Machado, R.C.; Javid, K.; Moraschini, V. The use of leukocyte- and platelet-rich fibrin in the management of soft tissue healing and pain in post-extraction sockets: A randomized clinical trial. *J. Craniomaxillofac. Surg.* 2020, *48*, 452–457. [CrossRef]
11. Lektemur Alpan, A.; Torumtay Cin, G. PRF improves wound healing and postoperative discomfort after harvesting subepithelial connective tissue graft from palate: A randomized controlled trial. *Clin. Oral Investig.* 2020, *24*, 425–436. [CrossRef] [PubMed]
12. Miron, R.J.; Xu, H.; Chai, J.; Wang, J.; Zheng, S.; Feng, M.; Zhang, X.; Wei, Y.; Chen, Y.; Mourão, C.; et al. Comparison of platelet-rich fibrin (PRF) produced using 3 commercially available centrifuges at both high (~700 g) and low (~200 g) relative centrifugation forces. *Clin. Oral Investig.* 2020, *24*, 1171–1182. [CrossRef]
13. Ahmed, M.; Shama, A.A.; Hamdy, R.; Ezz, M. Bioresorbable versus titanium space-maintaining mesh in maxillary sinus floor elevation: A split-mouth study. *Int. J. Oral Maxillofac. Surg.* 2017, *46*, 1178–1187. [CrossRef] [PubMed]
14. Taschieri, S.; Testori, T.; Corbella, S.; Weinstein, R.; Francetti, L.; Di Giancamillo, A.; Del Fabbro, M. Platelet-rich plasma and deproteinized bovine bone matrix in maxillary sinus lift surgery: A split-mouth histomorphometric evaluation. *Implant Dent.* 2015, *24*, 592–597. [CrossRef] [PubMed]
15. Schulz, K.F.; Altman, D.G.; Moher, D. CONSORT 2010 Statement: Updated guidelines for reporting parallel group randomised trials. *BMJ* 2010, *340*, c332. [CrossRef]
16. Kawase, T.; Mubarak, S.; Mourão, C.F. The Platelet Concentrates Therapy: From the Biased Past to the Anticipated Future. *Bioengineering* 2020, *7*, 82. [CrossRef]
17. Peterson, L.J. Principles of management of impacted teeth. In *Contemporary Oral and Maxillofacial Surgery*, 3rd ed.; Mosby: St. Louis, MO, USA, 1998; pp. 215–248.
18. Ghanaati, S.; Mourão, C.F.; Adam, E.H.; Sader, R.; Zadeh, H.H.; Al-Maawi, S. The role of centrifugation process in the preparation of therapeutic blood concentrates: Standardization of the protocols to improve reproducibility. *Int. J. Growth Factors Stem Cells Dent.* 2019, *2*, 41–44. [CrossRef]
19. Landry, R.G. *Effectiveness of Benzydamine HCl in the Treatment of Periodontal Post-Surgical Patients*; Faculty of Dentistry, University of Toronto: Toronto, ON, Canada, 1985.
20. Huskisson, E.; Jones, J.; Scott, P.J. Application of visual-analogue scales to the measurement of functional capacity. *Rheumatology* 1976, *15*, 185–187. [CrossRef]
21. Frey-Law, L.A.; Lee, J.E.; Wittry, A.M.; Melyon, M. Pain rating schema: Three distinct subgroups of individuals emerge when rating mild, moderate, and severe pain. *J. Pain Res.* 2013, *7*, 13–23. [CrossRef]
22. Hinkle, D.E.; Wiersma, W.; Jurs, S.G. *Applied Statistics for the Behavioral Sciences*; Houghton Mifflin College Division: Boston, MA, USA, 2003; Volume 663.
23. Biesbrock, A.; Yeh, C.H. Relationship of Surface Epithelium Concentrations of IL-1α and IL-1β to Cinical Inflammation during Experimental Gingivitis. In *Assessment of Oral Health*; Karger Publishers: Berlin, Germany, 2000; Volume 17, pp. 20–31.
24. Perkins, M.A.; Osterhues, M.A.; Farage, M.A.; Robinson, M.K. A noninvasive method to assess skin irritation and compromised skin conditions using simple tape adsorption of molecular markers of inflammation. *Skin Res. Technol.* 2001, *7*, 227–237. [CrossRef] [PubMed]
25. Jaedicke, K.M.; Preshaw, P.M.; Taylor, J.J. Salivary cytokines as biomark 164–183. [CrossRef]
26. Nunes, Q.M.; Li, Y.; Sun, C.; Kinnunen, T.K.; Fernig, D.G. Fibroblast growth factors as tissue repair and regeneration therapeutics. *PeerJ* 2016, *4*, e1535. [CrossRef]
27. Bao, P.; Kodra, A.; Tomic-Canic, M.; Golinko, M.S.; Ehrlich, H.P.; Brem, H. The role of vascular endothelial growth factor in wound healing. *J. Surg. Res.* 2009, *153*, 347–358. [CrossRef]
28. Eshwar, S.S.P.; Victor, D.J.; Sangeetha, S.; Prakash, P. Platelet Rich Plasma in Periodontal Therapy. *J. Pharm. Sci. Res.* 2017, *9*, 965–971.
29. Zhang, Y.; Alexander, P.B.; Wang, X.-F. TGF-β family signaling in the control of cell proliferation and survival. *Cold Spring Harb. Perspect. Biol.* 2017, *9*, a022145. [CrossRef] [PubMed]
30. Miron, R.J.; Chai, J.; Zhang, P.; Li, Y.; Wang, Y.; Mourão, C.; Sculean, A.; Fujioka Kobayashi, M.; Zhang, Y. A novel method for harvesting concentrated platelet-rich fibrin (C-PRF) with a 10-fold increase in platelet and leukocyte yields. *Clin. Oral Investig.* 2019, *24*, 2819–2828. [CrossRef] [PubMed]
31. Belstrøm, D.; Damgaard, C.; Könönen, E.; Gürsoy, M.; Holmstrup, P.; Gürsoy, U.K. Salivary cytokine levels in early gingival inflammation. *J. Oral Microbiol.* 2017, *9*, 1364101. [CrossRef]

32. Kitamura, Y.; Watanabe, T.; Nakamura, M.; Isobe, K.; Kawabata, H.; Uematsu, K.; Okuda, K.; Nakata, K.; Tanaka, T.; Kawase, T. Platelet Counts in Insoluble Platelet-Rich Fibrin Clots: A Direct Method for Accurate Determination. *Front Bioeng. Biotechnol.* 2018, *6*, 4. [CrossRef]
33. Kawase, T.; Nagata, M.; Okuda, K.; Ushiki, T.; Fujimoto, Y.; Watanabe, M.; Ito, A.; Nakata, K. Platelet-Rich Fibrin Extract: A Promising Fetal Bovine Serum Alternative in Explant Cultures of Human Periosteal Sheets for Regenerative Therapy. *Int. J. Mol. Sci.* 2019, *20*, 1053. [CrossRef] [PubMed]
34. He, Y.; Chen, J.; Huang, Y.; Pan, Q.; Nie, M. Local Application of Platelet-Rich Fibrin During Lower Third Molar Extraction Improves Treatment Outcomes. *J. Oral Maxillofac. Surg.* 2017, *75*, 2497–2506. [CrossRef] [PubMed]
35. Sirintawat, N.; Sawang, K.; Chaiyasamut, T.; Wongsirichat, N. Pain measurement in oral and maxillofacial surgery. *J. Dent. Anesth. Pain Med.* 2017, *17*, 253–263. [CrossRef] [PubMed]
36. Lesaffre, E.; Philstrom, B.; Needleman, I.; Worthington, H. The design and analysis of split-mouth studies: What statisticians and clinicians should know. *Stat. Med.* 2009, *28*, 3470–3482. [CrossRef] [PubMed]

5 Anexo V

healthcare

MDPI

Review

Digital Management Systems in Academic Health Sciences Laboratories: A Scoping Review

Margareth Timóteo [1,2], Emanuelle Lourenço [3], Ana Carolina Brochado [4], Luciana Domenico [1], Joice da Silva [1], Bruna Oliveira [1], Renata Barbosa [4], Pietro Montemezzi [5], Carlos Fernando de Almeida Barros Mourão [1,4,*], Beni Olej [1] and Gutemberg Alves [1,*]

[1] Clinical Research Unit, Antônio Pedro Hospital, Fluminense Federal University, Niteroi 24020-140, Brazil; margatimoteo@gmail.com (M.T.); ldqueiroz@id.uff.br (L.D.); joicepearl@gmail.com (J.d.S.); brunsoliver4@gmail.com (B.O.); beniolej@id.uff.br (B.O.)
[2] Post-Graduation Program in Medical Sciences, Fluminense Federal University, Niteroi 24020-140, Brazil
[3] Post-Graduation Program in Dentistry, Fluminense Federal University, Niteroi 24020-140, Brazil; emanuelle_stellet@yahoo.com.br
[4] Post-Graduation Program in Science and Biotechnology, Fluminense Federal University, Niteroi 24020-140, Brazil; anacarol.batista.b@gmail.com (A.C.B.); renata_licaa@hotmail.com (R.B.)
[5] Independent Researcher, 24128 Bergamo, Italy; m.montemezzi@libero.it
* Correspondence: carlosmourao@id.uff.br (C.F.d.A.B.M.); gutemberg_alves@id.uff.br (G.A.); Tel.: +1-941-830-1302 (C.F.d.A.B.M.); +55-21-26299255 (G.A.)

Abstract: Good laboratory practices (GLP) increase the quality and traceability of results in health sciences research. However, factors such as high staff turnover, insufficient resources, and a lack of training for managers may limit their implementation in research and academic laboratories. This Scoping Review aimed to identify digital tools for managing academic health sciences and experimental medicine laboratories and their relationship with good practices. Following the PRISMA-ScR 2018 criteria, a search strategy was conducted until April 2021 in the databases PUBMED, Web of Sciences, and Health Virtual Library. A critical appraisal of the selected references was conducted, followed by data charting. The search identified twenty-one eligible articles, mainly originated from high-income countries, describing the development and/or implementation of thirty-two electronic management systems. Most studies described software functionalities, while nine evaluated and discussed impacts on management, reporting both improvements in the workflow and system limitations during implementation. In general, the studies point to a contribution to different management issues related to GLP principles. In conclusion, this review identified evolving evidence that digital laboratory management systems may represent important tools in compliance with the principles of good practices in experimental medicine and health sciences research.

Keywords: scoping review; academic health centers; software; laboratory management

Citation: Timóteo, M.; Lourenço, E.; Brochado, A.C.; Domenico, L.; da Silva, J.; Oliveira, B.; Barbosa, R.; Montemezzi, P.; Mourão, C.F.d.A.B.; Olej, B.; et al. Digital Management Systems in Academic Health Sciences Laboratories: A Scoping Review. *Healthcare* 2021, 9, 739. https://doi.org/10.3390/healthcare9060739

Academic Editors: Giovanni Improta and Paolo Gargiulo

Received: 15 May 2021
Accepted: 9 June 2021
Published: 16 June 2021

1. Introduction

Laboratory research plays an essential role in providing evidence for translational medicine and sustainable solutions to healthcare [1]. However, the reliance on experimental medicine demands increased traceability and data integrity, ensuring the quality of transferrable results to the clinical setting. In recent years, the scientific community experienced awareness regarding a reproducibility crisis related to factors such as the pressure for publication, low statistical power, and insufficient supervision [2]. On the other hand, adequate management, training, and good practices may increase data quality by improving workflow, avoiding errors, and providing traceability [2].

Good laboratory practices (GLP) may be defined as a quality system encompassing organizational processes and conditions under which studies are planned, executed, monitored, registered, and reported [3]. The Principles of Good Laboratory Practice were first developed by a group of GLP experts led by the USA, established in 1978 under the Special

Program on the Control of Chemicals, based on the FDA's regulations for non-clinical laboratory studies. The Organization for Economic Cooperation and Development (OECD) published the Principles of Good Laboratory Practice and Compliance Monitoring in January 1998 [3]. Since then, it represents the primary set of standards available worldwide to ensure quality, reliability, and integrity, providing a solid approach to the management of research laboratories [4].

However, academic laboratories experience several critical barriers to developing and implementing a GLP-compliant infrastructure [5]. These limitations include poor training on management, lack of funding for compliance costs, and high staff turnover due to a dependence on students as temporary personnel [6]. Therefore, laboratory managers at academic centers should explore tools that facilitate supervision and identify critical steps in the laboratory workflow. In this context, digital systems are among the most important tools available for efficient management, ranging from dedicated computer programs to smartphone applications. Laboratory information management systems (LIMS) offer databases and automation [7] that allow experimental data tracking and storage [8]. Other software and digital services that fall outside of the original LIMS classification provide a broader offer of solutions to laboratory management [6,9], coping with other aspects of quality assurance related to communication, staff, multiuser equipment schedule and maintenance, standard procedures, and inventory control, which are fundamental in the full spectrum of a laboratory's workflow [10,11].

Despite the potential effectiveness of these digital tools in meeting specific aspects of laboratory management, it remains unclear how these systems may directly or indirectly contribute to adherence to the GLP principles. In this context, the present review aimed to provide evidence on the theme by scoping the scientific literature for the available digital tools designed to manage health sciences and experimental medicine laboratories and discuss the assessments of effectiveness, acceptance, and their potential for compliance to different aspects of good laboratory practices.

2. Materials and Methods

2.1. Protocol and Registration

This review followed the PRISMA recommendations for scoping reviews (PRISMA-ScR) [12], as shown in the Supplementary Table S1. The study protocol was registered in the Open Science Framework database under the Digital Object Identifier doi:10.17605/OSF.IO/KPC3Q on 15 July 2020.

2.2. Sources of Information and Research Strategy

The broad question that guided the review was: "Are there available digital tools for the management of academic health sciences laboratories?" Strategies were developed to search for data sources in three different databases: PUBMED (www.ncbi.nlm.nih.gov/pubmed (accessed on 26 April 2021)), Web of Science (WoS) (clarivate.com/webofsciencegroup (accessed on 26 April 2021)), and the Virtual Health Library (VHL) (bvsalud.org (accessed on 26 April 2021)). The research was carried until April 2021. Grey literature was consulted through the OpenGrey Database (available at http://www.opengrey.eu/ (accessed on 24 May 2021)). The search keys are described in Table 1, with various combinations of Medical Subject Headings (MeSH) descriptors selected to cover as many articles as possible coping with management software approaches in academic or research settings.

Table 1. Search keys applied to the three consulted databases.

Database	Search Key
PUBMED	(laborator*[tiab] OR Laboratories[mh]) AND (management[tiab] OR "Organization and Administration"[mh] OR "Information Management"[mh]) AND (software[tiab] OR computer*[tiab] OR virtual[tiab] OR Software[mh] OR "Mobile Applications"[mh]) AND (academic OR Universities[mh] OR research[tiab] OR research[mh] OR "Biomedical Research"[mh] OR "Translational Medical Research"[mh]) AND (health OR clinic*)
Web of Science	TOPIC: ((laboratory) AND (management OR "Organization and Administration" OR "Information Management") AND (software OR computer OR virtual OR "Mobile Applications") AND (academic OR University OR research OR "Biomedical Research" OR "Translational Medical Research") AND (health OR clinic)). Time stipulated: all years. Indices: SCI-EXPANDED, SSCI, A&HCI, CPCI-S, CPCI-SSH, ESCI.
Virtual Health Library	(laboratory) AND (management OR organization) AND (software OR computer OR virtual OR "Mobile Applications") AND (academic OR University OR research) AND (health OR clinic)

2.3. Selection of Sources of Evidence

The eligibility criteria were determined on a PIO (Population, Intervention, Outcome) variant of the PICO framework for the selection of studies, more adequate for qualitative reviews [13].

A structured question was produced, in which, Population (P): academic health sciences laboratories, Intervention (I): the use of digital tools, and Outcomes (O): management for quality. After the references were retrieved from the database search, a group of five trained and calibrated reviewers read all titles and abstracts, applying the eligibility criteria, which included complete works on digital tools that aid in the administration of laboratories in academic or research environments, in health or biomedical sciences, including collections and biorepositories. Studies were excluded if they (i) were entirely out of the subject, (ii) did not address laboratory management, (iii) did not deal with software or digital tools, and (iv) were not proposed or discussed for health sciences or biomedical research. Additionally, articles on software that exclusively assessed experimental data management were considered outside the scope of this review. The inter-examiner reliability was assessed through simultaneous assessment of references by five evaluators, obtaining a Cohen's Kappa coefficient of 0.93. Doubts and disagreements were resolved in weekly meetings conducted during this stage.

2.4. Critical Appraisal

A critical appraisal was conducted with the selected references, applying an instrument described by Whittemore and Knafl [14], considering two relevant criteria: (i) methodological and theoretical soundness and (ii) relevance of the data to the proposed question of the review. The methodological assessment considered whether studies presented adequate identification and traceability of the software, evaluating effectiveness, applicability, or acceptance. The adherence to the review's question was considered according to the description of management functions, target users and environment, and software limitations. Each present parameter was scored with 1 point, to a maximum of 4 points. No study was excluded based on this assessment classification, even though the score was included as a variable in the data analysis stage. In general, studies of lower scores contributed less to the analytical process.

2.5. Synthesis of Results and Data Charting

The main characteristics of the selected studies were collected and tabulated, including year and country of conduction, name and type of digital tool, topics of laboratory

management issued by the software, target public and environment of application, accessibility, and whether the software was free or paid. The data extraction was performed in conjunction with five authors in regular meetings. A specific table was produced solely with the studies that performed evaluations of effectiveness or acceptance, with the respective outcomes. A chart was produced connecting the management topics issued by the different tools and the respective sections/chapters from the Organization for Economic Cooperation and Development (OECD) GLP Principles [3].

3. Results

Figure 1 shows the results for the search strategy and screening of databases. The PUBMED database provided 855 entries, while 183 entries were identified in WoS and 550 in the VHL. After combining the 3 results, 352 duplicate articles were identified and excluded. After applying the exclusion criteria, 523 articles were considered off-topic, appearing in searches because of common words and often dealing with clinical/hospital-related issues, but not with experimental medicine. Of the total articles identified, 160 were excluded because they did not deal with software or digital systems, and 534 did not speak about management. From the screening result, 19 articles were selected to compose this Scoping Review, and 2 additional articles were identified manually upon reading the selected references. The twenty-one elected references included studies proposing new software or revisiting already available tools for novel management applications. Some authors also evaluated the impact of changes during and after implementing the systems, either qualitatively or quantitatively.

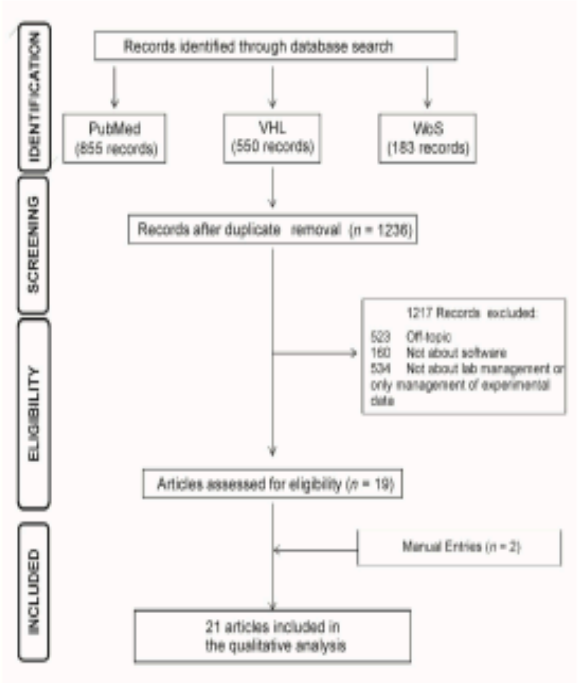

Figure 1. PRISMA flowchart of study screening and selection.

Table 2 shows a critical appraisal performed for the selected articles at the methodological level and relevance to our broad question. Of the 21 articles selected, 9 evaluated the effectiveness and pointed out the limitations. Another eight did not evaluate but described limitations, and four studies did not evaluate or point out the limitations of the systems used, only describing the implementation or development of the systems in an expository manner. Nevertheless, all articles adequately identified the investigated software, their

management purposes, and the environment/professionals served by its functionalities were considered relevant and contributed to some extent to the qualitative discussion on the theme.

Table 2. Critical appraisal of the sources of evidence.

	Adequacy to the Research Question		Methodological Soundness		
Reference	Description of Software Limitations	Description of Functions and Users/Environment	Evaluation of Applicability, or Acceptance	Adequate Identification and Traceability	Final Score
Delorme and Cournoyer [15]	1	1	1	1	4
Godmann et al. [16]	1	1	0	1	3
Nayler and Stamm [17]	1	1	0	1	3
Selznick et al. [18]	1	1	1	1	4
Anderson et al. [19]	1	1	1	1	4
Viksna et al. [20]	0	1	0	1	2
Milisavljevic et al. [8]	1	1	0	1	3
Yousef et al. [21]	1	1	1	1	4
Machina and Wild [22]	1	1	0	1	3
Allwood et al. [23]	1	1	0	1	3
Calabria et al. [24]	1	1	1	1	4
Perkel [9]	0	1	0	1	2
Boutin et al. [25]	0	1	0	1	2
Catena et al. [26]	1	1	0	1	3
Dirnagl et al. [27]	1	1	1	1	4
Manca et al. [28]	1	1	1	1	4
Paul et al. [29]	0	1	0	1	2
Gaffney et al. [11]	1	1	0	1	3
Dennert Friedrich and Kumar [1]	1	1	1	1	4
Timoteo et al. [6]	1	1	1	1	4
Cooper et al. [30]	1	1	0	1	3

To quantify the criteria, "1" means present, and "0" means absent.

Table 3 describes the main characteristics of the twenty-one selected studies related to the present research question. It can be observed that the selection ranged from studies of the earlier days of the use of personal computers in laboratories [15,16] to current cloud computing and mobile applications [25,29]. In addition, some references studied the complexities of the concomitant use of several integrated tools [11,30]. In accordance with the search criteria, the studied environments consisted of academic, health-related laboratories, as well as biorepositories and biobanks. Consistently, the target users were managers and staff common to these laboratories, including technicians, researchers, doctors, and students.

Thirty-three programs/systems were identified in the twenty-one studies, with eight exclusively available for installation on desktop computers and the rest available online, including cloud-based systems, that is, with storage on online servers and availability on demand. Twenty-one of the studied systems were commercially available, charged programs/services, while twelve were free-of-charge for some of their functionalities. Among the non-charged software, two were custom systems designed exclusively for the studied laboratory (Biobank Portal and CCLMS).

Table 4 summarizes the results of the nine studies that assessed the impact of implementing computerized management systems. All of them reported positive results with the use of digital-assisted management. However, problems were identified related to technical constraints (either hardware or software) and limited acceptance of users who resist changing already established procedures, thus impairing the use of some systems to their full potential. Furthermore, the need for staff training and participative management was also recognized to achieve engagement of users to digital-assisted laboratory administration.

Table 3. Main characteristics of the selected studies.

Reference	Country	Software	Availability	Managed Activity	Environment	Target Users	Costs
Delorme and Cournoyer [15]	UK	Customer Information Control System/Virtual Storage (CICS/VS)	Desktop	Tax and administrative tasks, quality control of data and techniques, epidemiological assistance, and teaching and research in the different subspecialties of microbiology.	Microbiology laboratory at a university hospital	Medical Doctors, researchers, and students	Charged
Godmann et al. [16]	USA	LabFlow	Desktop	Workflow in large-scale biology research laboratories.	Research Laboratory	Researchers and laboratory users	Free
Nayler and Stamm [17]	Germany	ScienceLab Database (SLD)	Desktop	Stock of reagents and biological samples, protocols, library, vendor information.	Molecular biology laboratory	Laboratory professionals	Charged
Selznick et al. [18]	USA	Cell Culture Laboratory Management System (CCLMS)	Desktop	Cell culture laboratory management: modules for registering cell counts, frozen cell records, user records, and culture vessel specifications.	Cell culture laboratory	Researchers and users of cell culture laboratories	Custom prototype
Anderson et al. [20]	USA	MGEA	Desktop	Experimental workflow, integration with laboratory equipment, storage, and statistical analysis of experimental data.	Genetic research laboratory	Researchers, laboratory professionals, biostatistics, students.	Charged
Viksna et al. [20]	UK	Patient and Sample System for Information Management (PASSIM)	Desktop/ online	Study participants, samples, and results.	Biorepository and biomedical research labs	Researchers and students	Free and open source
Milisavljevic et al. [8]	Canada	Laboratory Animal Management Assistant (LAMA)	Online	Management of mouse colonies.	Biotery.	Researchers	Free
Allwood et al. [23]	Canada	Lennie	Smartphone	Maintenance and management of animal colonies.	Vivarium.	Researchers	Free
Yousef et al. [21]	USA	LINA	Desktop	Track collections of biologically relevant materials.	Molecular biology academic laboratories.	Medical Doctors, researchers and students	Free
Machina and Wild [22]	USA	Electronic Laboratory Notebook (ELN)	Desktop	Automation of lab tests; register of equipment-related data (use, and calibration). Laboratory inventories.	General laboratories.	Researchers and laboratory users	Charged
Calabria et al. [24]	USA	AdLIMS	online	Biological samples; metadata from patient samples; experimental procedures, workflow, and data for DNA samples.	Genetic sequencing laboratories.	Researchers and users of cell culture laboratories	Charged

Table 3. *Cont.*

Reference	Country	Software	Availability	Managed Activity	Environment	Target Users	Costs
Perkel [9]	USA	Quartzy; LabGuru; LINA; StrainControl; CISPro; mLIMS; OpenFreezer	Online/ smartphone	Sample tracking and inventory.	Research laboratories and Academic Institutions	All levels of laboratory staff	Free and charged tools
Boutin et al. [25]	USA	STARLIMS; GIGPAD; Crimson; Constrack; EMSI; Biobank portal	Online/ smartphone	Genomic data transfer, sequencing, genotyping, sample inventory, workflow, DNA and RNA sample processing and tracking; patient data.	Research laboratories, biobanks, collection clinics, hospitals	Coordinators, research subjects, researchers, IT staff.	A combination of custom/ free/ charged tools
Catena et al. [26]	Switzerland	AirLab	Online/ smartphone	Reagent and sample inventory; database of antibodies.	Research laboratories, mainly molecular.	Researchers and laboratory students	Free
Dirnagl et al. [27]	Germany	LabCIRS (Laboratory critical incident report)	Online	Risk/error management.	Research Laboratories	Research groups, laboratories, and institutions	Free
Manca et al. [28]	USA	Laboratory Center (LC)	Online	Virtual biorepository.	Antibacterial Research Laboratory; biorepository	Researchers	Charged
Paul et al. [29]	USA	BlazeLIMS; FreezerPro; WebLIMS; BioTracer	Cloud	Biobanking.	Biobanks	Doctors and researchers	Charged
Gaffney et al. [11]	USA	GEM•NET	Online	Access control, data and protocol storage, project monitoring, teamwork, internal communication, engagement, and biorepositories.	Academic Research Laboratories—Biorepository of specimens	Researchers and laboratory students	A combination of free/charged tools
Timoteo et al. [6]	Brazil	Quartzy	Online	Staff and workflow management of an academic research lab including documentation, equipment, inventory, and communication.	Academic Research Laboratories	Researchers, and laboratory users.	Free/charged versions
Dennert, Friedrich and Kumar [1]	USA	Database—SDLC System	Online; LAN.	Inventory Management System	Research laboratories; Biorepository of specimens	Researchers and laboratory staff	Charged
Cooper et al. [30]	USA	LabDB	Online; LAN.	Manages experimental data and organizes personnel and inventory.	Research laboratories.	Researchers	Charged

Table 4. Results of the studies that assessed the impact of implementing computerized management systems.

System/Software	Reference	Objective	Test Groups	Method	Results
Customer Information Control System/Virtual Storage (CICS/VS)	Delorme and Cournoyer [15]	Qualitative and quantitative evaluation of system limitations and impact on workflow and man/hour relationships	Software developers and users at the Hospital Lab (N.D.)	Qualitative evaluation of the development of integrated modules; during field testing, the workflow was accessed by the evaluation of patient entry forms, the results of sample and data processing, and the final reports.	- Technical limitations were identified in the software and hardware; changes on the systems solved software-related issues. - More accurate patient and sample reports; control over the destination of the requested tests; easier control of billing; faster delivery and retrieval of results.
CCLMS	Selznick et al. [18]	Test system improvement on organization and control of collections.	Cell culture specialists from 2 labs (n = 6)	Qualitative and quantitative evaluation of usability through the system usability scale (SUS) and field notes.	- CCLMS improved the laboratory's organization set, increased efficiency and reliability.
MGEA	Anderson et al. [19]	Assess the impact on experimental workflow for gene expression analysis.	Researchers (n = 7)	A qualitative longitudinal study. Immersion in the work environment. Interviews, observations, and field notes were coded and analyzed.	- The system performed as a measurement tool rather than the "total laboratory analysis solution" desired initially. - The acceptance of software tools was specific to their function and objectives. - The tool was not used to its full potential.
LINA	Yousef et al. [21]	Effectiveness and acceptance of an inventory system for management of oligonucleotides, strains, and cell lines	Lab staff (n = 10)	Qualitative analysis of the implementation process; quantitative evaluation of usability through the SUS.	- The LINA project achieved its original objectives, as the system obtained an adequate mean SUS score of 86.25.
AdLIMS	Calabria et al. [24]	Evaluate effectiveness on sample tracking in genomic studies.	Developers and potential users/clients (N.D.)	Analysis of requirements and expectations of functionalities from users/clients in terms of functionalities; qualitative analysis of the development process.	- Improved workflow by reducing the time spent on repetitive tasks through interfaces with smartphones and tablets. - Reduced manual errors, standardizing pharmacovigilance monitoring of gene therapy patients. - Compatible with regulatory requirements.

Table 4. *Cont.*

System/Software	Reference	Objective	Test Groups	Method	Results
LabCIRS	Dirnagl et al. [27]	Assess the acceptability, usability of a software of risk assessment for traceability of reported cases.	Lab staff (n = 31)	Statistical and qualitative analysis of the data before and after the implementation of the tool. Online questionnaire with two questions on software usability	- Increased responsibility and maturity to deal with and prevent errors. - Differences in the frequency of digital and paper reporting. - Increased quality, safety, and communication. - Improvement of prevention policies.
LC Virtual Biorepository of the Antibacterial Resistance Leadership Group (ARLG)	Manca et al. [28]	Assess the impact of the implementation of a virtual repository on the management of data and biological collections.	Customers from research labs and diagnostic companies (N.D.)	Qualitative evaluation of the efficiency of the primer bank sequences. Quantitative retrospective assessment of impacts on services provided.	- The software provided sound technical and scientific support to diagnostic companies and platforms. - More than 200 samples/year were provided for research laboratories and diagnostic companies.
Quartzy	Timoteo et al. [6]	Assess the impact of the implementation in the workflow and the perception of users at an academic laboratory.	Lab staff (n = 30)	Qualitative analysis of the team's attitude towards implementation, including a structured questionnaire (and focus group assessments). Management performance indicators were also compared before and after implementation.	- There was a perception of improvement in the workflow in relation to the organization, data logging, traceability, distribution, and overall workflow. - Constant training and a management plan are essential if the potential use of supporting software is exploited to the full.
SDLC	Dennert, Friedrich, and Kumar [1]	Evaluate the development steps of a database of biological sample inventories	Researchers from different fields of medicine (N.D.)	Immersion in the work environment: The cycles of all resources have been developed and tested. User training and interviews were conducted to assess the applicability and identify user's needs.	- The efficiency, traceability, and cost savings led to significant improvements in the workflow and consolidated inventories, reducing storage needs.

N.D.: non-determined number of participants.

Regarding the management subjects issued according to each laboratory, digital systems were employed for several different uses, from purchases and administrative tasks to control of cell collections, inventories in general, as well as data storage and management of animal colonies.

All the thirty-two described software issued one or more topics of management recommended by documents of good laboratory practices [3], including experimental workflow, data storage, integration with laboratory equipment, statistical analysis, comparison of experimental data, animal colonies, biorepositories, inventory, and risks. The integration

of work demands of academic health sciences laboratories and items of compliance with the GLP guidelines are identified in the chart presented in Figure 2.

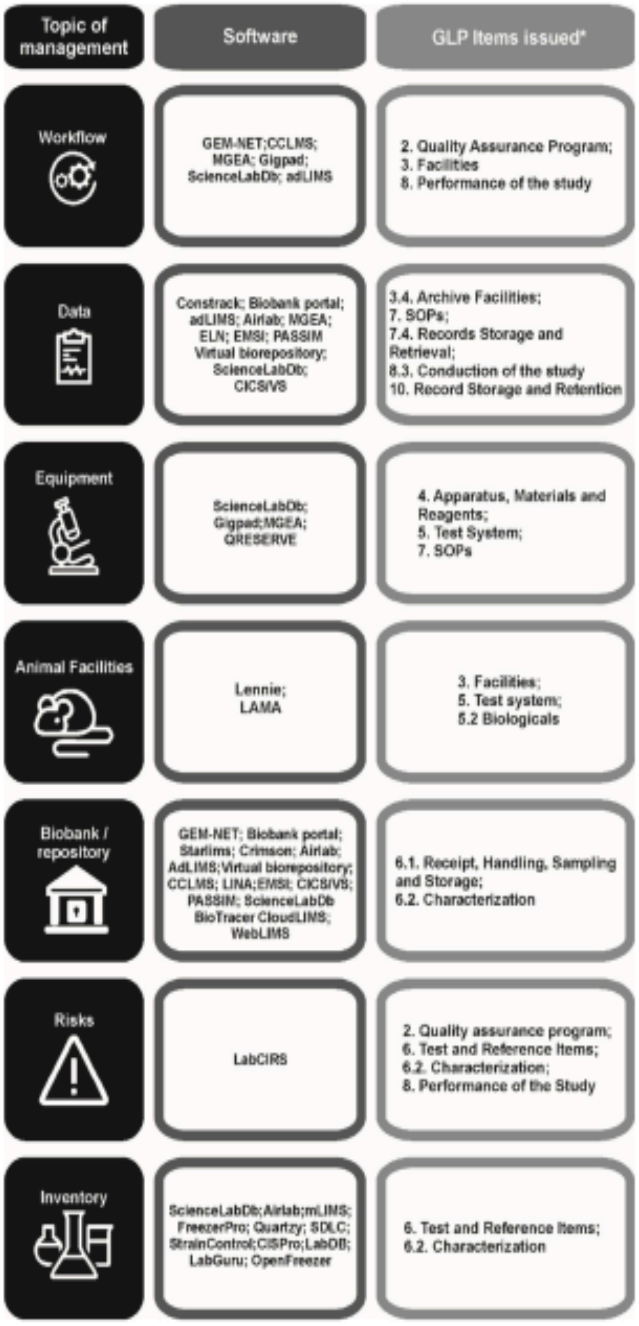

Figure 2. The main applications of the identified software on the different sections and chapters of the OECD GLP Principles [3].

4. Discussion

4.1. Contributions to Adherence to GLP Principles

While the search strategy from the present review identified several different laboratory management systems, few of the eligible studies provided a focused discussion on this topic. The lack of direct scientific evidence limits the present review to quantitatively assess to what extent digital systems can collectively contribute to accreditation achievement. On the other hand, all the identified software accounted for management issues related to at least one of the GLP principles, and, in some studies, more than one software was used to meet the different demands related to quality systems.

In this sense, the approach proposed by Timoteo et al. [6] could be applied to the present sources of data to chart the main topics of management affected by these programs and systems related to good practice guidelines. The chart presented in Figure 2 shows how the types of management supported by the software in academic laboratories are related to several items from Section II of the OECD GLP Principles [3]. Such relationship is revealed by an emphasis on the responsibilities of staff and facilities management, work planning, availability of standard operational procedures (SOPs) that cover all study activities, procedure analysis, use and maintenance of equipment, as well as the application of standards for receiving test samples, its chain of custody and logistics, control of inventory, and the traceability of reagents and validation of methods.

For a better understanding of the functions of these systems, a brief presentation of them will be made, with an emphasis on meeting the computerized systems to the GLP principles listed in Figure 2.

4.1.1. Workflow

The GLP principles require precise definitions of the different steps during the performance of the study, as described in item #8 of the OECD document [3], including the responsibilities of the personnel involved, the facilities and status of equipment employed (item #3), among other factors. Furthermore, quality assurance (item #2) requires identifying and monitoring critical steps, checkpoints, and possible sources of errors. Among the different systems identified in the present review, some described digital tools dedicated to managing such workflow of study performance in a systematized fashion.

In the late 1990s, Goodman and colleagues [16] presented Labflow, a software dedicated to genetics and mapping studies. Workflow management was not recognized as a study topic at that time and, while LIMS already existed, there was no commercial LIMS product that supported workflow management in a specific sense. In this scenario, LabFlow appeared among the first digital solutions, with a workflow model in which objects flow different laboratory tasks (such as DNA extraction, selection of clones, sequence analysis) under programmatic control. An essential point of this software was already allowing the programmer to customize their workflows to different laboratory needs.

Anderson et al. [19] described, in 2007, the implementation of the Microarray Gene Expression Analysis (MGEA), a software package developed by Rosetta Biosoftware (a subsidiary of Merck Inc.), that helped to integrate workflow information related to experimental design, data collection, and bioinformatic analysis of genomic results. Despite the high costs of the license and its renewals, the authors expected that implementing a commercially available service would bring advantages such as security in terms of support for operation and uniformity between different research centers, thus facilitating communication between employees. However, their qualitative analysis observed that the system was not used to its full potential, and its acceptance by staff would demand ongoing training and even an evolution of academic curricula towards the use of bioinformatics tools.

In 2019, Gaffney et al. [11] described the design and implementation of GEM-NET, a software that allowed members of the C-GEM (Center for Genetically Encoded Materials, USA) to integrate research efforts connecting six laboratories spread across three university campuses. GEM-NET was designed to support science and communication by integrating task management, scheduling, data sharing, and internal communications. A set of more

than 20 tools was organized, including two applications customized for the Institution's specific needs of workflow management. The tools are highly interconnected, but the set can be divided into access control, data storage, data navigation, project monitoring, teamwork, internal communication, and public engagement. The authors conclude that GEM-NET provides a high level of security and reliability in workflow management.

4.1.2. Data Management

In different items of the GLP principles, a need is described for the secure storage, filing, and retrieval of research data (item #7.4), including study plans, raw data, final reports, test system samples, and specimens (item #8.3), and their related archiving facilities (item #3.4). Furthermore, item #7 (standard operating procedures) requires the preparation and observance of documents that guarantee the quality and integrity of the data generated by the studies. Sub-item #7.4, for example, describes that in the case of computerized systems, validation, operation, maintenance, security, change control, and the backup system must be observed.

Within the selected studies, we found the report of computerized systems to manage data from various laboratory environments and how they were made available to the research groups. In the early 1980s, Delorme and Cournoyer [15], in a microbiology laboratory of a University Hospital, tested the CCIS/VS (Customer Information Control System/Virtual Storage), consisting of customer data repository, using a central computer shared with medical records databases, admission offices, patient accounting, and other medical-administrative services. The system also served as a virtual storage system, including data from microbiological samples. It performed activities such as report printing, data quality control, epidemiological assistance, germ identification, teaching, and research in the different subspecialties of microbiology. The authors carried out a qualitative and quantitative assessment identifying an improvement of workflow without increasing personnel, together with a reduction in the time for the production of reports, system downtime, and other parameters.

Viksna et al. [20] focused on collecting, storing, and retrieving data on research participants and biomedical samples through electronic management. For this, they proposed the PASSIM (Patient and Sample System for Information Management), a web-based customizable system that could be used for sending, managing, and retrieving samples and data from the research subject, ensuring the confidentiality of the records. This tool was instrumental in managing information in clinical research studies involving human beings and replaced the more expensive LIMS, which requires investments of time, effort, and resources that were not always available.

Electronic laboratory notebooks (ELN) are programs designed to replace traditional research notebooks. These electronic tools may register protocols, field/lab observations, notes, and other data inserted through a computer or mobile device, offering several advantages over paper notebooks [19]. Machina and Wild [22] investigated the importance of ELNs when integrated with other computer tools, such as laboratory information management systems, analytical instrumentation, data management systems, and scientific data. They observed that the type of laboratory (analytical, synthesis, clinical, research) was a primary source of differences when trying to integrate ELN with the available tools. Therefore, based on the observation that there was no well-established path for the effective integration of these tools, the authors decided to review and evaluate some of the adopted approaches.

Calabria et al. [24], in 2015, introduced adLIMS, a software for managing biological samples (primarily DNA) and metadata for patient samples and experimental procedures. The authors described how it was possible to produce this system by customizing a previous open-source software, ADempiere ERP. First, they collected the requirements of the end-users, verifying the desired functionalities of the system and Graphical User Interface (GUI), and then evaluated the available tools that met the desired requirements, ranging from pure LIMS to content management and corporate information systems.

The authors report that the system supported critical issues of sample tracking, data standardization, and automation related to NGS (next-generation sequencing).

By 2021, Cooper et al. [30] reported using integrated systems that ensure the sharing of essential data for current research. The authors followed the 15 years of development and implementation of the LabDB system, initially projected to manage structural biology experiments, which could be improved into a sophisticated system that integrates a range of experimental biochemical, biophysical, and crystallographic data. The LabDB central software module handles data from the management of laboratory personnel, chemical stocks, and storage locations. It is currently used by the American/Canadian consortium CSGID (Center for Structural Genomics of Infectious Diseases) and several prominent research centers. The authors identified the difficulties and resistance of some researchers in adopting these systems as the main limitation, often due to the necessary effort to import data from electronic notebooks or laboratory spreadsheets, with which most researchers are already familiar. Nevertheless, the authors consider that this effort is worth it since these older approaches do not remove or even track inconsistencies and do not adapt well to the requirements of modern research.

It is essential to notice that, for accreditation purposes, hosted services (cloud archiving, backup, or processes) require written agreements describing the responsibilities of the informatics services. Test facility management must be aware of potential risks on data integrity resulting from third-party storage.

4.1.3. Equipment

Adherence to the GLP principles speaks to the adequate management of research equipment (OECD item #4), including their adequate calibration, maintenance, scheduling, and responsible staff in the test facility. Several commercially available systems, such as QRESERVE, cited by Perkel [9], are entirely dedicated to these functions, with integrated reservation calendars, administration of equipment status and availability, a repository of maintenance documentation, and a registry of use time. Other all-purpose management systems such as Labguru have most of these functions on a specific equipment module. That was also the case of the freely available (for individual researchers) Quartzy until 2016, as reported by Timóteo et al. [6]. This study described how the implementation of the software optimized the shared use of equipment on a multiuser clinical research unit and the advantages of allowing equipment scheduling, check-in, and check-out remotely, even using mobile phones.

4.1.4. Animal Facilities

Several procedures related to pre-clinical studies conducted with animals are issued in the GLP principles, mostly in item #5 of the OECD document (test system) and subsection #5.2 (Biologicals). These include a proper registry of housing, handling, and care of animal test systems to ensure the quality of the data. Additionally, records of source, date of arrival, and arrival condition of test systems should be maintained. Two selected studies described the use of vivarium monitoring software to ensure the remote control of stocking, accommodation, handling and care of animals, identification of colonies, and inventory of supplies.

Milisavljevic et al. [8] described, in 2010, the Laboratory Animal Management Assistant (LAMA), a software modified from the LIMS proposal to optimize small animal research management. It was initially developed to manage hundreds of new mouse strains generated by an extensive functional genomics program in Canada. The authors realized that they needed greater availability of suitable, easy-to-use systems and software interfaces. LAMA was implemented for a broad community of users, allowing individual research labs to track their colonies in a larger facility, independently. This open-access software is still available to the research community.

Allwood et al. [23] described, in 2015, how smartphones could help researchers in the remote management of animal colonies. The authors proposed Lennie, an app that

introduced a new method for managing small to medium-sized animal colonies, allowing users to remotely access the facilities, and create and edit several functions virtually from anywhere. Its use contributes to the optimization of workflow and planning of experiments, offering a user-friendly experience. Possible updates to the functionalities were also suggested, such as camera integration with the calendar, permission for data sharing, and permanent storage.

4.1.5. Biobank/Repository

In order to comply with the GLP standards, samples that arrive at a laboratory must have records that include the characterization and reference, date of receipt, expiration date, quantities, and storage data, following item #6.1 (receiving, handling, sampling, and storage). This issue is of utmost importance for managing biobanks and biorepositories, creating a need for specific software for successful management.

Boutin et al. [25] carried out a study on a complex system of various software that contributed to the management of a Biobank. The core object of management was an extensive repository of samples and data available to researchers. The platform requires robust software and hardware, as they work with large amounts of data stored and transferred to research groups. In the study, the authors described each of the five custom and commercially available information systems integrated into the existing clinical and research systems, and discuss safety, efficiency, and challenges inherent in the construction and maintenance of this infrastructure. Constrack was used to manage patient data. The Enterprise Master Specimen Index (EMSI) is a sample indexing system, STARLIMS manages inventory, GIGPAD manages data and integrates equipment, and the Biobank Portal is the customized application that connects all the systems.

Manca et al. [28] assessed the structure of a central laboratory of the Antibacterial Resistance Leadership Group (ARLG) in the USA. This group leads the evaluation, development, and implementation of laboratory-based research and supports standard or specialized laboratory services. The laboratory included both a physical and a virtual biorepository. They developed digital procedures for reviewing and approving strain requests, providing guidance during the selection process, and monitoring the transfer of strains from the distribution laboratories to the requesting investigators.

Paul et al. [29] also describe a Biobank management system, with great emphasis on data storage in clouds. The authors evaluated that biobanks have become an essential resource for health research and drug discovery. However, collecting and managing large volumes of data (bio-specimens and associated clinical data) requires biobanks to use more advanced data management solutions. Paul and Chatterjee [27] point out that in the current COVID-19 pandemic scenario, that requires global and quick actions, virtual biobanks present a crucial role in several different fronts, from diagnosis to research. Without the need to physically use biological samples, these banks may allow sharing medical data and networks for better cooperation between biobanks at the national and international levels.

Recently, Dennert, Friedrich, and Kumar [1] explained the various implications of the inventory management of biological samples from various research areas, employing different cryopreservation methods. Such management must ensure the availability of items, easy tracking, and the optimization of shared space among the various research groups. For this, the authors presented the various stages of developing an inventory data model using the Microsoft Access database, after several phases that included training, planning, implementation, and maintenance, as well as the establishment of manuals and protocols for standardized data entry. Using the software development lifecycle (SDLC), the authors attained a database construction model. This model requires frequent communication with users to provide transparency and quality improvement.

4.1.6. Risk Management

Identifying incidents and risk assessment is an essential part of the GLP standards that requires an adequate work plan and a quality assurance program (OECD document

item #2). Item #8.3 of the GLP states that all data changes during the conduction of a study must always be registered and responsible for the change to ensure traceability, enabling a complete audit trail to show all changes without masking the original data.

The work of Dirnagl et al. [27] discusses how error management is fundamental to comply with international standards while studying the implementation of the LabCIRS (Laboratory Critical Incident Reporting System), a simple, accessible, and open-source critical incident reporting system for pre-clinical and basic academic research groups. The software was implemented by establishing an electronic quality management system, which allowed accessibility through any laboratory computer, enabling incident reports that included photo uploads and automatic alerts for new reports and archiving.

4.1.7. Inventory

Item #6.2 of the GLP principles clearly states that all material from a study must be adequately identified, including the batch number, purity, composition, concentrations, or other characteristics, to define each item or reference item properly. It also indicates the need to keep the receipt and expiration dates, quantities received/used in the studies, and storage instructions for the stock of materials. In this review, several articles emphasized this need to monitor inventories with the help of computerized systems.

Nayler and Stamm [17], in 1999, described a laboratory management software, ScienceLab Database (SLD), which offered a management platform for molecular biology research laboratories. The program primarily manages the stock of biological samples, including plasmids, antibodies, cell lines, and protocols, and included an ordering and grants management system. The authors considered that this system met the specific needs of a small to medium-sized research laboratory, helping to organize inventories of valuable reagents, storing, and maintaining information about these items, and simplifying orders and processes.

By 2016, Catena et al. [26] developed the AirLab, a cloud-based tool with web and mobile interfaces, to organize antibody repositories and their multiple conjugates. Due to the large number of data generated by these collections, the authors recognized the need for dedicated software. The work demonstrated that Airlab simplifies the purchase, organization, and storage of antibodies, creating a panel to record results and share antibody validation data.

Yousef et al. [21] described the LINA (Laboratory Inventory Network Application) as a set of Windows-based inventory management software configured to work on a computer network with multiple users. Designed for small molecular biology laboratories, it uses Access databases to assign a new identifier to each new reagent, providing a library that helps with research and comparing DNA sequences. It later faced several features, such as expanding the types of tables available, compatibility with other operating systems, barcoding, and improvement of security issues. According to the authors, the resources provided by LINA are comparable to those available in commercial databases, with the advantage of providing a free database maintenance application for academic laboratories.

In an opinion article published in Nature's section "Toolbox", Perkel [9] describes several low-cost computerized electronic inventory systems as a means to overcome tortuous searches, old notebooks, out-of-date spreadsheets, and "frost-encrusted freezer boxes" to identify laboratory samples and resources. Besides programs discussed by other authors in this review, such as LINA and Quartzy, the article cites other systems such as OpenFreezer, a free web-based system to register sample data such as location, origin, and biological properties, the cloud-based StrainControl (DNA Globe, Sweden), a software free for individual researchers that provides support for managing different lab-organism strains, molecules, and chemicals, the mLIMS, developed by BioInfoRx (Madison, WI, USA), designed to track rodent colonies, LabGuru (BioData, Cambridge, MA, USA), a widely known paid cloud-based all-in-one Electronic Notebook, and CISPro (BioVia, Waltham, MA, USA), described as a functional Institute-wide tracking system for shared resources. Despite

differences in accessibility and several resources, all of these systems share similar search engines linked to customizable databases.

Timoteo et al. [6] evaluated, by 2020, the impact of implementing a multi-module, free-of-charge online management system (Quartzy, Quartzy Inc., Santa Clara, CA, USA) in the workflow of a Brazilian academic clinical research laboratory on the perception of users. Until 2016, the software modules could assist in various aspects and demands of the laboratory, including user communications, multiuser equipment management, material inventory, research documents, and tracking of supply orders. Unfortunately, Quartzy was recently updated to a simpler version, consisting only of an inventory and purchase tracking system that connects researchers to hundreds of life sciences brands and suppliers.

4.2. Evaluating Impacts and Limitations

Effectiveness is a fundamental point to be considered in the potential role of software for laboratory management. However, most of the eligible studies identified in our search did not investigate the reported systems' impact either through qualitative or quantitative assessments. Moreover, despite the performance of evaluations, few studies identified or discussed the limitations and drawbacks of the studied information systems. The studies with evaluations reported, among several aspects, improvement of the organization, workflow, traceability, reliability, acceptability, and good use of the software. Decreased process errors were reported that were made manually, thereby gaining productivity and reducing work. In some specific cases, they positively evaluated the control of frozen cells, generating efficiency and better results in partner laboratories. On the other hand, regarding limitations, older articles (before 2000) identified problems that were more related to system performance, which was sometimes slow and needed adjustments at a time when information technology was still incipient. The limitations from the most current systems are more related to a selective satisfaction and acceptance of software tools, specific according to the function and objective of each group and, in some cases, the resistance by researchers and staff to abandon old ways and migrate to digital tools, which were not used to their full potential within the laboratory.

To adequately assess the impact of these electronic management systems, different methodological approaches are available, such as pre/post-tests evaluating quantitative indicators of performance and provision of services. However, as Timoteo et al. [6] discussed, the complex nature of the provided services of multiuser, academic research facilities may impair the obtention of feedback through quantitative indicators. In this sense, the perception and attitudes of staff towards the management system may contribute to understanding its impact on the workflow and the search for quality at academic clinical research laboratories, as well as provide data for the development or improvement of actions and strategies toward quality and compliance [31–33]. In this sense, validated tools may provide a means to standardize the evaluation of laboratory management software, allowing comparisons on the effectiveness and adequacy of these systems in different applications. Two studies [18,21] proposed the use of an important tool to investigate the effectiveness and efficiency of the software, the system usability scale (SUS). This tool, developed by John Brooke at Redhatch Consulting (UK), consists of a simple, ten-item attitude questionnaire using a Likert scale to provide a global view of subjective assessments of usability, which was validated as providing reliable results even with small samples/study groups, which was the case of most identified studies in this review. Therefore, it may represent a potential tool (although underestimated until the present moment) for further studies on implementing laboratory management systems.

Different studies point out that staff training is one of the most important factors of success of the implementation of these systems and a key part in acceptance and adapting to a new management model. Dirnagl et al. [27] evaluated the impact on staff attitudes toward incident reporting after one year of implementation, observing that training led to greater adherence to the goal of complying with international quality standards and mature culture of error management. Timóteo et al. [6] performed a qualitative evaluation

of the staff perception on software implementation, where most users stated that constant training and leadership were pivotal for the successful use of the software. On the other hand, Anderson et al. [19] reported that limited access to training was a barrier to software use during the implementation of MGEA, and that the lack of ongoing training might have contributed to a progressive de-emphasizing of the system use among the laboratory staff. These data point to the need of careful planning by the PIs to ensure continuous and inclusive training on the implementation program of management systems.

4.3. Software Availability

Regarding availability and accessibility, until 2010, most of the identified programs had to be downloaded/installed to specific laboratory computers [19,30], but were sometimes able to integrate local area networks (LANs), as described by Delorme and Cournoyer in 1980 [15]. In the past decade, technology has advanced to online software, expanding even to applications (apps) on mobile phones, reflecting the current expectations of users and consumers. With app technology permeating all fields of our daily lives, it would be natural for this technological paradigm to reach laboratory and research technologies. Indeed, a big leap was identified towards the proper integration between lab management systems and the new mobile universe. Real-time communication makes it possible, for example, that inventory checks, equipment scheduling, and data verification of an animal colony be performed while in transit. Multicenter studies can share data in real-time, as recently observed in the fast development studies of vaccines against SARS-CoV-2 since 2020, relying heavily on technological development and efficient data management [34].

Begg et al. [35] discussed how computer systems are of particular importance in the process of GLP certification in low- and middle-income countries, even though their role is not always emphasized on accreditation systems around the world. This review identified that the knowledge on laboratory management software is mainly originated, as expected, from developed, high-income countries, with advanced information technology industries and significant investment in technology and support for universities and study centers (USA, Germany, Canada, United Kingdom, Switzerland). In a critical view, it may indicate an economic bias in the technological development on the theme, as developing countries maintain a role as consumers of technology and not as producers and developers, reflecting little investment in this (and other) technological areas.

The costs of implementing computerized systems may represent one of the main challenges for public Academic Health Centers since these Institutions, in general, face tight budgets to support several laboratories, researchers, and research lines. Such limitations are expected to be potentialized when considering low- to middle-income countries, which could benefit from low-cost or cost-free initiatives.

In general, the development and maintenance of information systems are made possible by providing subscription services to ensure the tool's sustainability. The present review identified some systems that addressed a full spectrum of fundamental issues in the management of academic laboratories, such as inventory control and organization and equipment scheduling, on a free-of-charge basis, as it incorporated catalogs from various sponsors (reagent suppliers) and suggests these products when orders are placed [9]. However, such a business model probably did not match the maintenance costs of the platform, as Quartzy has shut down all functions not related to inventory/purchases by 2016, and recently included a fee for Institutional users. It is also possible that users from outside the USA and Europe could not use the vendor-related functionalities, as customer services and representatives in regions such as South America would not connect directly to the system [6]. On the other hand, LINA is an example of a system that could remain free-of-charge, even though limited to the needs of small molecular biology laboratories [21], with much simpler functionalities compared to well-known commercial applications such as Labguru. Other services, such as QReserve, have both free and paid versions with increased functionalities, allowing low-budget academic laboratories to use some free resources, such as equipment reservation and management, through a more straightforward interface.

A usual profile among entirely free software originates from in-house academic software, such as Biobank Portal and CCLMS, customized for the personal use of the developer group, usually without widespread use in other institutions. Even though they may present advantages on issuing specific demands of developers, the lack of a profound, systematic evaluation of performance on most selected studies does not allow to infer whether these are more or less effective than commercial software. In this sense, Boutin et al. [25] report that the laboratory IT framework may face challenges common to industry settings, where cost-overrun is prevented by planning the cost-effectiveness of purchasing commercially available vs. designing in-house custom applications. An interesting way to achieve broader applicability for such software is to use open-source codes, such as Boutin et al. [25], paving the way for other programmers to adapt the tool to different laboratory specificities. It is important to notice that investments from government bodies worldwide could also contribute to the development of freely available tools as part of public policies focused on increasing overall quality and adherence to good practices in health sciences research. In this sense, the encouragement of startups involving interdisciplinary initiatives can turn universities and academic centers into important stakeholders in covering technological gaps in low- or middle-income countries [36].

4.4. Review Limitations

The present Scoping Review has limitations mainly related to the impossibility of exhausting the literature on laboratory software, reflected in the choice of not including programs that dealt only with the transmission and handling of analysis results and laboratory data, such as pure LIMS or analytical bioinformatics software. Despite their fundamental role, these types of software have already been widely discussed [37–40], and most of these systems were not designed to support the management of staff and shared resources, for example. Additionally, the scientific literature probably does not reflect the abundance of available software since developers and the scientific community usually treat them as a commercial tool rather than a research topic. Nevertheless, regardless of such limitations, the present review was able to map a framework that points to the great applicability of these systems in the search for quality and good practices in academic experimental medicine laboratories, where restrictions regarding the availability of resources and staff and limited management experience are common restrictions. Therefore, the gaps identified here can serve as an indication for new studies that seek to assess, quantitatively or qualitatively, the impact of implementing these tools on the best practices at academic health Institutions.

5. Conclusions

The present literature review mapped several studies in the last four decades, proposing and evaluating the impact of digital tools in the management of health sciences research laboratories to several different applications, ranging from administrative workflow management and data traceability to virtual biobanking. These functions have the potential to contribute to the adherence to different GLP principles. However, the evidence for their effectiveness is still limited and requires further investigative efforts.

Supplementary Materials: The following are available online at https://www.mdpi.com/article/10.3390/healthcare9060739/s1, Table S1: Preferred Reporting Items for Systematic reviews and Meta-Analyses extension for Scoping Reviews (PRISMA-ScR) Checklist.

Author Contributions: Conceptualization, G.A., M.T. and B.O. (Bruna Oliveira); methodology, G.A. and C.F.d.A.B.M.; software, P.M.; formal analysis, M.T., R.B., J.d.S. and L.D.; investigation, M.T., E.L., J.d.S. and G.A.; resources, P.M. and C.F.d.A.B.M.; data curation, C.F.d.A.B.M. and G.A.; writing—original draft preparation, M.T., E.L., A.C.B. and L.D.; writing—review and editing, G.A. and C.F.d.A.B.M.; project administration, B.O. (Beni Olej). All authors have read and agreed to the published version of the manuscript.

Funding: This research received no external funding.

Institutional Review Board Statement: Not applicable.

Informed Consent Statement: Not applicable.

Data Availability Statement: The data presented in this study are openly available in the Open Science Framework (OSF) database, at doi:10.17605/OSF.IO/KPC3Q.

Acknowledgments: The authors acknowledge the financial support in scholarships from the Brazilian agencies CNPq, CAPES, and FAPERJ. The authors acknowledge the technical support by Jean Carlos Nascimento.

Conflicts of Interest: The authors declare no conflict of interest.

References

1. Dennert, K.; Friedrich, L.; Kumar, R. Creating an Affordable, User-Friendly Electronic Inventory System for Lab Samples. *SLAS Technol.* 2020. [CrossRef]
2. Baker, M. Is there a reproducibility crisis? *Nature* 2016, *533*, 452–454. [CrossRef]
3. Organization for Economic Co-Operation and Development (OECD). OECD Principles of Good Laboratory Practice. In *Series on Principles of Good Laboratory Practice (GLP) and Compliance Monitoring*; OECD Environmental Health and Safety Publications: Paris, France, 1998; pp. 1–41.
4. World Health Organization (WHO). *Handbook—Good Clinical Laboratory Practice (GCLP)*; World Health Organization on behalf of the Special Programme for Research and Training in Tropical Diseases: Geneva, Switzerland, 2009; pp. 1–28.
5. Adamo, J.E.; Bauer, G.; Berro, M.; Burnett, B.K.; Hartman, K.A.; Masiello, L.M.; Moorman-White, D.; Rubinstein, E.P.; Schuff, K.G. A Roadmap for Academic Health Centers to Establish Good Laboratory Practice-Compliant Infrastructure. *Acad. Med.* 2012, *87*, 279–284. [CrossRef]
6. Timoteo, M.O.; Brochado, A.C.B.; Costa-Silva, D.; Granjeiro, J.M.; Olej, B.; Alves, G.G. The impact of online management systems: A qualitative assessment of staff perception at a clinical research laboratory. *Res. Soc. Dev.* 2020, *9*, e9239109188. [CrossRef]
7. Bianchi, V.; Ceol, A.; Ogier, A.G.; De Pretis, S.; Galeota, E.; Kishore, K.; Bora, P.; Croci, O.; Campaner, S.; Amati, B.; et al. Integrated Systems for NGS Data Management and Analysis: Open Issues and Available Solutions. *Front. Genet.* 2016, *7*, 75. [CrossRef] [PubMed]
8. Milisavljevic, M.; Hearty, T.; Wong, T.Y.; Portales-Casamar, E.; Simpson, E.M.; Wasserman, W.W. Laboratory Animal Management Assistant (LAMA): A LIMS for active research colonies. *Mamm. Genome* 2010, *5–6*, 224–230. [CrossRef]
9. Perkel, J.M. Lab-inventory management: Time to take stock. *Nat. News* 2015, *524*, 125–126. [CrossRef] [PubMed]
10. Gumba, H.; Musyoki, J.; Mosobo, M.; Lowe, B. Implementation of Good Clinical Laboratory Practice in an Immunology Basic Research Laboratory: The KEMRI-Wellcome Trust Research Laboratories Experience. *Am. J. Clin. Pathol.* 2018, *151*, 270–274. [CrossRef] [PubMed]
11. Gaffney, S.G.; Ad, O.; Smaga, S.; Schepartz, A.; Townsend, J.P. GEM-NET: Lessons in Multi-Institution Teamwork Using Collaboration Software. *ACS Cent. Sci.* 2019, *5*, 1159–1169. [CrossRef]
12. Tricco, A.C.; Lillie, E.; Zarin, W.; O'Brien, K.K.; Colquhoun, H.; Levac, D.; Moher, D.; Peters, M.D.; Horsley, T.; Weeks, L.; et al. PRISMA extension for scoping reviews (PRISMA-ScR): Checklist and explanation. *Ann. Intern. Med.* 2018, *169*, 467–473. [CrossRef]
13. Kelly, A.M.; Cronin, P. How to Perform a Critically Appraised Topic: Part 1, Ask, Search, and Apply. *Am. J. Roent.* 2011, *197*, 1039–1047. [CrossRef]
14. Whittemore, R.; Knafl, K. The integrative review: Updated methodology. *J. Adv. Nurs.* 2005, *52*, 546–553. [CrossRef] [PubMed]
15. Delorme, J.; Cournoyer, G. Computer system for a hospital microbiology laboratory. *Am. J. Clin. Pathol.* 1980, *74*, 51–60. [CrossRef] [PubMed]
16. Goodman, N.; Rozen, S.; Stein, L.D. The LabFlow system for workflow management in large scale biology research laboratories. *Proc. Int. Conf. Intell. Syst. Mol. Biol.* 1998, *6*, 69–77. [PubMed]
17. Nayler, O.; Stamm, S. ScienceLabDatabase: A computer program to organize a molecular biology laboratory. *Biotechniques* 1999, *6*, 1186–1191. [CrossRef]
18. Selznick, S.H.; Thatcher, M.L.; Brown, K.S.; Haussler, C.A. Development and application of computer software for cell culture laboratory management. *In Vitro Cell Dev. Biol. Anim.* 2001, *37*, 55–61. [CrossRef]
19. Anderson, N.R.; Ash, J.S.; Tarczy-Hornoch, P. A qualitative study of the implementation of a bioinformatics tool in a biological research laboratory. *Int. J. Med. Inform.* 2007, *76*, 821–828. [CrossRef]
20. Viksna, J.; Celms, E.; Opmanis, M.; Podnieks, K.; Rucevskis, P.; Zarins, A.; Barrett, A.; Neogi, S.G.; Krestyaninova, M.; McCarthy, M.I.; et al. PASSIM—An open-source software system for managing information in biomedical studies. *BMC Bioinform.* 2007, *8*, 52. [CrossRef] [PubMed]
21. Yousef, A.F.; Baggili, I.M.; Bartlett, G.; Kane, M.D.; Mymryk, J.S. LINA: A laboratory inventory system for oligonucleotides, microbial strains, and cell lines. *J. Lab. Autom.* 2011, *16*, 82–89. [CrossRef] [PubMed]
22. Machina, H.K.; Wild, D.J. Electronic Laboratory Notebooks Progress and Challenges in Implementation. *J. Lab. Autom.* 2013, *18*, 264–268. [CrossRef]

23. Allwood, M.A.; Griffith, D.; Allen, C.; Reed, J.; Mahmoud, Q.H.; Brunt, K.R.; Simpson, J.A. Lennie: A smartphone application with novel implications for the management of animal colonies. *Lab. Anim.* **2015**, *49*, 258–262. [CrossRef] [PubMed]
24. Calabria, A.; Spinozzi, G.; Benedicenti, F.; Tenderini, E.; Montini, E. adLIMS: A customized open-source software that allows bridging clinical and basic molecular research studies. *BMC Bioinform.* **2015**, *16*, S5. [CrossRef]
25. Boutin, N.; Holzbach, A.; Mahanta, L.; Aldama, J.; Cerretani, X.; Embree, K.; Leon, I.; Rathi, N.; Vickers, M. The Information Technology Infrastructure for the Translational Genomics Core and the Partners Biobank at Partners Personalized Medicine. *J. Pers. Med.* **2016**, *6*, 6. [CrossRef] [PubMed]
26. Catena, R.; Özcan, A.; Jacobs, A.; Chevrier, S.; Bodenmiller, B. AirLab: A cloud-based platform to manage and share antibody-based single-cell research. *Genome Biol.* **2016**, *17*, 142. [CrossRef]
27. Dirnagl, U.; Przesdzing, I.; Kurreck, C.; Major, S. A Laboratory Critical Incident and Error Reporting System for Experimental Biomedicine. *PLoS Biol.* **2016**, *14*, e2000705. [CrossRef] [PubMed]
28. Manca, C.; Hill, C.; Hujer, A.M.; Patel, R.; Evans, S.R.; Bonomo, R.A.; Kreiswirth, B.N. Laboratory Center of the Antibacterial Resistance Leadership Group (ARLG). Leading Antibacterial Laboratory Research by Integrating Conventional and Innovative Approaches: The Laboratory Center of the Antibacterial Resistance Leadership Group. *Clin. Infect. Dis.* **2017**, *64*, S13–S17. [CrossRef] [PubMed]
29. Paul, S.; Gade, A.; Mallipeddi, S. The State of Cloud-Based Biospecimen and Biobank Data Management Tools. *Biopreserv. Biobank.* **2017**, *15*, 169–172. [CrossRef]
30. Cooper, D.R.; Grabowski, M.; Zimmerman, M.D.; Porebski, P.J.; Shabalin, I.G.; Woinska, M.; Domagalski, M.J.; Zheng, H.; Sroka, P.; Cymborowski, M.; et al. State-of-the-Art Data Management: Improving the Reproducibility, Consistency, and Traceability of Structural Biology and in Vitro Biochemical Experiments. *Methods Mol. Biol.* **2021**, *2199*, 209–236. [PubMed]
31. Lulie, A.D.; Hiwotu, T.M.; Mulugeta, A.; Kebede, A.D.; Asrat, H.; Abebe, A.; Yenealem, D.; Abose, E.; Kassa, W.; Kebede, A.M.; et al. Perceptions and attitudes toward SLMTA amongst laboratory and hospital professionals in Ethiopia. *Afr. J. Lab. Med.* **2014**, *3*, 233. [CrossRef]
32. Presot, I.M.; Soares, R.P.P.; Madureira, A.P.; Bicalho, K.A.; Modena, C.M. Quality perception in research laboratories from Fiocruz after QMS implementation. *Rev. Adm. Pub.* **2014**, *48*, 237–252. [CrossRef]
33. Rusanganwa, V.; Gahutu, J.B.; Evander, M.; Hurtig, A.K. Clinical Referral Laboratory Personnel's Perception of Challenges and Strategies for Sustaining the Laboratory Quality Management System. *Am. J. Clin. Pathol.* **2019**, *152*, 725–734. [CrossRef] [PubMed]
34. Paul, S.; Chatterjee, M.K. Data Sharing Solutions for Biobanks for the COVID-19 Pandemic. *Biopreserv. Biobank.* **2020**, *18*, 581–586. [CrossRef]
35. Begg, S.; Wright, A.; Small, G.; Mosha, F.; Kirby, M.; Snetselaar, J.; Aziz, S.; Bharmal, J.; Dacombe, R.; Bates, I. Developing laboratory capacity for Good Laboratory Practice certification: Lessons from a Tanzanian insecticide testing facility. *Gates Open Res.* **2020**, *12*, 59. [CrossRef]
36. Rao, B.; Mulloth, B. The role of universities in encouraging growth of technology-based new ventures. *Int. J. Innov. Technol. Manag.* **2017**, *14*, 1750014. [CrossRef]
37. Kwok, R. How to pick an electronic laboratory notebook. *Nature* **2018**, *560*, 269–270. [CrossRef]
38. Stephan, C.; Kohl, M.; Turewicz, M.; Podwojski, K.; Meyer, H.E.; Eisenacher, M. Using Laboratory Information Management Systems as central part of a proteomics data workflow. *Proteomics* **2010**, *10*, 1230–1249. [CrossRef] [PubMed]
39. Zimmerman, M.D.; Grabowski, M.; Domagalski, M.J.; Maclean, E.M.; Chruszcz, M.; Minor, W. Data management in the modern structural biology and biomedical research environment. *Methods Mol. Biol.* **2014**, *1140*, 1–25.
40. Labarga, A.; Beloqui, I.; Martin, A.G. Information Management. *Methods Mol. Biol.* **2017**, *1590*, 29–39. [PubMed]